

nn 0201

773

L. SPEELMAN

631.333.53.022.9

FEATURES OF A RECIPROCATING  
SPROUT BROADCASTER IN THE  
PROCESS OF GRANULAR FERTILIZER  
APPLICATION

(with a summary in Dutch)

PROEFSCHRIFT

TER VERKRIJGING VAN DE GRAAD  
VAN DOCTOR IN DE LANDBOUWWETENSCHAPPEN  
OP GEZAG VAN DE RECTOR MAGNIFICUS,  
DR. H. C. VAN DER PLAS,  
HOGLERAAR IN DE ORGANISCHE SCHEIKUNDE,  
IN HET OPENBAAR TE VERDEDIGEN  
OP VRIJDAG 19 OKTOBER 1979  
DES NAMIDDAGS TE VIER UUR IN DE AULA  
VAN DE LANDBOUWHOGESCHOOL TE WAGENINGEN

H. VEENMAN & ZONEN B.V. - WAGENINGEN - 1979

150 27 3/2

LIBRARY  
1 SEP 79  
1979

This thesis is also published as Mededelingen Landbouwhogeschool Wageningen 79-8 (1979)  
(Communications Agricultural University Wageningen, The Netherlands)

Aan *Tiny*  
*Arianne*  
*Gerty*

## VOORWOORD

Bij het verschijnen van dit proefschrift past een woord van dank aan allen, die direct dan wel meer indirect hebben bijgedragen aan de totstandkoming ervan. De alom waargenomen trend tot nivelleren, zou aanleiding kunnen zijn dit voorwoord hiermee af te sluiten, daarmee het gevaar van het niet of juist te nadrukkelijk vermelden van personen vermijdend.

Echter het voor de auteur eenmalige karakter van de afronding van een dissertatie rechtvaardigt een uitgebreider, wellicht traditioneel te noemen aanpak.

Vandaar:

Hooggeleerde Moens, hooggeachte promotor, mijn hartelijke dank voor Uw stimulerende begeleiding en opbouwende kritiek. Waar de afronding van de in dit proefschrift beschreven onderzoek samenvalt met mijn vertrek van de vakgroep Landbouwtechniek, wil ik mijn erkentelijkheid uitspreken voor het vertrouwen dat ik van Uw zijde mocht ondervinden gedurende de afgelopen elf jaren.

Hooggeleerde Quast, uit de gevoerde discussies bleek dat een 'Delftse' en 'Wageningse' achtergrond zich uitstekend verenigen in het vakgebied van de Landbouwtechniek.

Wellicht nog belangrijker dan de kwaliteit van de laboratorium voorzieningen, is de werksfeer. De interesse en de vriendschap, die betoond werden door de leden van de vakgroep, waren van bijzondere betekenis voor mij.

Beste Wim Huisman, in jou heb ik het geluk gehad een collega te treffen, die als klankbord kon en wilde fungeren.

De uitvoering van dit onderzoek werd mede mogelijk gemaakt door de financiële en materiële steun van Vicon N.V. te Nieuw Vennepe, de Afdeling Beproeving en de Fotografische Afdeling van het IMAG en door de medewerking van de kunstmestindustrieën DSM, MEKOG en NSM. De medewerking van het Landbouwkundig Bureau van de Nederlandse Stikstofmeststoffenindustrie zij hier met nadruk vermeld.

Van de studenten, die tijdens hun doctoraalstudie geconfronteerd werden met de pendelstroomer wil ik noemen: Jan Bosma, Wim van Donselaar, Henk Peelen, Hans Peeten, Jan Reiling, Victor Roos, Hans Verhofstadt en Jan Meuleman. Het doet mij genoegen dat juist jij Jan, de landbouwwerktuigkundige sectie van onze vakgroep bent komen versterken. Je hulpvaardigheid en enthousiasme is voor de uitvoering van dit onderzoek van groot belang geweest.

Voor de technische ondersteuning bij een aantal experimenten ben ik Oscar Bergman, Willem van Brakel, Jordan Charitoglou, Jan van Loo en Geurt van der Scheur bijzonder erkentelijk.

De illustraties werden verzorgd door Eef van Donselaar, Oscar Bergman, Piet Rijpma en Egbert van de Wal.

Het typewerk werd op accurate wijze verzorgd door onze 'eigen' staf: Karen den

Outer, Ruby van Rhoon en Guus Tergast; bijgestaan door de 'ingehuurde' krachten Joke Noppert en Jennette Doeve. De tekst is gecorrigeerd door Mrs. Carol Odarty.

Tenslotte:

Beste vader en moeder, het feit dat jullie mij de gelegenheid boden de studie aan de Landbouwhogeschool te volgen, stemt mij tot grote dankbaarheid. Moge de afronding van dit proefschrift mede een bekroning zijn voor de belasting die mijn studie ongetwijfeld voor jullie moet hebben betekend.

Lieve Tiny, verdere woorden zouden afbreuk doen aan het feit, dat deze dissertatie aan jou en de kinderen is opgedragen.

# STELLINGEN

## I

De fysische eigenschappen, die bepalend zijn voor de beweging van granulaire meststofdeeltjes door de strooi pijp van de pendelstrooier, dienen een zodanige pluriformiteit te hebben, dat een maximale bijdrage kan worden geleverd aan de variatie in translatiesnelheid.

Dit proefschrift.

## II

Bij het gebruik van onregelmatigheidsindices die de kwaliteit van het verdeelpatroon van kunstmeststrooiers weergeven op basis van de relatieve afwijkingen ten opzichte van het gemiddelde, dient mede rekening te worden gehouden met de nagestreefde dosering van een nutriënt.

## III

Teneinde de door de O.E.S.O. opgestelde procedure voor het beproeven van kunstmeststrooiers geschikt te maken voor het karakteriseren van de regelmaat van samengestelde strooibeelden van mengsels van enkelvoudige meststoffen, dienen normatieve standaard meetmethoden te worden geïntroduceerd voor die fysische eigenschappen die in belangrijke mate bepalend zijn voor segregatie.

O.E.C.D. (1967) Standard Testing Procedure for Fertiliser Distributors. Paris.

## IV

Bij de innovatie van technische systemen in de landbouw dient een grotere plaats te worden ingeruimd voor systematisch, fundamenteel onderzoek.

## V

De meeropbrengsten die bij de precisiezaai van granen ten opzichte van eenvoudige rijenzaai op rijafstanden van 20 cm en meer worden verkregen, moeten eerder worden toegeschreven aan een regelmatigere verdeling van het zaaizaad in het verticale, dan in het horizontale vlak.

CROW, J. and B. HUGHES (1973) *Arable farming*, December: 5-8.  
HEEGE, H. J. (1967) *KTL-Ber. über Landtechnik* 112. Frankfurt/M.  
HEEGE, H. J. (1974) *Landtechnik*: 115-120.  
STROOKER, E. (1969) *I.L.R.* publ. 135. Wageningen.

## VI

Het massaal installeren van muzikale geluidsbronnen met toenemend vermogen in en rond de werkplek wijst op een afnemend vermogen in onze cultuur om stilte te waarderen.

BIBLIOTHEEK  
DER  
LANDBOUW HOOGESCHOOL  
WAGeningen

## VII

Door het verhogen van de efficiëntie bij de toepassing van bestrijdingsmiddelen wordt de belasting van het milieu verminderd. Daartoe dient binnen het kader van een geïntegreerde bestrijdingsvorm het onderzoek naar verbetering van de toepassingstechnieken krachtig te worden gestimuleerd.

## VIII

In het wetenschappelijk en hoger agrarisch beroepsonderwijs dient oefening van de studenten in de technieken van het schriftelijk rapporteren een geïntegreerd onderdeel te vormen van de vakstudie.

## IX

Projectonderwijs zal op de positieve elementen in de mens een stimulerende invloed hebben, indien eerlijkheid ten opzichte van elkaar uitgangspunt is voor de deelnemers.

Project 4E differentiatie, RHLS Groningen; juni 1979.

## X

Te vaak wordt ten onrechte de term alternatief geassocieerd met beter.

# CONTENTS

1. GENERAL INTRODUCTION AND OBJECTIVES OF THE STUDY . . . . .	1
1.1. Introduction . . . . .	1
1.2. Aims of the study . . . . .	1
1.3. Strategy . . . . .	3
1.4. Equipment used . . . . .	5
2. FERTILIZER DISTRIBUTION WITHIN THE FRAMEWORK OF AGRICULTURAL ENGINEERING . . . . .	7
2.1. Introduction . . . . .	7
2.2. Production and use of fertilizers . . . . .	7
2.3. Mineral fertilizers . . . . .	8
2.4. Development of fertilizer distributors . . . . .	10
2.5. The reciprocating sprout or pendulum system . . . . .	13
2.6. Standards for the review of fertilizer distributors . . . . .	16
2.6.1. Capacity and labour demand . . . . .	16
2.6.2. Work load . . . . .	20
2.6.3. Evenness of distribution . . . . .	21
3. DESCRIPTION AND INTERPRETATION OF THE DISTRIBUTION PATTERN OF THE RECIPROCATING SPROUT FERTILIZER BROADCASTER . . . . .	23
3.1. Introduction . . . . .	23
3.2. Description of the evenness of the distribution pattern . . . . .	24
3.2.1. Choice of sampling area . . . . .	24
3.2.2. Coefficients of irregularity . . . . .	26
3.3. The transverse distribution pattern . . . . .	30
3.4. The importance of evenness of distribution of fertilizer . . . . .	33
3.5. Discussion . . . . .	37
4. THE OSCILLATION CHARACTERISTIC OF THE DISTRIBUTOR DEVICE OF THE RECIPROCATING SPROUT BROADCASTER . . . . .	39
4.1. Introduction . . . . .	39
4.2. Theory . . . . .	40
4.2.1. The oscillation characteristics of the sprout . . . . .	40
4.2.2. The relation between construction variables and the character of oscillation . . . . .	44
4.2.2.1. The angle of oscillation $\varphi$ as a function of $C$ and $\alpha$ . . . . .	44
4.2.2.2. Angular and tangential velocity of the sprout in relation to $C$ and $\alpha$ . . . . .	46
4.2.2.3. Angular and tangential acceleration of the sprout in relation to $C$ and $\alpha$ . . . . .	48
4.2.2.4. Centripetal acceleration in relation to $C$ and $\alpha$ . . . . .	52
4.2.2.5. The velocity components in $X$ - and $Y$ -direction . . . . .	54
4.3. Simulation of the oscillation pattern . . . . .	54
4.3.1. Experiments . . . . .	54
4.3.2. Experimental results . . . . .	55
4.3.3. Measurements of the oscillation pattern of the distributor device . . . . .	56
4.3.3.1. Materials and methods . . . . .	56
4.3.3.2. Experimental results . . . . .	58
4.3.4. Influences of construction variables on the oscillation pattern . . . . .	61
4.3.4.1. Introduction . . . . .	61
4.3.4.2. Values of the system variables . . . . .	63
4.3.4.3. Experimental results . . . . .	63
4.4. Discussion . . . . .	69



5. PARTICLE MOVEMENT IN THE RECIPROCATING SPROUT . . . . .	71
5.1. Introduction . . . . .	71
5.2. Theory of particle motion on spinning disc broadcasters . . . . .	72
5.3. Analysis of particle motion in the oscillating sprout . . . . .	75
5.3.1. Introduction . . . . .	75
5.3.2. Materials and methods . . . . .	76
5.3.3. Experimental results . . . . .	79
5.3.3.1. Duration of particle stay and acting section in the sprout . . . . .	79
5.3.3.2. Description of velocity, velocity of outlet, and direction of outlet of particles . . . . .	85
5.3.4. Discussion . . . . .	94
5.4. Theory of particle motion in the oscillating sprout . . . . .	97
5.4.1. Introduction . . . . .	97
5.4.2. Particle motion during impact (discontinuous stage) . . . . .	98
5.4.3. Particle motion during sliding and rolling (continuous stage) . . . . .	103
5.4.4. Set-up and testing of the simulation model . . . . .	107
5.4.5. Experimental results . . . . .	110
5.4.6. Discussion . . . . .	122
6. EFFECTS OF DESIGN VARIABLES ON THE DISTRIBUTION PROCESS . . . . .	124
6.1. Introduction . . . . .	124
6.2. Sprout design and the effects on particle velocities and angles of outlet . . . . .	124
6.2.1. Materials and methods . . . . .	125
6.2.2. Experimental results . . . . .	125
6.2.3. Simulation experiments . . . . .	129
6.2.4. Experimental results . . . . .	130
6.3. Consequences of alteration of design variables for particle dispatch . . . . .	130
6.3.1. Introduction . . . . .	130
6.3.2. The input data file . . . . .	131
6.3.3. Interpretation of the experimental results . . . . .	132
6.3.4. Experimental results . . . . .	133
6.3.4.1. Sprout length and sprout angle . . . . .	134
6.3.4.2. Sprout length and rotary frequency of the driving shaft . . . . .	138
6.3.4.3. Sprout length and angle of oscillation . . . . .	139
6.3.4.4. Sprout length, angle of oscillation, and rotary frequency of the driving shaft . . . . .	141
6.4. Effects of accessories at the sprout end on the basic distribution pattern . . . . .	143
6.4.1. Materials and methods . . . . .	147
6.4.2. Experimental results . . . . .	147
6.5. Discussion . . . . .	151
7. PHYSICAL PROPERTIES OF FERTILIZERS AND THEIR CONSEQUENCES FOR THE DISTRIBUTION PROCESS . . . . .	154
7.1. Introduction . . . . .	154
7.2. Objectives, materials and methods . . . . .	155
7.2.1. Determination of the physical properties . . . . .	157
7.2.1.1. Coefficient of friction . . . . .	157
7.2.1.2. Coefficient of restitution . . . . .	159
7.2.1.3. Particle size distribution . . . . .	159
7.2.1.4. Bulk density . . . . .	160
7.2.1.5. Angle of repose . . . . .	160
7.2.1.6. Thousand kernel weight . . . . .	160
7.2.1.7. Moisture content . . . . .	160
7.3. Experimental results . . . . .	160
7.3.1. Coefficients of friction and restitution . . . . .	160
7.3.2. Other physical properties . . . . .	162
7.4. Effects of physical properties of fertilizers on the quality of the transverse distri-	

bution pattern . . . . .	166
7.4.1. Introduction . . . . .	166
7.4.2. Experimental results . . . . .	169
7.5. Discussion . . . . .	176
SUMMARY . . . . .	178
ACKNOWLEDGEMENTS . . . . .	183
SAMENVATTING . . . . .	184
REFERENCES . . . . .	189
APPENDIX I . . . . .	194
LIST OF SYMBOLS AND ABBREVIATIONS . . . . .	214

# 1. GENERAL INTRODUCTION AND OBJECTIVES OF THE STUDY

## 1.1. INTRODUCTION

In modern agriculture, fertilizer distributors are widely used for the application of mineral fertilizers. Decrease of physical load of men, increase of machine capacity, relatively low costs of purchase and maintenance, and possibility of obtaining an acceptable evenness of distribution were reasons for the introduction of fertilizer broadcasters of the spinning disc and pendulum systems on a large practical scale. Since their introduction, fertilizer broadcasters with the spinning disc system (Fig. 1.1) have been the subject of extensive studies to increase the knowledge of the spreading process. The information of theory of particle movement on the disc, and the resulting opinions about the fundamental connections between place and dimensions of the metering devices, the construction of discs and vanes, the relevant physical properties of the materials and particle trajectories, and the velocities and angles of outlet, have created a potential basis for the control and steering of the distribution process. Extension of research work to the behaviour of mass flows on such spreading devices, as well as on those parts of the discs with or without vanes, supported by the more practical research work including machinery testings, has contributed to a further increase in the level of knowledge. In this way, valuable outlines for machine designers, fertilizer producers and practical users have become available in order to realize suitable and acceptable distribution patterns.

About half a million of the fertilizer distributors produced up till now are working with a pendulum system. The fertilizer is spread by the horizontally oscillating motion of a sprout to the rear of the machine (Fig. 1.2). The development of these reciprocating sprout fertilizer broadcasters started about thirty years ago. Contrary to the spinning disc system, the pendulum system has been the subject of scientific research work only on a minor scale. (CASELLA, 1956; PELLIZZI, 1958; ROMANELLO, 1969). The still existing lack of knowledge of the fundamentals of the metering and distribution process were the reasons for starting a research project of which the first results are published in this thesis. In the first chapter, aims and strategy of the study will be pointed out.

## 1.2. AIMS OF THE STUDY

The present design of the reciprocating sprout fertilizer broadcaster is mainly based on empirical experiences gained from practice and machinery testings. This study is dealing with:

1. An analysis of procedures and norms which are used for examination and description of the quality of the distribution pattern, based on agricultural



FIG. 1.1. Fertilizer distributor of the spinning disc system; two disc type.



FIG. 1.2. Reciprocating sprout or pendulum type fertilizer broadcaster.

requirements. The quality of distribution is mainly determined by means of examination, quantification and qualification of the form of the basic transverse distribution pattern and the compound pattern which is a result of a necessary ratio of overlap. Some specific forms of distribution patterns will be examined and discussed with respect to the values of various coefficients of irregularity, working widths, and variation in ratio of overlap.

2. A qualitative and quantitative analysis of the spreading process of the pendulum system with a special emphasis on particle behaviour inside and when leaving the sprout. It is expected that a better knowledge of the fundamentals of the spreading process, and of the factors which might be of important influence, will create possibilities for increased machine capacity and evenness of distribution. Furthermore, a mutual adaption of the distributor system and some relevant physical properties of the mineral fertilizer will be taken into consideration.

3. The development of theoretical relations for the description of particle behaviour – e.g. trajectory, velocity, character of motion – inside the oscillating system. Based on this theory, and related to the kinematics of the distributor device a mathematical model has to be formulated as a tool for simulation of fertilizer particle behaviour inside the sprout. Comparison between the results of the simulation experiments and the results of actual spreading experiments should indicate if the method may be suitable for predicting the effects and the importance of the changing of design and/or fertilizer parameters.

4. An examination of the effects of some alternative designs of the distributor mechanism on the spreading process and their consequences for the potential capacity and evenness of distribution.

### 1.3. STRATEGY

In order to achieve the described aims of the research work, the following stages can be distinguished in the strategy of the study:

- a. characterization of the distribution patterns
- b. kinematic studies of the distributor device
- c. characterization of particle movement inside and when leaving the sprout
- d. formulation of a theoretical basis for description of the particle movement
- e. development of a model in order to perform simulation experiments
- f. performance of a number of simulation experiments with introduction of several alternative designs.

The stages c.–f. were supported by the results of spreading experiments under laboratory conditions both to develop and to control the value of the theory and the simulation model. It was further examined whether methods of research and results of studies of spinning disc broadcasters, described in literature, could be used.

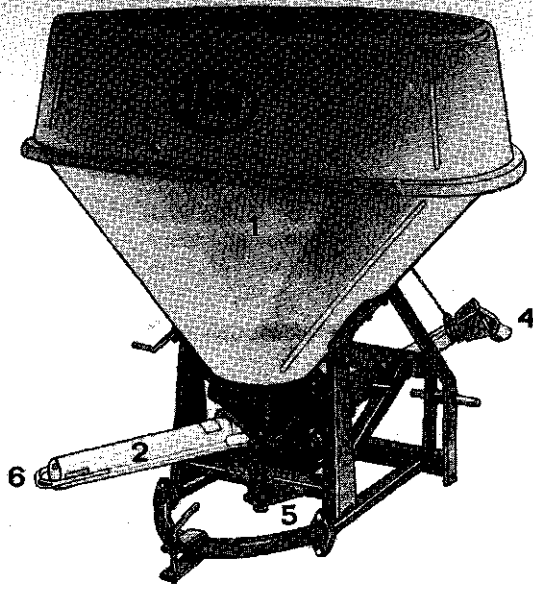


FIG. 1.3. Reciprocating sprout fertilizer broadcaster; 1: hopper, 2: sprout, 3: bowl, 4: driving shaft for p.t.o., 5: flywheel with elastic coupling and forked connection.

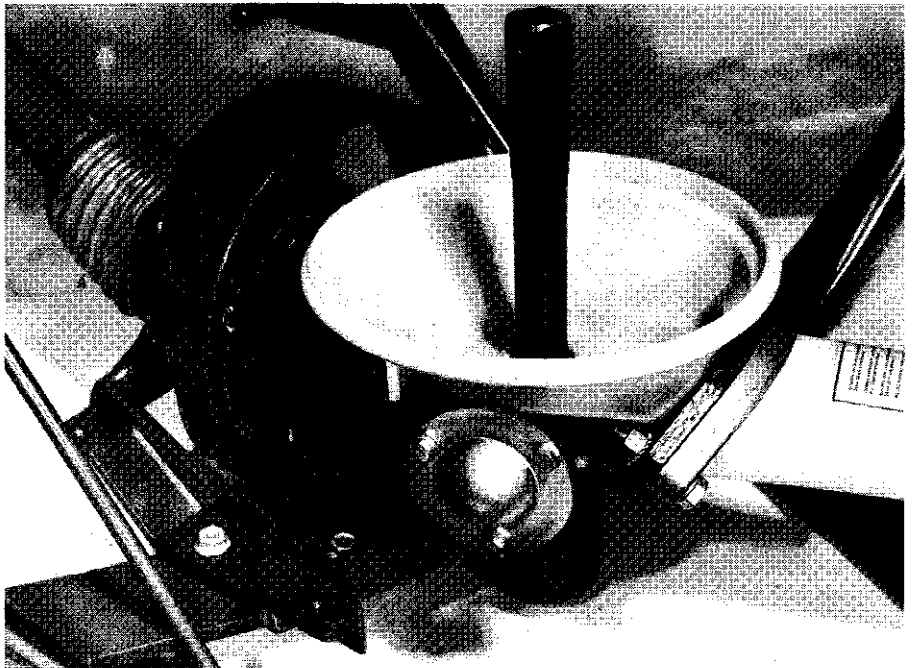


FIG. 1.4. Detail of flywheel, elastic coupling, forked connection, bowl, and entrance of the sprout.

#### 1.4. EQUIPMENT USED

Kinematics of the distribution mechanism as well as the dynamic behaviour of fertilizer particles passing through the sprout were studied using a Vicon reciprocating sprout broadcaster of the model 600 S (see Fig. 1.3). The distributor device consisted of a bowl to which the sprout was attached. The sprout consisted of a hollow, somewhat converging tube out of stainless steel or synthetic material. The distributor device was driven by the tractor power take off (p.t.o.) through a flywheel and elastic coupling. The circular motion of the flywheel was transferred into an oscillatory one for the bowl and sprout by means of a forked connection (Fig. 1.4 and Fig. 1.5). Metering of the fertilizer was controlled by a sliding shutter at the bottom of the hopper (Fig. 1.6).

Alternative construction forms and their effects on the spreading process were examined in a laboratory set-up, which was based upon the mechanism of the

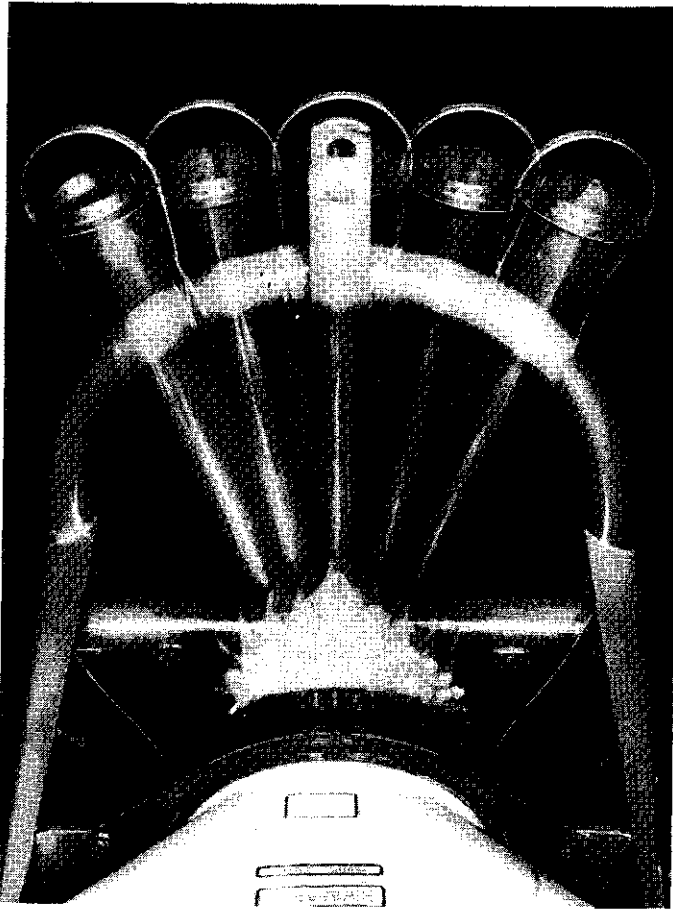


FIG.1.5. The oscillatory motion of the sprout with a bowl at the end of the sprout.

model 600 S. The experiments were carried out in the laboratory of the Department of Agricultural Engineering of the Wageningen Agricultural University. Spreading experiments on a more extensive and practical scale were performed on special patternators provided by Vicon Ltd. at Nieuw Vennep, and by the IMAG experimental farm 'Oostwaardhoeve' at Sloodorp, Wieringermeerpolder. The latter was designed according to international standards.

The characterization of particle movement was mainly based upon the results of high speed movie films. They were made by the Central Technical Institute of Applied Physical Research (CTI/TNO) at Apeldoorn and the Photographic Service of the Institute for Mechanization, Labour and Buildings (IMAG) at Wageningen. The simulation experiments were carried out using the computer facilities of the Computer Centre and the Department of Physics and Meteorology of the Wageningen Agricultural University. Calcium ammonium nitrate fertilizer was supplied by the Agricultural Office of the Dutch Nitrogen Fertilizer Industry at The Hague.

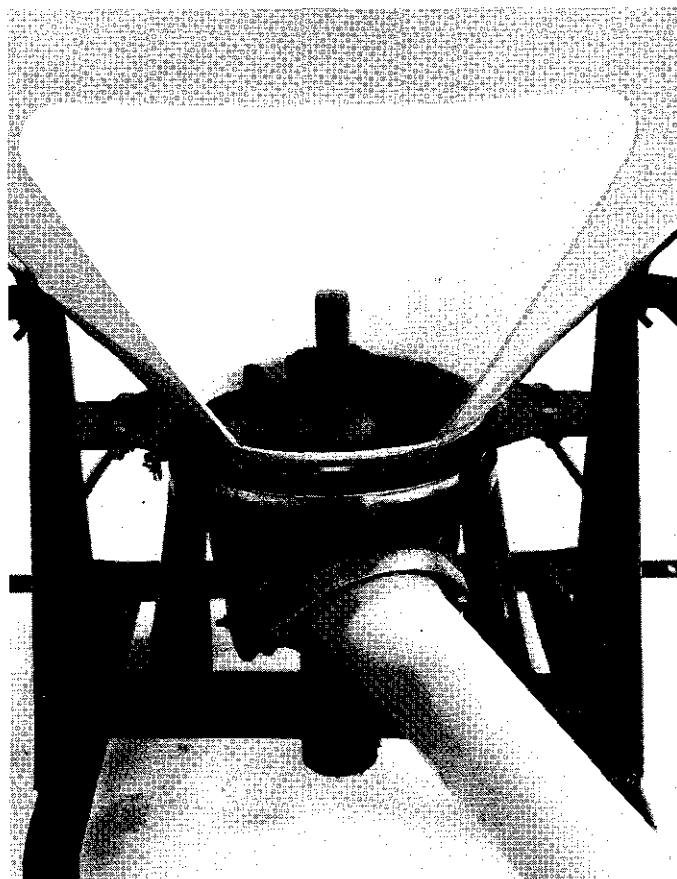


FIG. 1.6. View of metering device with sliding shutters and agitator.



## 2. FERTILIZER DISTRIBUTION WITHIN THE FRAMEWORK OF AGRICULTURAL ENGINEERING

### 2.1. INTRODUCTION

In this chapter a brief view of fertilizer production and use in the world will be given. Based on literature, the historical aspects of development of mechanical systems for fertilizer application are presented. Finally some criteria for the assessment of distribution systems are discussed.

### 2.2. PRODUCTION AND USE OF FERTILIZERS

In 1955/56 world production of nitrogen and ammonium fertilizers was 7.1 million tons N, of phosphatic fertilizers 8.0 million tons  $P_2O_5$  and of potassium fertilizers 7.1 million tons  $K_2O$  (MESKENS, 1975). In the period 1955–1973 the nitrogen fertilizer industry increased production more than five times, up to 38.0 million tons N. About 80% was produced in the U.S.A., the U.S.S.R., Japan, P.R. of China and the European Community countries. Although production in the developing countries increased, in 1972/73 their part was only 10% of total production.

In the same period, production of phosphatic fertilizers increased to 23.6 million tons  $P_2O_5$ . The main manufacturers were U.S.A. and U.S.S.R.. Again, production in the developing countries was still low: 8.5% of the total in 1972/73.

World production of potassium fertilizers increased to 20.2 million tons  $K_2O$ , mainly produced by the U.S.S.R.. In 1972/73 production in the developing countries was only 1.5%.

In 1972/73 more than 80% of N fertilizers were used in the developed countries. In the same season, the developing countries used 7.2 million tons N, of which 55% had to be imported. In the U.S.A., U.S.S.R. and E.C. countries about 50% or 11.0 million tons  $P_2O_5$  were used in 1972/73. The consumption by developing countries was 14%. More than half of this amount had to be imported. The consumption of potassium fertilizers by the developed countries was 17.0 million tons  $K_2O$  or about 90% of the world total. Only 1.7 million tons were used in the developing countries.

In general it may be stated that in the period 1955/56–1972/73 the total consumption of fertilizers increased more than three times. The consumption in developing countries increased to a rate of 15.5% of the world total in 1972/73. For their supply these countries were highly dependent on import. On a world scale, a relatively strong increase in use of N fertilizers with respect to  $P_2O_5$  and  $K_2O$  has to be noticed. In 1955/56 this ratio was 1 : 1.18 : 1.03; in 1972/73 it had changed to 1 : 0.63 : 0.52.

According to VOLLMER (1967) it was estimated that in 1965/66 about one third of the N fertilizers were applied in a liquid form. During that season in the U.S.A. about half of the total N fertilizing was done in this way.

Nevertheless, it may be concluded that, on a world scale, more than 80% of all fertilizers were applied in a fixed mineral form.

### 2.3. MINERAL FERTILIZERS

Mineral fertilizers represent highly diverse materials, making the task of distributor designers rather difficult. There are considerable differences between various fertilizers with respect to shape, size and physicochemical properties. As regards the initial structures, the following forms may be distinguished:

- dusty fertilizers (e.g. Thomas-slag)
- crystalline fertilizers (e.g. potassium salt)
- granulated fertilizers (e.g. calcium ammonium nitrate, granulated urea).

Dusty fertilizers are susceptible to wind influences and when using fertilizer broadcasters, working width can be limited and evenness of distribution poor. In general, crystalline fertilizers are highly hygroscopic. With increasing air humidity they can coagulate and bridge easily or even liquefy.

On the other hand, granulating of fertilizer (being a technological process

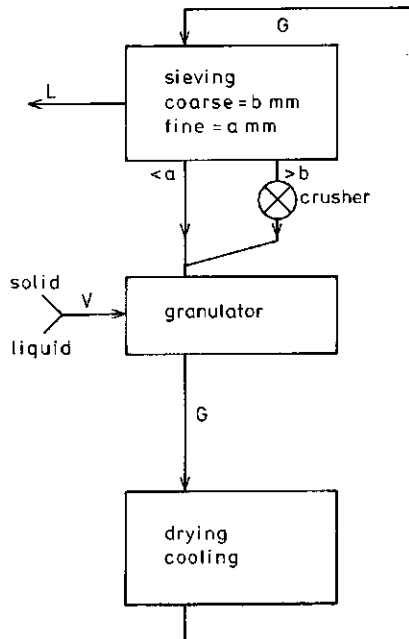


FIG. 2.1. Schematic representation of a technical granulation process. *V*: supply, *G*: granular material, *<a*: too fine fraction, *>b*: too coarse fraction, *L*: final product. (According to VANDER LEEK, 1977.)

during which any fertilizer mass is transformed into a well-defined kernel mass with respect to size and size distribution, shape, nature of surface, porosity, crushing strength, impact strength etc.) can create favourable conditions for the distribution quality of fertilizer broadcasters as it enables:

- the production of fertilizers with an adaptation of relevant physical properties such as particle size to the specific working mechanism of the distributors;
- the creation of better possibilities for the storage and handling in bulk, e.g. by means of coating the particles or other surface treatments to increase their hardness;
- the realization of greater working widths, and a better distribution pattern as the wind influence during spreading is decreased, especially compared to dusty and fine crystalline materials.

Some aspects of different granulation processes are described by VAN DER LEEK (1977). In fertilizer production, the prilling process (e.g. for urea and calcium ammonium nitrate) and the conglomerate granulation, sometimes followed by scaling granulation (e.g. for calcium ammonium nitrate) are applied. During prilling the melt is sprayed by means of special spraying devices. After solidification the hard spherical prills are obtained. Conglomerate granulation is the process during which the mass of fine solid particles, which are in movement with respect to each other, are forced to coagulate by adding a liquid phase. During scaling granulation, fine kernels increase in diameter by means of repeated spraying with melt or slurry. In Fig. 2.1 a scheme of the technical granulation process is presented, Fig. 2.2 shows some prilled and granulated fertilizer samples.

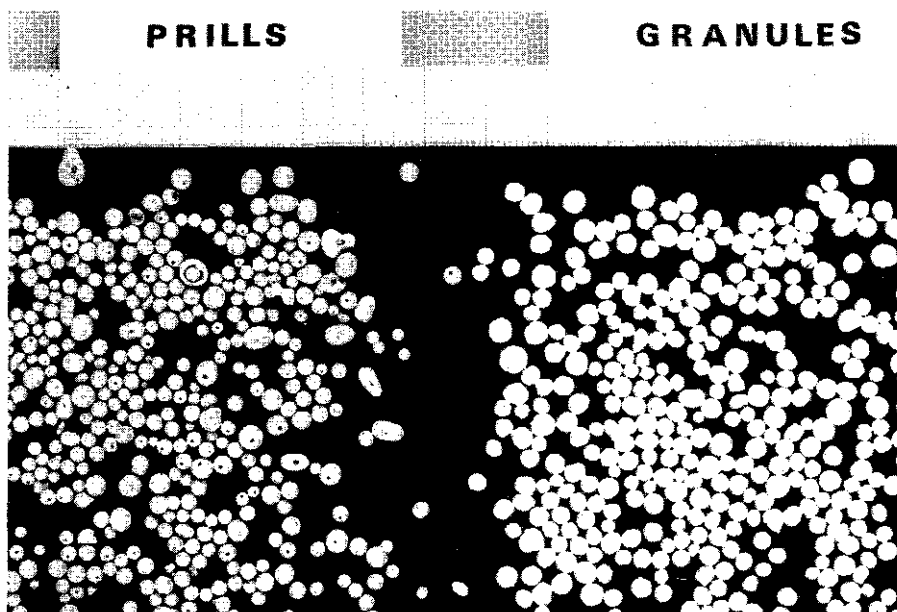


FIG. 2.2. Examples of fertilizer prills and granules.

## 2.4. DEVELOPMENT OF FERTILIZER DISTRIBUTORS

For the application of mineral fertilizers, farmers have used various spreading systems. Fig. 2.3 shows different methods of fertilizer application as well as an arrangement of distribution systems for broadcast application. The arrangement is based on characteristic dimensions of the metering and distribution devices in relation to the spreading width. Descriptions of design and working principles of the main types of construction are given by BAKKER ARKEMA (1957), SCHILLING (1958), SIMONS and TRAPHAGEN (1961), HEYDE (1963), and KANAFOJSKI (1972). For a short, but very clear presentation of fertilizer distributors including their official denominations we refer to the IMAG Trade Mark Guide by FOEKEN and KIERS (1977).

The purpose of broadcast application of fertilizer is to provide each surface unit with almost the same quantity of fertilizer. The oldest way of application was by hand. Scientific research about plant nutrition and fertilizing started around the beginning of the 19th century. However, already before that time equipment for the application of ashes, lime and gypsum was developed, described, and tested in

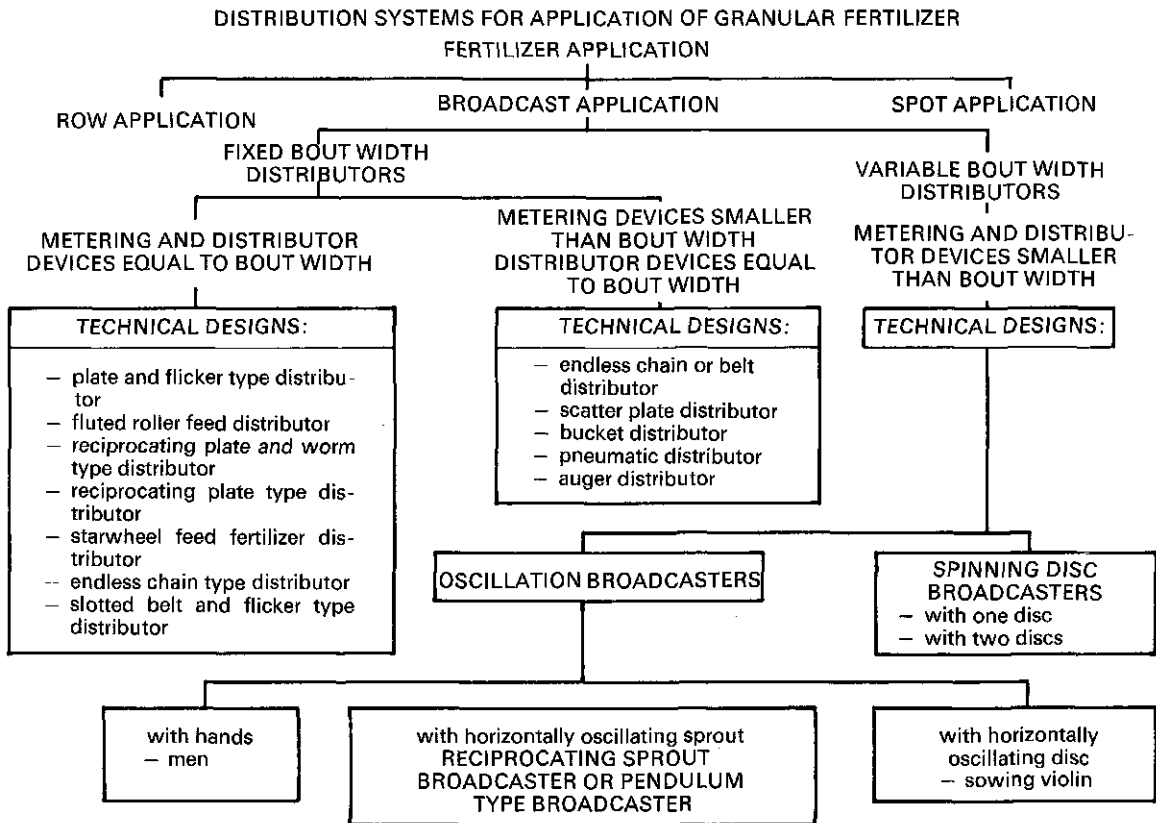


FIG. 2.3. Methods for fertilizer application and arrangement of distribution systems for broadcast application.

England (FUSSEL, 1952). The first use was the application of fertilizer in bands in or on the soil. Sometimes combinations of fertilizer distributor and sowing machine occurred. Examples of such equipment were the constructions by Ellis in 1745, Tull and Worlidge (about 1750), and the later design of Garrett (about 1850) described by VAN DER POEL and REINDERS (1962). Such developments took place simultaneously in North America. However, up to the middle of the 19th century there was hardly any progress in the development of fertilizer distributors (MATHES, 1969). In the second half of that century, mineral fertilizers such as Chilisalt-peter, ammonium sulphate, superphosphate, basic slag and potassium salts, were introduced (RINSEMA, 1959). Just as now, at that time people were somewhat sceptical about the unconditional use of mineral fertilizers. For example at the 36th Dutch Agricultural Economic Congress held in 1883, it was concluded by Dr. Adolf Mayer 'that the use of mineral fertilizer for the Dutch Reclaimed Peat Districts should not be recommended in general; however, it seems to be desirable to start trials with it as an additional nutrient' (ANON., 1928).

Then at the beginning of the 20th century, technical possibilities were found to fix atmospheric nitrogen to carbide (Caro and Frank), to oxygen (Birkeland and Eyde) and to hydrogen (Haber, Bosch, Fauser), and this proved to be of great importance. As a result, both the supply of different types of fertilizer and the demand for suitable spreading equipment increased. The application by hand of Chilisalt-peter and ammonium sulphate was heavy and unpleasant work. Besides that, skilled labour which would be able to obtain a sufficient, even distribution of fertilizer was scarce. Aside from so-called sowing violins, the first equipment for broadcast application of fertilizers belongs to the group of fixed bout width distributors: i.e. spreaders which have metering and/or distribution mechanisms equal to spreading width (see Fig. 2.3).

In the year 1852 'an apparatus for the even distribution of dry mineral fertilizers over the fields' was described in the Netherlands (COOLMAN and VAN DER POEL, 1964). At the same time, fixed bout width distributors were developed, which were the direct predecessors of the construction designs developed at a later stage. (Examples are the spreading systems with fluted roller feed and the agitator feed system.)

At the beginning of the 20th century, the endless chain, and the reciprocating plate and worm type distributors appeared. These had good practical success up

TABLE 2.1. Development of the number of fertilizer distributors in the Netherlands (Sources: DE WIDT, 1955; VAN DER POEL, 1967; CBS, 1965, 1970, 1975).

Year	1892	1895	1904	1950	1960	1965	1975
Variable bout width distributors*					17,646	63,631	
Fixed bout width distributors	42	48	606	19,041	24,526	21,250	102,000

\* sowing violins not included

till the thirties. Furthermore the system of Schloer and Salchow (with a hopper which was movable with respect to a spiked roller distributor system) was introduced (REINDERS, 1892; MATHES, 1969). Nevertheless, this did not create a break-through of the mechanization of fertilizer application. Reasons for this were its poor capacity, higher costs compared with hand-labour, irregular distribution of the fertilizer in the beginning, and the fact that cleaning of the machines was difficult. Important was the fact that 'with fertilizer distributors only good results can be obtained if granular fertilizers are available' (FISCHER, 1910). Between the first and second world wars, new distributor systems were developed such as the reciprocating plate type distributor and the very important plate and flicker type distributor. In general, the latter system showed less problems when using coarse granules, just like the reciprocating plate and worm type distributor. These compared with those systems where metering was regulated by a dosage cleft, as was the case with the fluted roller feed distributors, the endless chain type distributors, and the agitator feed type distributors. In addition, they were more suitable for the application of hygroscopic materials and employment under relatively wet conditions (KRUTIKOW et al., 1955; LORENZ and MATHES, 1955).

After 1955, the use on a practical scale of distributors of the spinning disc and pendulum type became important in the Netherlands (Table 2.1). According to their working principle they belong to the group of variable bout width distributors (see Fig. 2.3). In this publication they will be included in the group called 'fertilizer broadcasters'. In the U.K. their development started at an earlier time as

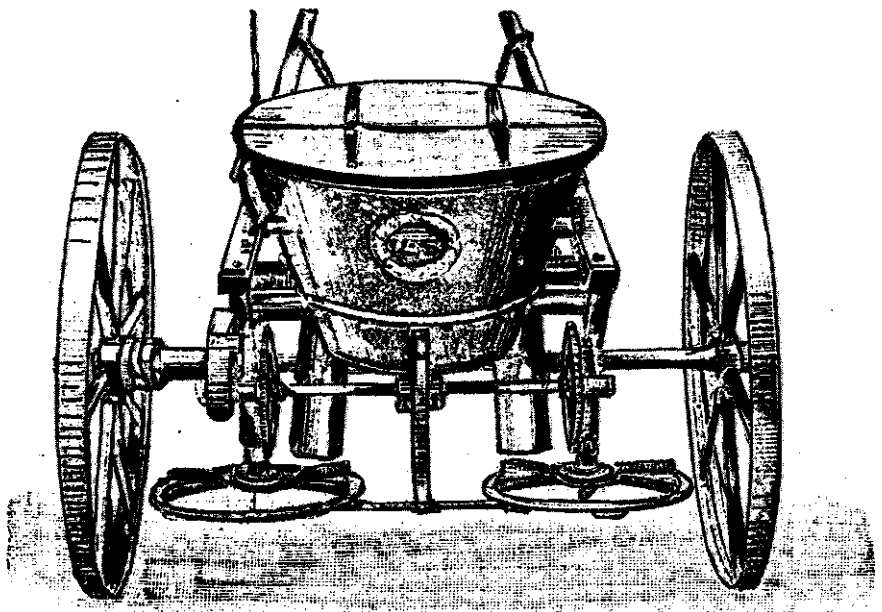


FIG. 2.4. Fertilizer broadcaster in the year 1919 with two spinning discs.

is indicated by the various types which were already shown at the so-called Smithfieldshow in 1955 (SPIJKERMAN, 1956). In 1960 the percentage of fertilizer broadcasters was about 27% in the Netherlands. By 1965 this percentage increased to almost 75%. In the German Federal Republic the same developments were noticed: in 1960 about 25% of the 40,000 fertilizer distributors sold belonged to the above-mentioned types.

In the beginning, people were sceptical about this new spreading equipment. The mostly unknown effects of the physical properties of fertilizer, negative influences due to wind, driving speed, and working width on the evenness of distribution often caused unexpectedly disappointing results. Besides that, the absence of spreading tables and failing data of the many specific properties and possibilities of the machines caused troubles. However, the simplicity of the construction and the relatively low costs of purchase compared to fixed bout width distribution systems (as the plate and flicker type distributors), together with the greater working width, opened possibilities.

In agriculture the principle of distributing materials by means of spinning discs was already used at the beginning of the 20th century (EYTH, 1906). In Canada such distributor systems were used for broadcast sowing of cereals giving the possibility of obtaining large working widths. In 1885 in Germany a fertilizer distributor with a horizontal disc and a great number of vanes was patented. The results of the first tests, however, were negative (BRUTSCHKE, 1900). The evenness of distribution was bad, due to the fact that there was a lack of knowledge about the right arrangement of the supply of the material to the disc. At that time a central supply along the whole circumference of the disc was used. As a result of this, the transverse distribution pattern showed two peaks as the material was distributed over a small circular strip. Due to the fine materials used, and because of air resistance, working widths of no greater than 3 or 4 m were obtained. The use of spreaders of the broadcast system remained limited to the application of lime, although already in 1919 in the Netherlands a fertilizer broadcaster with two spinning discs was for sale (Fig. 2.4).

The production of granular fertilizers, together with the fundamental and extensive studies of the behaviour of particles on rotating discs equipped with vanes, was most important for the introduction of the spinning disc fertilizer broadcasters.

Finally we may note that the increase of motorization in agriculture provided the opportunity of using the tractor p.t.o.. In this way, variable working width (as it was caused by variations in driving speed) could be decreased. The fact that this was more or less a real problem in practice with horse drawn types, can be illustrated by the fact that in England a broadcaster was developed which had a disc driven by a small engine (SPIJKERMAN, 1956).

## 2.5. THE RECIPROCATING SPROUT OR PENDULUM SYSTEM

Compared to spinning disc types, development of broadcasters with an oscillating distributor device is of a more recent date.

The development of the broadcaster used in this study started with an application for patent by Steffenino and Fassone on the May 14, 1954 (Italian patent 516291). The patent was for a broadcaster with an oscillating sprout, mounted to a bowl. The broadcaster was wheel-driven and a horizontally oscillatory motion was obtained by means of a crank connecting rod (Fig. 2.5). The angle of oscillation was adjustable by changing the length of the crank. This method of driving resulted in an asymmetrical pattern of velocity and acceleration. The characteristic of the system can be described as complex sine and cosine functions (PELLIZZI, 1958; QUAST, 1971).

In 1956 Steffenino designed a mounted broadcaster which was p.t.o.-driven. At the end of the sprout there were two grooves, and there was a spring construction in the crank to obtain smoother movement of the sprout. Metering was done by adjustable shutters which were fixed to the bowl. In the centre of the orifice of the sprout, a vertical strip was placed to improve the transverse distribution pattern.

During a Verona agricultural machinery exhibition, Mr. J. Vissers of Vicon Ltd. contacted Steffenino and Fassone, and obtained a licence for production of the broadcaster for all countries in the world except Italy. The broadcaster was presented under the name of 'Spandicar' (ANON., 1958).

The shape of the transverse distribution pattern was based on fixed bout width distributors: trapezoidally, with steep slopes (TAMBOER, 1976). It was hoped that problems of overlapping could be reduced to a minimum with this pattern, since the working width could be indicated rather accurately. However, the optimum ratio of overlapping was difficult to determine in practice. In addition, a deviation from the optimum ratio of overlap resulted in a high rate of unevenness of the

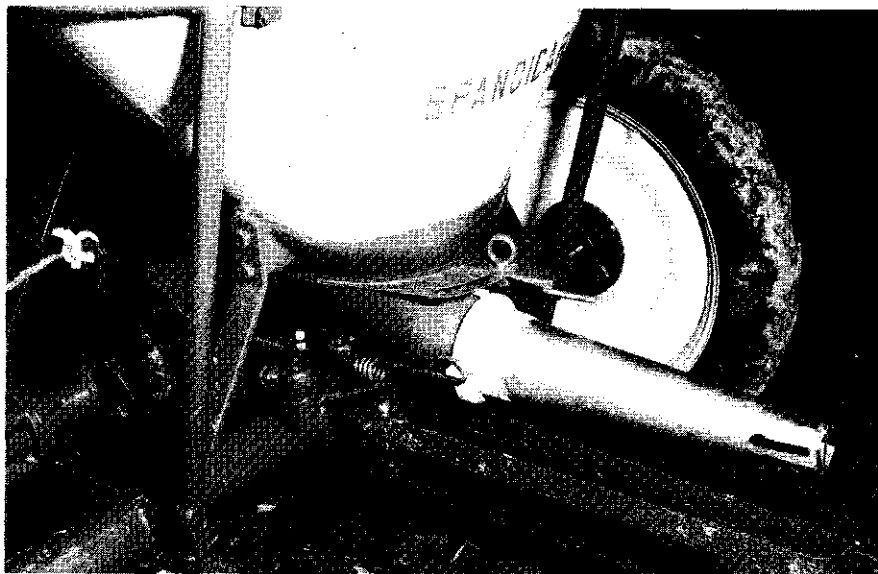


FIG. 2.5. Wheel-driven reciprocating sprout broadcaster (about the year 1958); the oscillatory motion of the sprout is obtained by means of a crank connecting rod mechanism.



transverse distribution pattern. With spinning disc broadcasters, the sides of the distribution pattern were less steep and as a consequence the latter had an advantage in practice.

Development and improvement of the reciprocating sprout fertilizer broadcaster continued with more than forty applications for patents (PESCHIER, 1974). Some important improvements in design can be mentioned. Until 1959 the crank connecting rod had been used as a driving mechanism. The asymmetry of sprout movement mentioned above acted in a negative way upon the distribution pattern. To avoid this, the vertical strip was arranged asymmetrically in the orifice. In addition, holes on one side of the sprout became smaller.

In the year 1959 two important changes in design were introduced: a forked connection between flywheel and oscillating bowl resulted in a symmetrical movement of the sprout, and at the end of the sprout a horizontal bow had been attached. Until then the typical two-peak transverse distribution pattern was a serious problem especially with granular fertilizers (CASELLA, 1956). Following these improvements, caking of fertilizer was prevented by the placement of a rubber lining inside the sprout (1960 and 1965) and, special attention was paid to the design of the metering devices allowing greater accuracy with positioning and dimensioning. Originally the shutters for the setting of the application rate were fixed to the oscillating bowl; for this reason, a more complex construction of the metering devices was required. In 1970, a new design placed the shutters between the hopper and the bowl and connected them to the fixed frame. For the mounted types of broadcasters, the frame was designed in such a way that unwanted vibrations were reduced to a minimum. Further improvements included the bearings of the crank in the flywheel (1971), the introduction of polyester hoppers and sprouts (1972), and the placement of a counterweight in the flywheel (1972).

Production of drawn broadcasters having hoppers with a greater capacity started at the beginning of 1960. An even supply of the fertilizer to the metering and distributor devices was obtained by auger constructions (single and double augers at the bottom of the hopper, floating augers on top of the fertilizer mass).

The construction of the bow and its relation to the design of the orifice of the sprout has had continuing interest. It appeared that changing other parts of the distributor device mostly required a mutual adaption of both the design of the bow and orifice.

The 1978 design enables three ranges of spreading width by changing the angle of oscillation of the sprout.

During the period 1956–1960 about 15,000 broadcasters were produced. Since 1960 the average yearly production of broadcasters of the mounted types is about 30,000 (GESCHIERE, 1976). The average yearly production of the types with a hopper capacity of more than  $1 \text{ m}^3$  is about 1,970. At this time reciprocating sprout fertilizer broadcasters are sold in more than 75 countries with Europe as the most important market.

## 2.6. STANDARDS FOR THE REVIEW OF FERTILIZER DISTRIBUTORS

The review of possibilities for distribution of fertilizer broadcasters of the spinning disc and pendulum system is based upon the following aspects: capacity and labour demand, physical load of men, and quality of the distribution pattern.

### 2.6.1. Capacity and labour demand

Several work methods are available for the distribution of mineral fertilizers (SCHAAFSTAL and DE LINT, 1973). Throughout the year, a relatively small part of the total labour available is needed for fertilizing.

For grassland in the Netherlands, the period when nitrogen fertilizing can be performed generally extends from the second half of February until the beginning of April. There are exceptions due to climatical circumstances and designated use of the land, i.e. pasturing or forage harvesting (OOSTENDORP, 1964; JAGTENBERG, 1966; VAN BURG, 1968).

In arable farming it is important that fertilizers are applied within a short period. The net number of available hours for the application of N fertilizers depends on the duration of this period, which is determined by the specific requirements for growth of the crops. In addition, the percentage of workable hours within such a period has to be taken into account (VAN DEN BERG, 1970).

The duration of the fertilizing period is determined by specific stages of development of the crops, such as 'date of the start of growth' (colza, winter cereals) and 'date of the start of sowing' (spring cereals). On the other hand, the 'date of the start of flowering - 10' (colza), the date of reaching stage 4 according to Feekes (beginning of the rise of the pseudo-stem for winter cereals), the date of reaching of stage 2 for spring cereals (starting of the stool) limits this period. A combination of functional relationships between the duration of the application period as it is determined by the development of growing, the available days with workable weather, and the fraction of workable hours per day, results in the net number of workable hours which are available for the performance of fertilizing

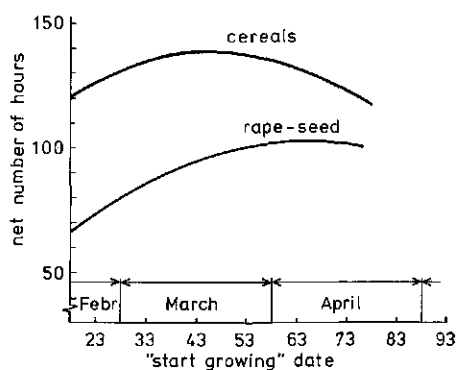


FIG. 2.6. Net number of hours available for N application depending on the 'start growing date' of cereals and rape-seed. (According to VAN DEN BERG, 1970.)

TABLE 2.2 Comparison between task times for the application of a one-man method for loading, transport, and spreading of sacked fertilizer (A); and loading, transport, and spreading of bulk fertilizer (B). Farm trailers are used for transport. (According to SCHAAFFSTAL and DE LINT, 1973.)

Boat width (m) · working speed (km h <sup>-1</sup> )	Number of transports per plot	Distance plot- storage	Task times (A) and differences between task times (B-A) in mh ha <sup>-1</sup> at a plot width of 100 m and a length (m) of											
			100		200		300		400		600			
			A	B-A	A	B-A	A	B-A	A	B-A	A	B-A		
24	1	0.5	2.15	+0.17	1.45	0.00	1.22	-0.07	1.22	-0.20	1.05	-0.13		
		1.0	2.24	+0.36	1.50	+0.10	1.25	0.00	1.24	-0.14	1.08	-0.10		
	2	0.5	1.54	+0.03	1.54	+0.03	1.28	-0.05	1.26	-0.15	1.10	-0.10		
		1.0	1.63	+0.14	1.63	+0.14	1.34	+0.01	1.31	-0.13	1.13	-0.08		
48	1	0.5	1.65	+0.20	1.10	-0.01	0.91	-0.07	0.82	-0.12	0.78	-0.20		
		1.0	1.74	+0.39	1.15	+0.09	0.94	0.00	0.84	-0.04	0.81	-0.17		
	2	0.5	1.19	+0.02	1.19	+0.02	0.97	-0.05	0.86	-0.05	0.83	-0.17		
		1.0	1.28	+0.12	1.28	+0.12	1.06	-0.02	0.91	-0.03	0.86	-0.15		
72	1	0.5	1.47	+0.19	0.99	-0.02	0.81	-0.08	0.72	-0.11	0.63	-0.14		
		1.0	1.56	+0.38	1.04	+0.08	0.84	-0.01	0.74	-0.03	0.65	-0.10		
	2	0.5	1.08	+0.01	1.08	+0.01	0.87	-0.06	0.76	-0.04	0.66	-0.09		
		1.0	1.17	+0.11	1.17	+0.11	0.93	0.00	0.81	-0.02	0.69	-0.07		
96	1	0.5	1.43	+0.13	0.95	-0.03	0.77	-0.08	0.68	-0.11	0.59	-0.14		
		1.0	1.52	+0.32	1.00	+0.07	0.80	-0.01	0.70	-0.03	0.61	-0.10		
	2	0.5	1.04	0.00	1.04	0.00	0.83	-0.06	0.72	-0.04	0.62	-0.09		
		1.0	1.13	+0.10	1.13	+0.10	0.89	0.00	0.77	-0.02	0.65	-0.07		

Additional specifications: Application rate: 500 kg ha<sup>-1</sup>; sacked fertilizer in building; bulk fertilizer in silo; 2 passes per hopper; loading in (high-level) tipping trailers. Driving speeds: on farmyard 4 km h<sup>-1</sup>, on field road 12 km h<sup>-1</sup>, and on the plot 6 km h<sup>-1</sup>.

(Fig. 2.6; VAN DEN BERG, 1970). Generally the optimal period has a duration of about 14 days starting from the date of 'the start of growth' (SELKE, 1965; JÜRGENS, 1971; ISENSEE, 1973).

As a result, the need to fertilize may be in competition with other field operations such as seedbed preparation, sowing, and crop protection. For this

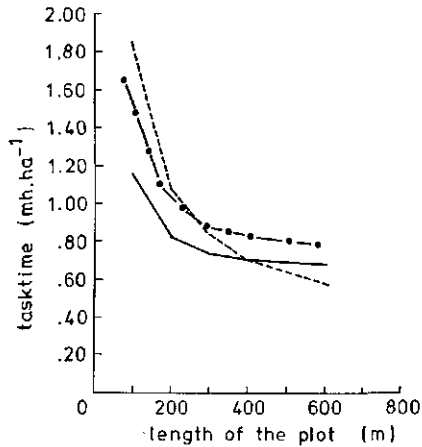


FIG. 2.7. Task time as a function of plot length for some transport methods of bulk and sacked fertilizers. ●—●: farm trailer and sacked fertilizer, ---: farm trailer and bulk fertilizer, —: distributor used for transport. Additional specifications; application rate:  $500 \text{ kg ha}^{-1}$ , bout width: 8 m, working speed:  $6 \text{ km h}^{-1}$ , 1 transport per plot (farm trailer), 1 transport per ha (distributor), distance plot-storage: 500 m, plot width: 100 m.

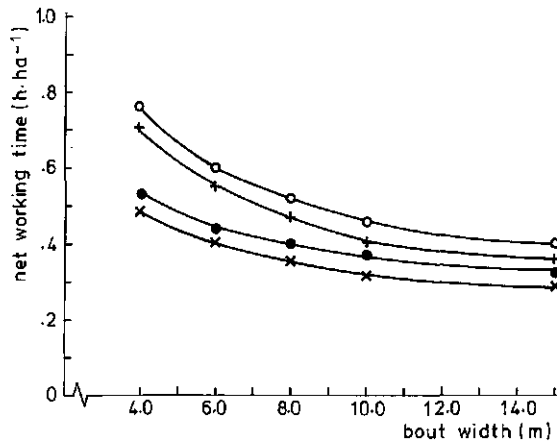


FIG. 2.8. Relationship between net working time and bout width, depending on working speed and hopper content. ○—○:  $6 \text{ km h}^{-1}$ , 400 kg; +—+:  $6 \text{ km h}^{-1}$ , 2000 kg; ●—●:  $12 \text{ km h}^{-1}$ , 400 kg; ×—×:  $12 \text{ km h}^{-1}$ , 2000 kg. Additional specifications: plot size  $100 \times 200 \text{ m}$ , application rate  $600 \text{ kg ha}^{-1}$ .

TABLE 2.3. Net working time for bulk fertilizer application with a spinning disc broadcaster, depending on driving speed, bout width, application rate, hopper content, and size of the plot.

plot size	Net working time (h ha <sup>-1</sup> )						Net working time (h ha <sup>-1</sup> )					
	100 x 200 m			2000 kg			400 kg			2000 kg		
	200	600	1000	200	600	1000	200	600	1000	200	600	1000
hopper content												
application rate (kg ha <sup>-1</sup> )												
driving speed (km h <sup>-1</sup> )												
bout width (m)												
4	0.95	1.01	1.07	0.95	0.97	1.07	0.88	0.94	0.96	0.87	0.90	0.92
6	0.68	0.76	0.84	0.68	0.70	0.72	0.65	0.71	0.73	0.64	0.67	0.69
8	0.59	0.65	0.72	0.59	0.61	0.63	0.53	0.59	0.61	0.52	0.55	0.57
12	0.47	0.53	0.61	0.47	0.49	0.51	0.42	0.48	0.50	0.41	0.44	0.46
4	0.68	0.76	0.87	0.68	0.70	0.72	0.64	0.72	0.74	0.63	0.66	0.68
6	0.53	0.60	0.71	0.53	0.55	0.57	0.49	0.57	0.59	0.48	0.51	0.53
8	0.46	0.52	0.63	0.46	0.48	0.50	0.41	0.49	0.51	0.40	0.43	0.45
12	0.38	0.44	0.55	0.38	0.40	0.42	0.33	0.41	0.43	0.32	0.35	0.37
4	0.57	0.64	0.72	0.57	0.59	0.61	0.53	0.58	-	0.51	0.54	0.57
6	0.45	0.52	0.60	0.45	0.47	0.49	0.42	0.47	-	0.40	0.43	0.46
8	0.39	0.46	0.54	0.39	0.41	0.43	0.36	0.41	-	0.34	0.37	0.40
12	0.33	0.40	0.48	0.33	0.35	0.37	0.30	0.35	-	0.28	0.31	0.34
4	0.48	0.56	0.58	0.48	0.50	0.52	0.45	-	-	0.44	0.47	0.49
6	0.38	0.46	0.48	0.38	0.40	0.42	0.36	-	-	0.35	0.38	0.40
8	0.33	0.41	0.43	0.33	0.35	0.37	0.32	-	-	0.31	0.34	0.36
12	0.29	0.37	0.39	0.29	0.31	0.33	0.27	-	-	0.26	0.29	0.31
4	0.42	0.48	0.64*	0.42	0.44	0.46	0.38	-	-	0.35	0.38	0.42
6	0.34	0.40	0.54*	0.34	0.36	0.38	0.32	-	-	0.29	0.32	0.36
8	0.31	0.37	0.51*	0.31	0.33	0.35	0.29	-	-	0.26	0.29	0.33
12	0.27	0.33	0.47*	0.27	0.29	0.31	0.26	-	-	0.23	0.26	0.30

\*: one pass.

reason, the labour demand for different fertilizing work methods must be examined in more detail.

The application of bulk and sacked fertilizers can be distinguished in a systems analysis. Besides a decrease of physical load (2.3.2), the application of bulk fertilizers can save labour (Table 2.2). This advantage is obtained if the size of a plot is more than 3 hectares. If the application rate increases to more than 500 kg per hectare the advantages of bulk application increases even more (correction of task times for sacked fertilizer: + 0.05 manhours per hectare per 100 kg of increase of application rate; correction for bulk fertilizer: + 0.008 manhours per hectare per 100 kg). When lengths of the plot exceed 300 m, tipping trailers or the distributor itself can be used for transport of the fertilizer from storage to the plot as this enables a savings in labour demand. The hopper content must be at least 500 kg in this case. For plot lengths smaller than 300 m, the use of bulk fertilizers only results in a savings of labour demand if the distributor is used for transport too (Fig. 2.7).

Net working time is influenced by the size of the plot, the application rate, and distribution-dependent variables such as: driving speed, working width, and hopper content (Table 2.3).

Task times decrease with increased forward speed, hopper content, and working width (Fig. 2.8). The larger the values of these factors, the smaller the decrease in labour demand.

#### 2.6.2. *Work load*

Mechanization in relation to fertilizer application has contributed to a decrease of work load. Mechanization of the distribution process itself and the introduction of methods with optimal work load have acted positively.

Based on studies of energy consumption, the jobs of hand-spreading and application by means of a horse-drawn fixed bout width distributor can be described as moderately heavy tasks (VAN LOON, 1959; ZANDER, 1972). During handspreading on a harrowed even field, net energy consumptions of 22.7–23.9 kJ min<sup>-1</sup> were measured (WIRTHS, 1956). The greater part of energy was spent on walking. As a result, such a heavy load must be alternated with frequent periods of rest. The application by tractor with a fixed bout width distributor reduced the net energy consumption to 5.6 kJ min<sup>-1</sup> (WIRTHS, 1956); and in addition pulse-rate was at an almost constant and acceptable level (VAN LOON, 1959). Although recent data for energy consumption for the combination tractor-variable bout width broadcasters are not available, we may expect that they will show fair agreement with the system of tractor-fixed bout width distributors.

Energy consumption during handling of fertilizers on a farm depends on bulk or sack handling. Comparative method-studies show that for the 'traditional' method (including i.e.: supplies in sacks of 50 kg, unloaded from a trailer by hand, and stored in 12–13 layers; transportation to the plot, and filling of the hopper) a net energy consumption of 65.9 kJ per 100 kg has been recorded. This is the sum for both truckdriver and farmer.

When using bulk fertilizers, allowing transport by tipping trailers and storage in

bulk on the farm savings in energy consumption of 25–35% can be obtained (SPOELSTRA, 1973). Loading of the transport equipment in a further stage has to be done by a tractor-loader. An equivalent method is bulk transport and storage in silos or the use of tipping trailers and buffering on the plot.

The handling by hand, especially, of sacked fertilizer on a farm has to be considered a moderately heavy or even heavy task. During loading and unloading the net energy consumption varies from 19.3 to 22.2 kJ min<sup>-1</sup> or from 14.5 to 16.6 kJ per 100 kg handled product (WIRTHS, 1956). It may be further noted that the application of trolleys can reduce the work load to an acceptable level of 120–125 heartbeats per minute (ZANDER, 1972; ISENSEE, 1973).

### 2.6.3. *Evenness of distribution*

The characterization of the evenness of distribution, its norms, coefficients of irregularity, and its effects on crop yield will be discussed extensively in chapter 3.

However, in this section we will give a brief description of the improved qualities in the distribution pattern in the framework of the continuing progress in design of the equipment.

Evenness in fertilizer distribution by hand depends on the skill of the worker. When hand-spreading is accurately performed, a minimum value of the coefficient of variation (*C.V.*; see also chapter 3) of 16% can be obtained. This value is based upon measurement of the amounts collected from areas of 0.5 m<sup>2</sup> (PRUMMEL and DATEMA, 1962). Under practical conditions a mean value of *C.V.* of 26% was measured with extremes of 17–34%. RÜHLE (1975) presents similar values for *C.V.*: 25% for the longitudinal distribution pattern, and 22% for the transverse distribution pattern. Spreading by hand from a farm trailer generally results in a worse distribution (mean value of *C.V.*: 38%).

As was mentioned before, the more fundamental research of the fertilizer distribution process started at the beginning of the sixties. At that time the plate and flicker type distributors performed the best (mean values of *C.V.*: 22%; extreme values: 12–45%). With the spinning disc fertilizer broadcasters a mean value of *C.V.* of 33% (extremes: 12–64%) could be obtained. With the reciprocating sprout broadcaster the results were relatively poor: mean value of *C.V.* of 47% with extremes from 11–97% (PRUMMEL and DATEMA, 1962). Obviously, as was pointed out in section 2.2.3, the more critical ratio of overlap played a negative role in the use of this last type of broadcaster.

Evenness of the longitudinal distribution pattern of fixed bout width fertilizer distributors is influenced negatively by vibrations or bumps caused when crossing tractor or equipment wheel tracks. Variable bout width broadcasters often provide a relatively better longitudinal distribution pattern. Values of *C.V.* of 3.5–7% can be obtained (HERPERD and PASCAL, 1959; PRUMMEL et al., 1959; PRUMMEL and DATEMA, 1962; ANON., 1974; RÜHLE, 1975). Design properties, (e.g. the use of chain distributors, bad placement of the metering devices, caking of the fertilizer on the distributor device, and abrasion) can cause an asymmetric transverse distribution (HOOGLAND, 1955; MARKS, 1963).

In Germany, research work about evenness of distribution of fixed bout width

distributors tends to show the same results as given by PRUMMEL and DATEMA. Depending on type and construction, coefficients of variation of 13 to 32% can be obtained (LORENZ, 1954). Lower values for *C.V.* (4–10%) are given by MARKS (1963).

Reports from the National Institute of Agricultural Engineering in the U.K. (1965), in which the results of tests with 16 variable bout width broadcasters are given, show the following: when used at the correct ratio of overlap, 11 broadcasters did not exceed a value of *C.V.* 15%. With seven machines, a value of *C.V.* 11% could be obtained. This tendency to improved evenness of distribution is confirmed by later trials in practice in which values of 10–15% were not exceptional (GREEN, 1968).

It can be concluded, therefore, that with advanced technical development, evenness of transverse distribution has increased remarkably. The value of *C.V.* can be reduced to 4–10%. However, in practice values of *C.V.* of 100% are still found (ISENSEE, 1973; RÜHLE, 1975). In the beginning of 1970 yield losses due to deviations from optimal evenness in distribution were still estimated at 3% of the potential yield when applying N fertilizer, and at 1% when spreading P and K fertilizers with variable bout width broadcasters (ISENSEE, 1973). Comparative machinery tests contributed to continuous quality control and indirectly to further improvement of distribution properties (ANON., 1967; ANON., 1972).



### 3. DESCRIPTION AND INTERPRETATION OF THE DISTRIBUTION PATTERN OF THE RECIPROCATING SPROUT FERTILIZER BROADCASTER

#### 3.1. INTRODUCTION

The application of fertilizer can be defined as a dynamic process limited by the static terms dosage or application rate on one hand, and distribution pattern on the other. Both of the static terms can be expressed by means of amounts of weight per surface-unit. The dynamic character of the spreading process includes the terms metering and distributing. Metering is the process of discharging an amount of fertilizer out of the hopper per unit of time (e.g.  $\text{kg s}^{-1}$ ); distributing is the process of supplying a certain area with an amount of fertilizer ( $\text{kg m}^{-2}$ ). The area is the product of working width and forward speed.

The distribution pattern represents the amount of fertilizer which is gained on a plot of a relevant size. A section of the distribution pattern, according to a coordinate parallel to the direction of movement of the distributor, results in the longitudinal distribution pattern. Likewise, a section according to a coordinate perpendicular to the direction of movement results in the transverse

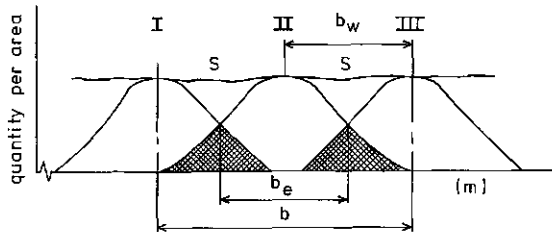


FIG. 3.1. Transverse section of the distribution pattern. I/III: basic transverse distribution patterns, S: compound pattern,  $b_w$ ,  $b_e$ : bout width or effective spreading width,  $b$ : spreading width.

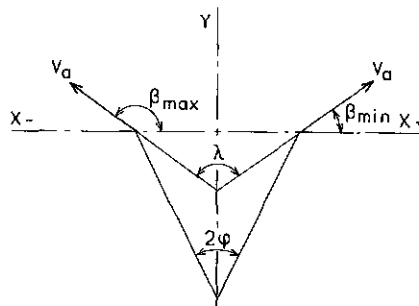


FIG. 3.2. Angle of dispatch or outlet  $\beta$ , and spreading angle  $\lambda$ ;  $\phi$ : oscillation angle,  $V_a$ : absolute particle velocity of outlet or dispatch (stationary situation).

distribution pattern. In practice, this transverse distribution pattern is the result of a partial overlap of basic distribution patterns (Fig. 3.1).

The single or basic distribution pattern can be considered a transverse section of the distribution pattern from which the amount of fertilizer is collected after one passing.

The distribution or spreading width is determined by the maximum trajectory of flow of the particles and the value of the so-called spreading angle. Of the reciprocating sprout broadcaster this value is derived from the difference in the maximum and minimum values of the angles of outlet. They are determined by the angle between the direction of the absolute particle velocity of outlet and the positive  $X$ -coordinate. Depending on the distributor system used, and due to the necessary ratio of overlap, the effective spreading width or working width ( $b_e$ ) is smaller than the spreading width ( $b$ ). The ratio of overlap ( $O$ ) which is determined by consideration of two neighbouring transverse basic patterns, is derived from:

$$O = (b - b_e)/b \quad (3.1)$$

In theory, an absolutely even transverse distribution pattern is obtained when triangular or trapezoidal distribution patterns are created, with the shapes being half overlapped. Deviations from the optimum ratio of overlap or from the optimum working width have a more negative influence when the slopes of the distribution patterns are steeper (OEHRING, 1964; DOBLER and FLATOW, 1969; PAPTHEODOSSIOU, 1970; BERRY, 1970).

In practice the longitudinal, as well as the transverse distribution pattern, will show a certain rate of unevenness. Several coefficients of irregularity are available for its characterization.

## 3.2. DESCRIPTION OF THE EVENNESS OF THE DISTRIBUTION PATTERN

### 3.2.1. Choice of sampling area

A basis for the calculation of evenness of fertilizer distribution is found in the amount of fertilizer which is obtained from relevant areas of equal size. This relevancy includes the question, within what size of area the evenness of distribution of broadcasted fertilizer can be considered to be indifferent with respect to potential yield. First of all, this can be considered a fertilizing-technical problem. From an agricultural engineering point of view, it is of further importance that calculations of the several coefficients of irregularity are based on a standardized area as this enables a comparison between the results of various research work.

From the investigations of ELLEN (1973), the conclusion can be drawn that the value of the coefficient of variation depends on the size of the area. This statement is supported by the work of BRÜBACH (1969). From his investigations the following conclusions can be drawn. When using trays with a width of 0.10, 0.20, 0.30, and 0.40 m, the minimum value for the coefficient of variation was

found for a similar ratio of overlap of 0.40. The minimum value of the coefficient of variation decreased from 8 to 5% when increasing the width of the trays from 0.10 to 0.40 m. Increase of width to 0.50 m resulted in a different ratio of overlap (0.33) and a coefficient of variation of 7.5%.

Discussions about a standardized size of area as a basis for calculation of evenness of distribution have had a rather long history. In the year 1931 the introduction of an area of  $0.2 \times 0.2$  m as a standard was proposed by Von Müller. This proposal was based on the idea that the action of soil moisture was neglectable with respect to redistribution of fertilizer. Character, size and development of the root system of the crop and its importance for the leveling of unevenly fertilized neighbouring areas were not taken into consideration (HEYDE, 1957).

However, research by VAN DER PAAUW (1940) and ZSCHUPPE (1968) indicated a necessary difference between the consequences of uneven distribution within a short distance (0.5 m) and uneven distribution due to irregularities extending over relatively long distances. Character and size of the crop root system were important. It was stated that potatoes, having an extensive and relatively flat root system, were able to perform a nutrient uptake from locations at a distance of more than 0.5 m from the plant.

Within this context we want to make the remark that soil cultivations during the growing season such as ridging and mechanical weed control, can also contribute to a redistribution of the fertilizer. This effect is more important with increasing row widths.

Crops like oats which have a relatively less extensive root system in the horizontal plane are more affected by uneven distribution of fertilizer. Uneven distribution of nitrogen extending over distances of 0.25 m resulted in yield losses (VAN DER PAAUW, 1940). Unevenness in N fertilizer distribution over distances of 0.083 m resulted in an irregular start of growing, although this was compensated during the growing season. Research performed in England during the same period showed that for winter wheat, such unevenness in distribution of nitrogen over a distance of 0.25 m did not affect crop yield in a negative way (WEST et al., 1940). This antithesis may be explained by the differences in root development as well as the longer growing season.

When applying nitrogen on winter rye, ZSCHUPPE (1968) concluded from his field trials that unevenness in distribution on differently fertilized subplots of  $0.5 \times 0.5$  m hardly influenced yield in a negative way. For this reason the cited author defeated the  $0.2 \times 0.2$  m standard for investigation of unevenness.

The final conclusion can be drawn that there are a few figures available, based on plant growing experiments which can contribute to the creation of a standard for judging the unevenness of fertilizer distributions.

In practical engineering terms a subdivision of the collecting trays with a width of 0.5 m seems to be justifiable. If more detailed information has to be obtained, a further subdivision (e.g. to a tray width of 0.25 m) can be favourable as the value of the coefficient of variation will tend towards a higher level. The

effects of minor changes in design of the fertilizer distributor or changes in physical properties of fertilizer can especially be examined more carefully as extremes will appear more clearly.

In the Standard Testing Procedure for Fertiliser Distributors of the ORGANIZATION for ECONOMIC COOPERATION and DEVELOPMENT (1967) a maximum collecting tray width of 0.5 m is recommended for fertilizer broadcasters, and one of 0.25 m is recommended for fixed bout width distributors. Narrow trays may be used provided that the width is a simple fraction of 0.50 (or 0.25) m. The collecting trays should be at least 0.10 m deep and, as much as possible, steps should be taken to prevent particles from ricocheting out of the trays. No tray should have an area less than 0.25 m<sup>2</sup>.

### 3.2.2. Coefficients of irregularity

The evenness of distribution of fertilizer can be described in various ways (SPEELMAN, 1972). The suitability of some coefficients of irregularity for the description of the evenness of fertilizer distribution was examined by HOLLMANN and MATHES (1962).

In the next section some coefficients will be discussed:

a. The difference between the two most extreme values of the compound transverse distribution pattern in ratio to the mean value:

$$v = \frac{x_{max} - x_{min}}{\bar{x}} \quad (3.2)$$

In this expression  $x_{max}$  and  $x_{min}$  represent the greatest and smallest amount of fertilizer in a certain tray;  $\bar{x}$  represents the mean value per tray in the compound distribution pattern.

Due to the fact that the review of the distribution pattern of variable bout width distributors is based on a large number of observations (20–80), the coefficient mentioned above is less suitable for this purpose (WEBER, 1957).

The same is true for a coefficient of irregularity used by PRUMMEL et al. (1959) and HOOGLAND (1955). Evenness of distribution was calculated by adding the deviations downwards and upwards, expressed as percentages of the mean.

b. The mean value of the total of absolute deviations from the mean expressed as a percentage of the arithmetical mean. This coefficient is sometimes called linear deviation from the mean and it is expressed as a percentage (RÜHLE, 1975).

Its value is expressed by:

$$\bar{d} = \frac{100 \cdot \sum_{i=1}^n |x_i - \bar{x}|}{n \cdot \bar{x}} \quad (3.3)$$

The use of  $\bar{d}$  as a coefficient of irregularity is limited by the fact that when using a large number of trays ( $n$ ), which is usually the case when testing fertilizer broadcasters, a leveling of differences between distribution patterns may occur. Several relatively small deviations may lead to a similar value as some few relatively great deviations; the negative influences of the latter, however, are much more unfavourable.

c. The coefficient of variation expressing the ratio between the square root out of the variance and the mean:

$$C.V. = \frac{100}{\bar{x}} \cdot \left\{ \frac{\sum_{i=1}^n (x_i - \bar{x})^2}{n-1} \right\}^{1/2} \quad (3.4)$$

As the coefficient of variation depends on squaring of the individual deviations, its application is recommended if a large number of trays (> 50) are used, or if characteristic extreme values in the distribution pattern are expected.

In literature (CASELLA, 1956/57; PRUMMEL and DATEMA, 1962; MATHES and PREISBERG, 1967; ZSCHUPPE, 1967, 1968; HOLMES, 1968; BRÜBACH, 1969; GASPARETTO, 1969; BERRY, 1970; REED and WACKER, 1970; DAVIS, 1971; HEYMANN et al., 1971; DAVIES, 1972; GÖHLICH and KESTEN, 1972; GLOVER and BAIRD, 1973; RÜHLE, 1975) the coefficient of variation is widely used in characterizing the evenness of the transverse distribution patterns of fertilizer broadcasters.

d. Especially for the description of evenness of the fertilizer distribution pattern a number of irregularity was developed by BUREMA (1968, 1970). The basic thought behind this number was that extreme values in the distribution pattern should be indicated clearly. For this reason the number of irregularity  $R$  depends on both the mean value ( $\bar{d}$ ), as described under b, as well as on the maximum deviation from the arithmetical mean. The value of the latter is calculated according to:

$$d_{max} = \frac{|x_{extr} - \bar{x}|}{\bar{x}} \cdot 100 \quad (3.5)$$

With the aid of (3.3) and (3.5), Burema's number of irregularity  $R$  now is defined in its general form by:

$$R = c \cdot \left\{ \left( \frac{\bar{d}}{a} \right)^k + \left( \frac{d_{max}}{b} \right)^k \right\}^{1/j} \quad (3.6)$$

For fixed values of  $c, j$  and  $k$  the relation between  $R, \bar{d}/a$  and  $d_{max}/b$  can be given in nomograms. If  $\bar{d}/a$  and  $d_{max}/b$  are plotted linearly along the  $y$ - and  $x$ -coordinate, respectively the level lines for  $R$  will appear as curves in the plane. By providing the coordinates with a double scale gradation (assigning values to  $a$  and  $b$ ) these nomograms also show the relation between  $R, \bar{d}$  and  $d_{max}$ . At increasing values of  $k$ , the curves for the  $R$  values become more angular as the shape of the  $R$  curve is determined by the value of  $k$ . For  $j = k$  the  $R$  curves are equidistant, since the value of  $j$  determines the scale gradation for the  $R$  curves system. For  $j = k = 8$  the shape of the  $R$  curves is such, that the horizontal and vertical part are almost equidistant to the  $x$ - and  $y$ -coordinate. In addition they tangent the level lines indicated by values of  $\bar{d}/a$  and  $d_{max}/b$ . When setting the linear scale enlargement factor  $c$  at 100, and adding values of 20 resp. 40 to  $a$  and  $b$ , Burema's number of irregularity can be expressed as:

$$R = 100 \cdot \left\{ \left( \frac{\bar{d}}{20} \right)^8 + \left( \frac{d_{max}}{40} \right)^8 \right\}^{1/8} \quad (3.7)$$

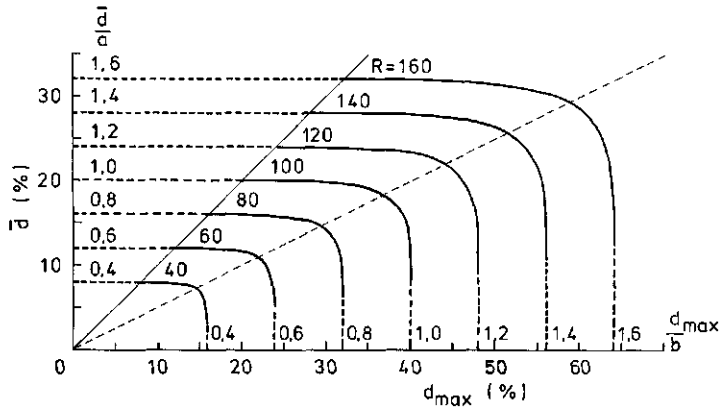


FIG. 3.3. Representation of Burema's number of irregularity  $R$ .

$$\text{Nomogram for } R=100 \left\{ \left( \frac{\bar{d}}{a} \right)^8 + \left( \frac{d_{\max}}{b} \right)^8 \right\}^{1/8}$$

(According to BUREMA, 1970.)

A nomogram for this expression is given in Fig. 3.3.

It has been proven that there is a mutual relation between the coefficients of irregularity mentioned under  $b$ ,  $c$  and  $d$ . It was indicated by HOLLMANN and MATHES (1962) that the ratio between  $\bar{d}$  and  $C.V.$  can reach a maximum value of 1. This is true if all individual deviations from the mean have the same value. Depending on the number and weight of the extremes, in practice the value of  $\bar{d}$  will be smaller than  $C.V.$  It was concluded by HOLLMANN and MATHES (1962) that the ratio between  $\bar{d}$  and  $C.V.$  for broadcasters reads:  $\bar{d}/C.V. = 1/1.1$ . As a consequence, only small extremes are to be expected in compound transverse distribution patterns. In a later report by RÜHLE (1975), a ratio between  $\bar{d}$  and  $C.V.$  of  $1/1.27$  was mentioned. It should be noted, however, that this figure was obtained from investigations of pneumatic fertilizer distributors. The tray width used by HOLLMANN and MATHES was 0.40 m. In RÜHLE'S work a tray width of 0.20 m was used, which enables a clearer demonstration of extremes.

Nevertheless, taking into account the above-mentioned considerations, it is possible to make a rough comparison between the results represented as  $\bar{d}$  and those represented as  $C.V.$

Based on a tray width of 0.5 m, the relation between Burema's number of irregularity and the coefficient of variation can be described by (ANON., 1976):

$$R = 5.05 \cdot C.V. + 0.96 \quad (3.8)$$

A comparison between the coefficients of irregularity mentioned under  $b$ ,  $c$  and  $d$  is shown in Fig. 3.4.

When testing the distribution patterns of fixed bout width distributors, for which the longitudinal evenness of distribution also must be taken into consideration, methods were described by LORENZ (1955) and MASCHE (1955).

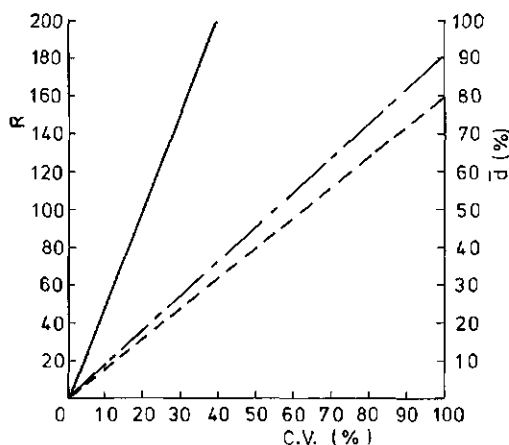


FIG. 3.4. Relationship between the coefficient of variation  $C.V.$ , Burema's number of irregularity  $R$ , and the linear deviation from the mean  $\bar{d}$  (—:  $R$ , ---:  $C.V./\bar{d} = 1.25$ , - · - ·:  $C.V./\bar{d} \approx 1.1$ ).

Analysis of variance and the  $t$ -test were used to determine the evenness of fertilizer distribution in transverse and longitudinal directions. Quality of fertilizer distribution by variable bout width distributors is mainly dependent on a compound transverse distribution pattern which is the result of a certain ratio of overlap of the single or basic pattern. For this reason the methods of LORENZ and MASCHE are less interesting.

Based on a Mitscherlich production law, HEYDE (1957) developed a method in which crop yields were compared for even and uneven fertilizer distribution patterns. The applied amount of fertilizer per area was transformed into relative yields according to:

$$y = A \cdot (a - 10^{-cx}) \quad (3.9)$$

in which  $y$  = yield;  $x$  = amount of fertilizer per area;  $A$  = maximum yield;  $c$  = proportion factor (for N:0.2;  $K_2O$ :0.4;  $P_2O_5$ :0.6).

The quality of the distribution pattern is expressed by a coefficient of irregularity  $W$ . Its value is found by determining the ratio between the mean of all  $y$  values as they arise from the individual amounts of fertilizer, and the  $y^*$  value as it arises from the mean amount of fertilizer  $x$  in the distribution pattern. The method of calculation is complex. In addition, a number of objections can be made against the use of this Mitscherlich production law as a standard (HOLLMANN and MATHES, 1962). One of the most important objections is the fact that depressions in yield can be frequently observed when the optimum fertilizer amount is exceeded. Due to interactions of growth factors, the proportion factors  $c$  are not constant. Contrary to Mitscherlich's statements, an absolute value of  $c$  has no general validity (VAN DIEST, 1971). The curve for  $W$  shows, under same conditions, a similar tendency to that of  $\bar{d}$  and  $C.V.$ , resulting in the same optimum working width. However, the difference between  $W$  values

representing sufficient and insufficient distribution patterns is small (LORENZ, 1957).

Until now no further investigations were performed to obtain more information about possible correlations between yield losses and other production functions (e.g. higher degree polynomials) and coefficients of irregularity.

### 3.3. THE TRANSVERSE DISTRIBUTION PATTERN

The compound transverse distribution pattern is the result of a certain ratio of overlap of the basic pattern. Evenness of distribution of a compound distribution pattern can be shown by means of diagrams. A certain coefficient of irregularity is plotted against working width. Based on a number of practical considerations it can be indicated which types of basic transverse distribution patterns result in acceptably even transverse distributions when choosing certain ratios of overlap.

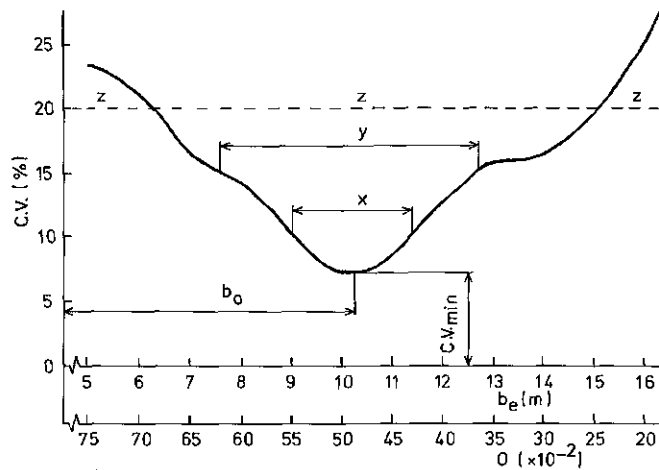


FIG. 3.5. Representation of a curve for the coefficient of variation  $C.V.$  depending on the ratio of overlap  $O$ , and the bout width  $b_e$ .

For example, in Fig. 3.5 the coefficient of variation is plotted against working width and ratio of overlap. With respect to the shape of  $C.V.$  the following standards can be handled in practice.

The general level of  $C.V.$  must be as low as possible. From a technical point of view, such a low level indicates the quality aspects of the broadcaster design. Furthermore it implies that the fertilizer is applied in an efficient and economical way, since rates of over- and underdoses are low.

The minimal value of  $C.V.$  must coincide with a value of the optimal working width  $b_o$ , which is as high as possible. In this way the capacity of the broadcaster is influenced favourably.



The curve of  $C.V.$  must have such a character that deviations from the optimum working width result in a minimum increase of the values for  $C.V.$  The possibility for variation in the ratio of overlap minimizes negative effects of unevenness due to variations from the set value of bout width. In practice, maintenance of a certain set value of working width is sometimes difficult, especially when no marking points are used.

Large relative deviations (57–132 %) from a set value of bout width can occur in practice. According to investigations by HANUSCH (1969), only one quarter of the tractor drivers involved, succeeded in realizing variations of less than 1 m from the set value of 8 m working width.

Based on the above-mentioned considerations, a distribution diagram as shown in Fig. 3.5 has to be qualified more favourably when the values of  $x$  and  $y$  are as great as possible. The value indicated by  $z$  should not be exceeded at all (see also Table 3.1).

When applying the work method of forwards and backwards spreading (instead of round and round driving), a symmetrical basic transverse distribution pattern is desired. The round and round driving method is most suitable for minimizing negative effects of skew transverse distribution patterns.

It was mentioned in chapter 2 that at their early stage of development, fertilizer broadcasters often performed a two-peak distribution pattern. With such patterns, it is difficult to realize compound distributions showing a high rate of evenness over a great ratio of overlap. This problem is more serious when peaks are relatively high or when they are situated far out of centre (NORDBY and HAMAN, 1965). Deviations from the optimum ratio of overlap will rapidly result in unacceptably high levels of unevenness, although at a certain ratio of overlap an acceptable value for a coefficient of irregularity can be obtained.

In extensive theoretical studies BERRY (1970) and DAVIS (1971) have examined the advantages and disadvantages of a great number of basic distribution patterns. Comparisons were made based on the behaviour of the value of the coefficient of variation ( $C.V.$ ) as a function of the variable ratio of overlap. From these studies the following aspects can be discussed. It is possible to obtain a minimum value of  $C.V.$  at a relatively small ratio of overlap for transverse distribution patterns with a two-peak character. However, peaks should be situated relatively close to the centre at a distance of about 0.2 times half the spreading width. Relative amounts of fertilizer in the peaks should be from 1.05, up to 1.20 times the amount of fertilizer supplies in the centre. This includes a relatively great working width, which can be obtained since values for the ratio of overlap  $O$  vary between 0.4 and 0.44. In these situations the very low values of 2.0 to 4.2 % for  $C.V.$  can be obtained. For a spreading width of 20 m such ratios of overlap would enable working widths of 11.2 to 12.0 m. However, deviations from this range in the ratio of overlap immediately lead to a very strong increase in the value of  $C.V.$  Under the most favourable circumstances, deviations from  $O = 0.4$  to  $O' = \pm 0.04$  and  $O' = O \pm 0.08$  lead to an increase of the value of  $C.V.$  up to 6.4 and 9.4 %. For deviations from the ratio of overlap  $O = 0.44$  to  $O' = O \pm 0.04$  and  $O' = O \pm 0.08$ , an increase in the value of  $C.V.$  up

to 9.0 and 12.8% has to be expected.

Speaking in practical terms, a variation of  $\pm 0.8$  m in working width at a value of  $b_0$  of 11–12 m results in a considerable decrease of evenness of transverse distribution for such distribution patterns. Distribution patterns showing peaks at a distance of 0.7 to 0.8 times half the spreading width, and with a relative fertilizer supply of 0.65 to 0.75 with respect to the amount in the centre, require a much greater value for the optimum ratio of overlap. Deviations from this optimum ratio of overlap and working width result in much worse compound distribution patterns.

Trapezoidal basic distribution patterns, create in principle, the opportunity for obtaining completely even distributions. As the steepness of the shapes increases, the optimum ratio of overlap decreases. Deviations from this optimum (e.g. due to steering failures) result in a very rapid increase of the unevenness of distribution (OEHRING, 1964).

A correct arrangement of the supply device(s) with respect to the distributor device (spinning disc broadcasters), and the application of a bow at the end of the sprout (reciprocating sprout broadcasters) have the objective of avoiding these two-peak distribution patterns. The answer to the question which type of basic transverse distribution pattern will create best opportunities with respect to evenness of distribution, can be limited to consideration of one-peak patterns. The maximum amount of fertilizer must be applied straight behind the

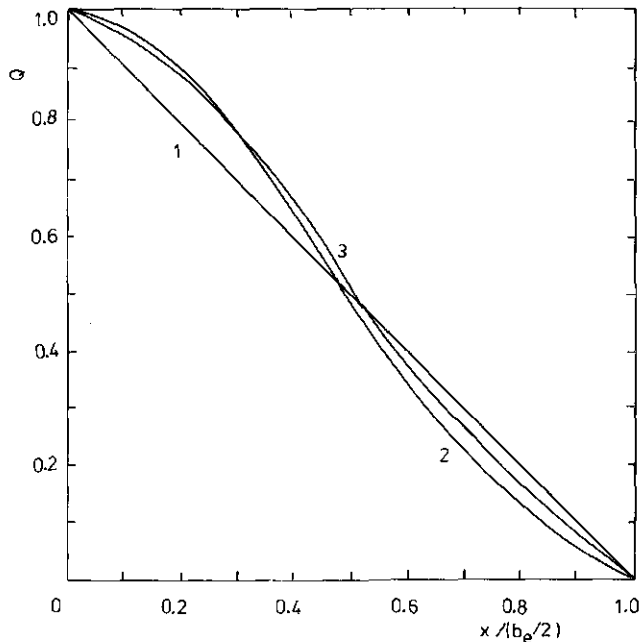


FIG. 3.6. Shapes of three basic transverse distribution patterns. 1: triangular pattern, 2: basic pattern according to DAVIS (1971), 3: basic pattern according to BERRY (1970),  $x/(b_0/2)$ : relative distance from the centre,  $Q$ : relative amount of fertilizer.

broadcaster, so that the amounts of fertilizer decrease continuously with increasing distance from the centre.

Fig. 3.6 shows some basic transverse distribution patterns as they were calculated and designed by BERRY (1970) and DAVIS (1971). As a comparison, the triangular shape of distribution pattern is given. The levels of the coefficient of variation in relation to the ratio of overlap are shown in Fig. 3.7. It appears that curve 3 enables a ratio of overlap of 0.4. In this case the coefficient of variation reaches a value of 8%. In general, curve 3 is better than the triangular distribution pattern; its optimum value for the ratio of overlap (with the minimum value of *C.V.*) is found for  $O = 0.56$ . The value of *C.V.* is 1.3%. Deviations from  $O = 0.56$  to  $O' = O \pm 0.06$  and  $O' = O \pm 0.12$  result in an increase of the value of *C.V.* up to 2.4 and 3.1%. With curve 2 very even compound distribution patterns can be found within the range  $O = 0.5-0.8$ .

In the section 2.3.3, it was mentioned that for the transverse distribution patterns of fertilizer broadcasters in practice, values of *C.V.* of 4-10% could be realized. In the next section, we will deal with the question of whether agricultural requirements support further improvement of the technical design of fertilizer broadcasters with respect to the evenness of distribution.

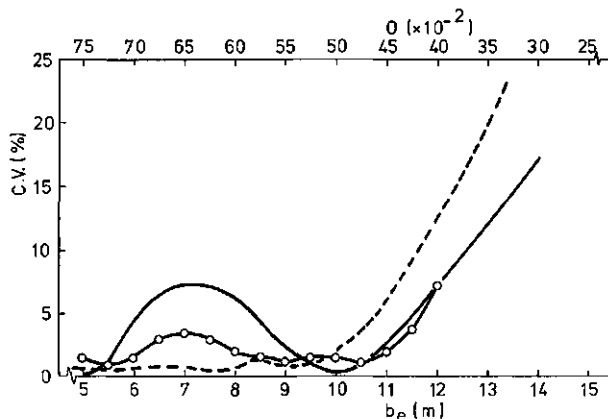


FIG. 3.7. Curves for the coefficient of variation *C.V.*, as a function of the ratio of overlap ( $O$ ) and bout width ( $b_e$ ), for three shapes of basic transverse distribution patterns. —: triangular basic pattern 1; (see Fig. 3.6). - - - - -: according to DAVIS (1971), basic pattern 2. ○—○ according to BERRY (1970), basic pattern 3.

#### 3.4. THE IMPORTANCE OF EVENNESS OF DISTRIBUTION OF FERTILIZER

There is great complexity in defining which values of coefficients of irregularity are tolerable in practice. This is connected with factors which are related to the variability of soil types, crops, climatological circumstances, types of fertilizer and types of distribution patterns. The problems which arise are formulated by MARKS (1959) in the following striking way: 'Very often the need for performing of trials is emphasized; however, at the same time the complexity

connected with such performance and the interpretation of the results is emphasized even more'.

Until now no generally valid standards of requirements are available with respect to the evenness of fertilizer distribution and its consequences for crop yield. Due to its complexity, it is impossible to formulate such a general

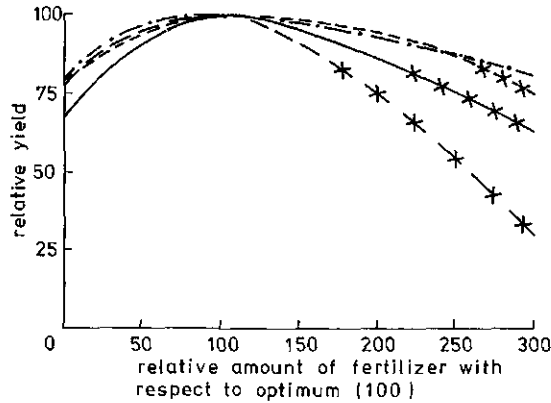


FIG. 3.8. Yield curves for some crops depending on N fertilizer supply. —: cereals (grain yield), - - -: rice (grain yield), ·····: potatoes (tuber yield), — · — ·: sugar beets (sugar yield). (According to PRUMMEL and DATEMA, 1962; GASPARETTO, 1969.)

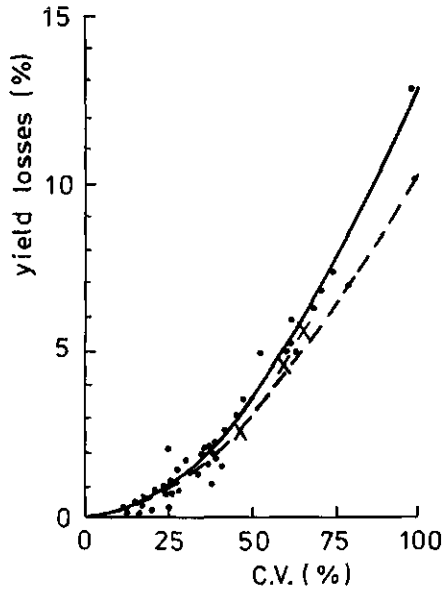


FIG. 3.9. Yield losses for N fertilizing of some crops as a function of the coefficient of variation *C.V.*. —: cereals; ●: calculated values, ×: experimental values. (According to PRUMMEL and DATEMA, 1962.) - - -: mean calculated yield losses for cereals, rice, sugar beets and potatoes. (According to GASPARETTO, 1969.)

standard. Nevertheless, in our opinion it is useful to describe and discuss the consideration on which the several recently used standards are based.

Incidentally, attempts have been made to obtain information about the consequences of uneven fertilizer distribution on crop yield, based on hypotheses concerning supposed or observed relationships between the growing factor of (anorganic) nutrients and potential crop yield (PRUMMEL and DATEMA, 1962; HOLLMANN and MATHES, 1962; ZSCHUPPE, 1968; GASPARETTO, 1969).

The relationship between relative crop production and relative amount of fertilizer can be demonstrated by means of production curves, as shown in Fig. 3.8 (PRUMMEL and DATEMA, 1962; GASPARETTO, 1969). The curves used by these authors represent an average and specific shape: per crop and per soil type, considerable year to year variations are possible. The relationship between the irregularities in the distribution pattern and the yield losses can be derived from transformation of the amount of fertilizer per area into relative yields which can be calculated from the production curves. In this way an uneven distribution pattern can be expressed by means of, for example, the coefficient of variation; its value can be correlated to the decrease in yield which must be expected (Fig. 3.9).

The relationship presented by PRUMMEL and DATEMA (1962) was based on about 60 fertilizer distributions obtained from the use of different distributors in practice. The results of a number of experiments in which the unevenness of distribution was created in an artificial way agreed well with the presented shape of the curve.

As far as it concerns values of *C.V.* < 50%, the results presented by GASPARETTO (1969) agreed reasonably with the relationships as they were shown by PRUMMEL and DATEMA (1962). This is understandable since the experiments were partly based on comparable relationships between nutrient supply and crop production. Fertilizer distributions were obtained from differing distributors and the method of calculation of the results differed slightly.

The effect of unevenness of fertilizer distribution on crop yield is influenced by the assumed production curves and the specific character of the irregularities in the distribution pattern. Considering a production curve as it is formulated by Mitscherlich's hypothesis, showing a continuous increase of production at increasing amounts of fertilizer, the following effects can be derived. Depending on the character of the distribution pattern, values of the coefficient of variation of about 13% will result in yield losses of 0.1 to 0.4%. For a coefficient of variation of 40%, losses will vary from 1.3 to 3.3%. However, when after reaching a maximum, the production curve has a depressive character, the negative effect of uneven fertilizer distribution will be considerably greater. Under these circumstances yield losses for the above-mentioned values of *C.V.* are calculated at 0.5 to 4% respectively 1.6 to 17.5% (HOLLMANN and MATHES, 1962). For production curves with a more depressive shape than those shown in Fig. 3.8, the yield losses for N fertilizing on cereals were calculated at 7% for a value of *C.V.* of 50% (PRUMMEL and DATEMA, 1962).

The specific character of a distribution pattern is represented by the way in

TABLE 3.1. Standards for the rate of unevenness of fertilizer distribution. (When needed, the coefficients of irregularity are translated into the value of the coefficient of variation *C.V.*).

Author/year	Coefficients of irregularity		Remarks
	$d_{max}$	<i>C.V.</i>	
HEYDE / 1957	≈ 50 %		trays: 0.2 × 0.2 m
HOLLMAN and MATHES / 1962		≈ 25 %	
PRUMMEL and DATEMA / 1962*		≈ 40 %	P, K fertilizers
PRUMMEL and DATEMA / 1962*		≈ 25 %	N fertilizers (cereals)
OHRING / 1963	≈ 20 %	≈ 13 %	
ZSCHUPPE / 1968*	≈ 50 %	≈ 20 %	N fertilizers
ZSCHUPPE / 1968*	≈ 50 %	≈ 30 %	P, K fertilizers
HOLMES / 1968		≈ 10 %	potatoes
HOLMES / 1968		≈ 15 %	winter wheat, grassland
GASPARETTO / 1969*		≈ 28 %	P, K fertilizers (mean for cereals, rice, sugar beets, potatoes)
GASPARETTO / 1969*			
IMAG / 1974		≈ 20 %	machine testings
ISO / 1974		≈ 13 %	machine testings
DLG / 1975 (BRD)		≈ 13 %	machine testings
Statens Masking Provingar (Sweden)		≈ 10 %	sufficient distribution
		≈ 5 %	good distribution

\* results obtained from calculations based on field trials.

which deviations appear in the compound transverse distribution pattern. Some possible variants with respect to their effects on yield losses were examined in a number of model studies by HOLLMANN (1962) and GASPARETTO (1969) and in a number of field trials (ZSCHUPPE, 1968). If a certain rate of unevenness (e.g. a value of *C.V.* > 35 %) is the result of some extremely high over- or underdoses (e.g. values of  $d_{max}$  > 50 %), a relatively large negative effect on crop yield has to be expected. This negative effect increases if the extremes are found at greater distances from each other and if the over- resp. underdoses cover a great area. Furthermore, the effect will be more negative if the average application rate is higher. The conclusions of GASPARETTO (1969) with respect to the negative effects of his so-called extreme distribution (in which the coefficient of irregularity only depends on two extremes extending over a width of 0.30 m in the distribution) contradicts with the results of HOLLMANN and MATHES (1962). It should be noted that the calculated results of HOLLMANN and MATHES (1962) are supported by field experiments performed later on by ZSCHUPPE (1968). Moreover, the starting points of GASPARETTO's considerations are, in our opinion, rather removed from actual practical situations.

When using fertilizer broadcasters in practice, it can happen that under certain conditions (wind, steering faults) false ratios of overlap result in extreme deviations which are found at relatively great distances from each other in the distribution pattern.

In England it was observed that when applying N.P.K. with the aid of the reciprocating sprout broadcaster, deviations of about 1.70 m from the optimum working width resulted in subsequent decreases in potential yield. Grain losses of 10% were recorded for cereals. Sugar production decreased by 18% for sugar beets, tuber yields with 10% for potatoes. A decrease in dry matter yield of 16% was recorded for grassland (MITCHELL, 1974, 1975).

In Table 3.1 a review is presented of the limits to the requirements for evenness of fertilizer distribution which are used by testing and research stations or are proposed by some authors. The table shows a certain rate of unanimity between the standards. A tendency towards more stringent standards can be noticed especially in the testing stations in The Federal Republic of Germany and in Sweden. At first glance, this tendency seems not to be supported by the requirements which can be formulated when considering the results of field experiments presented by above-cited authors. In the final discussion in section 3.5 we will return to this subject.

Nevertheless, more stringent standards – even when they are mainly dictated by the suggestion that the majority of modern fertilizer broadcasters can meet such requirements – can act favourably on further improvement in the various technical designs. However, unjustifiable increases of requirements should be avoided since they can lead to development of technically complicated and economically unattractive distribution systems.

In addition to the absolute value of the coefficients of irregularity which can be obtained, attention should be paid to the behaviour of these coefficients when deviations from the optimum ratio of overlap occur. Under such circumstances it is important that the curves which are representing the values of the coefficients of irregularity show a rather plane trajectory. In this way the risk on a very annoying source for failures in practice is minimized.

### 3.5. DISCUSSION

The quality of the distribution pattern of fertilizer broadcasters of the spinning disc and reciprocating sprout systems is mainly determined by the evenness of the compound transverse distribution pattern. This characteristic is mostly specified by means of several coefficients of irregularity. Widely used coefficients of irregularity are the coefficient of variation  $C.V.$  (%) and the mean linear deviation from the mean  $\bar{d}$  (%). In the Netherlands and South Africa testing stations are using Burema's number of irregularity  $R$ . It is pointed out that there is a relationship between the values of  $C.V.$  and  $R$ , creating a basis for comparison of results. A rough basis for comparison is also available for the results represented by  $\bar{d}$  and  $C.V.$

The width of the collecting trays up to 0.5 m hardly influences the values of the coefficients of irregularity, and in testing procedures a tray width of 0.5 m can be considered a reasonable and acceptable value.

Yield losses which must be expected due to uneven fertilizer distribution are in

the first instance determined by crop properties. In addition, the type of fertilizer, the amount of fertilizer supplied, and the character of the irregularities in the distribution pattern play an important role. The negative effect of an over- or underdose is more serious if the width of extension increases, or if the deviations are less randomly distributed over the transverse pattern. Soil type and climatical circumstances also have to be taken into consideration. One of the most important sources for failures is an incorrect ratio of overlap resulting in over- or underdosage. In principle, a formulation of generally valid standards based on agricultural requirements for the coefficients of irregularity is impossible. However, the results of incidentally performed trials tend towards a certain rate of agreement. There is an impression that testing stations, taking into account the progressing technical developments of distributor systems, tend towards an increase in the level of the standards. This can be considered as an adaptation to the quality of the distribution patterns which presently can be realized by the majority of the spinning disc and reciprocating sprout broadcasters.

Statements of various authors not directly based on the results of experiments also show a tightening up of the standards which should be realized. In our opinion an increase in the level of fertilizing and the use of highly concentrated N fertilizers justify such an augmentation. The contradiction arises that the use of the coefficients of irregularity described in the previous sections in principle enable an increase of the variations together with an increase of the average level of fertilization. Within this scope it should be examined if present standards which are expressing relative deviations from the setvalues of the application rate, should be replaced in future by absolute limit values. These should not be exceeded with respect to unevenness of distribution.

The availability of computer facilities and simulation techniques, in our opinion, can contribute to a valuable way of tackling problems in order to create a more fundamental basis against which these aspects of the working quality of fertilizer distributors can be weighed.



## 4. THE OSCILLATION CHARACTERISTIC OF THE DISTRIBUTOR DEVICE OF THE RECIPROCATING SPROUT BROADCASTER

### 4.1. INTRODUCTION

In this chapter kinematic aspects of the distributor device will be discussed. It is expected that kinematics will affect particle movement inside and when leaving the sprout.

The oscillation characteristic was described by PELLIZZI (1958) and ROMANELLO (1969) based on the crank connecting rod mechanism which was used for driving the sprout at that time. This mechanism resulted in an asymmetrical movement of the sprout (see also section 2.5). PELLIZZI (1958) derived equations of motion for the sprout; however, they were not directly related to the properties of the distribution pattern and the kinematic studies were restricted to velocity properties. The ratio between the crank and connecting rod (which determines the angle of oscillation) was not taken into further consideration. The contradiction between the asymmetry of velocity due to the driving mechanism used, and the pursued symmetry of the transverse distribution pattern, was ignored. Furthermore, spreading experiments were performed with different types of fertilizers and various designs of the sprout. Under all conditions the compound transverse distribution pattern showed a high rate of unevenness resulting in values of the coefficient of variation of 60% to about 80%. The spreading width was 6 to 8.5 m which resulted in a working width (depending on the type of fertilizer) of 4.2 to 7 m.

Comparable values were obtained some years before by CASSELLA (1956/57). In his studies it appeared that a decrease of the length of the sprout from 410 mm to 365 mm, as well as an increase of both the diameters of entrance and outlet from 80 to 85 mm resp. to 40 and 45 mm, resulted in a considerable improvement of the transverse distribution pattern. The working width was not influenced to any extent. For the types of fertilizers studied, an average decrease of the value of *C.V.* from 62 to 26% was obtained. Improvement was most noticeable for granular fertilizers which showed a decrease of the value of *C.V.* from 93 to 32%.

ROMANELLO (1969) stated in his kinematic studies that the absolute particle velocity of outlet was equal to the vectorial sum of the velocity components of the sprout in longitudinal and transverse directions. Based on these assumptions particle trajectories were calculated, while ignoring air resistance. In our opinion these assumptions are too simple and are fundamentally incorrect since it has been widely proven by experiments that air resistance cannot be ignored (MENNEL and REECE, 1963). In ROMANELLO's calculations particle trajectories were overestimated. Even more controversial is the fact that the production process of particle energy was not taken into account. In principle it is very well tenable that the process of kinetic energy production leads to higher absolute

velocities of outlet than are calculated on the basis of ROMANELLO's assumptions. No further experiments were performed in order to verify this hypothesis.

The agreement between the calculated values of the particle trajectories and working widths of 5–6 m should not be considered as a proof of the validity of the hypothesis. It can only be concluded that the opposite effects of incorrect starting points lead to final calculated results which are in possible agreement with the experimental results. The fact that working widths of about the same size were obtained in the experiments of CASSELLA (1956/57) and PELLIZZI (1958) should not be considered as a support of ROMANELLO's hypothesis.

Our final conclusion is, therefore, that the three investigations discussed above did not deal to a sufficient degree with the possible relationships between kinematics of the sprout and the process of particle movement; as a result, they ignored the consequences for particle velocity and direction of dispatch.

Since a part of our study is a fundamental analysis of the process of energy transfer from the oscillating distributor device to the particles, we will in the next sections deal with more extensive analyses of the character of sprout oscillation. This will be based on the mechanism of the Vicon reciprocating sprout fertilizer broadcaster in its present design. The relationship between some construction variables used in the driving mechanism and the kinematic aspects of the character of sprout oscillation will be discussed. These relationships will be compared with the results of a number of experiments including the systems of tractor and mounted distributors. Furthermore, some effects of the elastic coupling, the flywheel, and the counterweight – which are all part of the driving mechanism – will be examined.

## 4.2. THEORY

### 4.2.1. *The oscillation characteristics of the sprout*

In Fig. 4.1 a schematic drawing of the driving mechanism is given. Fig. 4.2 shows the code for signs which we will use to describe the components of velocity and the angle of oscillation in the different quadrants.

A point  $B$  on the centre line of the sprout at a distance  $RB$  of the oscillation point  $P$  describes from the centre position a part of an arc with a length of  $\pi \cdot RB \cdot \phi_{max}/180^\circ$ .

It should be noted that  $\phi$  is defined as the angle of oscillation in this thesis; in fact, the actual angle of oscillation of the sprout in practice has a value of  $2\phi$ .

The value of the angle of oscillation  $\phi$  depends on the length of the crank  $RA$ , the length of the connecting rod  $L$ , and the angle of rotation  $\alpha$ . It holds:

$$\phi = \operatorname{atan}\left(\frac{RA \cdot \cos \alpha}{(L^2 - RA^2)^{1/2}}\right) \quad (4.1)$$

For the values of  $\alpha = k\pi$ , in which  $k = 0, 1, 2, 3, \dots, n$ , a maximum value for the angle of oscillation is obtained.

So:

$$\phi_{max} = \operatorname{atan}\left(\frac{RA}{(L^2 - RA^2)^{1/2}}\right) \quad (4.2)$$

For  $k = 0, 2, 4, \dots$   $\phi_{max}$  has positive values, and for  $k = 1, 3, 5, \dots$  its value will be negative.

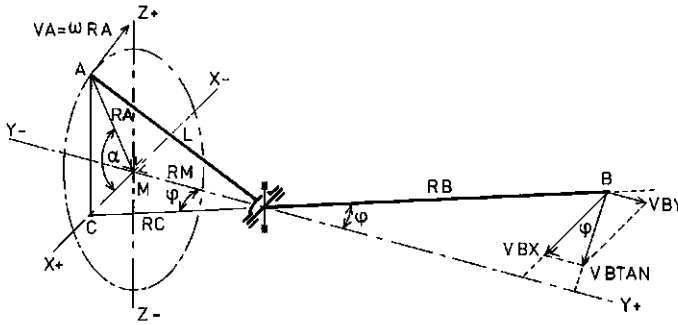


FIG. 4.1. Schematic representation of the characteristic of motion of the oscillating distributor device (abbreviations and symbols are explained in the text and in the list on page 214).

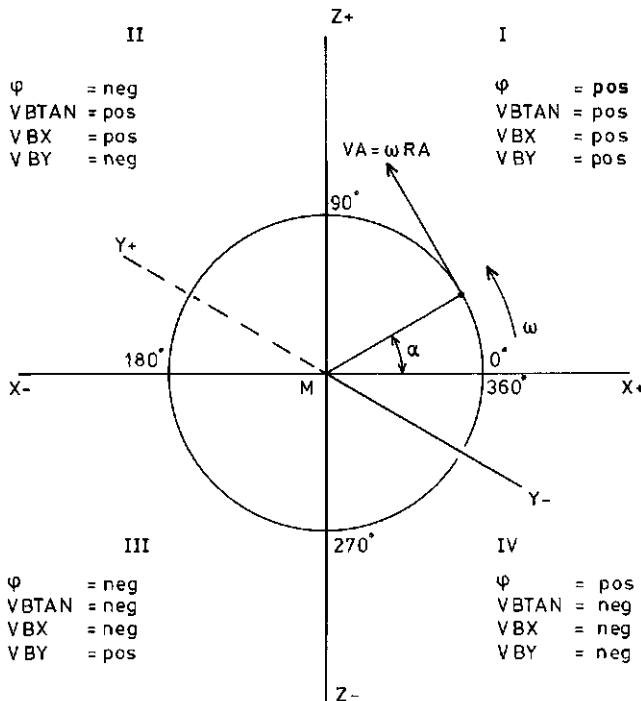


FIG. 4.2. Code for signs (abbreviations and symbols are explained in the text and in the list on page 214).

As:

$$\dot{\phi} = \frac{d\phi}{d\alpha} \cdot \frac{d\alpha}{dt} = \omega \cdot \frac{d\phi}{d\alpha} \quad (4.3)$$

the angular velocity can be found from:

$$\dot{\phi} = \frac{-\omega \cdot RA \cdot \sin \alpha \cdot (L^2 - RA^2)^{1/2}}{L^2 - RA^2 \cdot \sin^2 \alpha} \quad (4.4)$$

The tangential velocity component of point *B* will be now, taking into account the code for signs:

$$V_{BTAN} = -\dot{\phi} \cdot RB \quad (4.5)$$

or:

$$V_{BTAN} = \frac{\omega \cdot RA \cdot RB \cdot \sin \alpha \cdot (L^2 - RA^2)^{1/2}}{L^2 - RA^2 \cdot \sin^2 \alpha} \quad (4.6)$$

The tangential acceleration of a point *B* can be found from:

$$a_{BTAN} = \frac{d V_{BTAN}}{dt} = -\ddot{\phi} \cdot RB \quad (4.7)$$

with:

$$\ddot{\phi} = \frac{d\dot{\phi}}{dt} = \frac{d\dot{\phi}}{d\alpha} \cdot \frac{d\alpha}{dt} = \omega \cdot \frac{d\dot{\phi}}{d\alpha} \quad (4.8)$$

we obtain:

$$\ddot{\phi} = -\frac{\omega^2 \cdot RA \cdot \cos \alpha \cdot (L^2 - RA^2)^{1/2} \cdot (L^2 + RA^2 \cdot \sin^2 \alpha)}{(L^2 - RA^2 \cdot \sin^2 \alpha)^2} \quad (4.9)$$

So:

$$a_{BTAN} = \frac{\omega^2 \cdot RA \cdot RB \cdot \cos \alpha \cdot (L^2 - RA^2)^{1/2} \cdot (L^2 + RA^2 \cdot \sin^2 \alpha)}{(L^2 - RA^2 \cdot \sin^2 \alpha)^2} \quad (4.10)$$

Besides the tangential acceleration, point *B* has a centripetal acceleration. Its value is found from:

$$a_{BCEN} = \frac{(V_{BTAN})^2}{RB} = \dot{\phi}^2 \cdot RB \quad (4.11)$$

Taking into consideration the Eq. (4.4) this leads to:

$$a_{BCEN} = \frac{\omega^2 \cdot RA^2 \cdot RB \cdot \sin^2 \alpha \cdot (L^2 - RA^2)}{(L^2 - RA^2 \cdot \sin^2 \alpha)^2} \quad (4.12)$$

Finally, the components of the tangential velocity *V*<sub>BTAN</sub> in the *X*- and *Y*-

direction can be written as:

$$VBX = VBTAN \cdot \cos \phi \quad (4.13)$$

so:

$$VBX = \frac{\omega \cdot RA \cdot RB \cdot \sin \alpha \cdot (L^2 - RA^2)}{(L^2 - RA^2 \cdot \sin^2 \alpha)^{3/2}} \quad (4.14)$$

and:

$$VBY = VBTAN \cdot \sin \phi \quad (4.15)$$

so:

$$VBY = \frac{\omega \cdot RA^2 \cdot RB \cdot \sin \alpha \cdot \cos \alpha \cdot (L^2 - RA^2)^{1/2}}{(L^2 - RA^2 \cdot \sin^2 \alpha)^{3/2}} \quad (4.16)$$

Since we can now understand the character of oscillation of the distributor device in terms of size and shape of the angle of oscillation, angular velocity, and angular acceleration, the following conclusions can be made. Character of oscillation depends on the following driving and construction variables: the angular speed  $\omega$  of the driving shaft. The length of the sprout  $RB$ , the length of the crank  $RA$ , and the length of the connecting rod  $L$ . In the existing design of the reciprocating sprout fertilizer broadcaster, the actual values of  $RA$ ,  $L$ ,  $RB$ , and  $\omega$  are respectively 0.095 m, 0.200 m, 0.63 m and  $56.55 \text{ rad s}^{-1}$ . Table 4.1 lists the

TABLE 4.1. The (absolute) values for  $VBTAN$ ,  $VBX$ ,  $VBY$ ,  $aBTAN$ ,  $aBCEN$  and  $\phi$  as a function of  $\alpha$ , for a reciprocating sprout broadcaster ( $\omega = 56.55 \text{ rad s}^{-1}$ ,  $RB = 0.63 \text{ m}$ ,  $RA = 0.095 \text{ m}$  and  $L = 0.20 \text{ m}$ ).

	$VBTAN$	$VBX$ ( $\text{m s}^{-1}$ )	$VBY$	$aBTAN$	$aBCEN$ ( $\text{m s}^{-2}$ )	$\phi$ (deg)
$\alpha$	0	0	0	842.08	0	28.36
(deg)	5	1.30	1.15	843.20	2.68	28.27
	10	2.60	2.30	846.40	10.76	27.99
	15	3.91	3.47	851.22	24.31	27.54
	20	5.23	4.67	856.81	43.44	26.90
	25	6.56	5.89	862.01	68.26	26.07
	30	7.89	7.15	865.26	98.83	25.05
	35	9.22	8.44	864.58	135.11	23.85
	40	10.56	9.76	857.66	176.87	22.46
	45	11.87	11.09	841.84	223.60	20.89
	50	13.15	12.42	814.30	274.41	19.13
	55	14.37	13.73	772.25	327.98	17.20
	60	15.52	14.99	713.26	382.48	15.10
	65	16.56	16.15	635.58	432.62	12.85
	70	17.47	17.18	538.64	484.71	10.46
	75	18.22	18.04	423.28	526.89	7.95
	80	18.77	18.69	292.05	559.40	5.42
	85	19.11	19.09	149.13	579.95	2.69
	90	19.23	19.23	0	586.98	0

resulting values for the angle of oscillation  $\phi$  and the tangential velocity and acceleration for point  $B$  on the centre line at the end of the sprout. In addition, the components in the  $X$ - and  $Y$ -direction of the tangential velocity are given. The  $Y$ -coordinate coincides with the direction of forward movement of the broadcaster. Finally the values for the centripetal acceleration are given. All values are considered during a period of rotation  $0 \leq \alpha \leq \pi/2$ .

#### 4.2.2. *The relation between construction variables and the character of oscillation*

The angle of oscillation, the velocities, and the accelerations are all functions of the angle of rotation  $\alpha$  ( $= \omega \cdot t$ ) of the driving shaft. Velocities and accelerations are linearly resp. quadratically positively correlated with the angular velocity  $\omega$  of the driving shaft. Velocities and accelerations of the sprout are linearly positively correlated with the length  $RB$ .

The effect of the construction variables  $RA$  (crank length) and  $L$  (length of connecting rod) on the oscillation pattern is more complicated. Their relationship will be analyzed. This analysis will be based on the pattern of  $\phi$ ,  $\dot{\phi}$  and  $\ddot{\phi}$  and the centripetal acceleration  $aBCEN$ , as a function of the ratio between  $RA$  and  $L$  during the period  $0 \leq \alpha \leq \pi$ . These functions will be characterized further by calculating the absolute maximum values of  $\dot{\phi}$ ,  $\ddot{\phi}$  and  $aBCEN$ . In addition, it will be examined for which values of  $\alpha$  these maximum values are obtained during the period considered. Except for the maximum values, the levels of the means and the ratios between both can contribute to a better knowledge of the character of velocities and accelerations in the oscillation pattern. This knowledge can be increased when considering the moment (as a function of  $\alpha$ ) at which these mean values are obtained.

High values of the absolute velocity of outlet – or more concretely, the  $X$ -component of this velocity – will create the possibility for obtaining large working widths. Therefore, the hypothesis can be stated that the character of the oscillation pattern should create an opportunity for energy transfer to the particles on a level as high, and also during a period as long, as possible.

##### 4.2.2.1. *The angle of oscillation $\phi$ as a function of $C$ and $\alpha$*

It can be assumed that the angle of oscillation affects the velocity of outlet and the angle of dispatch of the particles. In this section the relation between the angle of oscillation and the design parameters affecting its value are examined.

The ratio between the length of the crank  $RA$  and the length of the connecting rod  $L$  can be expressed as  $C = RA/L$ , in which  $0 < C < 1$ .

The Eq. (4.1) can now be rewritten as:

$$\phi = \text{atan} \left( \frac{\cos \alpha}{(C^{-2} - 1)^{1/2}} \right) \quad (4.17)$$

The values of  $\alpha$  for which the maximum value of  $\phi$  is obtained can be calculated by differentiating and zero setting of Eq. (4.17). With the aid of Eq. (4.4) it can be

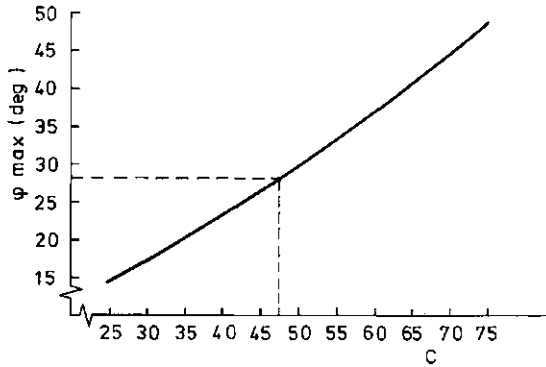


FIG. 4.3. The maximum angle of oscillation  $\phi_{max}$  as a function of the ratio  $C$  between length of the crank  $RA$  and connecting rod  $L$ .

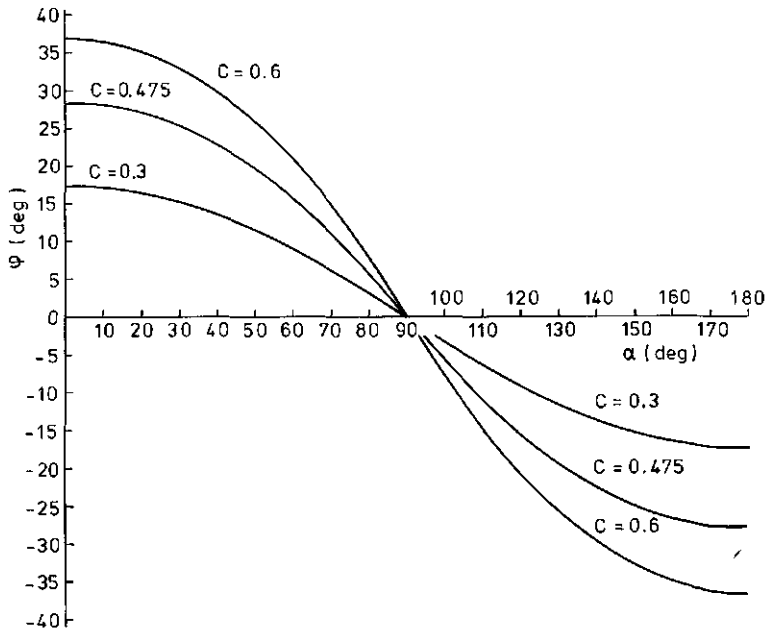


FIG. 4.4. The angle of oscillation  $\phi$  as a function of the angle of rotation  $\alpha$  for three values of  $C$ .

stated that:

$$\phi/\omega = -\frac{\sin \alpha \cdot (C^{-2} - 1)^{1/2}}{C^{-2} - \sin^2 \alpha} \quad (4.18)$$

Maximum values for the angle of oscillation are now found for those values of  $\alpha$  for which  $\sin \alpha = 0$ . As a result of this we find:

$$\phi_{max} = \text{atan} (C^{-2} - 1)^{-1/2} \quad (4.19)$$

The relationship between  $\phi_{max}$  and  $C$  is represented in Fig. 4.3. It can be concluded that at increased values of  $C$ , the value of  $\phi_{max}$  increases somewhat more than linearly. In Fig. 4.4 the curves for  $\phi$  as a function of  $\alpha$  during the period  $0 \leq \alpha \leq \pi$  is given for values of  $C = 0.3, 0.475$ , and  $0.6$ .

#### 4.2.2.2. Angular and tangential velocity of the sprout in relation to $C$ and $\alpha$

The relationship between the angular velocity of the sprout and  $C$  and  $\alpha$  has already been presented in Eq. (4.18). This equation also represents the curve for the tangential velocity as  $V_{BTAN}/\omega \cdot RB = -\dot{\phi}/\omega$ . The (absolute) maximum values of  $\dot{\phi}/\omega$  can be found from Eq. (4.9), which can be transferred into:

$$\dot{\phi}/\omega^2 = -\frac{\cos \alpha \cdot \{(C^{-2} + \sin^2 \alpha) \cdot (C^2 - 1)^{1/2}\}}{(C^{-2} - \sin^2 \alpha)^2} \quad (4.20)$$

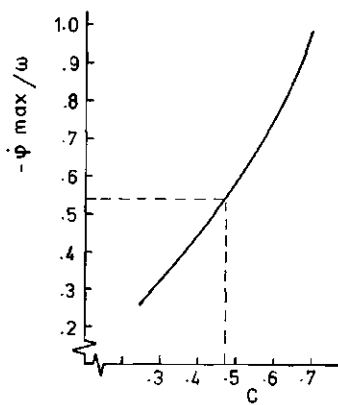


FIG. 4.5. The maximum angular velocity of the sprout (expressed by the ratio  $-\dot{\phi}_{max}/\omega$ ) as a function of  $C$ .

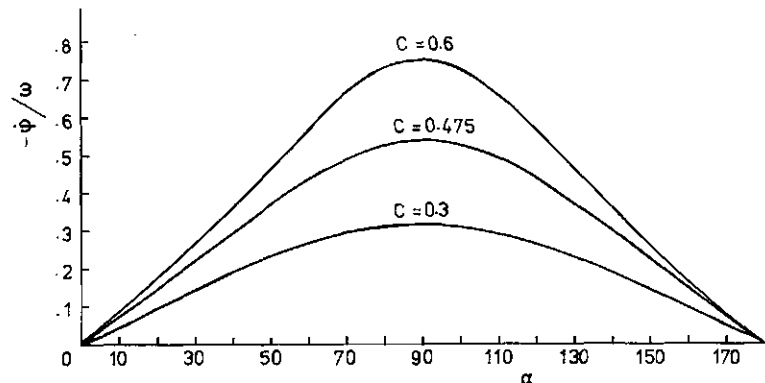


FIG. 4.6. The angular velocity of the sprout (expressed by the ratio  $-\dot{\phi}/\omega$ ) as a function of the angle of rotation  $\alpha$  for three values of  $C$ .



TABLE 4.2. Ratio between mean and maximum values of the tangential velocity and tangential acceleration and of the centripetal acceleration as a function of  $C$ .

$C$	$VBTANGEM$	$aBTANGEM$	$aBCEMGEM$
	$VBTANMAX$	$aBTANMAX$	$aBCENMAX$
0.30	0.62	0.70	0.48
0.35	0.61	0.73	0.47
0.40	0.60	0.76	0.46
0.45	0.59	0.79	0.45
0.50	0.58	0.81	0.43
0.55	0.56	0.81	0.42
0.60	0.54	0.79	0.40
0.65	0.52	0.77	0.38
0.70	0.50	0.73	0.36

Maximum values are found for those values of  $\alpha$  for which  $\cos \alpha = 0$ . Taking into account Eq. (4.18) we obtain:

$$-\dot{\phi}_{max}/\omega = (C^{-2} - 1)^{-1/2} \quad (4.21)$$

From Fig. 4.5 it can be seen that the (negative) value of  $\dot{\phi}_{max}/\omega$  increases progressively with a linear increase of the value of  $C$ . According to the relation between  $\dot{\phi}$  and  $VBTAN$ , it has to be taken into account that the tangential sprout velocity increases strongly during the second half of the period  $0 \leq \alpha \leq \pi/2$  at increased values of  $C$  (Fig. 4.6). The specific shape of the velocity curve will be more clearly explained when considering  $\dot{\phi}/\omega^2$  for the same conditions.

The mean value for the angular oscillation velocity  $\dot{\phi}_{gem}$  is determined in the following way. Using the relationships for  $\phi$  and  $\dot{\phi}$ , it can be derived that:

$$-\dot{\phi}_{gem}/\omega = \frac{2}{\pi} \int_{\alpha=0}^{\pi/2} \dot{\phi} \cdot d\alpha = \frac{2}{\pi} \cdot \phi \Big|_{\alpha=0}^{\pi/2} \quad (4.22)$$

Taking into consideration Eq. (4.17) this now leads to:

$$-\dot{\phi}_{gem}/\omega = \frac{\text{atan}(C^{-2} - 1)^{-1/2}}{2 \cdot \text{atan } 1} \quad (4.23)$$

The ratio between the mean and maximum values for  $\dot{\phi}$  respectively  $VBTAN$  can now be determined with the aid of the Eq. (4.21) and (4.23). Therefore:

$$\frac{\dot{\phi}_{gem}}{\dot{\phi}_{max}} = \frac{VBTANGEM}{VBTANMAX} = \frac{(C^{-2} - 1)^{1/2} \cdot \text{atan}(C^{-2} - 1)^{-1/2}}{2 \cdot \text{atan } 1} \quad (4.24)$$

As indicated in Table 4.2, the ratio between the mean and maximum value of  $VBTAN$  decreases as the value of  $C$  increases. It was shown above that during the period  $0 \leq \alpha \leq \pi/2$ , the value of  $\alpha$  (for which the maximum value of  $\dot{\phi}$  was obtained) was determined by  $\cos \alpha = 0$  or  $\alpha = \pi/2$ . The value of  $\alpha$  for which

during the same period the mean value of  $\dot{\phi}$  is obtained from:

$$\frac{\text{atan}(C^{-2} - 1)^{-1/2}}{2 \cdot \text{atan } 1} = \frac{\sin \alpha \cdot (C^{-2} - 1)^{1/2}}{C^2 - \sin^2 \alpha} \quad (4.25)$$

From this equation  $\alpha(\dot{\phi}_{gem})$  can be determined:

$$\begin{aligned} \alpha(\dot{\phi}_{gem}) &= \\ &= \text{asin} \left\{ \frac{-P \cdot \text{atan } 1 + (P^2 \cdot \text{atan } 1 + C^{-2} \cdot \text{atan}^2(P - 1)^{1/2})}{\text{atan}(P - 1)} \right\} \end{aligned} \quad (4.26)$$

in which:  $P = (C^{-2} - 1)^{1/2}$ .

The value of  $\alpha$  for which  $\alpha = \alpha(\dot{\phi}_{gem})$  increases from  $\alpha = 40.6^\circ$  to  $\alpha = 46.4^\circ$  as  $C$  increases from 0.3 to 0.7. Therefore, the ratio between  $\alpha(\dot{\phi}_{gem})$  and  $\alpha(\dot{\phi}_{max})$  increases slightly at increased values of  $C$ .

#### 4.2.2.3. Angular and tangential acceleration of the sprout in relation to $C$ and $\alpha$

The relationship between the angular acceleration expressed as  $\dot{\phi}/\omega^2$  and the tangential acceleration  $a_{BTAN}/\omega^2 \cdot RB$ , depending on the value of  $C$ , can be found from the given Eq. (4.20). According to Fig. 4.6 the value of  $\alpha$  (for which the maximum values of  $\phi$  and  $\dot{\phi}/\omega$  were found), was independent of  $C$ . On the other hand the value of  $\alpha$  for which the maximum values of  $\dot{\phi}/\omega^2$  are found is dependent on  $C$ . With:  $-y_{c(\omega)} = \dot{\phi}/\omega^2$  and  $-y_{c(\omega)} \cdot (C^{-2} - 1)^{-1/2} = y_p$  the differential of Eq. 4.20 yields to:

$$y'_p = \frac{\sin \alpha}{(p^2 - \sin^2 \alpha)^3} \cdot \{-\sin^4 \alpha + 2 \cdot (1 - 3 \cdot p^2) \cdot \sin^2 \alpha + 6 \cdot p^2 - p^4\} \quad (4.27)$$

in which  $p = 1/C$ .

Limitation of  $C$  to more practicable values  $0.3 \leq C \leq 0.7$  yields to  $10/7 \leq p \leq 10/3$ . For  $0 \leq \alpha \leq \pi/2$ ;  $y'_p = 0$ , if:  $\sin^4 \alpha - 2 \cdot (1 - 3 \cdot p^2) \cdot \sin^2 \alpha - 6 \cdot p^2 + p^4 = 0$  or if  $\sin \alpha = 0$ . So:  $\sin^2 \alpha = 1 - 3 \cdot p^2 + (1 + 8 \cdot p^4)^{1/2}$  or  $\alpha = 0$ .

On the condition that:  $0 \leq 1 - 3 \cdot p^2 + (1 + 8 \cdot p^4)^{1/2} \leq 1$ , and taking into account that  $p \geq 10/7$ , we finally obtain:  $10/7 \leq p \leq \sqrt{6}$ . So:

$$1/\sqrt{6} \leq C \leq 0.7 \text{ or } 0.408 \leq C \leq 0.7 \quad (4.28)$$

In this range of values of  $C$ ;  $-y_{c(\omega)}$  (which was  $y_p \cdot (C^{-2} - 1)^{1/2}$ ) increases for  $0 \leq \alpha < \alpha_c$  and decreases for  $\alpha_c \leq \alpha \leq \pi/2$ . In other words, for a value of  $C = 0.475$  ( $RA = 0.095$  m and  $L = 0.20$  m), for example, the angular acceleration first will increase since  $\alpha_c > 0$ . After reaching its maximum value at  $\alpha = \alpha_c$ , it will decrease to zero for  $\alpha = \pi/2$ . The maximum is found at a value of  $\alpha = \alpha_c$  which can be calculated from:

$$\alpha_c = \text{asin } C^{-1} \cdot \{C^2 - 3 + (C^4 + 8)^{1/2}\}^{1/2} \quad (4.29)$$

The absolute maximum values for the angular velocity and the tangential

velocity can be found from:

$$-y_{c(max)} = \frac{\{C^2 - 2 + (C^4 + 8)^{1/2}\} \cdot \{3 - (C^4 + 8)^{1/2} \cdot (1 - C^2)\}^{1/2}}{\{4 - C^2 - (C^4 + 8)^{1/2}\}^2} \quad (4.30)$$

In the range  $0.3 \leq C < 0.408$  it is found that the function for  $-y_{c(\omega)}$  is continuously decreasing during the period  $0 \leq \alpha \leq \pi/2$ . The maximum values for

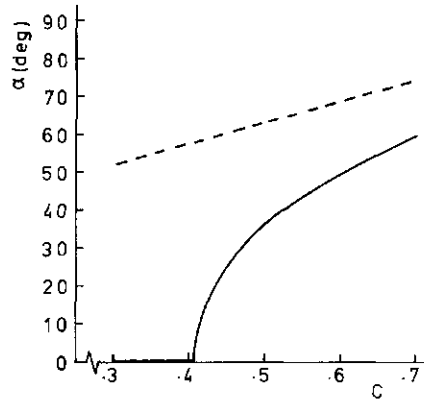


FIG. 4.7. The values of the angle of rotation  $\alpha$ , for which the mean and maximum tangential accelerations of the sprout are found as a function of  $C$ . (-----:  $aBTANGEM$ ; —:  $aBTANMAX$ ).

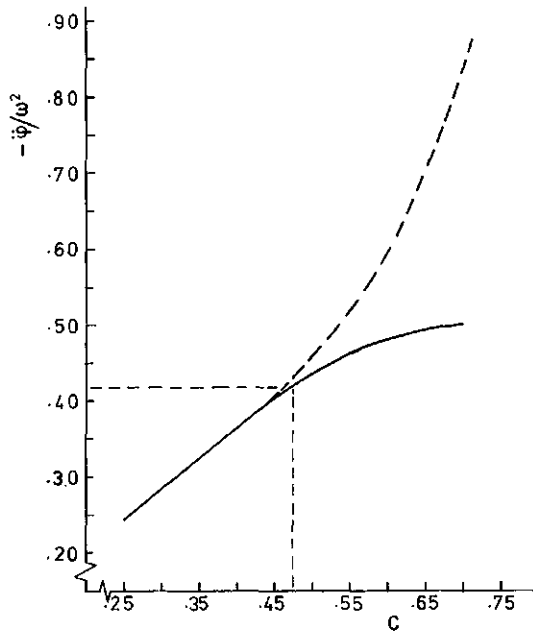


FIG. 4.8. Curves for the angular acceleration of the sprout as a function of  $C$ . (-----:  $-\ddot{\phi}_{max}/\omega^2$ ; —:  $-\ddot{\phi}/\omega^2$  for  $\alpha = 0^\circ$ ).

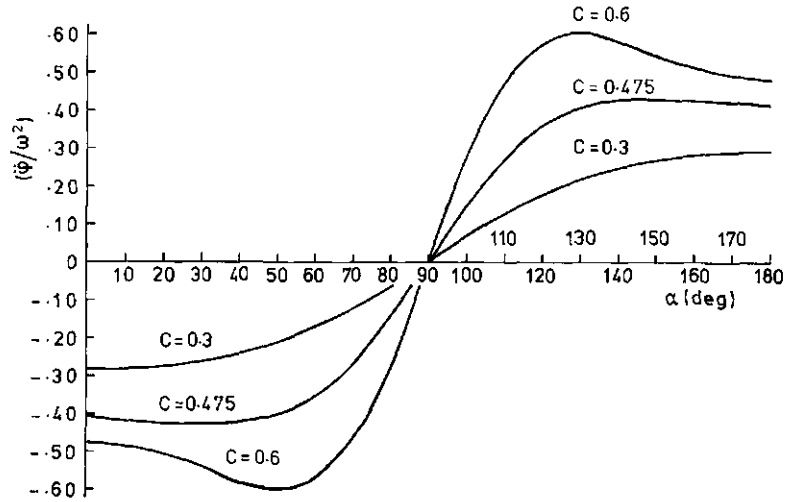


FIG. 4.9. The angular acceleration of the sprout (expressed by the ratio  $\ddot{\phi}/\omega^2$ ) as a function of the angle of rotation  $\alpha$  for three values of  $C$ .

angular and tangential accelerations are found at  $\alpha = 0$ . Just as the values for  $\alpha = 0$ , when  $C \geq 0.408$  the values are computed according to:

$$\begin{aligned} -y_{c(max)} &= -\dot{\phi}_{max}/\omega^2 = \\ &= aBTANMAX/\omega^2 \cdot RB = C \cdot (1 - C^2)^{1/2} \end{aligned} \quad (4.31)$$

The relation is given in Fig. 4.7 between  $C$  and the value of  $\alpha$  at which the maximum values for  $-\dot{\phi}/\omega^2$  resp.  $aBTAN/\omega^2 \cdot RB$  are obtained. For values of  $C \geq 0.408$ , the value of  $-\dot{\phi}_{max}/\omega^2$  increases and deviates more from the value of  $-\dot{\phi}_{(\alpha=0)}/\omega^2$  at increased values of  $C$  (Fig. 4.8). For the values of  $C = 0.3$ ,  $0.475$ , and  $0.6$  the curves of  $\dot{\phi}/\omega^2$  as functions of  $\alpha$  are given in Fig. 4.9.

As the functions of  $\dot{\phi}/\omega$  and  $\dot{\phi}/\omega^2$  have been derived previously, the mean values for angular and tangential acceleration can be found from:

$$-\dot{\phi}_{gem}/\omega^2 = \frac{2}{\pi} \int_{\alpha=0}^{\pi/2} \dot{\phi} \cdot d\alpha = \frac{2}{\pi} \cdot \dot{\phi} \Big|_{\alpha=0}^{\pi/2} \quad (4.32)$$

With Eq. (4.18) this yields to:

$$-\dot{\phi}_{gem}/\omega^2 = 2/\pi \cdot (C^{-2} - 1)^{1/2} \quad (4.33)$$

Application of Eq. (4.31) and (4.30) in the ranges of  $0.3 \leq C < 0.408$  resp.  $0.408 \leq C \leq 0.7$  yields for the calculation of the ratio between  $\dot{\phi}_{gem}$  and  $\dot{\phi}_{max}$  resp.  $aBTANGEM$  and  $aBTANMAX$  to:

$$\begin{aligned} \dot{\phi}_{gem}/\dot{\phi}_{max} &= aBTANGEM/aBTANMAX = 2/\pi \cdot (1 - C^2) \\ &\text{for } 0.3 \leq C < 0.408 \end{aligned} \quad (4.34)$$

and:

$$\dot{\phi}_{gem}/\dot{\phi}_{max} = \frac{2 \cdot C \cdot \{4 - C^2 - (C^4 + 8)^{1/2}\}^2}{\pi \cdot (1 - C^{-2}) \cdot \{C^2 - 2 + (C^4 + 8)^{1/2}\} \cdot \{3 - (C^4 + 8)^{1/2}\}^{1/2}} \quad (4.35)$$

for  $0.408 \leq C \leq 0.7$

From Table 4.2 it can be seen that the ratio between *aBTANGEM* and *aBTANMAX* at the beginning increased with increased values of *C*. After reaching the value of *C* = 0.55 where the maximum is obtained, a decrease in the ratio can be observed.

Determination of the values of  $\alpha$  for which the mean value of  $\dot{\phi}/\omega^2$  is obtained as a function of *C* during the period  $0 \leq \alpha \leq \pi/2$ , can be found from a numerical solution of the equation:

$$\frac{\cos \alpha \cdot \{C^{-2} + \sin^2 \alpha \cdot (C^{-2} - 1)^{1/2}\}}{(C^{-2} - \sin^2 \alpha)^2} = 2/\pi \cdot (C^{-2} - 1)^{1/2} \quad (4.36)$$

In Fig. 4.7 the relation between the mean value of the angular or tangential acceleration and  $\alpha$  is shown. At increasing values of *C*, the values of  $\alpha$  – for which the mean value of the tangential acceleration is obtained – are increasing also. In the range  $0.408 \leq C \leq 0.7$  the values for  $\alpha$ , at which the maximum tangential accelerations are obtained, increase relatively rapidly.

The conclusion can be drawn that the tangential acceleration of the sprout shows an increasing two-peak shape on a higher level at increased values of *C*. An increase of the value of *C* leads to increasing values of the angle of oscillation and to an increasing level of the potential energy source of the sprout since angular velocity will also increase to higher levels. However, since part of the

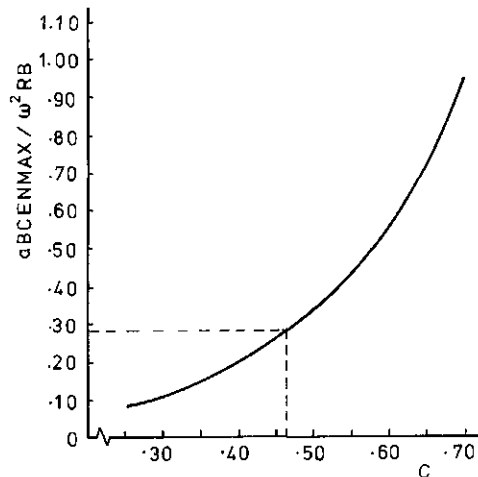


FIG. 4.10. The maximum centripetal acceleration (expressed by the ratio *aBCENMAX*/ $\omega^2 \cdot RB$ ) as a function of *C*.

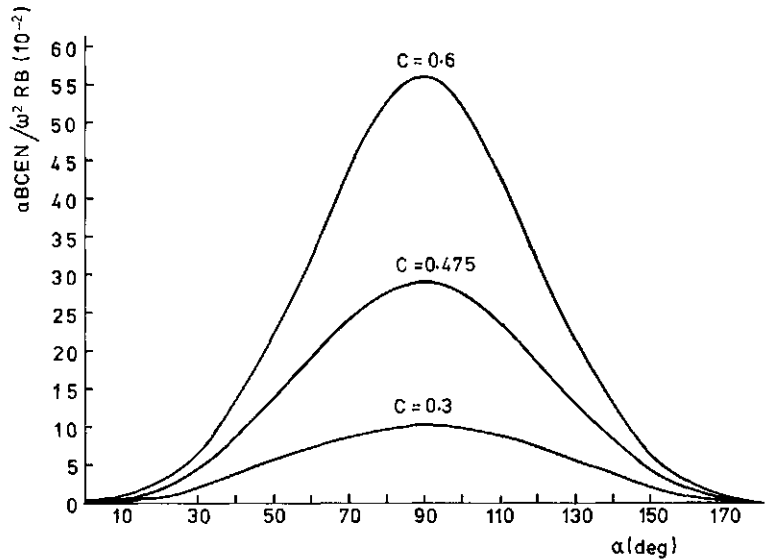


FIG. 4.11. The centripetal acceleration (expressed by the ratio  $aBCENMAX/\omega^2 \cdot RB$ ) as a function of the angle of rotation  $\alpha$  for three values of  $C$ .

mass forces of the distributor device are related to the tangential accelerations, it is expected that a more complex character of  $\dot{\phi}/\omega^2$  will lead to more complications in equilibrating the distributor system.

#### 4.2.2.4. Centripetal acceleration in relation to $C$ and $\alpha$

Centripetal acceleration  $aBCEN$  can be written as:

$$aBCEN/\omega^2 \cdot RB = (C^{-2} - 1) \cdot \sin^2 \alpha / (C^{-2} - \sin^2 \alpha)^2 \quad (4.37)$$

The conclusion can be easily drawn that its maximum value is obtained for the value of  $\alpha$ , for which  $VBTAN$  is maximal. As this was found for  $\alpha = \pi/2$  the maximum value for the centripetal acceleration can be found from:

$$aBCENMAX/\omega^2 \cdot RB = 1/(C^{-2} - 1) \quad (4.38)$$

The curve for the value of  $aBCENMAX/\omega^2 \cdot RB$  as a function of  $C$  is given in Fig. 4.10. Its values increase relatively strongly at increased values of  $C$ . Fig. 4.11 shows curves for  $aBCEN/\omega^2 \cdot RB$  as a function of  $\alpha$  for values of  $C = 0.3, 0.475$  and  $0.6$ . The mean value of the centripetal acceleration during the period  $0 \leq \alpha \leq \pi/2$  can be found from:

$$aBCENGEM/\omega^2 \cdot RB = (C^{-2} - 1) \cdot \frac{2}{\pi} \int_{\alpha=0}^{\pi/2} \frac{\sin^2 \alpha}{(C^{-2} - \sin^2 \alpha)^2} \cdot d\alpha \quad (4.39)$$

Integration yields to:

$$aBCENGEM/\omega^2 \cdot RB = C^2/2 \cdot (1 - C^2)^{1/2} \quad (4.40)$$

The ratio between mean and maximum values of the centripetal acceleration is found from:

$$a_{BCENGEM}/a_{BCENMAX} = (1 - C^2)^{1/2}/2 \quad (4.41)$$

The decrease in the ratio between both values at increased values of  $C$  is given in Table 4.2. From Eq. (4.37) and (4.40), the value of  $\alpha$  for which  $a_{BCEN} = a_{BCENGEM}$ , can be calculated for different values of  $C$ . Solution of:

$$C^2/2 \cdot (1 - C^2)^{1/2} = (C^{-2} - 1) \cdot \sin^2 \alpha / (C^{-2} - \sin^2 \alpha)^2$$

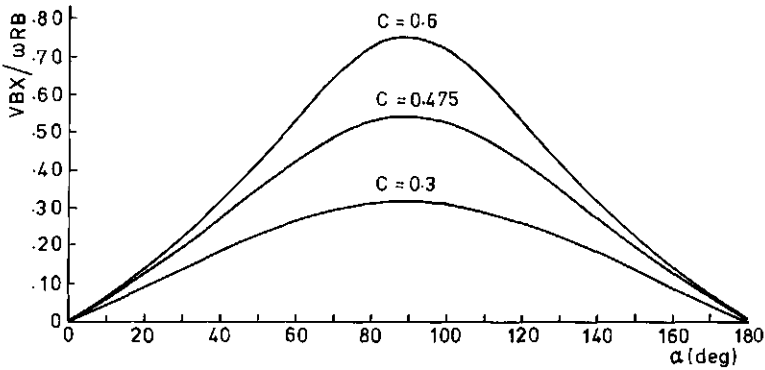


FIG. 4.12. Curves for the X-velocity component of the sprout (expressed by the ratio  $V_{BX}/\omega \cdot RB$ ) as a function of the angle of rotation  $\alpha$  for three values of  $C$ .

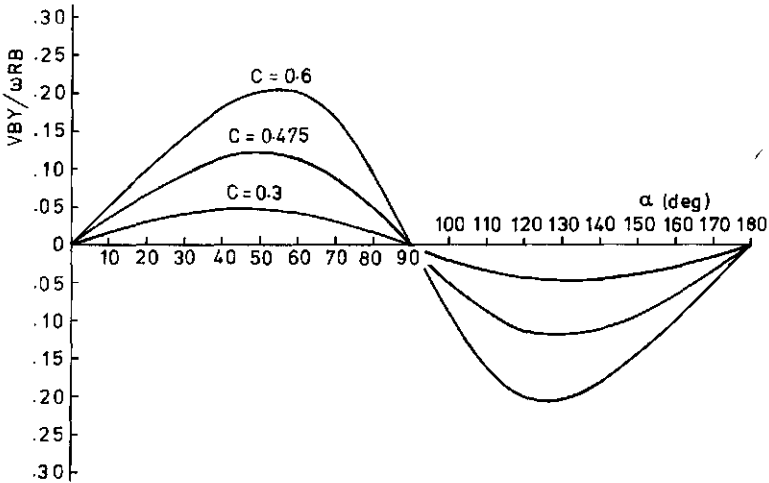


FIG. 4.13. Curves for the Y-velocity component of the sprout (expressed by the ratio  $V_{BY}/\omega \cdot RB$ ) as a function of the angle of rotation  $\alpha$  for three values of  $C$ .

yields to:

$$\alpha = \text{asin} \left[ \frac{-\{2 \cdot (1 - C^2)\}^{3/8} + \{2 \cdot (1 - C^2)^{3/2} + 4 \cdot C^2\}^{1/2}}{2 \cdot C^2} \right] \quad (4.42)$$

The value of  $\alpha$ , for which the mean value is obtained, increases from  $\alpha = 46.3^\circ$  to  $53.3^\circ$  as  $C$  increases from 0.3 to 0.7.

#### 4.2.2.5. The velocity components in X- and Y-direction

The components of the tangential velocity in X- and Y-direction can be derived from Eq. (4.14) and (4.16). Hence:

$$VBX / \omega \cdot RB = (C^{-2} - 1) \cdot \sin \alpha / (C^{-2} - \sin^2 \alpha)^{3/2} \quad (4.43)$$

and:

$$VBY / \omega \cdot RB = \sin \alpha \cdot \cos \alpha \cdot (C^{-2} - 1)^{1/2} / (C^{-2} - \sin^2 \alpha)^{3/2} \quad (4.44)$$

The values of these velocity components as a function of  $\alpha$  are presented in Fig. 4.12 and 4.13 for values of  $C = 0.3, 0.475, \text{ and } 0.6$ .

### 4.3. SIMULATION OF THE OSCILLATION PATTERN

The above description of the oscillation pattern is based on the principle of a constant rotation  $\omega$  of the driving shaft. As was described in the previous sections, the tangential acceleration (and as a result, the loading forces acting in the system) is variable with time. There are different possibilities available for the limitation of the vibrations which may be introduced in the system (VAN SANTEN, 1950). In the driving system of the reciprocating sprout broadcaster, a combination of flywheel and elastic coupling is used. In addition, the oscillating bowl is provided with a counterweight. In order to obtain more information about the effect of these provisions on the oscillation pattern, a number of simulation experiments were performed (BOSMA, 1976; CLEINE and YZERMAN, 1976). These experiments were made with the aid of the so-called bondgraph method (VAN DIXHOORN, 1972) and the simulation language THT-SIM.

#### 4.3.1. Experiments

In Fig. 4.14 a schematic presentation of the physical model is given, as well as the bondgraph of the system. In this conception the energy source consists of an ideal F-source, which value is assumed to be independent of the acting load. Under normal conditions the curve for the relation between couple and number of revolutions should be taken into consideration. However, the overdimensioning of the source seems to fit the assumption. The starting number of revolutions  $\Omega_1$  of the driving shaft is described by means of a first order system (F.I.O.). The time constant  $\tau$  is set at 0.3 so that after 1.5 s the number of revolutions reached more than 99% of their final value. The elastic coupling is considered as a torsian spring ( $K$ ) with a known spring characteristic. The mass moment of inertia of the



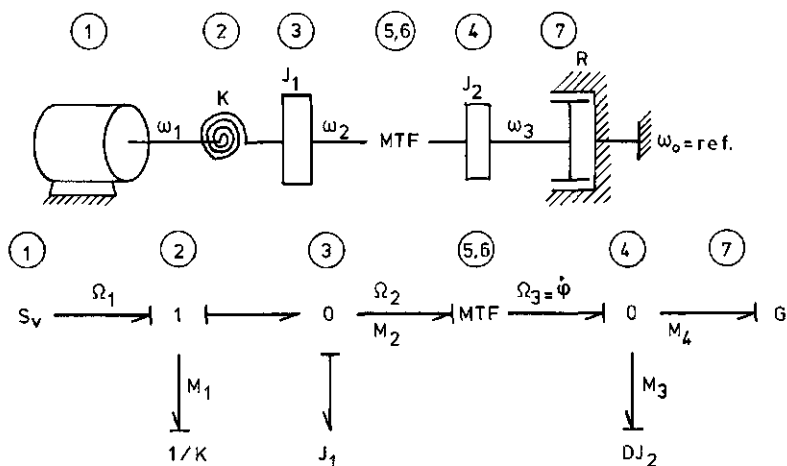


FIG. 4.14. Physical model and bondgraph of the oscillating distributor device. Values of the construction parameters;  $\omega_1$ :  $56.54 \text{ rad s}^{-1}$ ,  $1/K$ :  $0.00105 \text{ rad/N m}$ ,  $J_1$ :  $0.244 \text{ m}^2 \text{ kg}$ ,  $J_2$ :  $0.192 \text{ m}^2 \text{ kg}$ ,  $G$ :  $0.011 \text{ N m s rad}^{-1}$ ,  $C = 0.475$ .

flywheel is presented by  $J_1$ ; the sum of the mass moments of inertia of the sprout, bowl, counterweight and forked connection is represented by  $J_2$ . The rotational motion in the model is transferred to an oscillating one by means of a multigate transformer (M.T.F.). In the bondgraph shown in Fig. 4.14,  $J_2$  was included as a differentiated moment of inertia. The value of  $G$  was estimated from the kinetic energy of the mass flow inside the sprout. The gear ratio  $\dot{\phi}/\Omega_3$  could be derived from Eq. (4.4).

#### 4.3.2. Experimental results

The differences between simulated and calculated values of  $\phi$ ,  $\dot{\phi}$ , and  $\ddot{\phi}$  for  $C = 0.475$  are given in Table 4.3. The period is limited by  $t = t_{stationary} = 2.00 \text{ s}$  to  $t = 2.25 \text{ s}$ . Determination of  $t_{stationary}$  is based on review of the curves which were obtained for  $\phi_{simulated}$ . As will be explained later, the choice of  $\phi_{simulated}$  appeared to have consequences for the curves of  $\dot{\phi}_{simulated}$  and therefore for the calculation of the values of the differences between  $\phi_{simulated}$  and  $\dot{\phi}_{computed}$ .

From Table 4.3 it can be seen that for  $\phi = \text{maximal}$  when  $t = 0.025 (0.055) 0.245 \text{ s}$ , the mean absolute differences between  $\phi_{simulated}$  and  $\phi_{computed}$  can be estimated at 2% based on the computed values. This corresponds with  $0.011 \text{ rad} \approx 0.6^\circ$ . The mean absolute differences between  $\dot{\phi}_{simulated}$  and  $\dot{\phi}_{computed}$  when  $\dot{\phi} = \text{maximal}$ , are for  $t = 0.0525 (0.0550) 0.2175 \text{ s}$  about 11% or  $3.3 \text{ rad s}^{-1}$  based on  $\dot{\phi}_{computed}$ . For  $\ddot{\phi}_{max}$  it holds that the mean absolute differences for  $t = 0.025 (0.055) 0.245 \text{ s}$  are about 16% or  $349 \text{ rad s}^{-2}$ . The simulated oscillation pattern shows an asymmetrical character (Fig. 4.15). The criteria for the choice of  $t_{stationary}$  possibly contribute to an overestimation of the differences between computed and simulated values of  $\dot{\phi}$  since the large differences between

TABLE 4.3. Differences between simulated and computed values of  $\phi$ ,  $\dot{\phi}$  and  $\ddot{\phi}$ .  $C=0.475$ , other parameters according to Fig. 4.14.  $\phi_{com}$ ,  $\dot{\phi}_{com}$  and  $\ddot{\phi}_{com}$  according to Eq. (4.21), (4.31) and (4.30). Maximum values of  $\phi_{com}$ ,  $\dot{\phi}_{com}$  and  $\ddot{\phi}_{com}$  resp.: 0.495 rad (28.36°); 30.52 rad s<sup>-1</sup> and 1458.0 rad s<sup>-2</sup>.

$t-2$ (s)	$\phi_{sim} - \phi_{com}$ (rad)	$\dot{\phi}_{sim} - \dot{\phi}_{com}$ (rad s <sup>-1</sup> )	$\ddot{\phi}_{sim} - \ddot{\phi}_{com}$ (rad s <sup>-2</sup> )
0.00	-0.048	3.70	92.2
0.01	-0.011	3.11	-165.1
0.02	0.010	1.39	-171.7
0.03 $\phi_{max}$	0.015	-0.54	-221.4
0.04	-0.001	-2.92	-195.3
0.05	-0.034	-2.72	370.9
0.06	-0.037	2.53	541.8
0.07	-0.000	3.52	-289.3
0.08 $\phi_{max}$	0.011	-1.76	-602.5
0.09	-0.030	-5.49	-42.1
0.10	-0.070	-1.18	657.3
0.11	-0.051	3.98	163.9
0.12	-0.011	3.28	-220.5
0.13	0.010	1.15	-190.7
0.14 $\phi_{max}$	0.013	-0.59	-174.7
0.15	-0.002	-2.39	-155.3
0.16	-0.029	-2.43	286.8
0.17	-0.032	2.15	526.9
0.18	0.002	3.37	-250.2
0.19 $\phi_{max}$	0.012	-1.62	-583.9
0.20	-0.026	-5.39	-72.1
0.21	-0.067	-1.40	660.4
0.22	-0.049	4.11	196.3
0.23	-0.008	3.29	-269.2
0.24 $\phi_{max}$	0.011	0.84	-196.9
0.25	0.012	-0.62	-117.9

$\dot{\phi}_{simulated}$  and  $\dot{\phi}_{computed}$  (which are found for  $t = 0.08$  and  $0.19$  s) have to be taken into consideration.

The absolute differences between  $\phi_{simulated}$  and  $\phi_{computed}$  for  $\phi = 0$  and  $t = 0.0525$  (0.0550) 0.2175 s yield to a mean value of about 0.041 rad or 2.30° with respect to the computed values. For  $\dot{\phi} = 0$  and  $t = 0.025$  (0.055) 0.245 s the mean absolute differences between  $\dot{\phi}_{simulated}$  and  $\dot{\phi}_{computed}$  are about 1 rad s<sup>-1</sup>. For  $\ddot{\phi} = 0$  and  $t = 0.0525$  (0.0550) 0.2175 s the mean absolute differences are about 258 rad s<sup>-2</sup>. The variation in differences between  $\dot{\phi}_{simulated}$  and  $\dot{\phi}_{computed}$  which was noticed for  $\dot{\phi} = \text{maximal}$  has decreased considerably.

### 4.3.3. Measurement of the oscillation pattern of the distributor device

#### 4.3.3.1. Materials and methods

The experiments performed had the following objectives:

- to obtain information about the oscillation pattern of the distributor device; for this reason a distribution unit was placed in a laboratory set-up (Fig. 4.16) in order to examine the theoretical relationships of section 4.2.1 on their usefulness.

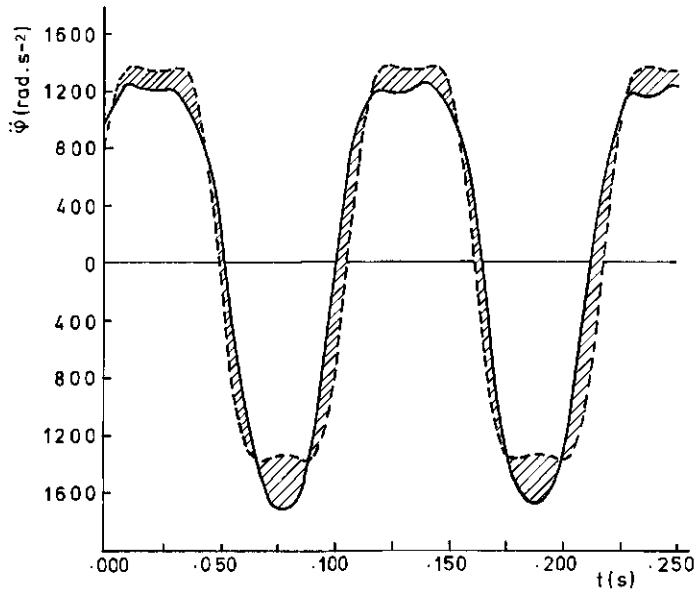


FIG. 4.15. Curves of  $\ddot{\psi}_{\text{simulated}}$  (—) and  $\ddot{\psi}_{\text{computed}}$  (---) for  $C: 0.475$  and  $\omega_1: 56.54 \text{ rad s}^{-1}$ . (Other construction parameters according to Fig. 4.14.)

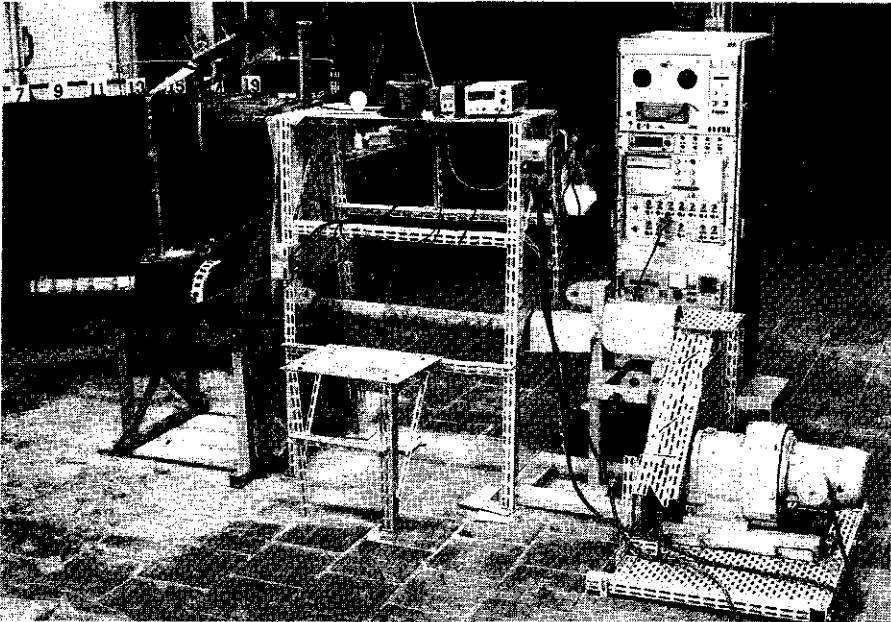


FIG. 4.16. Representation of the laboratory set-up for examination of the oscillation characteristics of the sprout.

b. to perform a more practical analysis of the oscillation pattern of the distribution device in the tractor-mounted broadcaster system. A rather simple method was used to examine the oscillation pattern of the distributor device in accordance with the first objective. The angle of oscillation  $\phi$  as a function of  $\omega \cdot t$  was recorded with the aid of a potentiometer connected with the oscillation point  $P$  (see also Fig. 4.1). The angle of oscillation was recorded by means of a U.V. recorder (Honeywell; type 2206/AC). Furthermore, the angular acceleration  $\ddot{\phi}$  was measured by the tangential attachment of an accelerometer on the sprout.

Determination of the oscillation pattern in accordance with the second objective was performed by measuring the tangential and centripetal accelerations ( $a_{BTAN}$  and  $a_{BCEN}$ ). Measurements were achieved with the aid of piëzo-electric accelerometers (Bruehl and Kjaer; type 4332). A disadvantage of this method was the fact that the conversion to a purely quantitative description of the oscillation characteristic was difficult due to the amplification factors which had to be used. In this respect, it should be noted that in our experiments a value of  $1000 \text{ m s}^{-2}$  corresponded with a paper width of  $0.125 \text{ m}$ . Vibrations with a frequency  $> 9 \text{ Hz}$  disturbed the recorded oscillation pattern. In addition it should be noted that the accelerometer must be attached accurately in order to avoid the wrong conclusion that the oscillation pattern shows either symmetry or asymmetry.

#### 4.3.3.2. Experimental results

As an example, Fig. 4.17 shows a part of the recorded values of  $\phi$  and  $\ddot{\phi}$ . Comparison between the measured values according to objective a, and the

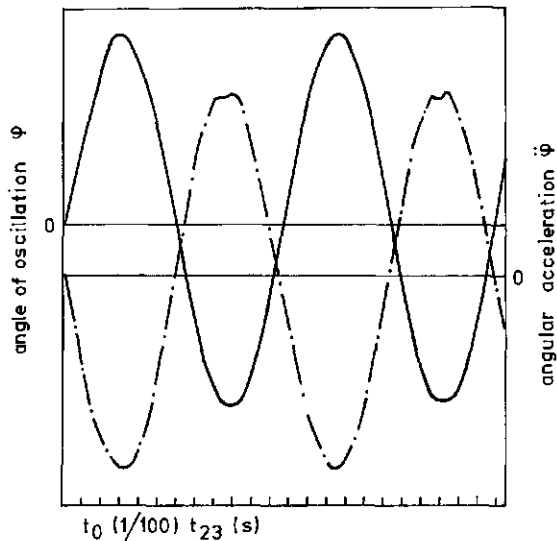


FIG. 4.17. Example of a part of the recorded values of  $\phi$  (—) and  $\ddot{\phi}$  (- · -), obtained from the laboratory experiments.  $C: 0.475, \omega_1 = 56.54 \text{ rad s}^{-1}$ .

computed values obtained with Eq. (4.1) shows that at the moments  $t = 0.01$  (0.01) 0.11 s, there are differences between the measured and computed values for  $\phi$ . Generally the absolute differences are smaller than those found between  $\phi_{\text{simulated}}$  and  $\phi_{\text{computed}}$  (Fig. 4.18). Especially for  $t = 0.08$  and 0.09 s, or  $\alpha = 260-290^\circ$ , the absolute differences between both values are considerable. As a result, the largest differences between  $\phi_{\text{measured}}$  and  $\phi_{\text{simulated}}$  are found at the same moments (0.065 rad  $\approx 3.7^\circ$ ). Otherwise, the mean difference between  $\phi_{\text{measured}}$  and  $\phi_{\text{simulated}}$  during the considered period, as it was computed from Table 4.3, is on the same level as that between  $\phi_{\text{measured}}$  and  $\phi_{\text{computed}}$  (0.013 rad  $\approx 0.75^\circ$ ).

Even more clearly, a similar tendency can be noticed between the curves for  $\ddot{\phi}_{\text{measured}}$  and  $\ddot{\phi}_{\text{simulated}}$  (compare Fig. 4.15 and Fig. 4.20). As was mentioned before, asymmetry for  $\ddot{\phi}_{\text{simulated}}$  may be over-estimated for  $\ddot{\phi} = \text{maximal}$ . Accurate examination of the measured values of  $\ddot{\phi}$  as they were recorded with the aid of the accelerometers, also shows a certain rate of asymmetry.

In Fig. 4.19a and Fig. 4.19b the tangential acceleration, and so the characteristic of  $\ddot{\phi}$ , is given for the combination tractor-mounted broadcaster, depending on the number of revolutions of the driving shaft. The recorded oscillation pattern shows an increased deviation from the computed one when the rotary frequency  $N$  of the driving shaft deviates more from the nominal value of  $540 \text{ min}^{-1}$ ; in addition, the oscillation pattern is more irregular. This can be

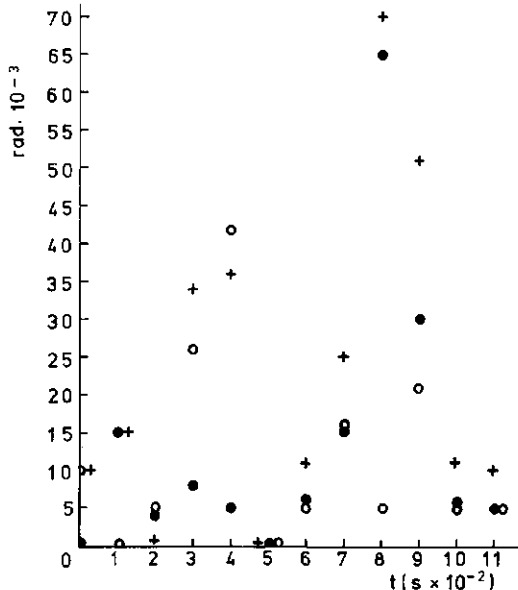


FIG. 4.18. Absolute values of the differences between:  $\phi_{\text{measured}} - \phi_{\text{simulated}}$  (●),  $\phi_{\text{measured}} - \phi_{\text{computed}}$  (○) and  $\phi_{\text{simulated}} - \phi_{\text{computed}}$  (+);  $C = 0.475$ ,  $\omega_1 = 56.54 \text{ rad s}^{-1}$ . (Other construction parameters according to Fig. 4.14.)

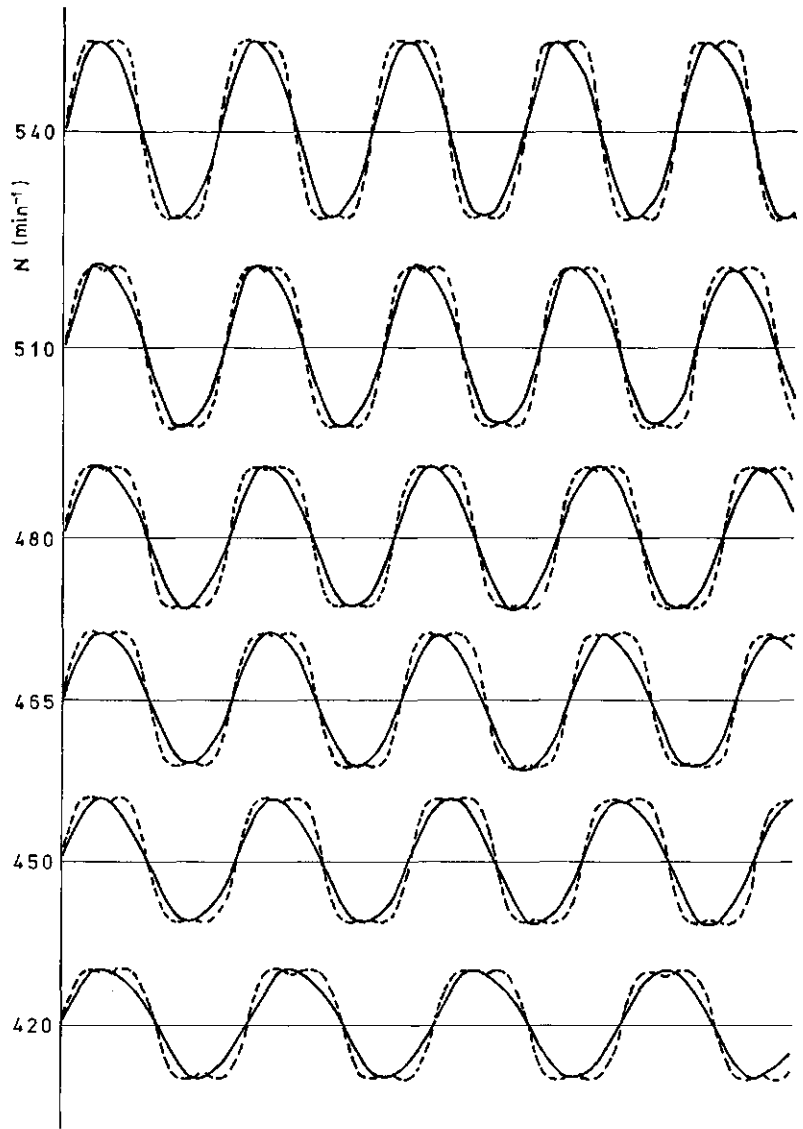


FIG. 4.19a. Oscillation characteristic of the sprout in a stationary set-up of the distribution device represented by the curve for the tangential acceleration (—), at various rotary frequencies  $N$  of the driving shaft. Calculated values are indicated by: - - -.

explained by the fact that the construction and balance of the distributor system is based on that nominal number of revolutions. Trials which were performed by the manufacturer have proved that irregularities in the oscillation pattern act negatively on the evenness of the transverse distribution pattern (BAECKE, 1976).

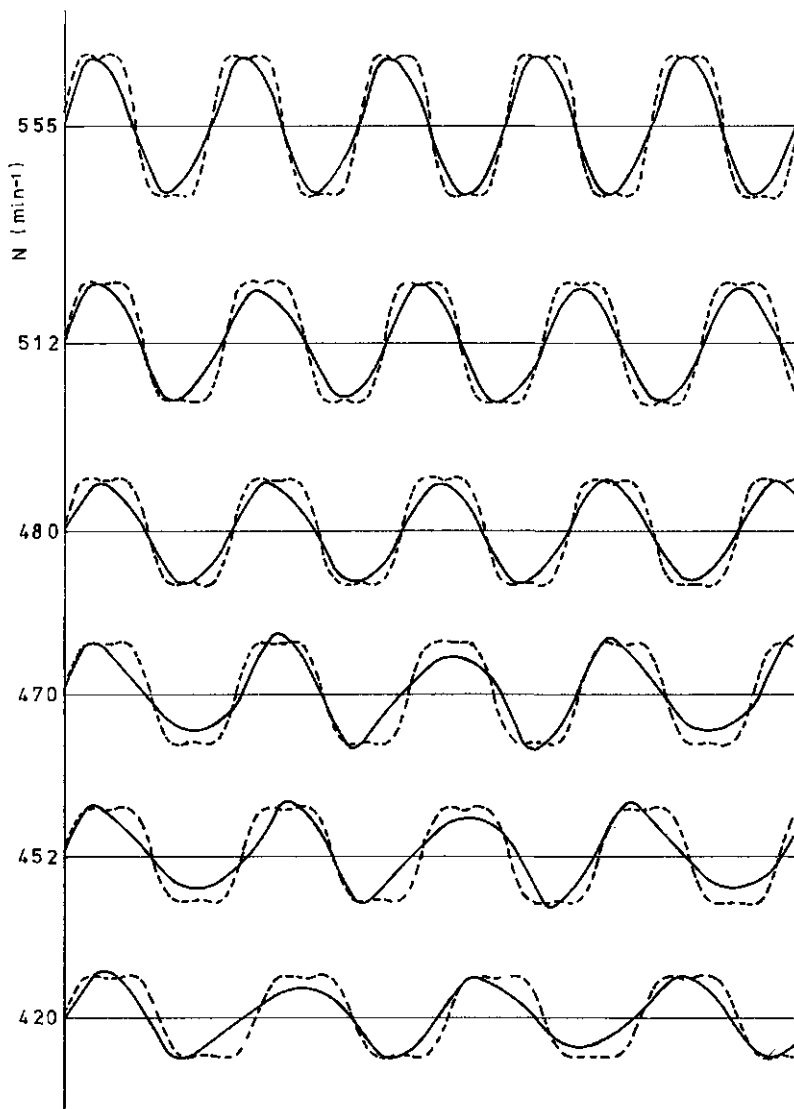


FIG. 4.19b. Oscillation characteristic of the sprout of a driving tractor-mounted broadcaster, represented by the curve for the tangential acceleration (—), at various rotary frequencies  $N$  of the driving shaft. Calculated values are indicated by: ---.

#### 4.3.4. Influence of construction variables on the oscillation pattern

##### 4.3.4.1. Introduction

In section 4.2.2 it was indicated to what extent the oscillation pattern theoretically changes when the values of  $RB$ ,  $\omega$  and  $C(= RA/L)$  were varied. In that section the possible effects of the flywheel, elastic coupling, and the mass moments of inertia were ignored.

Section 4.3.3.2 showed that the simulation experiments gave results which were different from those obtained from the laboratory experiments. Taking into consideration the fact that these differences were highly dependent on only one high value for  $t = 0.08$  (see Fig. 4.18), it seemed to be a reasonable conclusion that this simulation technique could be used to obtain information about the effects which could be expected when changing some system variables. Against this background, additional simulation experiments were performed using the methods which were described in sections 4.3 and 4.3.1 above.

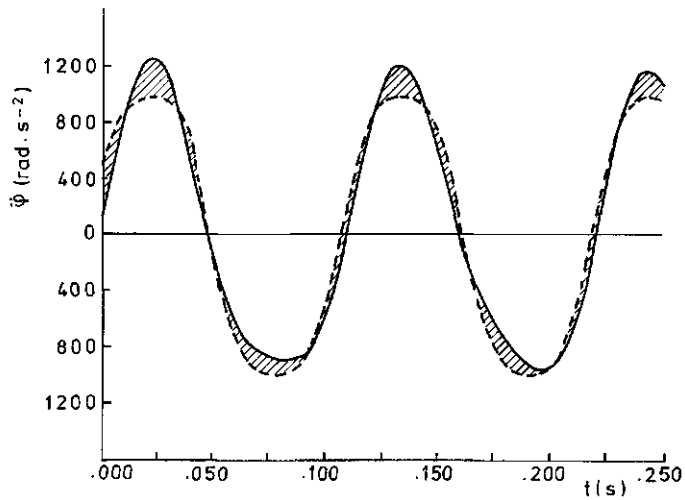


FIG. 4.20. Curves of  $\ddot{\phi}_{\text{simulated}}$  (—) and  $\ddot{\phi}_{\text{computed}}$  (---) at values for  $C: 0.325$ ,  $\omega_1: 56.54$   $\text{rad s}^{-1}$ , and  $G: 0.617$   $\text{N m s rad}^{-1}$ .

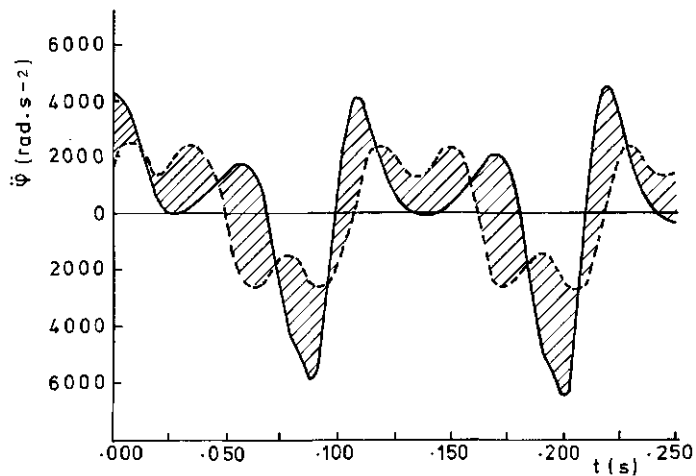


FIG. 4.21. Curves of  $\ddot{\phi}_{\text{simulated}}$  (—) and  $\ddot{\phi}_{\text{computed}}$  (---) at values for  $C: 0.630$ ,  $\omega_1: 56.54$   $\text{rad s}^{-1}$ , and  $G: 0.617$   $\text{N m s rad}^{-1}$ .



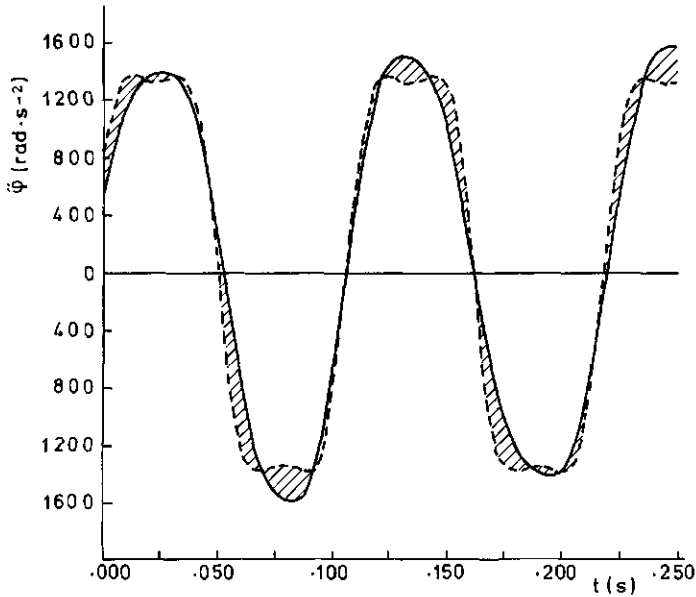


FIG. 4.22. Curves of  $\phi_{\text{simulated}}$  (—) and  $\phi_{\text{computed}}$  (---) at values for  $K$ :  $400 \text{ N m rad}^{-1}$ ,  $C$ :  $0.475$ ,  $G$ :  $0.617 \text{ N m s rad}^{-1}$ , and  $\omega_1$ :  $56.54 \text{ rad s}^{-1}$ .

#### 4.3.4.2. Values of the system variables

a. For a value of  $C = 0.475$  the influence of the size of the mass flow in the sprout on the oscillation pattern was examined. Mass flows were  $1 \text{ kg s}^{-1}$  and  $3 \text{ kg s}^{-1}$  resulting in values for  $G = 0.206 \text{ N m s rad}^{-1}$  and  $0.617 \text{ N m s rad}^{-1}$ . All other variables were kept at the same level as given in Fig. 4.14.

b. For  $G = 0.617 \text{ N m s rad}^{-1}$ , the value of  $C$  was varied according to  $C = 0.325$  resulting in a value of  $\phi_{\text{max}} = 0.331 \text{ rad} \approx 19^\circ$ , and  $C = 0.630$  resulting in  $\phi_{\text{max}} = 0.681 \text{ rad} \approx 39^\circ$ . Similar to a, all other variables were kept at the same levels.

c. Of spring constant  $K$ , the original value of  $952 \text{ N m rad}^{-1}$  was reduced to  $400 \text{ N m rad}^{-1}$ . Values for  $C$  were  $0.475$  and for  $G$ :  $0.617 \text{ N m s rad}^{-1}$ . All other system variables were the same as for a.

d. The mass moment of inertia of the flywheel, having an original value of  $0.244 \text{ m}^2 \text{ kg}$ , was varied according to  $J_1 = 0.100$  and  $0.500 \text{ m}^2 \text{ kg}$ , with  $C = 0.475$  and  $G = 0.617 \text{ N m s rad}^{-1}$ . All other variables were the same as for a.

#### 4.3.4.3. Experimental results

a. Change of mass flow does not contribute to a change of the oscillation pattern. A value of  $G = 0.011 \text{ N m s rad}^{-1}$ , which was derived from the maximum kinetic energy of a mass of  $0.060 \text{ kg}$  at a distance  $RB = 0.55 \text{ m}$  from the oscillation centre  $P$ , results in a mean absolute difference between  $\phi_{\text{simulated}}$  and  $\phi_{\text{computed}}$  of  $0.024 \text{ rad}$ . A mass flow of  $1 \text{ kg s}^{-1}$  which results in a value of  $G = 0.206 \text{ N m s rad}^{-1}$  as well as one of  $3 \text{ kg s}^{-1}$  ( $G = 0.617 \text{ N m s rad}^{-1}$ ) yields

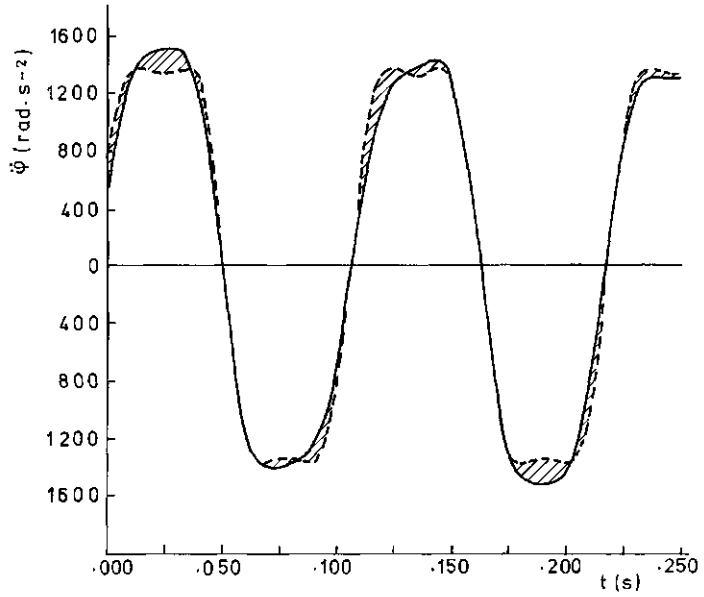


FIG. 4.23. Curves of  $\ddot{\phi}_{\text{simulated}}$  (—) and  $\ddot{\phi}_{\text{computed}}$  (---) at values for  $J_1$ : 0.500 m<sup>2</sup> kg,  $C$ : 0.475,  $G$ : 0.617 N m s rad<sup>-1</sup>, and  $\omega_1$ : 56.54 rad s<sup>-1</sup>

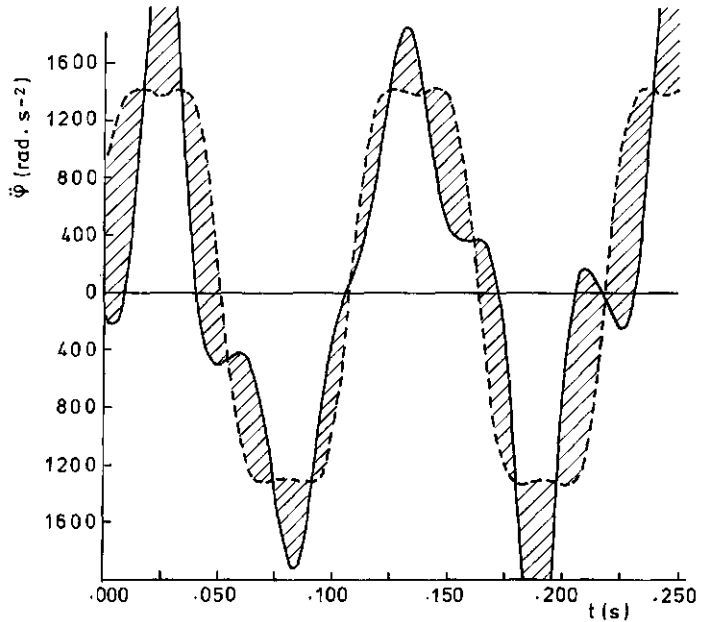


FIG. 4.24. Curves for  $\ddot{\phi}_{\text{simulated}}$  (—) and  $\ddot{\phi}_{\text{computed}}$  (---) at values for  $J_1$ : 0.100 m<sup>2</sup> kg,  $C$ : 0.475,  $G$ : 0.617 N m s rad<sup>-1</sup>, and  $\omega_1$ : 56.54 rad s<sup>-1</sup>.

to the same value of the mean absolute difference (0.025 rad) between  $\phi_{\text{simulated}}$  and  $\phi_{\text{computed}}$ .

b. From Table 4.4 it appears that at increased values of  $C$  the differences between simulated and computed values of  $\phi$ ,  $\dot{\phi}$  and  $\ddot{\phi}$  increase. During the period  $t = 2$  to 2.25 s the mean absolute differences between  $\phi_{\text{simulated}}$  and  $\phi_{\text{computed}}$  are with  $C = 0.325, 0.475$  and  $0.630$  resp.: 0.012 rad., 0.023 rad., and 0.195 rad. Expressed as a percentage of  $\phi_{\text{max}}$ , the differences are 3.6%, 4.6%, 28.6%.

For  $\phi_{\text{simulated}} - \phi_{\text{computed}}$  the following absolute differences can be found 1.06 rad s<sup>-1</sup> or 5.5% with respect to  $\dot{\phi}_{\text{max}}$  ( $C = 0.325$ ); 2.51 rad s<sup>-1</sup> or 8.2% with respect to  $\dot{\phi}_{\text{max}}$  ( $C = 0.475$ ) and 17.05 rad s<sup>-1</sup> or 37.2% with respect to  $\dot{\phi}_{\text{max}}$  ( $C = 0.630$ ).

The mean absolute differences between  $\ddot{\phi}_{\text{simulated}}$  and  $\ddot{\phi}_{\text{computed}}$  are resp.: 132.9 rad s<sup>-2</sup> or 13.5% with respect to  $\ddot{\phi}_{\text{max}}$ ; 286.4 rad s<sup>-2</sup> or 19.6% and 2056.9 rad s<sup>-2</sup> or 97.2% during the same period.

It can be concluded therefore, that especially for values of  $C$  greater than 0.475 considerable deviations from the computed oscillation character of the distributor system have to be expected. From Fig. 4.20 and Fig. 4.21 it can be concluded that these deviations must be considered a disturbing element in the oscillation characteristics especially for  $\dot{\phi}$ . Therefore, they act as a potential source for irregularities in the distribution pattern. A considerable increase of the angle of oscillation  $\phi$  over 28.36°, requires an appropriate correction in design of other system parameters.

c. In its present design, with a value for  $C = 0.475$  and  $\omega = 56.54$  rad s<sup>-1</sup>, the value of the spring constant  $K = 952$  N m rad<sup>-1</sup>. Decrease of the value of the spring constant to 400 N m rad<sup>-1</sup> yields to a decrease of the mean absolute differences between simulated and computed values for  $\phi$ ,  $\dot{\phi}$  and  $\ddot{\phi}$ . The values are resp.: 0.012 rad (for  $K = 952$  N m rad<sup>-1</sup>: 0.023 rad), 1.17 rad s<sup>-1</sup> (2.51 rad s<sup>-1</sup>) and 160.8 rad s<sup>-2</sup> (286.4 rad s<sup>-2</sup>). The complete results of these series of experiments during the period  $t = 2$  to 2.25 s are presented in Table 4.5. Comparison of Fig. 4.15 and 4.22 leads to the expectation that decreasing values of  $K$  contribute to improvement of the symmetry of the characteristic of the angular acceleration  $\ddot{\phi}$ . The two-peak character of  $\ddot{\phi}_{\text{computed}}$ , which is related to the value of  $C = 0.475$ , disappears.

d. From Table 4.6 it can be seen that an increase of the value of the mass moment of inertia  $J_1$  of the flywheel from 0.244 to 0.500 m<sup>2</sup> kg positively affects the oscillation pattern. Mean absolute differences between simulated and computed values of  $\phi$ ,  $\dot{\phi}$  and  $\ddot{\phi}$  are decreased to resp.: 0.010 rad, 0.82 rad s<sup>-1</sup> and 100.8 rad s<sup>-2</sup>. The symmetry of the angular acceleration pattern improves. The two-peak characteristic disappears (Fig. 4.23). A decrease of the mass moment of inertia to a value of 0.100 m<sup>2</sup> kg appears to act in a very negative way on the oscillation pattern (Fig. 4.24).

TABLE 4.4. Differences between simulated and computed values of  $\phi$ ,  $\dot{\phi}$  and  $\ddot{\phi}$  dependent on the value  $C (= RA/L)$ .

$t-2$	$\phi_{sim} - \phi_{com} \text{ (rad)}$			$\dot{\phi}_{sim} - \dot{\phi}_{com} \text{ (rad s}^{-1}\text{)}$			$\ddot{\phi}_{sim} - \ddot{\phi}_{com} \text{ (rad s}^{-2}\text{)}$		
	$C = 0.325$	$C = 0.475$	$C = 0.630$	$C = 0.325$	$C = 0.475$	$C = 0.630$	$C = 0.325$	$C = 0.475$	$C = 0.630$
.00	.031	-.048	-.294	-0.22	3.69	-10.91	-280.7	92.2	2102.1
.01	.018	-.012	-.129	-2.03	3.13	17.93	-71.3	-170.3	-277.7
.02	.001	.010	.014	-0.87	1.34	9.27	234.8	-178.4	-1210.5
.03	.005	.014	.037	1.53	-0.61	-5.35	184.6	-220.1	-1644.6
.04	.024	-.003	-.100	1.58	-2.98	-22.15	-133.8	-194.3	-1564.8
.05	.028	-.036	-.368	-0.68	-2.81	-26.69	-188.9	366.2	1205.8
.06	.015	-.040	-.512	-1.67	2.48	2.43	32.1	557.1	3823.5
.07	.001	-.002	-.321	-0.77	3.72	31.34	135.3	-263.8	1365.4
.08	.000	.011	-.029	0.50	-1.49	19.67	112.5	-612.5	-2891.0
.09	.009	-.027	-.007	1.30	-5.45	-16.72	37.3	-70.7	-3812.5
.10	.023	-.068	-.270	1.09	3.94	-24.36	-116.2	657.7	2308.5
.11	.026	-.050	-.343	-0.58	-1.30	10.09	-232.6	172.8	2873.3
.12	.013	-.010	-.161	-1.82	3.27	21.07	-21.5	-224.2	204.8
.13	.000	.010	.011	-0.40	1.09	11.51	232.5	-193.6	-1374.6
.14	.007	.013	.049	1.71	-0.64	-4.63	135.8	-169.9	-1758.6
.15	.024	-.002	-.087	1.28	-2.40	-22.49	-174.7	-153.9	-1728.0
.16	.025	-.030	-.373	-1.16	-2.50	-30.65	-185.5	276.6	686.7
.17	.008	-.034	-.572	-1.82	2.05	-3.44	88.3	535.4	4094.4
.18	.003	-.000	-.412	-0.38	3.50	32.39	175.4	-220.9	2320.4
.19	.000	.013	-.069	0.90	-1.33	26.92	79.6	-583.3	-2886.3
.20	.010	-.024	.013	1.09	-5.28	-13.01	-33.9	-99.3	-4531.0
.21	.019	-.064	-.266	0.42	-1.49	-30.39	-121.5	652.2	1901.8
.22	.017	-.047	-.388	-0.80	4.04	8.37	-156.5	202.3	3677.5
.23	.005	-.007	-.193	-1.35	3.23	23.95	21.5	-271.4	-95.1
.24	.002	.012	.006	0.06	0.76	13.66	196.0	-198.2	-1527.0
.25	.007	.011	.057	1.60	-0.67	-3.84	72.7	-111.3	-1847.8

$C = 0.325$ :  $\phi_{max} = 0.331 \text{ rad} = 18.97^\circ$ ;  $\dot{\phi}_{max} = 19.43 \text{ rad s}^{-1}$ ;  $\ddot{\phi}_{max} = 982.9 \text{ rad s}^{-2}$   
 $C = 0.475$ :  $\phi_{max} = 0.495 \text{ rad} = 28.36^\circ$ ;  $\dot{\phi}_{max} = 30.52 \text{ rad s}^{-1}$ ;  $\ddot{\phi}_{max} = 1458.0 \text{ rad s}^{-2}$   
 $C = 0.630$ :  $\phi_{max} = 0.681 \text{ rad} = 39.02^\circ$ ;  $\dot{\phi}_{max} = 45.87 \text{ rad s}^{-1}$ ;  $\ddot{\phi}_{max} = 2115.4 \text{ rad s}^{-2}$   
 $\omega_1 = 56.55 \text{ rad s}^{-1}$ ; other construction parameters according to section 4.3.4.2.  
 \* computed with resp. Eq. (4.21), (4.31) and (4.30).

TABLE 4.5. Differences between simulated and computed values of  $\phi$ ,  $\dot{\phi}$ , and  $\ddot{\phi}$  dependent on the spring constant  $K$ .

$t-2$	$\phi_{sim} - \phi_{com}$ (rad)		$\dot{\phi}_{sim} - \dot{\phi}_{com}$ (rad s <sup>-1</sup> )		$\ddot{\phi}_{sim} - \ddot{\phi}_{com}$ (rad s <sup>-2</sup> )	
	$K = 400$ N m rad <sup>-1</sup>	$K = 952$ N m rad <sup>-1</sup>	$K = 400$ N m rad <sup>-1</sup>	$K = 952$ N m rad <sup>-1</sup>	$K = 400$ N m rad <sup>-1</sup>	$K = 952$ N m rad <sup>-1</sup>
(s)						
.00	.001	.048	2.41	3.69	-243.7	92.2
.01	.011	-.012	-.030	3.13	-230.9	-170.3
.02	.002	.010	-1.13	1.34	16.2	-178.4
.03 $\phi_{max}$	-.006	.014	-.072	-.061	23.7	-220.1
.04	-.015	-.003	-1.37	-2.98	-122.5	-194.3
.05	-.035	-.036	-2.08	-2.81	160.7	366.2
.06	-.042	-.040	1.04	2.48	402.9	557.1
.07	-.020	-.002	2.77	3.72	-32.5	-263.8
.08 $\phi_{max}$	.000	.011	-.095	-1.49	-251.3	-612.5
.09	-.001	-.027	-1.36	-5.45	-100.9	-70.7
.10	-.012	-.068	-0.13	-1.30	167.9	657.7
.11	-.004	-.050	0.79	3.94	-123.1	172.8
.12	-.002	-.010	-0.31	3.27	-61.9	-224.2
.13 $\phi_{max}$	-.003	.010	-0.42	1.09	152.2	-193.6
.14	.008	.013	1.75	-0.64	65.5	-169.9
.15	.023	-.002	0.57	-2.40	-279.1	-153.9
.16	.011	-.030	-2.63	-2.50	-136.0	276.6
.17	-.012	-.034	-1.49	2.05	343.5	535.4
.18	-.013	-.000	1.06	3.50	139.5	-220.9
.19 $\phi_{max}$	-.000	.013	-1.19	-1.33	-58.9	-583.3
.20	.003	-.024	0.71	-5.28	-0.8	-99.3
.21	-.019	-.064	1.65	-1.49	90.9	652.2
.22	.037	-.047	1.28	4.04	-307.6	202.2
.23	.033	-.007	-2.01	3.23	-271.7	-271.4
.24	.003	.012	2.22	0.76	157.5	-198.2
.25 $\phi_{max}$	-.002	.011	0.09	-0.67	240.2	-111.3

$C = 0.475$ ;  $\phi_{max} = 0.495$  rad = 28.36°;  $\dot{\phi}_{max} = 30.52$  rad s<sup>-1</sup>;  $\ddot{\phi}_{max} = 1458.0$  rad s<sup>-2</sup>.  
 $\omega_1 = 56.55$  rad s<sup>-1</sup>; other construction parameters according to section 4.3.4.2.

TABLE 4.6. Differences between simulated and computed values of  $\phi$ ,  $\dot{\phi}$ , and  $\ddot{\phi}$  dependent on the value of the mass moment of inertia of the flywheel  $J_1$ .

t-2	$\phi_{sim} - \phi_{com}$ (rad)			$\dot{\phi}_{sim} - \dot{\phi}_{com}$ (rad s <sup>-1</sup> )			$\ddot{\phi}_{sim} - \ddot{\phi}_{com}$ (rad s <sup>-2</sup> )		
	0.100	0.244	$J_1$ (m <sup>2</sup> kg)	0.100	0.244	$J_1$ (m <sup>2</sup> kg)	0.100	0.244	$J_1$ (m <sup>2</sup> kg)
(s)									
.00	.047	-.048	.029	9.62	3.69	-0.12	-861.5	92.2	-297.3
.01	.082	-.012	.018	3.19	3.13	-1.85	-1295.9	-170.3	-56.3
.02	.016	.010	.002	-6.57	1.34	-1.05	728.8	-178.4	157.3
.03 $\phi_{max}$	.013	.014	.000	6.29	-0.61	0.64	1023.1	-220.1	151.4
.04	.082	-.003	.010	3.78	-2.98	1.17	-1106.6	-194.3	-43.1
.05	.060	-.036	.015	-6.97	-2.81	-0.27	-576.5	366.2	-72.9
.06	-.012	-.040	.010	-5.38	2.48	-0.58	732.6	557.1	53.7
.07	-.026	-.002	.005	2.10	3.72	-0.56	524.8	-263.8	-27.4
.08 $\phi_{max}$	.001	.011	-.002	1.59	-1.49	-0.90	-487.5	-612.5	-21.7
.09	-.008	-.027	-.010	-2.55	-5.45	-0.51	67.1	-70.7	110.5
.10	-.018	-.068	-.007	1.48	-1.30	1.42	-523.4	657.7	166.1
.11	.011	-.050	.012	2.98	3.94	1.71	-357.3	172.8	-214.8
.12	.016	-.010	.017	-1.83	3.27	-0.60	-372.6	-224.2	-211.4
.13 $\phi_{max}$	.002	.010	.006	-0.50	1.09	-1.45	486.3	-193.6	2.9
.14	.014	.013	-.006	2.74	-0.64	-0.95	-52.4	-169.9	66.9
.15	.020	-.002	-.013	-2.77	-2.40	-0.45	-790.6	-153.9	35.0
.16	-.039	-.030	-.017	-7.55	-2.50	-0.30	109.2	276.6	112.1
.17	-.085	-.034	-.015	0.15	2.05	-0.90	-1206.4	535.4	160.5
.18	-.036	-.000	-.004	7.39	3.50	1.00	-57.8	-220.9	-93.8
.19	-.002	.013	-.000	-2.57	-1.33	-.48	-1295.7	-983.3	-163.7
.20 $\phi_{max}$	-.061	-.024	-.012	5.67	-5.28	-1.62	699.2	59.3	38.8
.21	-.061	-.064	-.024	6.34	-1.49	-0.44	-1153.0	652.2	200.5
.22	.035	-.047	-.018	10.14	4.04	1.44	519.4	202.3	5.2
.23	.087	-.007	-.006	1.21	2.23	0.82	-1374.6	-271.4	-117.7
.24 $\phi_{max}$	.028	.012	-.001	7.52	0.76	0.18	343.3	-198.2	-27.5
.25	.005	.011	-.000	4.45	-0.67	-0.02	1285.3	-111.3	-30.2

$C = 0.475$ ;  $\phi_{max} = 0.495$  rad = 28.36°;  $\dot{\phi}_{max} = 30.53$  rad s<sup>-1</sup>;  $\ddot{\phi}_{max} = 1458.0$  rad s<sup>-2</sup>.  
 $\omega_1 = 56.55$  rad s<sup>-1</sup>, other construction parameters according to section 4.3.4.2.

#### 4.4. DISCUSSION

The oscillation pattern of the reciprocating sprout broadcaster in its present design can be characterized by: the angular velocity ( $\omega$ ) of the driving shaft, the distance between the centre of the driving shaft and the fastening point of the forked connection ( $RA$ ), the distance ( $L$ ) between the fastening point of the forked connection and the oscillation point ( $P$ ), and – as far as it concerns the values of the velocity and acceleration components of the sprout – the length of the sprout ( $RB$ ).

The value of the angle of oscillation is determined by the ratio between  $RA$  and  $L$ . Increase of this ratio leads to an increase of the value of  $\phi$ . The tangential velocity component of the distributor device is linearly proportional to  $RB$  and  $\omega$ . The tangential acceleration is linearly proportional to  $RB$  and quadratically proportional to  $\omega$ .

A change of the ratio  $RA/L = C$  at constant values of  $\omega$  and  $RB$  not only changes the level of the velocity and acceleration components of the sprout, it also changes the characteristics of their patterns. Increase of the value of  $C$  contributes to increased values of the angular velocity  $\dot{\phi}$ . During a period  $0 \leq \alpha \leq \pi/2$  the ratio between mean and maximum values decreases at increased values of  $C$ . Furthermore, the ratio between the values of  $\alpha$  (for which  $\dot{\phi} = \dot{\phi}_{gem}$  and  $\dot{\phi} = \dot{\phi}_{max}$ ) increases slightly over the range  $C = 0.3$  to  $0.7$ .

The change of  $C$  on the angular accelerations shows the following effects. Within the examined range of values of  $C$ , two trajectories can be distinguished. For values of  $C < 0.408$  a one-peak symmetrical acceleration characteristic arises. The maximum value of  $\ddot{\phi}$  is found for  $\alpha = 0$ . Values of  $C \geq 0.408$  result in a two-peak acceleration characteristic when a period of e.g.  $\pi/2 \leq \alpha \leq 3\pi/2$  is considered. Maximum values of  $\ddot{\phi}$  are found for values of  $\alpha \neq k\pi$  ( $k = 0, 1, 2, \dots, n$ ). At increased values of  $C$ , the values of  $\alpha$  for which  $\ddot{\phi} = \ddot{\phi}_{max}$  deviates more from  $\alpha = 0$ . In addition, the differences between  $\ddot{\phi}_{max}$  and  $\ddot{\phi}(\alpha) = 0$  increase.

Although the interaction between particle dynamics and kinematics of the distributor device is not discussed in the previous sections, a general assumption can be made that a high energy level of the sprout creates favourable opportunities for obtaining a high level of kinetic energy of the particles when leaving the distributor device. Under such conditions, working width can be increased.

Potential sources of particle energy production such as  $VTAN$  and  $aCEN$  move to a higher level at increased values of  $\omega$ ,  $RB$ , and  $C$ , or when a combination of these three variables is used. Since the effect of  $C$  proves to be rather complex, and only hypotheses of particle motion in the sprout are available, at this stage no detailed quantitative predictions can be given with respect to the effects of a higher level of sprout energy on particle movement.

The use of an elastic coupling and a flywheel in the driving mechanism affects the dynamic behaviour of the distributor device. It appears from measurements that there are deviations with respect to the calculated patterns for  $\phi$ ,  $\dot{\phi}$  and  $\ddot{\phi}$ . However, these deviations are of such a character that, in our opinion, it is

justified to use the theoretical kinematic relationships in the next chapter in which particle dynamics will be discussed.

The results of the simulation experiments show that in the present design of this type of broadcaster, an increase of the mass moment of inertia of the flywheel or a decrease of the spring constant of the elastic coupling can contribute to a better symmetrical pattern of the angular acceleration. In practice this would create favourable opportunities for maintenance or even improvement of the symmetry of the transverse fertilizer distribution patterns.

More generally, the simulation technique which was used on a limited scale in this systems analysis can be favourably applied to future machine design, since it can provide information about the effects of the alteration of relevant system variables on system behaviour.



## 5. PARTICLE MOVEMENT IN THE RECIPROCATING SPROUT

### 5.1. INTRODUCTION

During their stay in or on the distribution devices of spinning disc and reciprocating sprout fertilizer broadcasters, kinetic energy must be transmitted to the particles. The increase of the particle energy level on spinning disc broadcasters occurs under the influences of tangential and centrifugal forces at a constant value of the angular velocity of the rotating disc with vanes. The controlling of particle movement on a spinning disc (in the sense of reducing random motions) requires that the material is directed smoothly and without appreciable impact or bounce onto the distribution device (INNS and REECE, 1962; SMEETS, 1964; DOBLER and FLATOW, 1969; GÖHLICH and KESTEN, 1972; DAVIES, 1973; BRINSFIELD and HUMMEL, 1975). As a consequence of this particle motion on a spinning disc, there has to be a process of mainly continuous contact between fertilizer and distribution device. The tangential component of the absolute value of the outlet velocity depends linearly on angular velocity and radius of the disc. The relative velocity of the particles with respect to the vanes and therefore the radial component of the outlet velocity (as well as the angle of outlet), are influenced by the position and construction of the metering and distribution devices, certain physical properties of the fertilizer, and size of the mass flow (PATTERSON and REECE, 1962; KLAPP, 1965; DOBLER and FLATOW, 1968; DELITZ, 1969).

Considering its kinematics as described in the previous chapter, we may say that the reciprocating sprout fertilizer broadcaster is a special and more complex design than the spinning disc type. The sprout can be considered a special design of a vane. Furthermore, the angular velocity of the distribution device varies as the direction of movement reciprocates. During the period  $0 \leq \alpha \leq \pi/2$  the angular velocity increases; during the period  $\pi/2 < \alpha \leq \pi$  its value decreases.

Assuming that there is a certain rate of synchronism between the character of motion of the distribution device and the particles inside, transmitting of kinetic energy to the particles will mainly occur during the accelerating phase of the sprout motion or during periods. Based on the kinematics of the reciprocating sprout broadcaster we may state that from the point of view of particle dynamics, the spinning disc type can be considered as a simplification of the pendulum system. For this reason it is expected that the theory of particle movement on spinning discs can contribute only to a limited extent to the development of a theory describing particle movement in the oscillating sprout.

Nevertheless, we will in this chapter first briefly discuss the theory of particle motion on a spinning disc with vanes, especially because several stages in dynamic behaviour of particles can be distinguished (PATTERSON and REECE, 1962). This knowledge may contribute to the development afterwards of a more

complex theoretical model which can explain particle motion in the oscillating sprout. The model will be based on the results of previous qualitative and quantitative analyses of the character of particle motion inside the sprout. Finally, the value of the model will be discussed by comparing the results of simulation experiments with actual figures including mean absolute particle velocity of outlet and mean angle of outlet as they were obtained from high speed cinematography of the particle movements.

## 5.2. THEORY OF PARTICLE MOTION ON SPINNING DISC BROADCASTERS

The aims of the application of the theory of particle motion are: determination of the values of the absolute velocity of outlet (*VABS*) of particles; the relation between tangential and relative velocity components; the determination of the direction of particle movement when leaving the distribution device. Assuming a continuous contact between particles and vanes, we may write for *VABS* (see also Fig. 5.1):

$$VABS = \{(\omega \cdot a_2)^2 + (\dot{x}_{t_v})^2\}^{1/2} \quad (5.1)$$

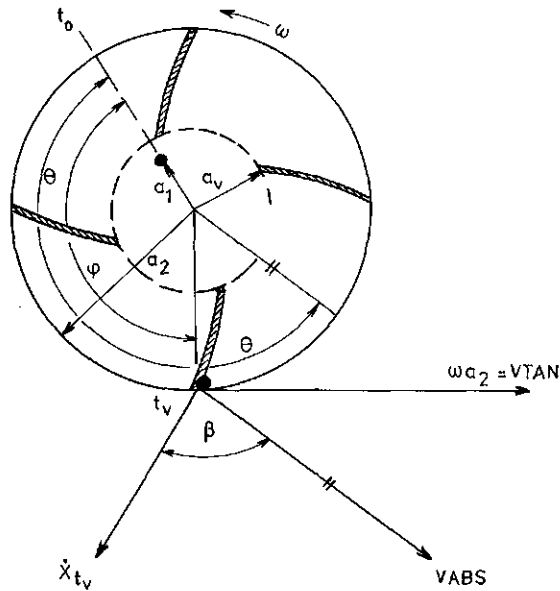


FIG. 5.1. Schematic representation of particle motion on a spinning disc broadcaster with backwards curved vanes;  $\omega$ : angular velocity,  $a_1$ : radius of particle supply,  $a_2$ : radius of the disc,  $a_v$ : free radius,  $\varphi$ : angle of rotation =  $\omega \cdot (t_r - t_o)$ ,  $\theta$ : angle of direction of motion =  $(\lambda = \theta_{max} - \theta_{min})$ ,  $\beta$ : angle of dispatch,  $\dot{x}_{t_v}$ : relative particle velocity component of outlet,  $\omega \cdot a_2$ : tangential particle velocity component of outlet, *VABS*: absolute particle velocity of outlet.

So the calculation of  $VABS$  is based upon the determination of  $\dot{x}_{tv}$  when  $a = a_2$ . For a conical disc with backwards curved vanes as shown in Fig. 5.2, we may write:

$$F_Z \cdot \cos \alpha \cdot \cos \beta - F_R - m \cdot g \cdot \sin \alpha \cdot \cos \beta - F = 0 \quad (5.2)$$

Introducing a coefficient of friction  $\mu = \mu_{d(isc)} = \mu_{v(anes)}$  the sum of the frictional forces will be:

$$F_R = (m \cdot g \cdot \cos \alpha \cdot \cos \beta) \cdot \mu + (m \cdot g \cdot \sin \alpha \cdot \sin \beta) \cdot \mu + (F_Z \cdot \sin \alpha \cdot \cos \beta) \cdot \mu + (F_C - F_Z \cdot \sin \beta) \cdot \mu \quad (5.3)$$

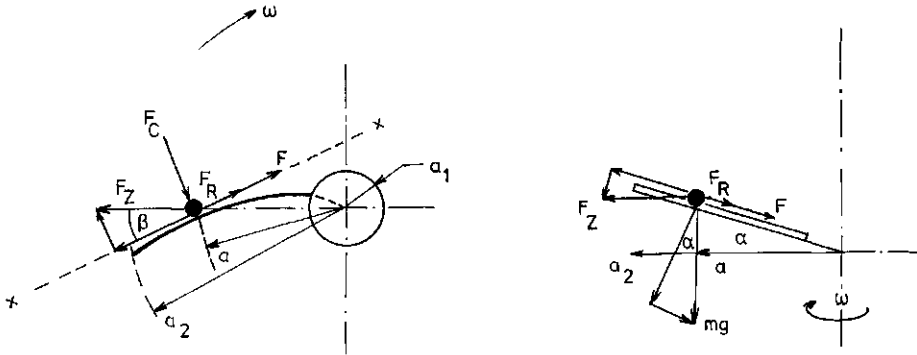


FIG. 5.2. Forces acting on a particle during motion over a conical disc with backwards curved vanes.  $F_Z$ : centrifugal force,  $F_C$ : Coriolis force,  $F_R$ : friction force;  $F$ : inertia resistance,  $\alpha$ : angle of slope of the disc,  $\beta$ : angle of backwards distortion of vane,  $a_1$ : radius of particle supply,  $a_2$ : radius of disc.

With:

$$F_Z = m \cdot \omega^2 \cdot a \text{ and } F_C = 2 \cdot m \cdot \omega \cdot x, \text{ we combine Eq. (5.2) and (5.3) to:}$$

$$\begin{aligned} \ddot{x} + (2 \cdot \omega \cdot x) \cdot \mu + (\omega^2 \cdot a \cdot \sin \alpha \cdot \cos \beta) \cdot \mu - \\ (\omega^2 \cdot a \cdot \sin \beta) \cdot \mu + (g \cdot \cos \alpha \cdot \cos \beta) \cdot \mu + \\ (g \cdot \sin \alpha \cdot \sin \beta) \cdot \mu - \omega^2 \cdot a \cdot \cos \alpha \cdot \cos \beta + \\ g \cdot \sin \alpha \cdot \cos \beta = 0 \end{aligned} \quad (5.4)$$

By substituting:  $x = k_1 \cdot a$ ; the radial component of the particle velocity can be computed from:

$$\begin{aligned} (k_1 \cdot \ddot{a}) + 2 \cdot \omega \cdot (k_1 \cdot \dot{a}) \cdot \mu + (\omega^2 \cdot a \cdot \sin \alpha \cdot \cos \beta) \cdot \mu - \\ (\omega^2 \cdot a \cdot \sin \beta) \cdot \mu + (g \cdot \cos \alpha \cdot \cos \beta) \cdot \mu + \\ (g \cdot \sin \alpha \cdot \sin \beta) \cdot \mu - \omega^2 \cdot a \cdot \cos \alpha \cdot \cos \beta + \\ g \cdot \sin \alpha \cdot \cos \beta = 0 \end{aligned} \quad (5.5)$$

For radial vanes and a flat disc, ( $k_1 = 1$ ,  $\alpha = 0$ ,  $\beta = 0$ ), Eq. (5.5) yields to:

$$\ddot{a} + 2 \cdot \omega \cdot \dot{a} \cdot \mu - \omega^2 \cdot a + g \cdot \mu = 0 \quad (5.6)$$

Solution of this differential equation leads to:

$$a_2 = \omega \cdot a_2 \cdot (\mu^2 + 1)^{1/2} - \mu \quad (5.7)$$

or with  $a_2 = \dot{x}_{iv} = \omega \cdot a_2 \cdot D$  the value for the absolute velocity of outlet can be found from:

$$VABS = \omega \cdot a_2 \cdot (1 + D^2)^{1/2} \quad (5.8)$$

According to PATTERSON and REECE (1962) four types of motion are possible with respect to particle mode of travel on a flat disc with radial vanes:

- sliding on both vane and disc
- sliding on disc and rolling on vane
- rolling on disc and sliding on vane
- rolling on both vane and disc.

It was determined that the particle slides on the disc when the radius of particles feed onto the disc:

$$a_f > \frac{7}{2} \cdot \frac{g}{\omega^2} \cdot \mu_d \quad (5.9)$$

When introducing representative values for  $\mu_{d(isc)}$  and  $\omega$  the limiting value of  $a_f$  proved to be very small. Therefore, the assumption can be made that particles start sliding on both disc and vane. During this phase, relative or radial velocity of the particles can be computed by means of Eq. (5.6).

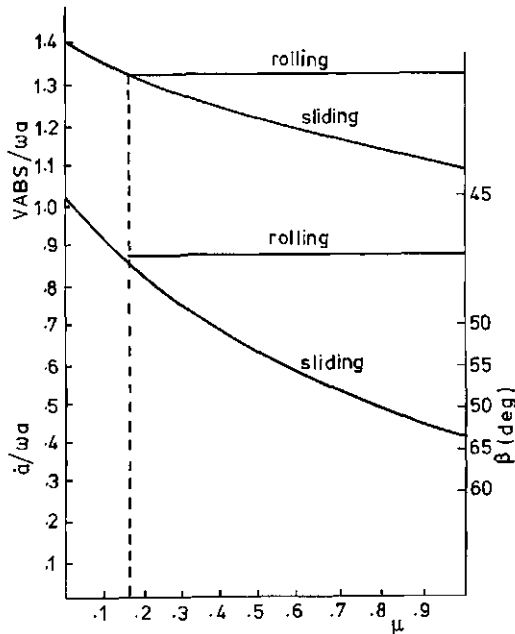


FIG. 5.3. Values for the absolute and the relative particle velocity of outlet (expressed by the ratio  $VABS/\omega \cdot a$  and  $\dot{a}/\omega \cdot a$ ), and the angle of dispatch  $\beta$ , for various values of the coefficient of friction  $\mu$ . (According to PATTERSON and REECE, 1962.)

However, increase in  $a$  leads to an increase of Coriolis friction torque acting on a particle. This provides the possibility for transition of a sliding motion into a rolling motion on the vanes. The equation of motion for this phase in particle movement (sliding on the disc, rolling on the vane) reads, according to PATTERSON and REECE (1962) and KLAPP (1965):

$$\ddot{a} - \omega_2 \cdot a + \frac{2}{5} \cdot \ddot{a} + \mu_d \cdot g = 0 \quad (5.10)$$

Hence:

$$\dot{a} = \left\{ \frac{5}{7} \cdot a \cdot (\omega^2 \cdot a - 2 \cdot \mu_d \cdot g) + C \right\}^{1/2} \quad (5.11)$$

The constant  $C$  can be found from the initial values of  $a$  and  $\dot{a}$  at the moment of transition from one mode of travel into the other.

The relation between the value of the absolute velocity of outlet and  $\omega \cdot a_2$  and that between  $\dot{a}$  and  $\omega \cdot a_2$  (depending on the value of  $\mu$ ) is given in Fig. 5.3. This figure also shows the value of the angle of dispatch  $\beta$ , being the angle between  $V_{ABS}$  and  $V_{RAD} = a_2$ .

From this theory we can gain the following conclusions with respect to particle dynamics in the reciprocating sprout. If, during the stage of continuous contact, particles can slide in the tube we can use equations of motion as given in Eq. (5.4)–(5.6) and Eq. (5.10). However, some extensions have to be taken into consideration, as we must introduce a tangential acceleration and retardation due to the irregular angular velocity of the sprout. Using spherical particles and a vane designed as a tube, the hypotheses can be stated that the mode of particle travel during continuous contact will be sliding, rolling, or sliding followed by rolling.

### 5.3. ANALYSIS OF PARTICLE MOTION IN THE OSCILLATING SPROUT

#### 5.3.1. Introduction

In this next section we will deal with experiments which have the objective of obtaining knowledge about particle trajectories, particle velocities, and accelerations in the reciprocating sprout. The trajectories and the production of velocity determine velocities of outlet and angles of outlet (dispatch) of the particles. These latter components define the shape of the basic transverse distribution pattern to an important rate. The analysis of particle motion has qualitative and quantitative aspects. The qualitative part deals with the production of kinetic energy of the particles when taking into account the discontinuity in the direction of movement of the distribution device. This phenomenon creates the possibility of a phase of discontinuous contact between the distribution device and the particles (in other words, a phase of impact during which the increase of particle velocity has a discontinuous character).

Depending on certain properties of the materials expressed by coefficients of friction and restitution, a phase of continuous contact may occur. During this phase the mode of particle dynamics may show a certain rate of similarity with that of particles on a spinning disc.

Quantitative analysis of the character of particle movement is also necessary to obtain the fundamentals for the development of a model of movement of the particles in the reciprocating sprout. Furthermore, such an analysis may contribute to the description of the possible relations between kinematics of the distribution device and particle dynamics.

### 5.3.2. *Materials and methods*

In order to determine particle trajectories, a high speed movie technique is

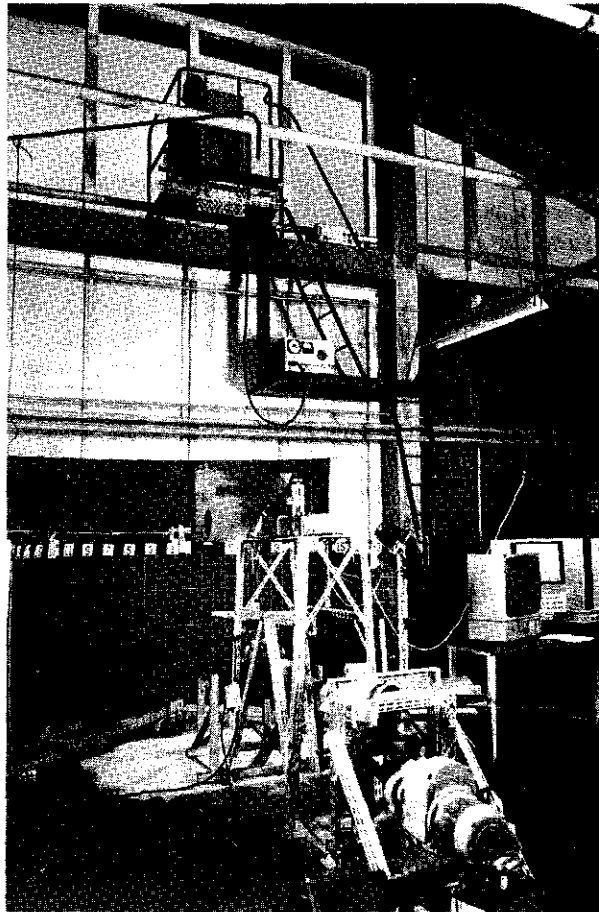


FIG. 5.4. Laboratory set-up for making the high speed movies. The camera is placed about 3.0 m above the sprout.

TABLE 5.1. Specifications of the reciprocating sprout broadcaster (mounted-type, hopper content: 600 dm<sup>3</sup>).

1. Rotary frequency of the driving shaft $N$ :	540 min <sup>-1</sup>
2. Length of the (polyester) sprout $RB$ :	0.63 m
3. Length of the crank $RA$ :	0.095 m
4. Length of the connecting rod $L$ :	0.200 m
5. Angle of oscillation $\phi$ :	23–28°
6. Diameter of the sprout orifice:	0.080 m
7. Sprout angle $\gamma$ :	+ 1°

used. Fertilizer kernels moving through a transparent polyester sprout are filmed using a film speed of 1,500 pictures/s (see Fig. 5.4).

The construction parameters of the broadcaster and the sprout are given in Table 5.1. The broadcaster is driven by an electric motor. In the laboratory experiments the rotary frequency is 540 min<sup>-1</sup>. The high speed movie technique sets some requirements and limits concerning the fertilizer which can be used.

The fertilizer particles must be as white as possible to provide contrast and they must have a sufficient size. Based on these considerations, two types of fertilizer are used of which the properties are described in Table 5.2. In order to analyze the separate kernels, dosage is decreased to the very low rate of 0.5 kg/min. This implies that the rate of mutual affection of the particles will be lower than under practical circumstances. The possible effects will be discussed later. Particle trajectories and velocity are determined by means of expressing the position of a certain particle each 0.002 s with respect to a  $X$ - $Y$  coordinate system. The origin of this system coincides with the center of rotation  $P$  of the sprout; the  $Y$ -coordinate with its centerline when the angle of oscillation  $\phi = 0^\circ$ .

For the determination of the particle trajectories, six films are analyzed including three of each type of fertilizer. On each film 36 trajectories are analyzed, subdivided into four groups of nine according to:

- one group, which starts with the analysis of values of the angle of rotation  $\alpha = 0^\circ$  and  $\phi =$  maximal and positive
- the same for  $\alpha = 90^\circ$  and  $\phi = 0^\circ$
- the same for  $\alpha = 180^\circ$  and  $\phi =$  maximal and negative
- the same for  $\alpha = 270^\circ$  and  $\phi = 0^\circ$ .

For this purpose a film motion analyzer is used. This analysis proved that each particle trajectory can be determined by 40–60 measuring points when taking into account a time interval of 0.002 s between two points.

The following results from the above analysis were obtained and treated by a computer (Fig. 5.5):

–  $R(I)$ , being the distance between the position of a kernel and the center of oscillation  $P$ , at the moment ( $I$ ).  $R(I)$  is computed according to:

$$R(I) = \{X(I)^2 + Y(I)^2\}^{1/2}.$$

– The alteration of the value of  $R(I)$  according to:

$$DR(I) = R(I) - R(I-1).$$

–  $DX(I)$  and  $DY(I)$  representing the alteration in position with respect to the  $X$

TABLE 5.2. Properties of the fertilizers used in the experiments.

Fertilizer	A Chilisałtpeter granules (not coated)	B Ammonium nitrate 'Nitram' prills (coated)
sieve fraction (mm)	2.8-3.4	2.8-3.4
1000 kernel weight (g)	19.8	18.2
coefficient of restitution	0.48	0.73
coefficient of friction	0.23	0.17

The methods for determination of the coefficients of restitution and friction are explained in section 7.2. The actual values were determined in a later stage of the research work.

and  $Y$  axis. These values are computed according to:  $DX(I) = X(I) - X(I-1)$  resp.  $DY(I) = Y(I) - Y(I-1)$ . From these values particle velocity components  $VKX(I)$  and  $VKY(I)$  can be derived.

$-VK(I)$ , being the absolute particle velocity at the moment ( $I$ ). The value is computed according to:

$$VK(I) = \{VKX(I)^2 + VKY(I)^2\}^{1/2}.$$

Particle accelerations in the  $X$ ,  $Y$ , and  $R$  direction as well as the value of the angle of rotation of the sprout  $\alpha(I)$  are computed. The direction of particle movement when leaving the sprout is expressed by the angle of outlet  $\beta$ , being the angle between the absolute velocity  $VK(I)$  and the positive  $X$  axis. Hence:

$$\beta = \text{atan} \{DY(I)/DX(I)\} \text{ when } DX(I) > 0 \text{ and}$$

$$\beta = 180^\circ - \text{atan} \{DY(I)/DX(I)\} \text{ when } DX(I) < 0.$$

Given the radial component of particle velocity:  $VK RAD(I) = DR(I)$ , the tangential component  $VKTAN(I)$  is computed from:

$$VKTAN(I) = \{VK(I)^2 - VKRAD(I)^2\}^{1/2}.$$

Before performing particle analysis, several preparatory experiments were carried out. Their objective was to obtain a better knowledge about the dimensions of the vertical section of the sprout in which particle movement takes place. Determination of the points on the sprout walls where particles are reciprocating may possibly contribute to more information about the section(s) where the sprout will wear out in practice. The points of particle reversal were examined by means of a black paper cone which was placed accurately inside the sprout. The fertilizer which was used for this part of the experiments was powdered with the fluorescent tracer Saturn Yellow A. After removal of the cone from the sprout, the dimensions of the active section, as is represented



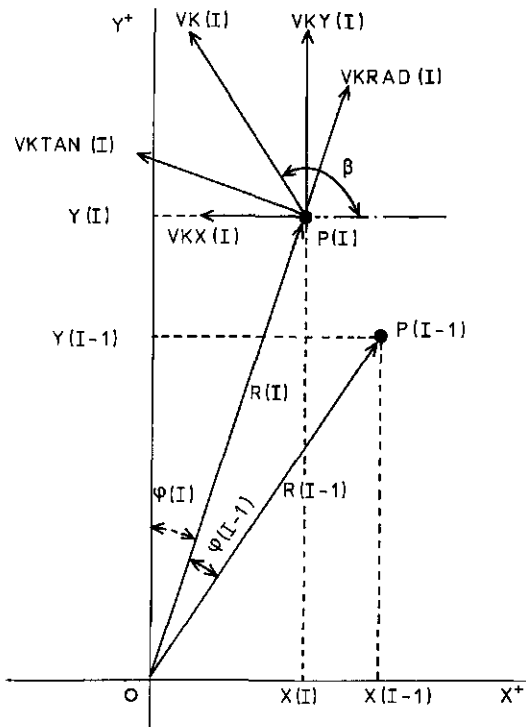


FIG. 5.5. Schematic representation of the method of analysis of particle positions and velocities (symbols are explained in the text and in the list of symbols on page 214).

by the points of reversal of the particle trajectories, was determined rather easily by examination of the colored points of impact.

### 5.3.3. Experimental results

#### 5.3.3.1. Duration of particle stay and acting section in the sprout

The time needed by the kernels to pass through the sprout from the first points of observation shows a considerable rate of variation. For fertilizer A it appears that the mean distance  $\bar{R}_0$  between the first point of observation and the center of rotation  $P$  was 21.5 cm. The minimum and maximum values for these initial radii are 16.7 and 30.1 cm. For the collection of analyzed initial radii ( $n = 98$ ) the mean duration of stay of the particles is 0.080 s. In 72% of the trajectories one point of reversal is noticed; and in 28% a reversal of the direction of movement is noticed twice.

For fertilizer B the mean value of the initial radii  $R_0$  is 22.1 cm, the extreme values being 16.6 and 28.3 cm ( $n = 99$ ). Mean duration of particle stay was 0.064 s, which is lower than for fertilizer A. In 89% of the particle trajectories one point of reversal was noticed; in 11% direction of movement reversed two times.

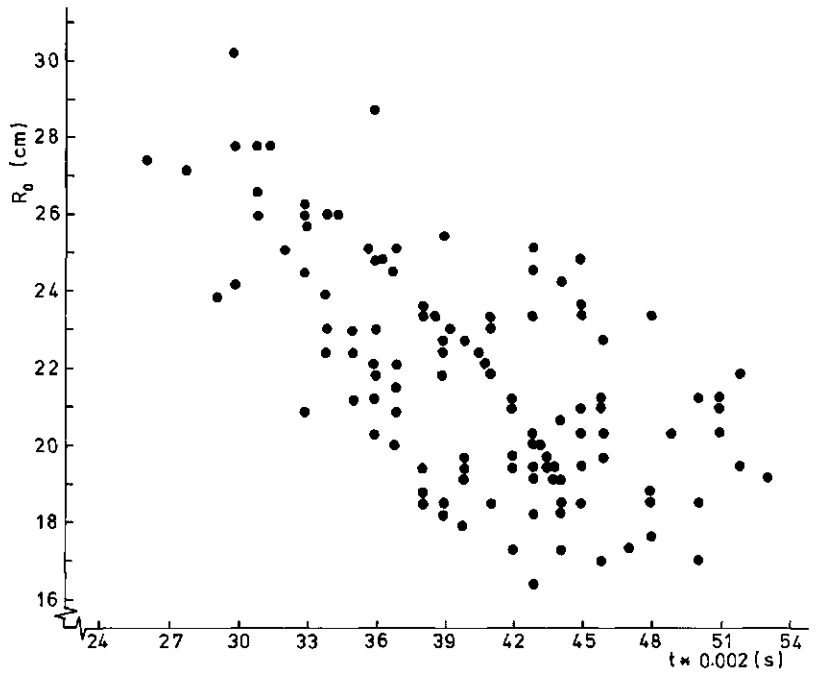


FIG. 5.6a. (FERTILIZER A) Relationship between the value of the initial radii  $R_0$  and duration of particle stay in the sprout  $t$ .

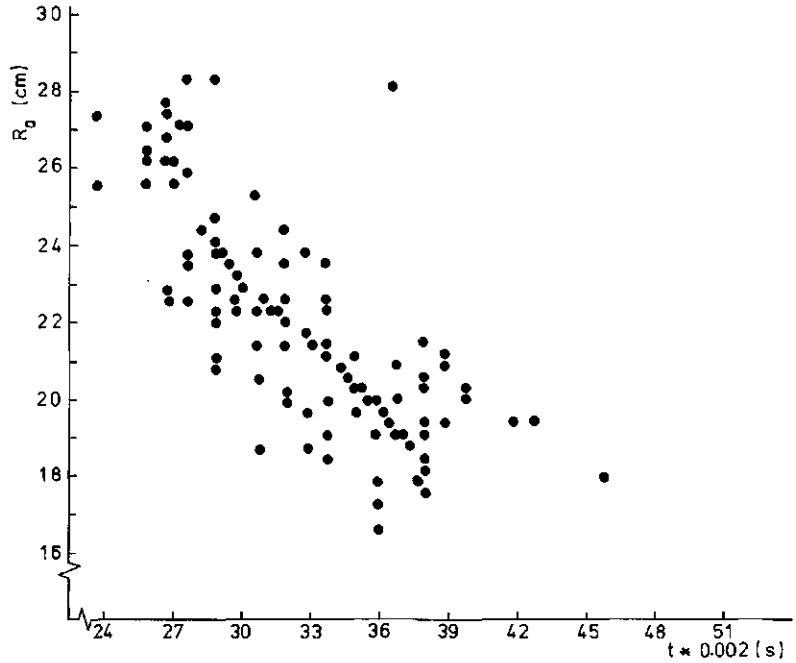


FIG. 5.6b. (FERTILIZER B) Relationship between the value of the initial radii  $R_0$  and duration of particle stay in the sprout  $t$ .

Duration of particle stay in the sprout is negatively correlated with the values of the initial radii  $R_0$  (the coefficients of correlation being  $-0.61$  for fertilizer A, and  $-0.73$  for fertilizer B). It should be noted that the initial radius does not necessarily coincide with the start of particle movement. It indicates only the value of  $R_0$  by which analysis of particle movement begins. At that time the particles have already a certain velocity in a particular direction.

This is caused by a number of factors, such as the flow of the fertilizer through the metering apertures, and the specific position of these apertures with respect to the bowl (resulting in varying angles of entrance and inlet velocities). Although spherical particles of a narrow sieve fraction were used, a considerable variation in velocities and directions of movement at the beginning of the analysis has to be expected. Due to this fact, the duration of particle stay inside the sprout can only partly (0.37 and 0.53) be explained by the initial position of the particles or by the trajectory (expressed in  $DR$ ).

The relationship between the values of the initial radii  $R_0$  and the duration of particle stay in the sprout (Fig. 5.6a and 5.6b) results in the conclusion that the radial component of particle outlet velocity will show a variation for both fertilizers ( $0 \leq \alpha \leq 360$ ). However, this radial component will show a higher mean level for fertilizer B. During one complete oscillation, and taking into account the starting positions of the analyses, the radial velocity component will show a rather smooth curve. When discussing angles and velocities of outlet we will return to this subject.

Results of the analyses of high speed films combined with the results of the determination of points of reversal of fluorescent-traced particles, shows that particle trajectories can be approximated by spirals which flatten in the vertical plane with an increase of the value of radius  $R$ .

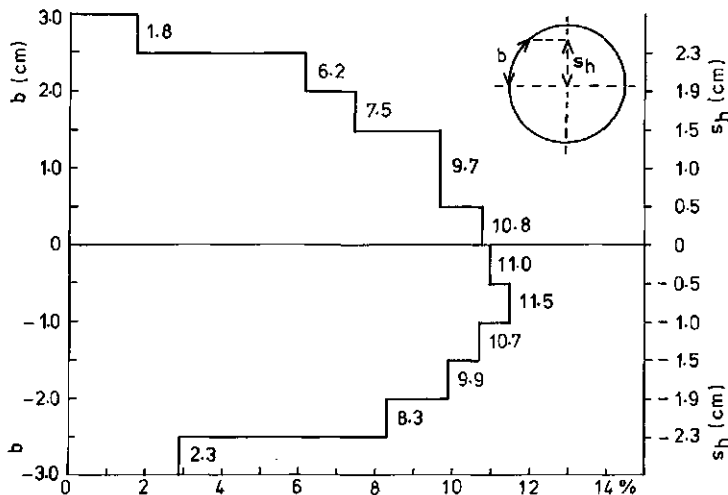


FIG. 5.7. Frequency distribution of the points of reversal of particle motion in the vertical section of the sprout ( $R > 0.33$  m;  $s_h$ : arc-height); ( $n = 391$ ).

For the sprout section  $0 < R \leq 0.33$  m, it holds that an average of 66.2% of the kernels have a reversal of the direction of motion in the vertical section of the sprout, limited by an arc-height ( $s_n$ ) of 1.9 cm on both sides of the horizontal axis. In the part of the sprout for which  $0.33 < R \leq 0.63$  m, this average percentage increases to 80.8%. The frequency distribution of the points of reversal in the vertical section of the sprout, related to the above-mentioned height of the arc, is given in Fig. 5.7.

Considering now the length of the sprout (expressed by  $R$ ), there is a strong concentration of the number of points of reversal in the trajectory  $0.10 \leq R \leq 0.12$  m. The percentage of the points of reversal decreases relatively strongly in the trajectory  $0.24 \leq R < 0.28$  m (Fig. 5.8). While also taking into account the results of the qualitative analyses of the filmed particle trajectories, the above percentages lead to the conclusion that three stages in particle motion can be distinguished. The first stage is characterized by the process of sorting-in of the particles in the bowl and the entrance of the sprout, after they have left the orifices of the metering devices. The second stage is characterized by the fact that at an increasing rate, energy from the walls of the oscillating sprout is added to the relatively highly concentrated mass flow of fertilizer particles. During this stage a certain rate of synchronism between particle movement and oscillation of the tube can be noticed. As a result of this, for the first time a general reversal of the direction of particle motion occurs due to contact with the walls of the

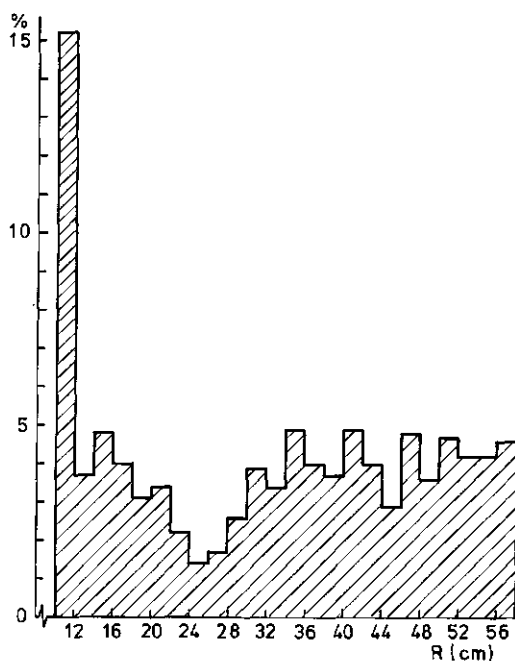


FIG. 5.8. Frequency distribution of the points of reversal of particle motion in the length  $R$  of the sprout ( $n = 803$ ).

sprout. This reversal of particle movement occurs during the last stage of the retarding movement of the sprout.

The third phase starts again with buildup of particle energy. Furthermore, it is characterized by the fact that the density of the mass flow decreases. Particle points of reversal are rather equally distributed along the sprout walls. The transition from the second to the third stage may be indicated by that part of the trajectory which shows relatively fewer points of reversal ( $R$ : 0.24–0.28 m).

Based on Fig. 5.8 we draw the conclusion that the process of wearing out at the end of the sprout which is notable in practice (starting at values of  $R$  of about 0.40 m) is due to the fact that the increase of particle velocity and mass flow is concentrating itself to an increasing rate into a smaller vertical section of the sprout.

From the results of our experiments we further draw the conclusion that the statement in practice that wear and tear of the sprout is the result of a highly concentrated mass of fertilizer around a certain value of  $R$  is incorrect.

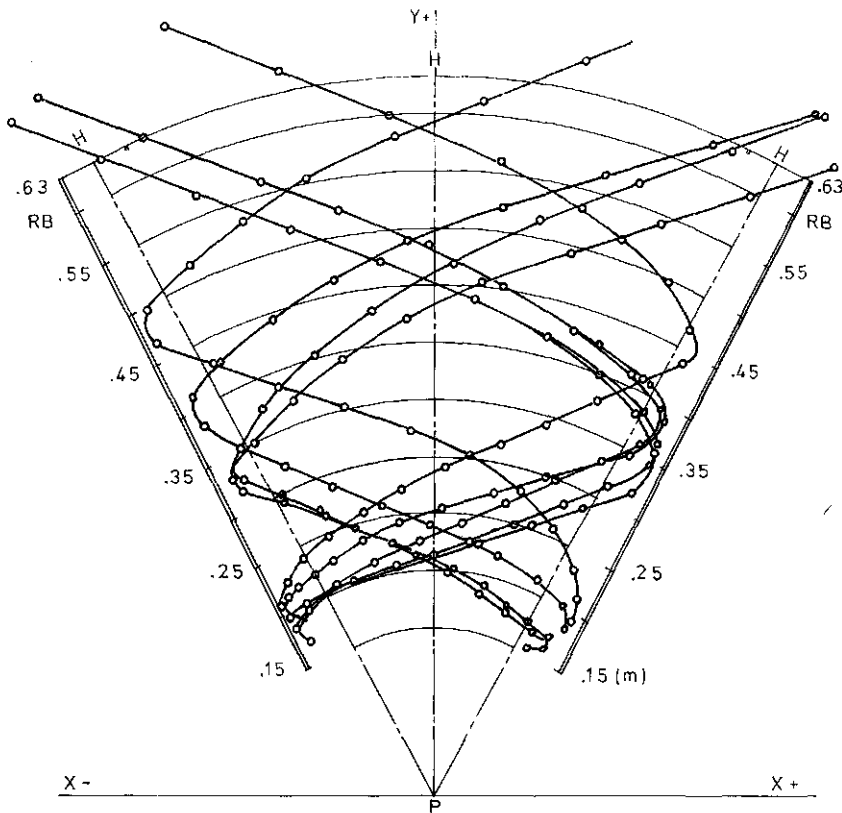


FIG. 5.9. Examples of absolute particle positions and trajectories with respect to an  $X$ - $Y$  system of coordinates. ( $PH$  indicates the positions of the centrelines when  $\phi$  has its maximum value;  $RB$ : sprout length.)

TABLE 5.3. Examples of momentary particle positions  $R_0$  and velocity components  $DX/DT$ ,  $DY/DT$ , and  $VK$  in relation to  $\alpha$ . Points of reversal of particle motion are printed in bold.

$t$	$\alpha$ (deg.)	$R_0$ (cm)	$DX/DT$ ( $m\ s^{-1}$ )	$DY/DT$ ( $m\ s^{-1}$ )	$VK$ ( $m\ s^{-1}$ )
1	22.0	20.3	23.9	20.1	20.9
2	28.5	21.0	24.5	20.8	21.4
3	35.0	21.2	25.1	21.2	22.1
4	41.4	21.6	25.4	21.4	22.6
5	47.9	21.9	25.7	21.8	23.1
6	54.4	22.2	25.6	21.8	23.2
7	60.8	22.8	25.8	22.3	23.6
8	67.4	23.0	25.8	22.8	23.8
9	73.8	24.1	26.0	22.8	23.9
10	80.3	24.5	26.3	23.4	24.2
11	86.8	25.0	26.7	24.1	24.5
12	93.3	25.7	27.2	24.3	25.1
13	99.7	26.3	27.7	25.5	25.5
14	106.2	27.0	28.1	25.7	26.0
15	112.7	27.8	28.7	26.7	26.7
16	119.2	28.5	29.6	27.5	27.4
17	125.7	29.3	30.2	28.4	28.2
18	132.2	30.2	31.0	29.2	29.0
19	138.6	31.3	32.3	29.9	29.9
20	145.1	32.3	33.3	31.2	30.9
22	158.1	34.7	35.6	33.3	32.9
23	164.6	35.9	37.1	34.8	34.1
24	171.0	37.4	38.4	36.2	35.6
25	177.5	38.8	39.6	37.6	36.9
26	184.0	40.3	41.3	39.0	38.3
27	190.5	41.1	42.8	40.5	39.7
28	197.0	41.7	43.9	41.3	41.3
29	203.4	42.7	44.9	42.5	42.9
30	209.4	43.4	46.0	43.2	44.4
31	216.4	44.3	46.7	44.1	45.3
32	222.9	45.3	47.1	44.7	46.1
33	229.4	45.8	47.7	45.6	46.6
34	235.8	46.6	48.5	46.3	47.2
35	242.3	47.1	49.5	47.2	47.9
36	248.8	48.3	50.3	48.0	48.9
37	255.3	49.3	51.4	49.0	49.7
38	261.8	50.8	52.4	49.7	50.4
39	268.2	52.2	53.7	50.8	50.8
40	274.7	53.7	55.2	51.9	52.1
41	281.2	55.8	56.6	53.5	53.2
42	287.7	57.7	58.2	55.0	54.4
43	294.2	60.0	59.8	56.7	55.6
44	300.6	62.8	61.7	58.5	57.1
45	307.1	65.4	63.8	60.7	59.0
46	313.6	68.5	66.2	63.2	61.2
47	-	-	69.0	65.9	63.6
48	-	-	316.6	304.6	-
49	-	-	323.0	311.0	-
50	-	-	-	-	-
51	-	-	-	-	-
52	-	-	-	-	-
53	-	-	-	-	-
54	-	-	-	-	-
55	-	-	-	-	-
56	-	-	-	-	-
57	-	-	-	-	-
58	-	-	-	-	-
59	-	-	-	-	-
60	-	-	-	-	-
61	-	-	-	-	-
62	-	-	-	-	-
63	-	-	-	-	-
64	-	-	-	-	-
65	-	-	-	-	-
66	-	-	-	-	-
67	-	-	-	-	-
68	-	-	-	-	-
69	-	-	-	-	-
70	-	-	-	-	-
71	-	-	-	-	-
72	-	-	-	-	-
73	-	-	-	-	-
74	-	-	-	-	-
75	-	-	-	-	-
76	-	-	-	-	-
77	-	-	-	-	-
78	-	-	-	-	-
79	-	-	-	-	-
80	-	-	-	-	-
81	-	-	-	-	-
82	-	-	-	-	-
83	-	-	-	-	-
84	-	-	-	-	-
85	-	-	-	-	-
86	-	-	-	-	-
87	-	-	-	-	-
88	-	-	-	-	-
89	-	-	-	-	-
90	-	-	-	-	-
91	-	-	-	-	-
92	-	-	-	-	-
93	-	-	-	-	-
94	-	-	-	-	-
95	-	-	-	-	-
96	-	-	-	-	-
97	-	-	-	-	-
98	-	-	-	-	-
99	-	-	-	-	-
100	-	-	-	-	-

Taking into account the positions at the beginning of the movie analyses and combining these results with those obtained from the performed experiments for defining the particle points of reversal, we conclude that under the circumstances particles are reversing their direction of movement on an average of two times since they are sorted-in. This number of reversals of particle motion is one fourth to one fifth the expectation of the constructors. Their expectation was based on the assumption that the particle trajectories could be described by a part of an arc during the accelerating phase of the sprout movement, and by a tangential line during the connecting phase of retardation.

### 5.3.3.2. Description of velocity, velocity of outlet, and direction of outlet of particles

In Fig. 5.9 some examples of particle positions are given as they relate to a system of  $X$ - $Y$  coordinates of which the  $Y$ -coordinate coincides with the forward speed of the broadcaster. Furthermore, in Fig. 5.10 a representative number of relative particle positions are shown in which the sprout is in its extreme positions, its middle position, and its two positions on both sides. Finally, for a number of particle trajectories, the particle positions (and velocity components which can be derived from them) are shown (Table 5.3).

From this and the multitude of other analyzed material we can draw the following conclusions.

At increasing values of  $R$  there is an increase in the rate of synchronism between particle and sprout movement. As a result of energy transfer, the  $X$ -component of particle velocity increases during the accelerating phase. It appears from the analysis of particle trajectories that during a part of the phase of retardation this component still increases. Apparently, relative particle

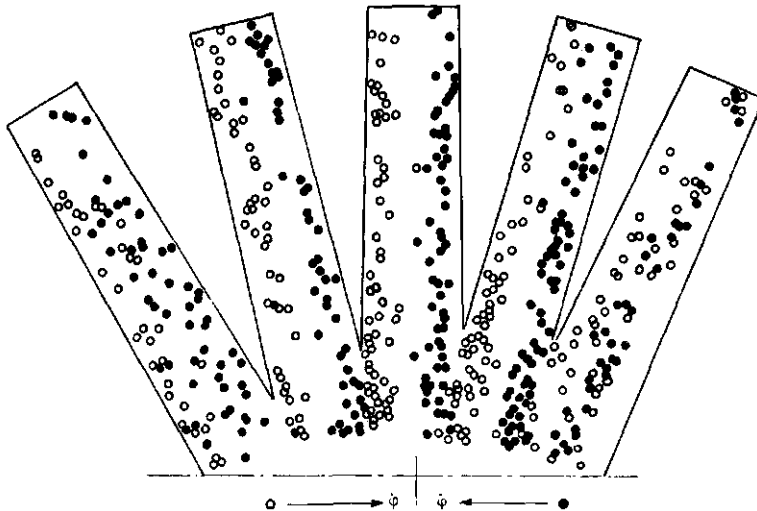


FIG. 5.10. Relative positions of the particles with respect to the sprout.

motion has such a character that in the model of motion this phenomenon has to be taken into account when formulating criteria for the initial conditions. (When discussing the results of the simulation experiments obtained with the model, we will return to this subject.) When the direction of motion reverses or when particles impact on the retarding sprout wall, a decrease of the  $X$ -velocity component is noted frequently for values of  $\alpha$  around  $180^\circ$ ; situations are also found in which particles impact on the opposite sprout wall before the value of  $\alpha$

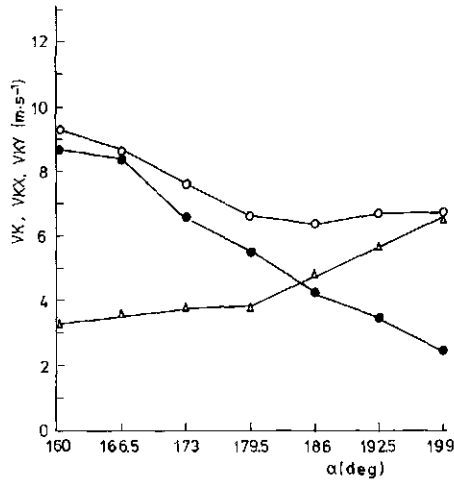


FIG. 5.11a. The absolute particle velocity  $VK$ , and its  $X$ - and  $Y$ -components as a function of the angle of rotation  $\alpha$ , in the range  $160^\circ \leq \alpha \leq 199^\circ$ .  $\circ$ — $\circ$ :  $VK$ ,  $\bullet$ — $\bullet$ :  $VKX (= DX/DT)$ ,  $\triangle$ — $\triangle$ :  $VKY (= DY/DT)$ . (FERTILIZER A; mean values obtained from 35 analyses.)

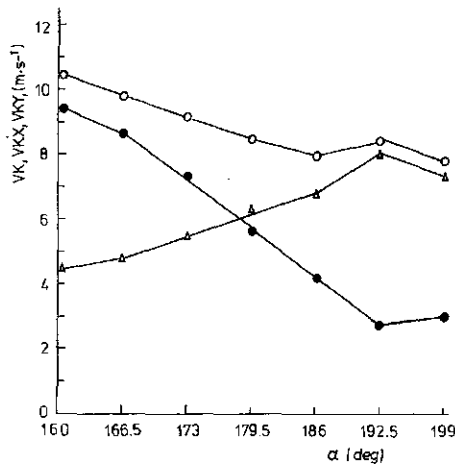


FIG. 5.11b. The absolute particle velocity  $VK$ , and its  $X$ - and  $Y$ -components as a function of the angle of rotation  $\alpha$ , in the range  $160^\circ \leq \alpha \leq 199^\circ$ .  $\circ$ — $\circ$ :  $VK$ ,  $\bullet$ — $\bullet$ :  $VKX (= DX/DT)$ ,  $\triangle$ — $\triangle$ :  $VKY (= DY/DT)$ . (FERTILIZER B; mean values obtained from 35 analyses.)



$= 180^\circ$ . After reversal of the direction of particle motion, the  $X$ -velocity component increases quickly and on a higher level. Just as before, this increase continues during the first phase of retardation.

The  $Y$ -component of velocity has the following features: during the phase of acceleration and a greater part of the phase of retardation of the sprout, its value hardly depends on the angle of oscillation or angular velocity or the value of the radius  $R$ . Variations appear at random and have perhaps to be explained by limitations in accuracy of the method of analysis. During the stage of oscillation, when direction of sprout movement reverses, or when the particles impact on the opposite sprout wall, an increase of the  $Y$ -velocity component can be noted. After starting the process of sprout motion in the opposite direction, this velocity component stabilizes on the new, higher level. Just as before, random variations in the value of the velocity component are noticeable.

The composed image of both velocity components results in a decrease of the absolute particle velocity during the reversal of particle motion. Reversal of the direction of particle motion occurs just before, during, or just after the reversal of the direction of sprout motion (Fig. 5.11a and 5.11b).

The phenomenons above are noted for both types of fertilizer. Under comparable circumstances, however, the level of all components was higher for fertilizer B (see also section 5.3.3.1).

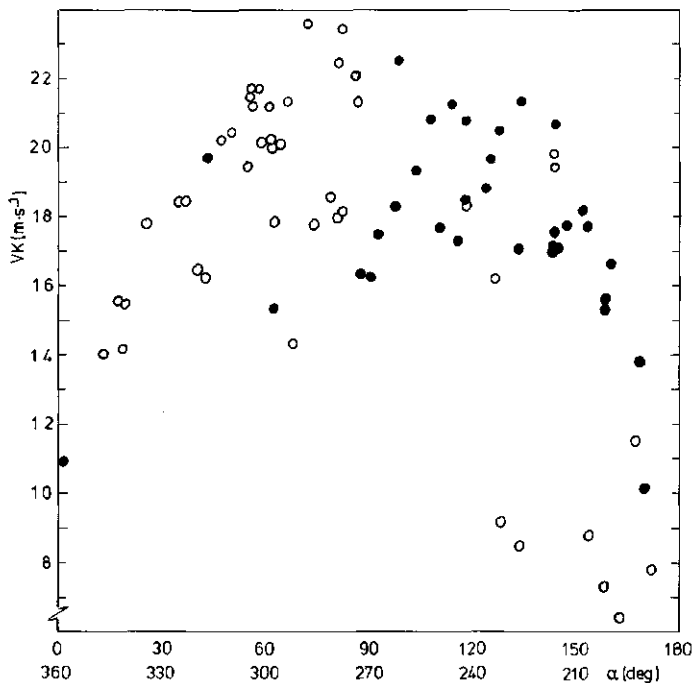


FIG. 5.12a. The absolute particle velocity of outlet  $VK$  as a function of the angle of rotation  $\alpha$ . ●:  $VK$  for  $0^\circ \leq \alpha \leq 180^\circ$ , ○:  $VK$  for  $180^\circ < \alpha \leq 360^\circ$ . FERTILIZER A.

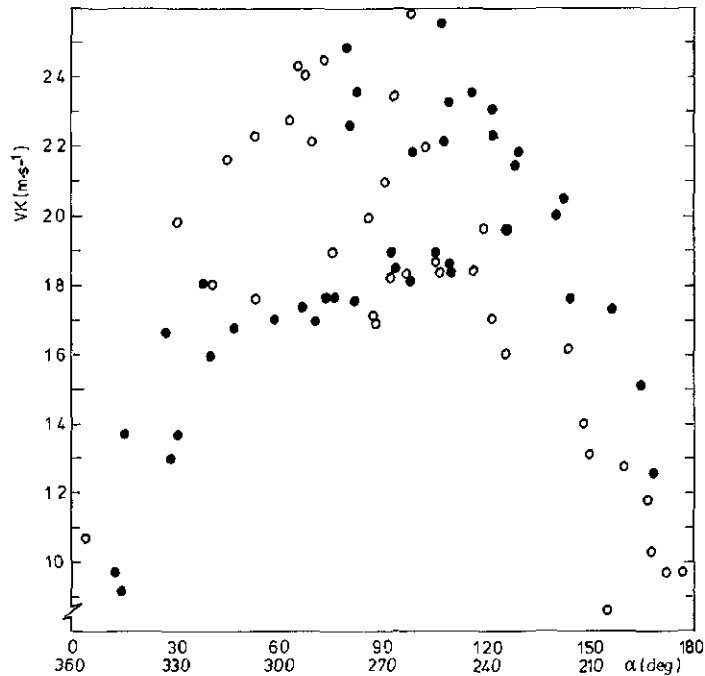


FIG. 5.12b. The absolute particle velocity of outlet  $VK$  as a function of the angle of rotation  $\alpha$ . ●:  $VK$  for  $0^\circ \leq \alpha \leq 180^\circ$ , ○:  $VK$  for  $180^\circ < \alpha \leq 360^\circ$ . FERTILIZER B.

During the last phase of particle motion within the sprout, the  $X$ -component of the absolute velocity increases continuously. As a result of this, the value for the angle of dispatch which was defined in section 5.3.2, decreases if this value is recorded as  $\beta$  resp.  $(180^\circ - \beta)$ .

The following remarks have to be made with respect to the values of the absolute velocity of outlet, its tangential and radial components, and the angle of dispatch. For both fertilizers A and B, the absolute particle velocity of outlet  $VK$  depends on the angle of rotation  $\alpha$ , and therefore on the angle of oscillation  $\phi$  (Fig. 5.12a and 5.12b). Velocities of outlet increase during the accelerating phase of sprout motion and during about one-third of the successive phase of retardation. Particle velocities are at a lower level throughout the last part of the phase of retardation. This can be explained as follows: during the last part of the phase of retardation, particles coming from a position with a lower value of the effective radius are able to leave the sprout. (The effective radius is defined as the distance between the oscillation point and that momentary position of the particles on the wall when, due to the contact between both, energy can be transferred for the last time.) In addition, particles can already impact on the opposite wall before the maximum angle of oscillation is obtained. Depending on the elastic properties of the impacting materials, the kinetic energy of the particles will decrease. The low values of absolute particle velocities of outlet at

the beginning of the phase of sprout acceleration can be explained in a similar way.

We may note that the maximum value for the absolute velocity of outlet is on a higher level for fertilizer B. Due to differing material properties of this type of fertilizer, the rate of energy transfer seems to be on a higher level.

The tangential component of particle velocity ( $VKTAN$ ) shows a similar pattern to absolute particle velocity (Fig. 5.13a and 5.13b). The largest values are found during the last stage of the accelerating phase and the first stage of the phase of retardation of the sprout. Again, the low values during the period of reversal of the direction of sprout motion can be explained by the possibilities for lower effective radii and impacts on the opposite wall.

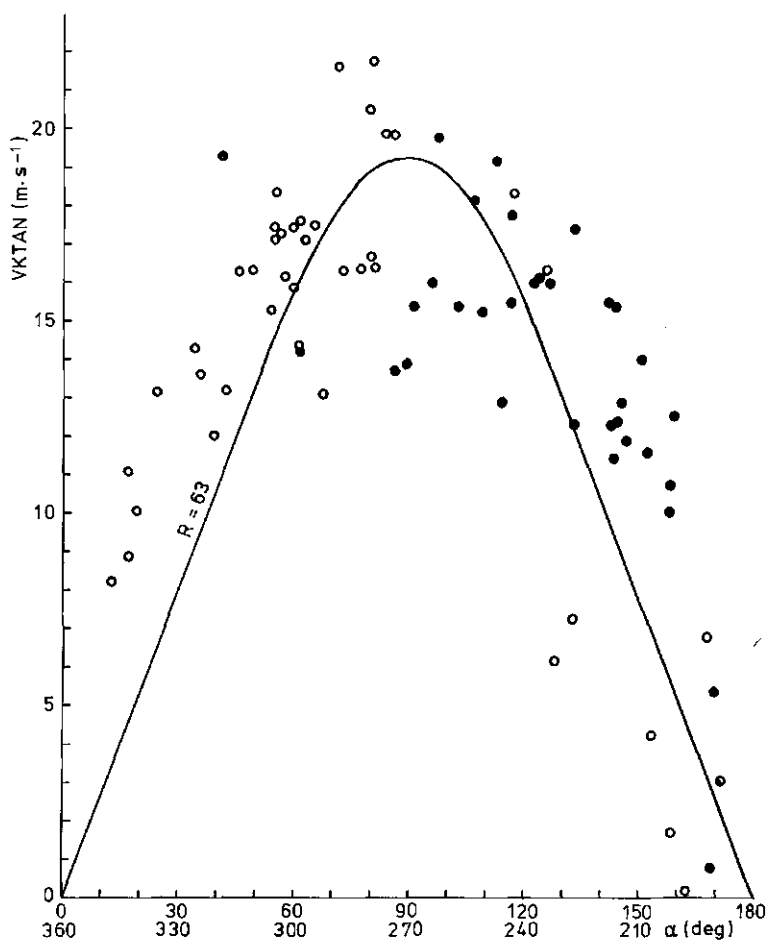


FIG. 5.13a. The tangential component  $VKTAN$  of the particle velocity of outlet  $VK$ , as a function of the angle of rotation  $\alpha$ . ●:  $VKTAN$  for  $0^\circ \leq \alpha \leq 180^\circ$ , ○:  $VKTAN$  for  $180^\circ < \alpha \leq 360^\circ$ ; —: velocity of the sprout for  $RB = 63$  cm. FERTILIZER A.

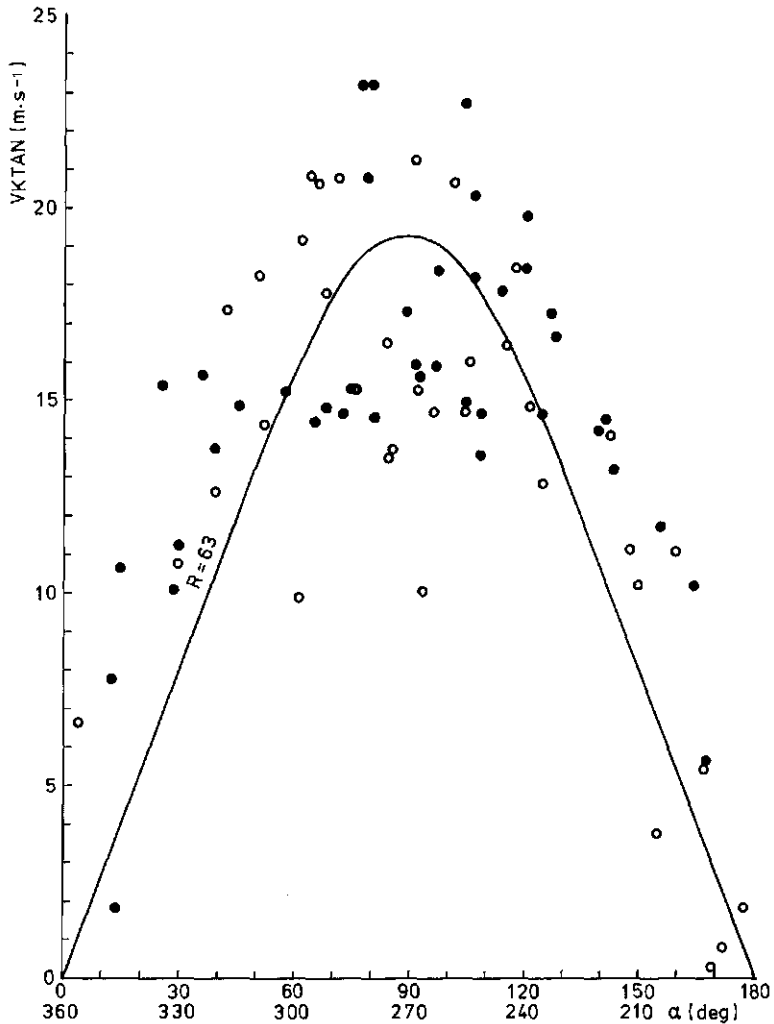


FIG. 5.13b. The tangential component  $VKTAN$  of the particle velocity of outlet  $VK$ , as a function of the angle of rotation  $\alpha$ . ●:  $VKTAN$  for  $0^\circ \leq \alpha \leq 180^\circ$ , ○:  $VKTAN$  for  $180^\circ < \alpha \leq 360^\circ$ ; —: velocity of the sprout for  $RB = 63$  cm. FERTILIZER B.

The radial velocity component ( $VK RAD$ ) reaches its largest values during the phase of retardation of the sprout. The level of the values of  $VK RAD$  during this oscillation period is relatively constant (Fig. 5.14a and 5.14b). Generally the part of the oscillation period during which this velocity component increases is larger than for  $VK$  and  $VKTAN$ . In addition, the level of the radial velocity component is lower than that of the tangential component.

The angle of dispatch  $\beta$ , indicating the angle between the velocity of outlet  $VK$  and the positive  $X$ -coordinate and which value is represented by  $\beta$  resp.  $(180^\circ - \beta)$ ,

decreases asymptotically as  $\alpha$  increases from  $0^\circ$  to  $180^\circ$  resp. from  $180^\circ$  to  $360^\circ$  (Fig. 5.15a and 5.15b). The X-component of the velocity of outlet will increase relative to the Y-component at increased angles of oscillation during the phase of sprout retardation. This feature combined with the values of the velocity of outlet has the following consequences (Fig. 5.16a and 5.16b). Generally the particles which have high values of outlet velocity and which therefore contribute to high values of the particle trajectories after leaving the sprout, have low values of  $\beta$  or  $(180^\circ - \beta)$ . So in practice there exists the opportunity for obtaining large spreading widths.

However, it can be noted that, due to the frequency of the number of particles that combine high velocities of outlet with low values of the angle of dispatch, a two-peak basic transverse distribution pattern is created. This statement is supported by the figures in Table 5.4 and Fig. 5.17. During the phase of retardation, the mean velocity of outlet is at a high level in contrast to the mean values for  $\beta$  which are low. Especially during the second half of the phase of

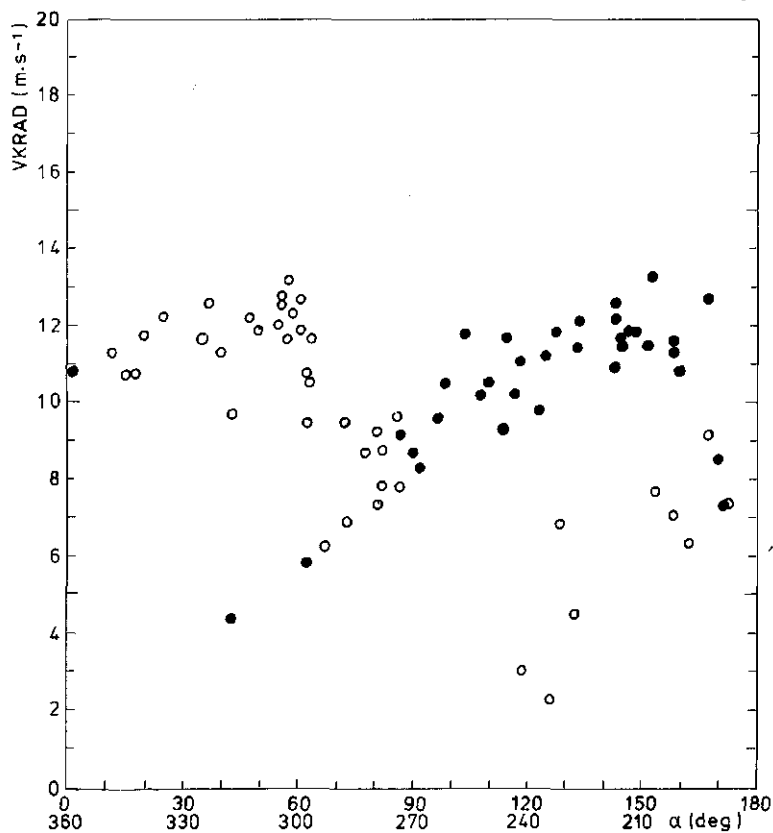


FIG. 5.14a. The radial velocity component  $V_{KRAD}$  of the particle velocity of outlet  $V_K$  as a function of the angle of rotation  $\alpha$ . ●:  $V_{KRAD}$  for  $0^\circ \leq \alpha \leq 180^\circ$ , ○:  $V_{KRAD}$  for  $180^\circ < \alpha \leq 360^\circ$ . FERTILIZER A.

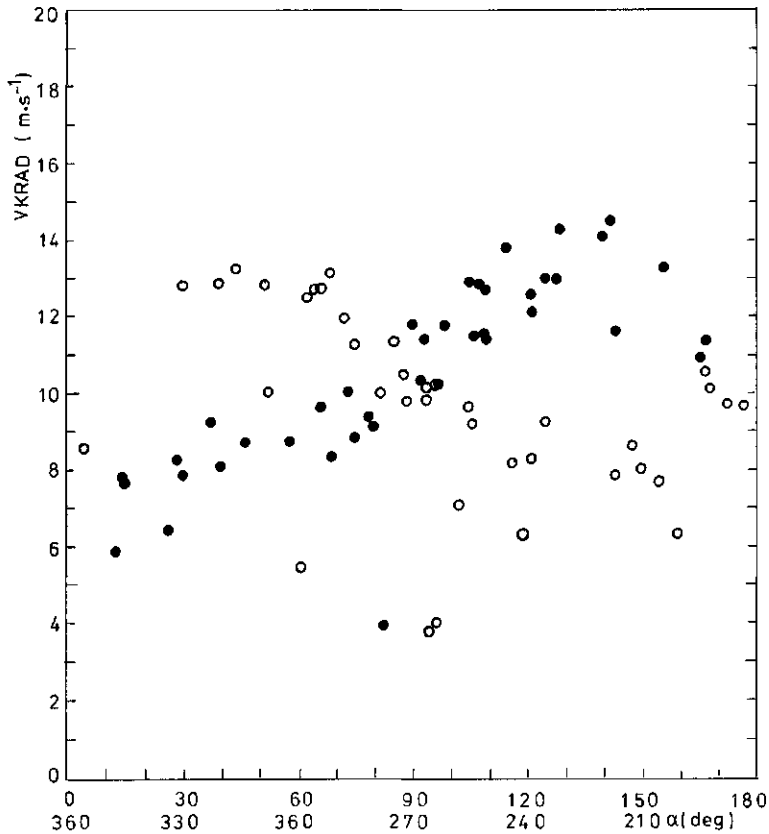


FIG. 5.14b. The radial velocity component  $VK_{RAD}$  of the particle velocity of outlet  $VK$  as a function of the angle of rotation  $\alpha$ . ●:  $VK_{RAD}$  for  $0^\circ \leq \alpha \leq 180^\circ$ , ○:  $VK_{RAD}$  for  $180^\circ < \alpha \leq 360^\circ$ . FERTILIZER B.

retardation, a relatively high percentage of particles leave the sprout.

Since the peaks are not necessarily situated close to the centre, the following remarks can be made. The direction of the velocity of outlet of the particles has to be changed in such a way – e.g. by attachment of special additional constructions at the end of the sprout – that a greater number of the particles are

TABLE 5.4. Values of particle velocity of outlet ( $\overline{VK}$ ) and the angle of dispatch ( $\overline{\beta}$ ) in relation to the angle of oscillation of the sprout. (Fertilizer: ammonium nitrate; sieve fraction: 3.35–4.00 mm.)

Angle of oscillation	28.36/14.18° (acceleration of the sprout)	14.18/0°	0/–14.18° (retardation of the sprout)	–14.18/–28.36°
$\overline{VK}$ (m s <sup>–1</sup> )	14.0	19.0	22.0	18.5
$\sigma_{VK}$ (m s <sup>–1</sup> )	2.5	2.5	2.0	3.5
$\overline{\beta}$ (deg)	60	36	23	20
$\sigma_\beta$ (deg)	11	9	6	5

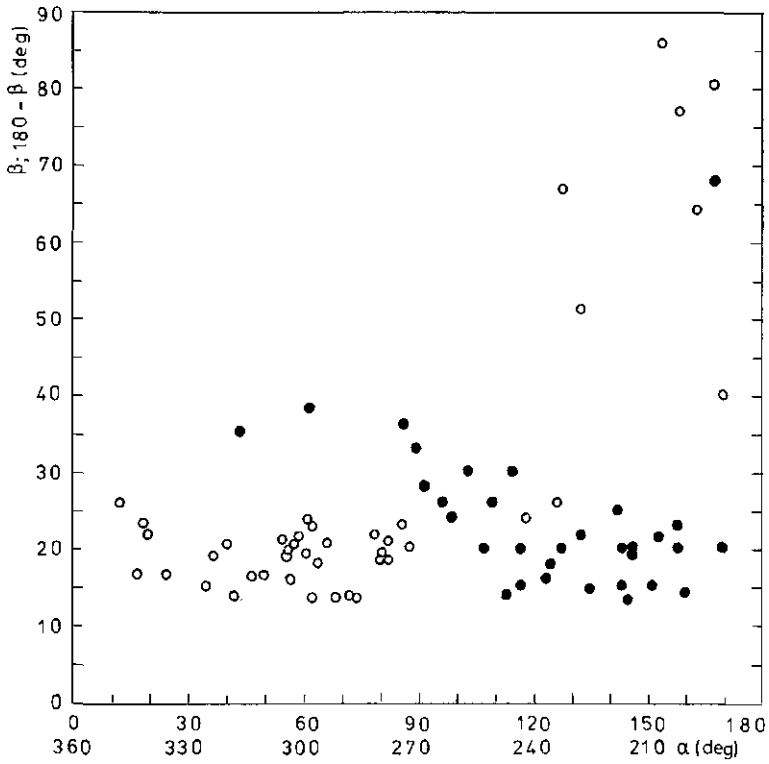


FIG. 5.15a. The angles of particle dispatch  $\beta$  as a function of the angle of rotation  $\alpha$ . ●:  $\beta$ ,  $(180^\circ - \beta)$  for  $0^\circ \leq \alpha \leq 180^\circ$ ; ○:  $\beta$ ,  $(180^\circ - \beta)$  for  $180^\circ < \alpha \leq 360^\circ$ . FERTILIZER A.

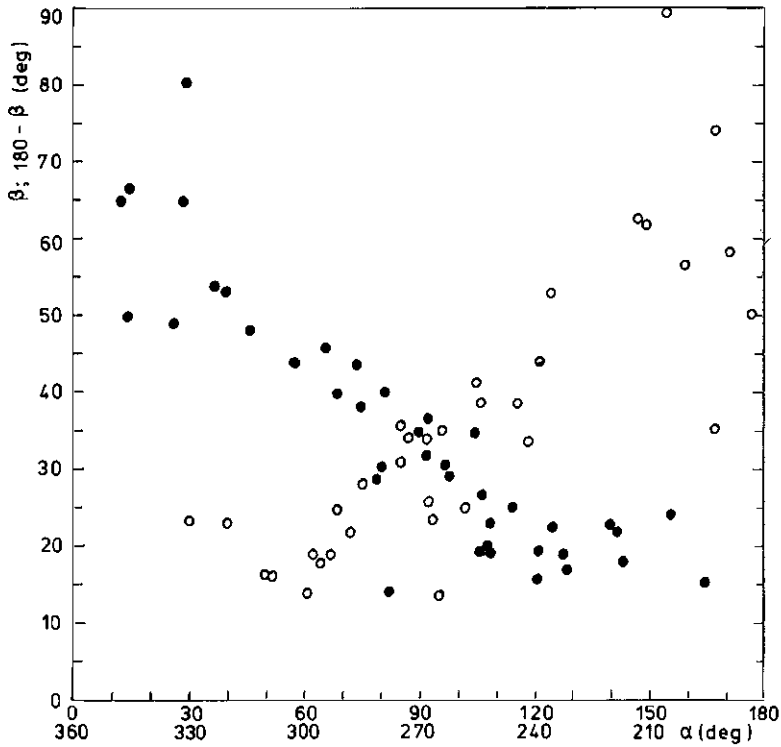


FIG. 5.15b. The angles of particle dispatch  $\beta$  as a function of the angle of rotation  $\alpha$ . ●:  $\beta$ ,  $(180^\circ - \beta)$  for  $0^\circ \leq \alpha \leq 180^\circ$ ; ○:  $\beta$ ,  $(180^\circ - \beta)$  for  $180^\circ < \alpha \leq 360^\circ$ . FERTILIZER B.

directed towards the centre of the distribution pattern.

In its present design such a change to a one-peak transverse distribution pattern, which is acceptable in practice, is supported by the attachment of a bow or other special devices at the end of the sprout, combined with a specially shaped orifice such as the attachment of grooves in the sides of the sprout. The effects of such devices on particle motion (velocity and angle outlet) will be discussed in chapter 6.

#### 5.3.4. Discussion

From the qualitative analyses of particle behaviour, it can be concluded that particle trajectories within the sprout can be described as spirals which flatten near the end. During the last phase of particle movement in the sprout, the

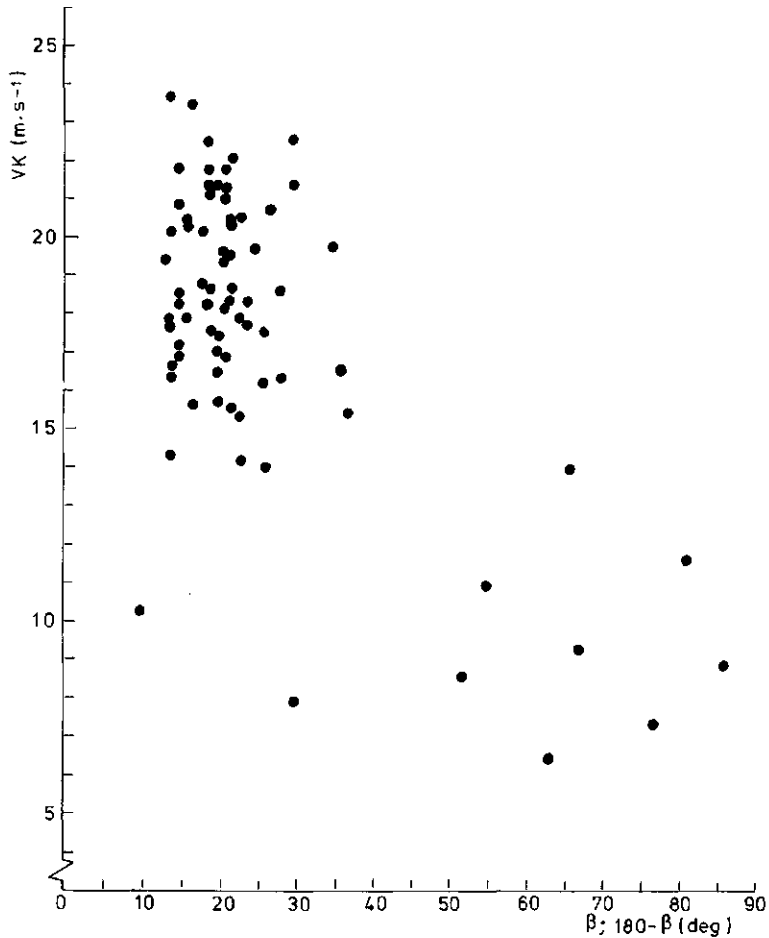


FIG. 5.16a. Relation between absolute particle velocity of outlet  $VK$  and angle of dispatch  $\beta$ , ( $180^\circ - \beta$ ). FERTILIZER A.



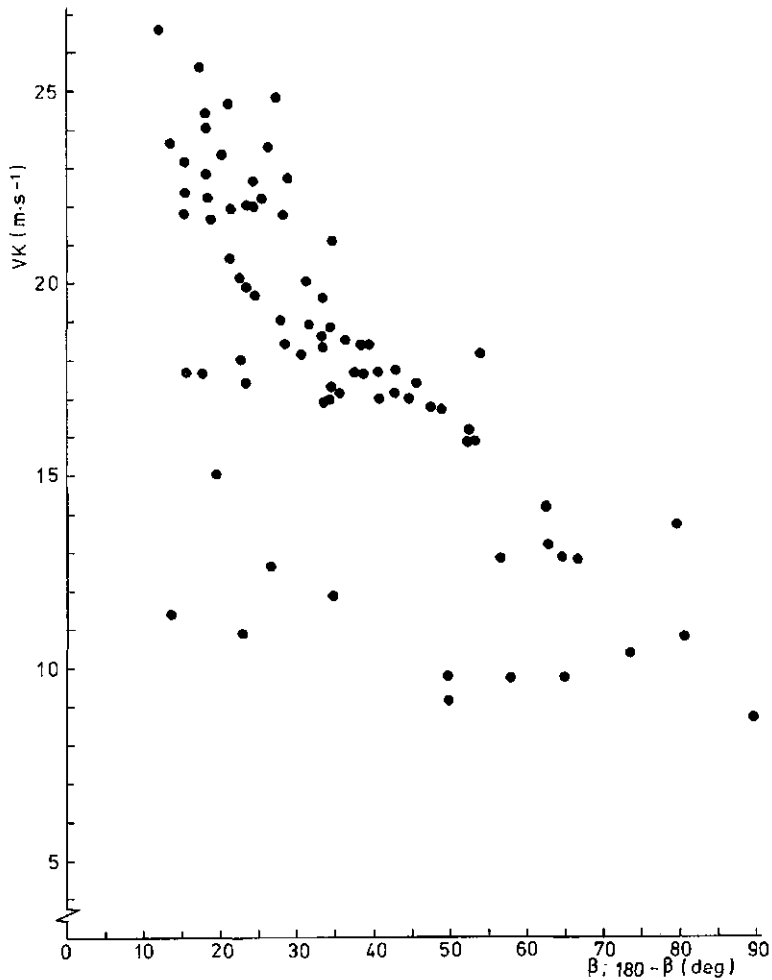


FIG. 5.16b. Relation between absolute particle velocity of outlet  $V_K$  and angle of dispatch  $\beta$ , ( $180^\circ - \beta$ ). FERTILIZER B.

assumption is tenable that particle trajectories can be reasonably approximated by considering them as movements in a horizontal plane.

In particle motion, stages of continuous and discontinuous contact between particles and sprout can be distinguished. Qualitative analyses of particle motion show that, depending on material properties, the phase of discontinuous contact can be observed during a relatively long period just before, during, or after reversal of the direction of sprout motion.

For the two types of fertilizer observed, it appears that the stage of discontinuous contact is followed by a stage of continuous contact. This stage is noticed during the second part of the phase of sprout acceleration and a part of the successive phase of retardation. Relative particle motion can be sliding

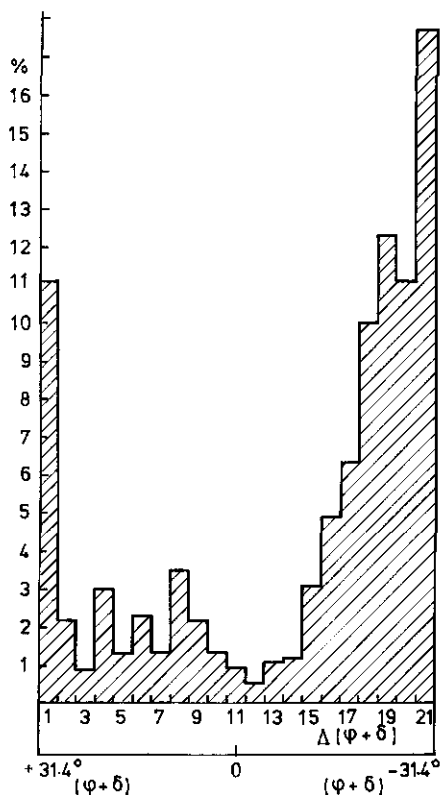


FIG. 5.17. Frequency distribution of the particle dispatch as a function of the angle of oscillation  $\phi$  of the sprout. ( $0^\circ \leq \alpha \leq 180^\circ$ ;  $n = 818$ ).

and/or rolling. The method of analysis does not permit accurate observation of the transition between these types of motion. However, rotation of the particles can be observed clearly.

Quantitative analysis of a number of particle trajectories shows an increase of kinetic energy of the particles during the phase of sprout acceleration. This increase continues during a part of the successive phase of retardation. Reversing the direction of the sprout movement especially affects the tangential component of the absolute particle velocity. As a result, the values of the angle of dispatch  $\beta$  or  $(180^\circ - \beta)$  are high during this phase of sprout motion.

The frequency of the number of particles leaving the sprout during the first part of the accelerating phase is relatively low. During the further course of the (half) oscillation period, the angles of dispatch decrease to mean values of about  $20^\circ$ . In addition, it must be noted that during the last part of the phase of retardation, the frequency of the number of particles leaving the sprout is high. Moreover, these particles have obtained a rather high mean velocity of outlet of about  $20 \text{ m s}^{-1}$ . As a result of this, fertilizer leaves the sprout in two divergent

mass flows. The highest density of these mass flows is found at values of  $\beta$  of about  $25^\circ$  resp.  $155^\circ$ . Without further additional constructions a two-peak transverse distribution pattern is created. The value of the spreading angle  $\lambda$  (see also Fig. 3.2) is  $130-150^\circ$ . Taking into consideration the related velocities of outlet, this leads to the conclusion that conditions are created which enable practical working widths of reciprocating sprout broadcasters which are comparable to those of the greater number of spinning disc broadcasters.

#### 5.4. THEORY OF PARTICLE MOTION IN THE OSCILLATING SPROUT

##### 5.4.1. Introduction

In the section of the sprout which was examined ( $RB > 0.17\text{ m}$ ), production of particle velocity can be subdivided into two successive stages. During the first

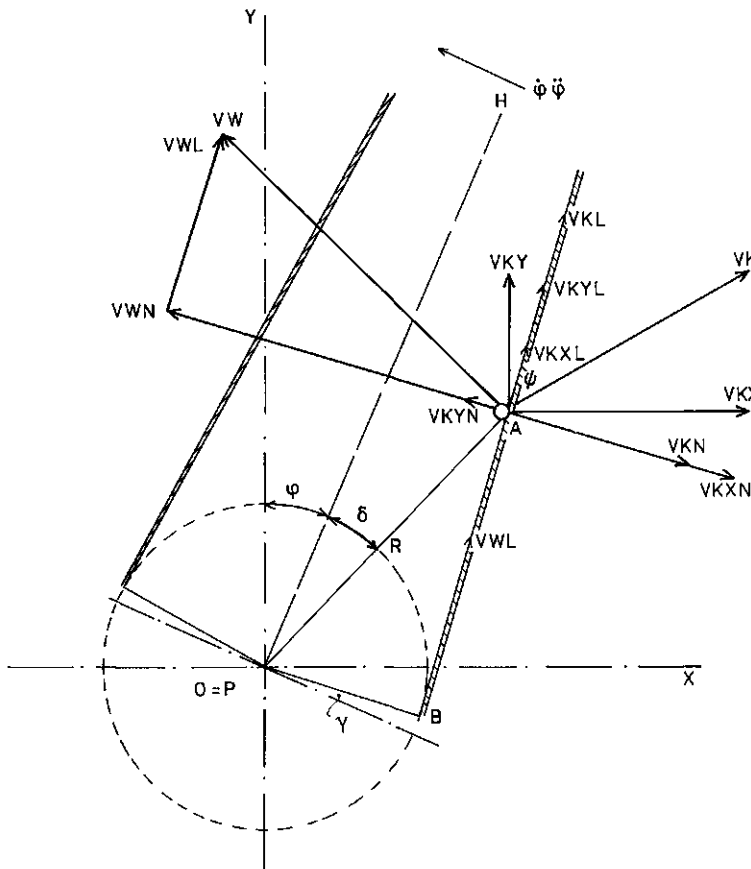


FIG. 5.18. Velocity characteristics of the oscillating sprout and an impacting particle. (Abbreviations and symbols are explained in the text and in the list of symbols on page 214.)

stage of sprout acceleration ( $\phi = \phi_{max} \rightarrow \phi = 0$ ) particle impact dominates. Depending on elastic and friction properties of the particles and the sprout material, as well as the direction of particle movement, a stage of continuous contact can occur (sliding/rolling). At this stage the equation of motion shows a certain rate of agreement with the equations presented for the description of particle movement on a spinning disc (see section 5.2.).

The theoretical analysis and the set-up of the model for particle motion in the oscillating sprout is based on the assumption that particles are moving in the horizontal section according to the centre line  $PH$ . This simplification includes the possibility that variations in velocities and angles of outlet will be underestimated, and the variation in angles of elevation will be neglected.

#### 5.4.2. Particle motion during impact (discontinuous stage)

The description of particle behaviour during the process of impact is based on the model situation as represented in Fig. 5.18. In the section of the sprout which coincides with the plane in which the centre line  $PH$  oscillates, a spherical particle with a mass  $m$  and a radius  $r$  impacts the sprout wall at point  $A$ . Particle movements as well as movements of the oscillating system are characterized by relevant velocities with respect to a fixed  $X-Y$  system of coordinates. Particle impact starts at  $t = 0$  and ends when  $t = \Delta t$ . The kernel impacts the right wall with an angle  $\psi$  (see Fig. 5.18). It is:

$$VKX = VK \cdot \cos(90 - \phi + \gamma - \psi) \quad (5.12)$$

and:

$$VKY = VK \cdot \sin(90 - \phi + \gamma - \psi) \quad (5.13)$$

Now the components derived parallel and perpendicular to the wall are:

$$VKXL = VKX \cdot \sin\theta \quad (5.14)$$

and:

$$VKXN = VKX \cdot \cos\theta \quad (5.15)$$

Similarly:

$$VKYL = VKY \cdot \cos\theta \quad (5.16)$$

$$VKYN = VKY \cdot \sin\theta \quad (5.17)$$

In these equations  $\gamma$  stands for the sprout angle which indicates the convergent ( $\gamma > 0$ ) or divergent ( $\gamma < 0$ ) shape of the sprout (walls). For the right wall it holds  $\theta = \phi - \gamma$ , and for the left wall  $\theta = \phi + \gamma$ .

It yields:

$$VKL = VKXL + VKYL \quad (5.18)$$

and:

$$VKN = VKXN + VKYN \quad (5.19)$$

$V_{KL}$  and  $V_{KN}$  are considered to be positive when their direction coincides with the positive  $Y$ -resp.  $X$ -coordinate.

At the time  $t = 0$  kernel rotation is indicated by  $\omega_1$ , its value is considered to be positive when the rotation is clockwise. During the period  $0 < t \leq \Delta t$  velocities of the sprout wall are supposed to be constant.

For the sprout wall it can be derived that it holds for the point of impact  $A$ :

$$VW = -\frac{\omega \cdot R \cdot \sin \alpha \cdot (C^{-2} - 1)^{1/2}}{C^2 - \sin \alpha} \quad (5.20)$$

in which  $R = PA$ .

The component of  $VW$  parallel to the wall is:

$$VWL = | \dot{\phi} \cdot PB | \quad (5.21)$$

Here,  $PB$  represents the perpendicular line from  $P$  to the sprout wall. Its length can be derived from the dimensions of the sprout. For the right wall

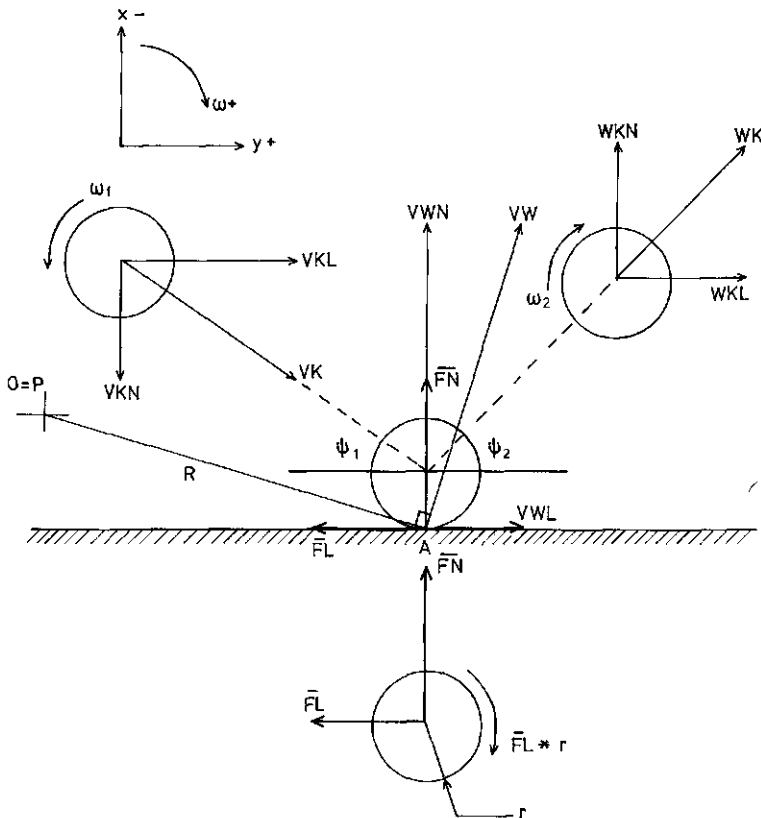


FIG. 5.19. Schematic representation of a particle impact on an oscillating sprout wall. (Abbreviations and symbols are explained in the text and in the list of symbols on page 214.)

velocity and  $\alpha \leq 180^\circ$  and so for the left wall velocity and  $\alpha > 180^\circ$  it holds that:  $VWL = -VWL$ .

The component of  $VW$  perpendicular to the wall can be found from:

$$VWN = (VW^2 - VWL^2)^{1/2} \quad (5.22)$$

It should be noted that when  $\alpha > 180^\circ$ :  $VWN = -VWN$ . So  $VWL$  and  $VWN$  have a positive value if their direction coincides with the positive  $X$ - and  $Y$ -coordinates.

During discontinuous contact the following impacts are acting on the particle parallel and perpendicular to the wall:

$$\overline{FL} \cdot \Delta t = \int_0^{\Delta t} FL \cdot dt \quad (5.23a)$$

$$\overline{FN} \cdot \Delta t = \int_0^{\Delta t} FN \cdot dt \quad (5.23b)$$

At the time  $t = 0$ , the particle has the following velocity components with respect to point  $A$  of the right sprout wall (see Fig. 5.19):

a. parallel to the wall:

– at the circumference of the particle:  $VKL - VWL - p \cdot \omega_1 \cdot r$  in which  $p = +1$  for an impact on the right wall and  $p = -1$  for an impact on the left wall

– in the centre point of the particle:  $VKL - VWL$

b. perpendicular to the wall:  $VKN - VWN$

c. rotation:  $-\omega_1$ .

According to ADAM (1960) the mathematical description of the impact process is based on two model situations. The first, which is indicated as stick impact, results in an angle of reflection which is dependent on the initial kernel rotation, just as in billiard and tennis games. In addition, only the elastic properties of the impacting materials affect the process. On the contrary, it is pointed out that for the second situation, which is indicated as sliding impact, initial particle rotation does not affect the angle of reflection. For the description of this impact process, elastic as well as friction properties of the materials have to be taken into consideration.

At the time  $t = \Delta t$  the following relative particle velocities are recorded:

a. parallel to the wall:

– at the circumference of the particle:  $WKL - VWL - p \cdot \omega_2 \cdot r$

– in the centre point of the particle:  $WKL - VWL$

b. perpendicular to the wall:  $WKN - VWN$

c. rotation:  $\omega_2$ .

These considerations lead to the following equations for the description of the process of impact:

$$\overline{FL} \cdot \Delta t = m \cdot (WKL - VKL) \quad (5.24)$$

A change in velocity parallel to the sprout wall has the same sign as an impact on the particle in this direction. In the same way it holds for the direction

perpendicular to the wall:

$$\overline{FN} \cdot \Delta t = m \cdot (WKN - VKN) \quad (5.25)$$

Taking into consideration the code for the signs and also Eq. (5.24), the change in rotational velocity can be found from:

$$-\overline{FL} \cdot \Delta t \cdot r = J \cdot (\omega_2 - \omega_1) \cdot p \quad (5.26)$$

For a spherical particle the mass moment of inertia is  $J = \frac{2}{5} m \cdot r^2$ .

For a stick impact it holds that:

$$WKL = VWL + \omega_2 \cdot r \cdot p \quad (5.27)$$

With the aid of Eq. (5.24), (5.26), and (5.27) it can be derived for this situation that:

$$WKL = \frac{5}{7} \cdot VKL + \frac{2}{7} \cdot VWL + \frac{2}{7} \cdot \omega_1 \cdot r \cdot p \quad (5.28)$$

Due to the fact that the mass of the wall  $M$  is much greater than the mass of the particle  $m$ ,  $WWN = VWN$ , and introducing a coefficient of restitution  $\varepsilon$  ( $0 < \varepsilon < 1$ ), we find with the aid of:

$$M \cdot VWN + m \cdot VKN = M \cdot WWN + m \cdot WKN \text{ and}$$

$$\frac{1}{2} M \cdot (VWN)^2 + \frac{1}{2} m \cdot (VKN)^2 =$$

$$= \frac{1}{2} M \cdot (WWN)^2 + \frac{1}{2} m \cdot (WKN)^2$$

$$WKN = VKN + (1 + \varepsilon) \cdot (VWN - VKN) \quad (5.29a)$$

or:

$$WKN = (1 + \varepsilon) \cdot VWN - \varepsilon \cdot VKN \quad (5.29b)$$

From Eq. 5.26 and 5.28 follows:

$$\omega_2 = \frac{2}{7} \cdot \omega_1 + \left( \frac{5}{7} \cdot (VKL - VWL) / r \right) \cdot p \quad (5.30)$$

For a sliding impact, taking into account a coefficient of friction  $\mu$ , it holds:

$$|\overline{FL}| = \mu \cdot |\overline{FN}| \quad (5.31)$$

When  $\overline{FL} = +\mu \cdot |\overline{FN}|$ , it can be derived with the aid of Eq. (5.24), (5.25), and (5.29a) that:

$$WKL = VKL + \mu \cdot (1 + \varepsilon) \cdot |VWN - VKN| \quad (5.32)$$

In addition when  $\overline{FL} = -\mu \cdot |\overline{FN}|$ :

$$WKL = VKL - \mu \cdot (1 + \varepsilon) \cdot |VWN - VKN| \quad (5.33)$$

The Eq. (5.29b) already showed that:

$$WKN = (1 + \varepsilon) \cdot VWN - \varepsilon \cdot VKN$$

So the velocity after impact and the angle of reflection are independent of the initial particle rotation.

With the aid of Eq. (5.24) and (5.26) particle rotation after impact can be calculated from:

$$\omega_2 = \omega_1 + \frac{5}{2} \cdot \{(VKL - WKL)/r\} \cdot p \quad (5.34)$$

With the aid of Eq. (5.32) and (5.33) this yields to:

$$\omega_2 = \omega_1 - \frac{5}{2} \cdot \mu \cdot (1 + \varepsilon) \cdot (|VWN - VKN|/r) \cdot p \quad (5.35)$$

and:

$$\omega_2 = \omega_1 + \frac{5}{2} \cdot \mu \cdot (1 + \varepsilon) \cdot (|VWN - VKN|/r) \cdot p \quad (5.36)$$

The transition from a sliding impact to a stick impact is derived from the absolute value of the ratio between velocity components of particle and sprout, perpendicular and parallel to the wall. With the aid of Eq. (5.30) and (5.35) or (5.36), or with Eq. (5.28) and (5.32) or (5.33) we find:

$$\left| \frac{VWN - VKN}{VKL - VWL - \omega_1 \cdot r \cdot p} \right| > \frac{2/7}{\mu \cdot (1 + \varepsilon)} \quad (5.37)$$

The simulation experiments, as far as they are based on this part of the theory, are performed using the following initial conditions:

- the particle impacts the right wall of the sprout with a positive absolute velocity  $VK$  and with an angle of impact  $\psi$ . The direction of  $VK$  with respect to the positive  $X$ -coordinate is represented by angle  $\beta$ , ( $0 < \beta \leq 90$ ) for which yields:  $\beta = 90 - |\phi| + \gamma - \psi$
- the first impact occurs when  $t = 0$  and  $\phi = \phi_{max}$  and so  $\dot{\phi} = 0$ .

The choice of the initial conditions is so arbitrary that there is no fundamental difference between a first impact on the right wall or one on the left wall. As was explained in the previous chapter, the oscillation pattern is symmetrical and therefore conditions for particle energy production and motion are, also.

Asymmetry in the transverse distribution pattern, which has sometimes been noticed in spreading tests, must be attributed to 'external circumstances', such as behaviour of the particles when passing the metering device, and/or the effects of the bow at the end of the sprout. In addition, when the broadcaster is not centrally and horizontally mounted to the tractor, there exists another source for asymmetry. The negative effect of deviations from the nominal revolutions of the driving shaft on the oscillation pattern of the sprout must also be taken into consideration.



The preference for starting the simulation process of the impact phase at the moment when  $\phi = \phi_{max}$  is based on the following considerations. The motion analyses show the extreme positions of the sprout which can be determined reasonably accurately. It is true that the mathematical procedure which was developed for the determination of particle positions of trajectories also enables the determination of the centre position of the sprout (MEULEMAN, 1976). Nevertheless, the fact remains that the initial velocity and angle of impact can be determined more accurately if  $\phi = \phi_{max}$ . Both can be derived from the particle position during the phase of retardation of the sprout. It appears, that during the last part of this phase, and taking into account the accuracy of the method of analysis, velocity and angle of impact can be determined most accurately, especially since the value of the former is relatively great.

#### 5.4.3. Particle motion during sliding and rolling (continuous stage)

The theory which was presented in the previous section for the stage of discontinuous contact holds as long as the particles are inside the sprout and as long as the perpendicular component of wall velocity is different from that of particle velocity ( $V_{WN} \neq V_{KN}$ ).

Continuous contact can now be understood as that stage of particle motion during which the perpendicular component of particle velocity and sprout wall velocity are equal and have the same direction. So:  $V_{WN} = V_{KN}$ .

As it is unlikely that at the beginning of the stage of continuous contact the relative particle velocity of translation is equal to the velocity of rotation or peripheral velocity of the particles ( $\omega r \neq \dot{x}$ ), the first phase of the stage of continuous contact will generally be a sliding motion. So the first strategy for solving the problem will be focused on a calculation of the relative particle velocity during its sliding and rolling motion. This problem is to a certain extent more or less related to the determination of the relative or radial component of the particle velocity of outlet on spinning disc broadcasters.

The change in the absolute position of a particle in a fixed  $X$ - $Y$  system of coordinates can be determined from (Fig. 5.20):

$$X = R \cdot \sin(\phi + \delta) \quad (5.38)$$

and:

$$Y = R \cdot \cos(\phi + \delta) \quad (5.39)$$

with  $\phi$  being the angle of oscillation and  $\delta$  being the angle between  $R$  and the centre line of the sprout.

With:  $\delta + \gamma = \text{asin } c/R = \text{acos } (R^2 - c^2)^{1/2}/R$  in which  $\gamma$  represents the sprout angle and  $c$  is a function of the known sprout width at the entrance of the sprout, the position vectors can be expressed as:

$$X = (R^2 - c^2)^{1/2} \cdot \sin(\phi - \gamma) + c \cdot \cos(\phi - \gamma) \quad (5.40)$$

and:

$$Y = (R^2 - c^2)^{1/2} \cdot \cos(\phi - \gamma) - c \cdot \sin(\phi - \gamma) \quad (5.41)$$

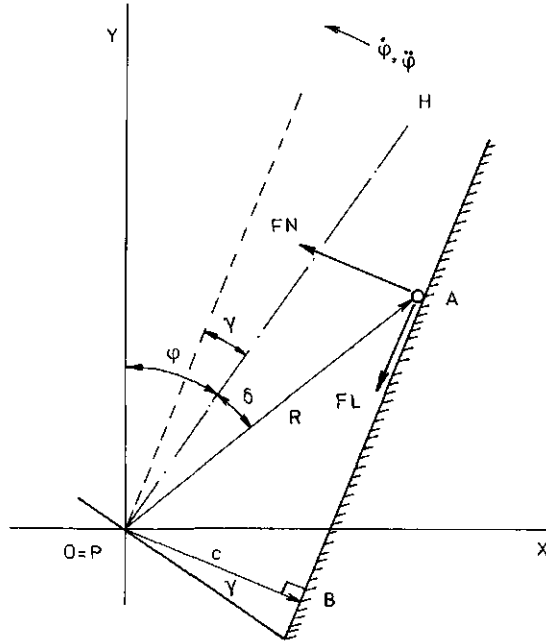


FIG. 5.20. Schematic representation of the determination of absolute velocity of a particle (o) during the stage of continuous contact. (Abbreviations and symbols are explained in the text and in the list of symbols on page 214.)

It can be derived that:

$$\dot{X} = \frac{\dot{R} \cdot R \cdot \sin(\phi - \gamma)}{(R^2 - c^2)^{1/2}} + \dot{\phi} \cdot (R^2 - c^2)^{1/2} \cdot \cos(\phi - \gamma) - c \cdot \dot{\phi} \cdot \sin(\phi - \gamma) \quad (5.42)$$

and:

$$\dot{Y} = \frac{\dot{R} \cdot R \cdot \cos(\phi - \gamma)}{(R^2 - c^2)^{1/2}} - \dot{\phi} \cdot (R^2 - c^2)^{1/2} \cdot \sin(\phi - \gamma) - c \cdot \dot{\phi} \cdot \cos(\phi - \gamma) \quad (5.43)$$

Additionally:

$$\begin{aligned} \ddot{X} = & \frac{\ddot{R} \cdot R \cdot \sin(\phi - \gamma)}{(R^2 - c^2)^{1/2}} - \frac{\dot{R}^2 \cdot c^2 \cdot \sin(\phi - \gamma)}{(R^2 - c^2)^{3/2}} \\ & + \frac{2 \cdot \dot{R} \cdot R \cdot \dot{\phi} \cdot \cos(\phi - \gamma)}{(R^2 - c^2)^{1/2}} + \ddot{\phi} \cdot (R^2 - c^2)^{1/2} \cdot \cos(\phi - \gamma) \\ & - \dot{\phi}^2 \cdot (R^2 - c^2)^{1/2} \cdot \sin(\phi - \gamma) - c \cdot \ddot{\phi} \cdot \sin(\phi - \gamma) \\ & - c \cdot \dot{\phi}^2 \cdot \cos(\phi - \gamma) \end{aligned} \quad (5.44)$$

and:

$$\begin{aligned} \ddot{Y} = & \frac{\ddot{R} \cdot R \cdot \cos(\phi - \gamma)}{(R^2 - c^2)^{1/2}} - \frac{\dot{R}^2 \cdot c^2 \cdot \cos(\phi - \gamma)}{(R^2 - c^2)^{3/2}} \\ & - \frac{2 \cdot \dot{R} \cdot R \cdot \dot{\phi} \cdot \sin(\phi - \gamma)}{(R^2 - c^2)^{1/2}} - \ddot{\phi} \cdot (R^2 - c^2)^{1/2} \cdot \sin(\phi - \gamma) \\ & - \dot{\phi}^2 \cdot (R^2 - c^2)^{1/2} \cdot \cos(\phi - \gamma) - c \cdot \ddot{\phi} \cdot \cos(\phi - \gamma) \\ & + c \cdot \dot{\phi}^2 \cdot \sin(\phi - \gamma) \end{aligned} \quad (5.45)$$

Introduction of the forces  $FL$  and  $FN$  acting perpendicular and parallel to the sprout wall yields to:

$$m \cdot \ddot{X} = -FL \cdot \sin(\phi - \gamma) - FN \cdot \cos(\phi - \gamma) \quad (5.46)$$

and:

$$m \cdot \ddot{Y} = -FL \cdot \cos(\phi - \gamma) + FN \cdot \sin(\phi - \gamma) \quad (5.47)$$

So:

$$FL = -m \cdot \{\dot{X} \cdot \sin(\phi - \gamma) + \dot{Y} \cdot \cos(\phi - \gamma)\} \quad (5.48)$$

and:

$$FN = -m \cdot \{\dot{X} \cdot \cos(\phi - \gamma) - \dot{Y} \cdot \sin(\phi - \gamma)\} \quad (5.49)$$

If  $FL = \mu \cdot FN$  it can be derived from Eq. (5.48) and (5.49) that:

$$\begin{aligned} \dot{X} \cdot \sin(\phi - \gamma) + \dot{Y} \cdot \cos(\phi - \gamma) = & \mu \cdot \{\dot{X} \cdot \cos(\phi - \gamma) \\ - \dot{Y} \cdot \sin(\phi - \gamma)\} \end{aligned} \quad (5.50)$$

Combination of the Eq. (5.44), (5.45), and (5.50) yields into:

$$\begin{aligned} \frac{\ddot{R} \cdot R}{(R^2 - c^2)^{1/2}} - \frac{\dot{R}^2 \cdot c^2}{(R^2 - c^2)^{3/2}} - \dot{\phi}^2 \cdot (R^2 - c^2)^{1/2} - c \cdot \ddot{\phi} \\ - \frac{2 \cdot \mu \cdot \dot{R} \cdot R \cdot \dot{\phi}}{(R^2 - c^2)^{1/2}} - \mu \cdot \ddot{\phi} \cdot (R^2 - c^2) + \mu \cdot \dot{\phi}^2 \cdot c = 0 \end{aligned} \quad (5.51)$$

Relative particle motion with respect to the sprout wall can be determined by introduction of a new  $x$ - $y$  system of coordinates, and using the following relations (Fig. 5.21). One can write for  $R$ ,  $\dot{R}$  and  $\ddot{R}$  resp.:

$$R = (x^2 + c^2)^{1/2} \quad (5.52)$$

$$\dot{R} = x \cdot x / (x^2 + c^2)^{1/2} \quad (5.53)$$

and:

$$\ddot{R} = \ddot{x} \cdot x / (x^2 + c^2)^{1/2} + x^2 \cdot c^2 / (x^2 + c^2)^{3/2} \quad (5.54)$$

The combination of Eq. (5.52)–(5.54) with Eq. (5.51) yields to the following differential equation of the relative motion of a particle with respect to the sprout wall:

$$\ddot{x} - 2 \cdot \mu \cdot \dot{\phi} \cdot \dot{x} \cdot p - \mu \cdot \ddot{\phi} \cdot x \cdot p - \phi^2 \cdot x - \dot{\phi} \cdot c \cdot p + \mu \cdot \phi^2 \cdot c = 0 \quad (5.55)$$

Taking into account the code for the signs of the angle of oscillation  $\phi$  we notice that  $p = +1$  for the right sprout wall and so  $p = -1$  for the left wall.

Now it holds, since  $FL = \mu \cdot FN$ :

$$FN/m = -\dot{\phi} \cdot x \cdot p + \phi^2 \cdot c - 2 \cdot \dot{\phi} \cdot \dot{x} \cdot p \quad (5.56)$$

and:

$$FL/m = +\dot{\phi} \cdot c \cdot p + \phi^2 \cdot x - \ddot{x} \quad (5.57)$$

Due to the force at right angles  $FN$  acting on the particle, a moment  $\mu \cdot r \cdot FN$  is created. It holds:

$$\mu \cdot r \cdot FN = J \cdot \dot{\omega} \quad (5.58)$$

With the aid of Eq. (5.56), the angular acceleration of a spherical particle can be written as:

$$\dot{\omega} = \frac{5}{2} \cdot \mu \cdot (-\dot{\phi} \cdot x \cdot p + \phi^2 \cdot c - 2 \cdot \dot{\phi} \cdot \dot{x} \cdot p) / r \quad (5.59)$$

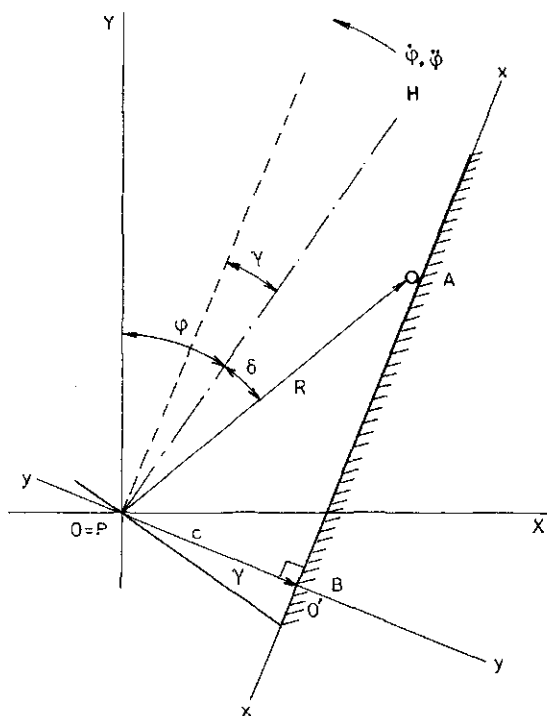


FIG. 5.21. Schematic representation of the determination of the relative velocity of a particle (o) by means of introduction of a system of x-y coordinates. (Abbreviations and symbols are explained in the text and in the list of symbols on page 214.)

The differential equations (5.55) and (5.59) can be solved with the aid of a Runge-Kutta method (ROOS, 1978).

A following possible stage in particle motion is that of the particle rolling along the sprout wall.

So:  $\dot{x} = \omega \cdot r$ . When ignoring rolling resistance it holds:

$$FL \cdot r = J \cdot \dot{\omega} \quad (5.60)$$

Combination of Eq. (5.57) with (5.60) leads to:

$$\ddot{x} = \frac{5}{7} \cdot (\ddot{\phi} \cdot c \cdot p + \dot{\phi}^2 \cdot x) \quad (5.61)$$

By numerical solution of Eq. 5.61 and with  $\omega = \dot{x}/r$  it is possible to calculate particle movement during rolling. The stage of continuous contact is ended when  $FN < 0$  and so not *a priori* if  $\alpha = \pi/2$  or  $\phi = 0^\circ$ . The various movement sub-routines are repeated as long as the particle remains within the sprout. Mostly the successive calculation will start with the process of impact on the opposite wall.

#### 5.4.4. Set-up and testing of the simulation model

Based on the formulated theory of the previous section, a simulation program was written (ROOS, 1978)\*. A flow chart of this program is given in Fig. 5.22. At first, the values of the construction variables of the broadcaster as well as the sprout are read. They include (see also Fig. 4.1): the rotary frequency ( $N$ ) of the driving shaft of the broadcaster ( $\text{min}^{-1}$ ), the length of the crank  $RA$  (m), the length of the connecting rod  $L$  (m), the length of the sprout  $RB$  (m), as well as its diameter at the entrance (m). The design of the sprout is expressed by the value of the sprout angle  $\gamma$  indicating the convergent ( $\gamma > 0$ ) or divergent ( $\gamma < 0$ ) shape of the walls.

Next, a number of particle variables are presented to the program. They consist of (see also Fig. 5.18 and 5.19): the velocity of impact  $VK$  of the particles on the wall ( $\text{m s}^{-1}$ ), the angle of impact  $\psi_1$  (deg), the radius  $r$  of the (spherical) particles (m), the initial rotation  $\omega_1$  of the particles ( $\text{rad s}^{-1}$ ), a coefficient of restitution ( $\epsilon$ ), and a coefficient of friction ( $\mu$ ). The set values of the last three variables need some explanation.

A reasonably accurate determination of the initial rotation ( $\omega_1$ ) of the particles is hardly possible for the spherical particles.

For a stick impact and for  $\dot{\phi} = 0$  it would be in principle possible to calculate the value of  $\omega_1$  from:

$$\omega_1 = VKL \cdot \left( \frac{7}{2} \cdot \frac{\epsilon}{A} - \frac{5}{2} \right) / r \quad (5.62)$$

in which  $A = \tan \psi_2 / \tan \psi_1$ .

\* This program is available at the Department of Agricultural Engineering, Agricultural University Wageningen; The Netherlands.

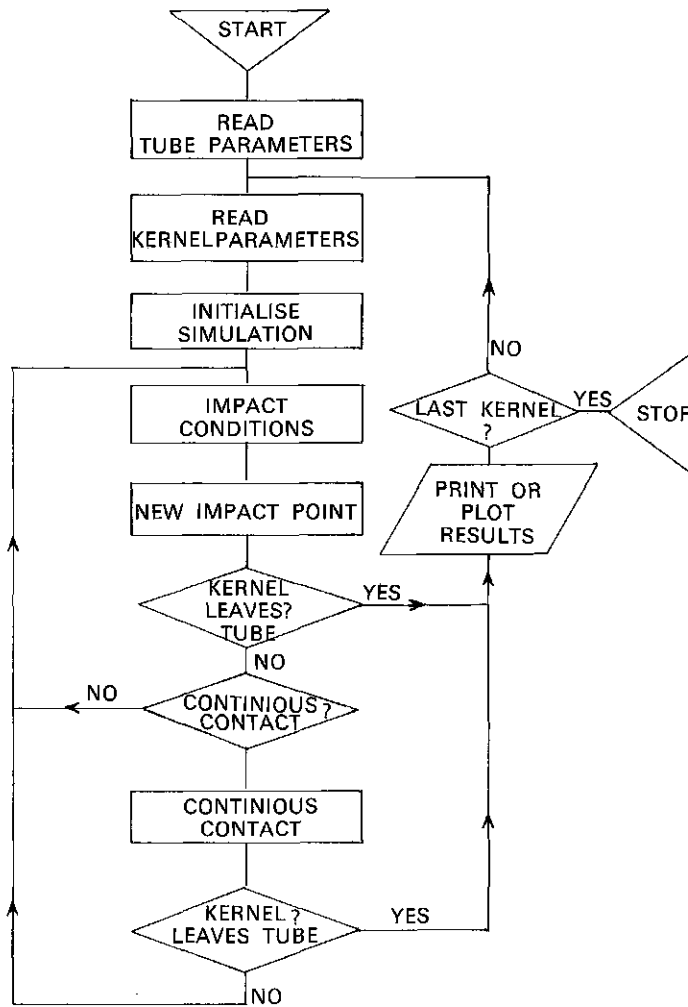


FIG. 5.22. Flow chart of the simulation model.

So if  $\psi_2$  and  $\psi_1$  are measured accurately, the value  $\omega_1$  would only depend on  $\varepsilon$ . However it has been proved that the value of  $\varepsilon$  depends on the value of the velocity of impact  $VK$ , the angle of impact  $\psi$ , and so on  $|VKL - VWL|$  (SHARMA and BILANSKI, 1971; HOEDJES, 1978). In addition, the method which is used in the performance of the experiments plays an important role. Transformation of the results of model experiments with accurate set-values of initial variables to differing situations is unacceptable. In addition, the experimental values of  $\varepsilon$  show a considerable variance even when using narrow fractioned fertilizers and accurate set-values of the initial energy levels and angles of impact (REILING, 1976; HOEDJES, 1978).

As the characteristics of particle motion during the stage of impact are complex and variable, the following procedure is chosen for the adjustment of  $\varepsilon$ . In the simulation model a variable  $\varepsilon^*$  was introduced mainly representing the effect in the model of the elastic properties of the materials. It is assumed that during particle motion, the value of  $\varepsilon^*$  will remain a constant magnitude. Based on the above cited experiments, it is expected that the value of this imaginary coefficient of restitution  $\varepsilon^*$  will be in the range of 0.25–0.80.

With respect to the value of the coefficient of friction  $\mu$ , problems are similar to those which arise in the calculation of the relative velocity component for spinning disc broadcasters (DOBLER and FLATOW, 1968). The adjustment and use of a constant value for a dynamic coefficient of friction seems to be discussable, due to the variation of acting forces and the resulting possibilities for the characteristics of movement.

For this reason we will, just like above, introduce a variable  $\mu^*$  which will be indicated as an imaginary coefficient of friction.

The testing of the simulation model was done in the following way. Firstly, the values of construction variables of the distribution device which were used in these experiments have to be indicated in the program. They are presented in Table 5.1. Secondly, initial particle variables are presented to the program.

For fertilizer A, the mean of the values of  $VK$  was  $8.6 \text{ m s}^{-1}$  and of  $\psi$ :  $38.1^\circ$ . The initial mean radius  $\bar{R}$ , was  $0.37 \text{ m}$ . As a result the mean values for  $VKL$  and  $VKN$  were resp.  $6.7 \text{ m s}^{-1}$  and  $5.2 \text{ m s}^{-1}$ .

For fertilizer B the values were the following:  $\overline{VK} = 8.8 \text{ m s}^{-1}$ ,  $\overline{\psi}_1 = 35.2^\circ$ , and  $\bar{R} = 0.40 \text{ m}$ . As a result of these, the values for  $\overline{VKL}$  and  $\overline{VKN}$  were resp.:  $7.2$  and  $5.0 \text{ m s}^{-1}$ . For both types of fertilizer the radius of the particles was  $1.5 \text{ mm}$ . The values of  $\omega_1$ ,  $\varepsilon^*$ , and  $\mu^*$  were varied according to:  $\omega_1 = -1000(-1000) - 6000 \text{ rad s}^{-1}$ ;  $\varepsilon^* = 0.2 (0.1) 0.8$ ; and  $\mu^* = 0.1 (0.1) 0.6$ .

The initial values of the velocity of impact  $VK$  and the angle of impact  $\psi_1$  were obtained from the analyses of a number of particle trajectories during the last half of the period of sprout oscillation.

Comparison of the results obtained from the simulation experiments with those obtained from the analyses is made according to the following procedure. A. The mean simulated value of the velocities of outlet ( $\overline{VK}$ ) has to agree with the mean measured value of  $VK$ . It should be noted that the measuring error for the determination of the mean value of  $VK$  is  $\pm 0.5 \text{ m s}^{-1}$ .

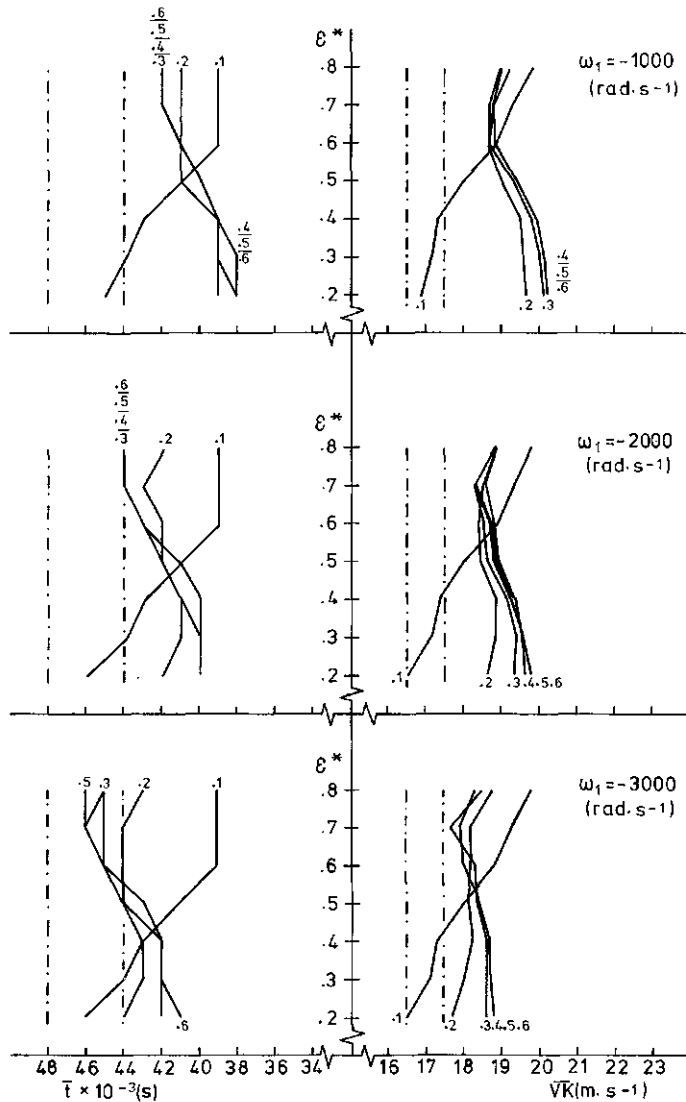
B. In addition to what was mentioned under A, the mean time required for particle motion through the sprout from the initial radii to the orifice (found from the simulation experiments) should be in agreement with the measured mean time of particle stay. Again, it should be noted that a measuring error  $t = \pm 0.002 \text{ s}$  has to be taken into consideration.

First, those combination of  $\omega_1$ ,  $\mu^*$ , and  $\varepsilon^*$  were considered which fulfilled the requirements of A and B. An additional selection was found by considering the simulated and measured values of the angle of dispatch  $\bar{\beta}$ . Its value depended indirectly upon the ratio between e.g. the radial and tangential component of the

velocity of outlet. Considering the accuracy of the determination of the absolute particle velocity, the measuring error in the determination of the mean angle of outlet was  $\pm 1.5^\circ$ .

#### 5.4.5. Experimental results

The results of the simulation experiments are presented in Fig. 5.23 and 5.24. For each experiment the calculated mean values of the velocity of outlet ( $\overline{VK}$ ), and the mean duration ( $\bar{t}$ ) of particle movement within the sprout (from the initial radii to the orifice) are given, in relation to the set values of  $\omega_1$ ,  $\epsilon^*$ , and  $\mu^*$ .





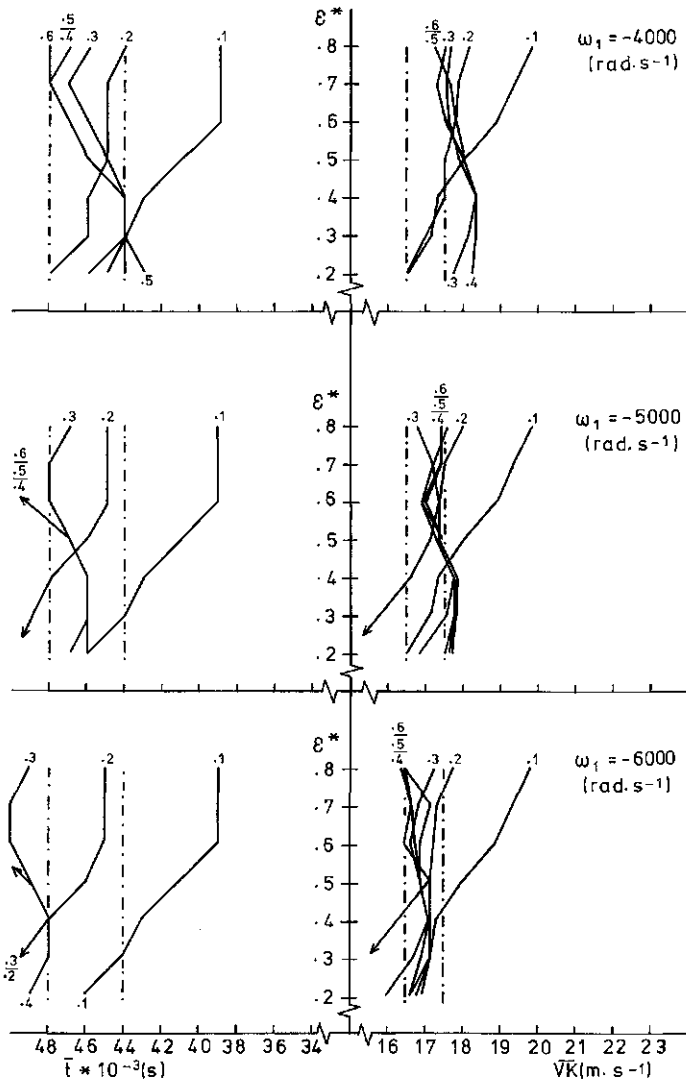
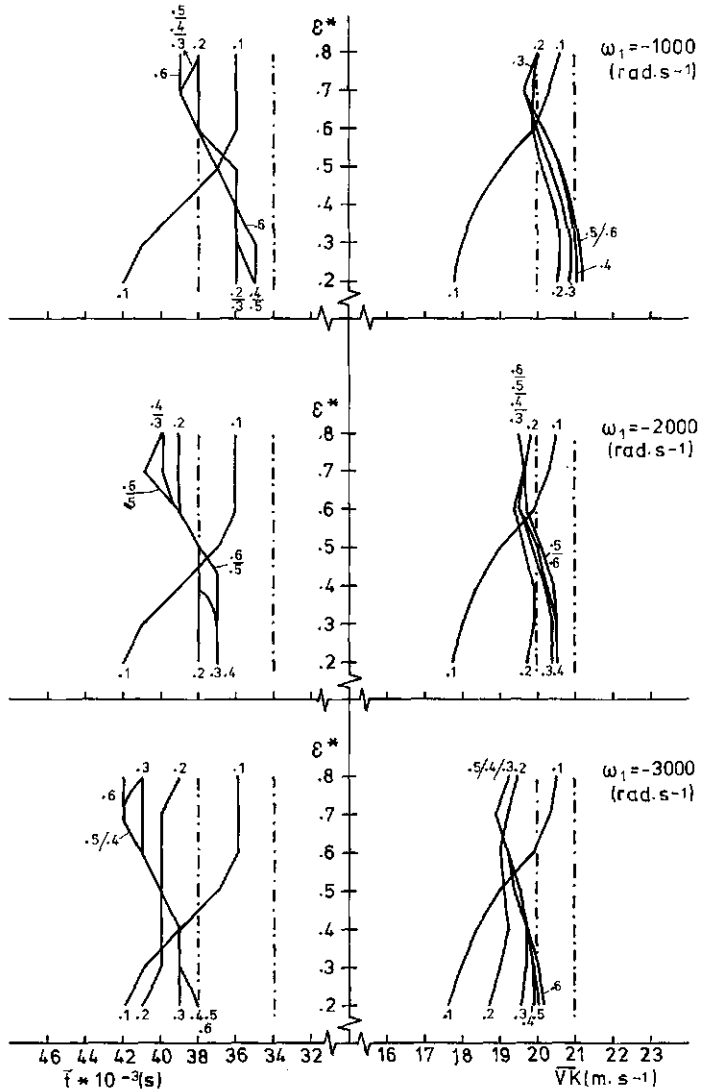


FIG. 5.23. Results of the simulation experiments. The mean values of particle velocity of outlet  $\overline{VK}$  and duration of particle stay in the sprout  $\bar{t}$  as functions of the values of initial particle rotation  $\omega_1$ , imaginary coefficient of restitution  $\epsilon^*$ , and imaginary coefficient of friction  $\mu^*$  (—). Limits of the measured values of  $\overline{VK}$  and  $\bar{t}$  are represented as: - - -. FERTILIZER A.

With respect to fertilizer A the following remarks can be made. For a value of the imaginary coefficient of friction  $\mu^* = 0.1$ , the effect on  $\overline{VK}$  and  $\bar{t}$  at increased values of  $\epsilon^*$  is similar for all examined values of  $\omega_1$ . Thus it can be seen that the initial particle rotation combined with such a low value of  $\mu^*$  does not affect the values of  $\overline{VK}$  and its component parallel to the wall. This can be explained by the fact that the entire impact process during particle motion can be described by

means of equations given for a sliding impact during the stage of discontinuous contact between particles and sprout wall. Under such conditions the value of  $WKL$  does not depend on the particle rotation  $\omega_1$ . In agreement with the previous statement, the mean value of the time needed for particle motion between the given limits does not depend on the initial value of particle rotation. An increase of the imaginary coefficient of restitution  $\varepsilon^*$  leads to an increase of the values of the velocity components after impact  $WKL$  and  $WKN$ , and therefore finally to an increase of the mean velocity of outlet  $\overline{VK}$ .



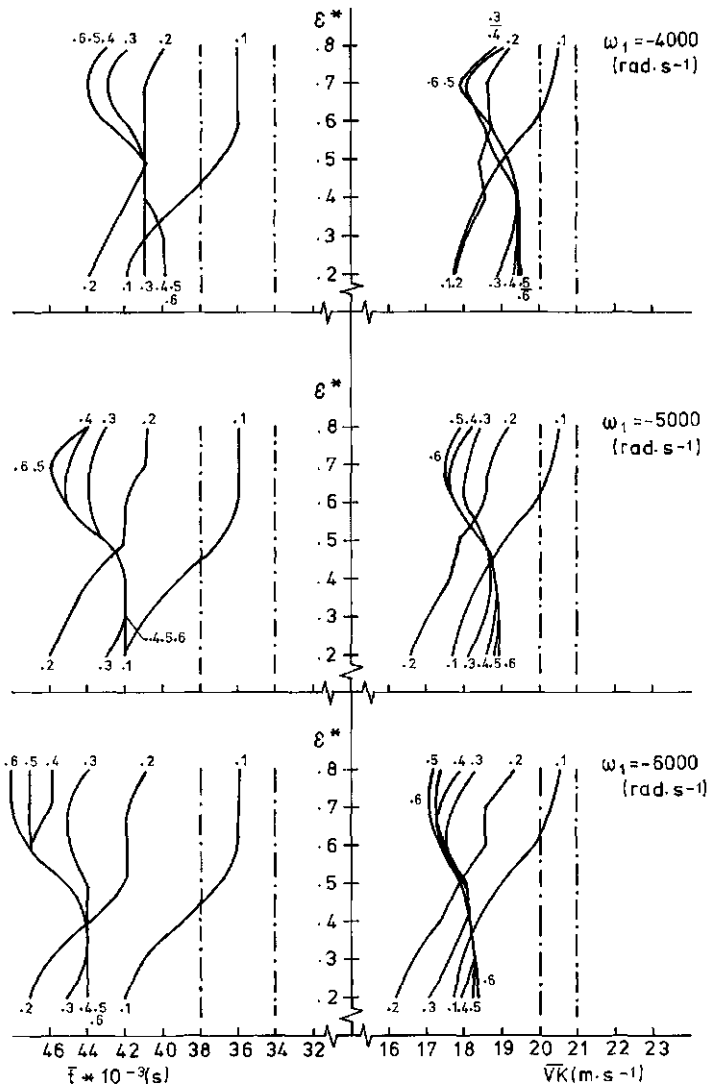


FIG. 5.24. Results of the simulation experiments. The mean values of particle velocity of outlet  $\bar{VK}$  and duration of particle stay in the sprout  $\bar{t}$  as functions of the values of initial particle rotation  $\omega_1$ , imaginary coefficient of restitution  $\varepsilon^*$ , and imaginary coefficient of friction  $\mu^*$  (—). Limits to the measured values of  $\bar{VK}$  and  $\bar{t}$  are represented as: —. FERTILIZER B.

For values of  $\mu^* \geq 0.2$  the influence on  $\bar{VK}$  and  $\bar{t}$  is dependent on the value of  $\omega_1$ , hence  $WKL$  depends on the value of  $\omega_1$ . Therefore, the assumption should be made that during a part of the continuous stage of contact the characteristics of particle motion have to be described with the aid of equations which were given for the stick impact conditions.

An increase of the absolute value of  $\omega_1$  results in a decrease of  $\bar{VK}$  for the Meded. Landbouwhogeschool Wageningen 79-8 (1979)

TABLE 5.5. FERTILIZER A.

Review of the combinations of  $\omega_1$ ,  $\mu^*$ , and  $\varepsilon^*$  which give experimental results for  $\overline{VK}$  and  $\bar{t}$  that are in agreement with the measured values. Combinations for which there is an agreement between simulated and measured values for  $\bar{\beta}$  are printed in bold. ( $16.5 < \overline{VK} < 17.5 \text{ m s}^{-1}$ ;  $0.044 < \bar{t} < 0.048 \text{ s}$ ;  $23.5 < \bar{\beta} < 26.5^\circ$ ).

$\mu^* = 0.1$	$\varepsilon^*$						
$\omega_1 = -1000 \text{ rad s}^{-1}$	0.2	0.3					
-2000	0.2	0.3					
-3000	0.2	0.3					
-4000	0.2	0.3					
-5000	0.2	0.3					
-6000	0.2	0.3					
$\mu^* = 0.2$	$\varepsilon^*$						
$\omega_1 = -4000 \text{ rad s}^{-1}$	<b>0.2</b>	<b>0.3</b>	<b>0.4</b>		<b>0.6</b>		
-5000			0.4	0.5	<b>0.6</b>	0.7	0.8
-6000				0.5	<b>0.6</b>	0.7	
$\mu^* = 0.3$	$\varepsilon^*$						
$\omega_1 = -4000 \text{ rad s}^{-1}$						0.7	0.8
-5000	<b>0.2</b>	<b>0.3</b>		<b>0.5</b>	<b>0.6</b>	0.7	
-6000			<b>0.4</b>				
$\mu^* = 0.4$	$\varepsilon^*$						
$\omega_1 = -4000 \text{ rad s}^{-1}$					0.6	0.7	0.8
-5000	<b>0.2</b>			0.5		0.7	
-6000			0.4				
$\mu^* = -4000 \text{ rad s}^{-1}$	$\varepsilon^*$						
-5000				0.5		0.7	0.8
-6000		0.3	0.4		0.6		

range  $\mu^* \geq 0.2$  and  $0.2 \leq \varepsilon^* \leq 0.8$ ; accordingly, the value of  $\bar{t}$  increases. Increase of the absolute initial value of particle rotation results in the tendency towards conformity between the values for  $\mu^* = 0.1$  and  $\mu^* = 0.2$ , under the conditions that  $\varepsilon^* \leq 0.4-0.5$  and  $\omega_1 = \leq -4000 \text{ rad s}^{-1}$ . In addition, this increase influences the shape of the curves of  $\mu^* = 0.1$  and  $\mu^* \geq 0.2$  in such a way that the intersections are found at ever lower values of  $\varepsilon^*$ . In addition, the curves for  $\mu^* \geq 0.2$  show a tendency towards divergence which at the beginning is most strongly noted for the lower values of  $\mu^*$  and  $\varepsilon^*$ . As the absolute values of  $\omega_1$  increase, this divergence of the curves appears also at higher values of  $\varepsilon^*$ . This phenomenon is most clear with relatively low values of  $\mu^*$ . With respect to the shape of  $\overline{VK}$ , the interaction between  $\mu^*$  ( $\mu^* \geq 0.2$ ) and  $\varepsilon^*$  is apparently such that at first, for values of  $\omega_1 \leq -3000 \text{ rad s}^{-1}$ , an increase of  $\mu^*$  and  $\varepsilon^*$  results in a slight decrease of  $\overline{VK}$ .

At increasing values of  $\omega_1$  ( $\omega_1 \geq -3000 \text{ rad s}^{-1}$ ) the value of  $\overline{VK}$  increases first for  $\mu^* = 0.2$  and later also for  $\mu^* = 0.3$  at increased values of  $\epsilon^*$ . However, the effect of differences of the value of  $\mu^*$  remains small for values of  $\epsilon^* \geq 0.5$ .

Coherence between the variables  $\omega_1$ ,  $\mu^*$  and  $\epsilon^*$  appears to be complex. Their relationship is such that it is not *a priori* allowed to assume that high values of the imaginary coefficient of restitution combined with low values of the imaginary coefficient of friction will result in high mean values of the velocity of outlet of the fertilizer particles.

When trying to answer the question, which combinations of  $\omega_1$ ,  $\mu^*$ , and  $\epsilon^*$  give simulation results which can be considered to be in agreement with the measured values, Table 5.5 shows that based on the criteria under A and B, a number of combinations have to be discussed.

The addition to these criteria of the condition that the simulated mean values of the angles of dispatch  $\beta$  also should show an agreement with the measured values, results in a further restriction of the possible combinations.

Applying the combination:  $\omega_1 = -1000 \text{ rad s}^{-1}$ ,  $\mu^* = 0.1$  and  $\epsilon^* = 0.2$  requires the use of a low value of  $\epsilon^*$ . This value differs considerably from the results of experiments performed by REILING (1976). In his experiments, values for the coefficient of restitution of 0.46–0.64 were obtained. The impact velocity of the particles was  $4.5 \text{ m s}^{-1}$ . In REILING's experiments a reflection plate of the same material as the sprout was used. Although situations during particle impacts within the sprout can differ substantially from the model experiments by REILING, it is justified, in our opinion, to conclude that the value of  $\epsilon^* \geq 0.3$ . The next possible combinations are:  $\omega_1 = -4000 \text{ rad s}^{-1}$ ,  $\mu^* = 0.2$  and  $\epsilon^* = 0.3, 0.4$ . Accepting  $\mu^* = 0.2$  as a possible value means that  $WKL$  and therefore  $WK$

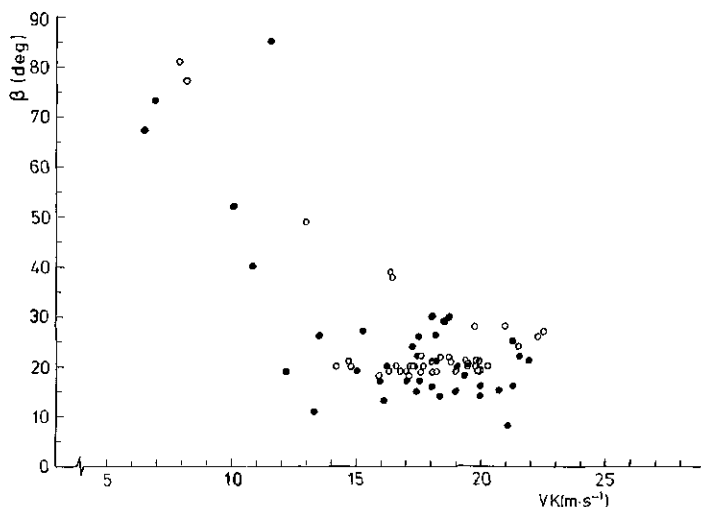


FIG. 5.25. The relation between simulated (o) and measured values (●) of the angles of particle dispatch ( $\beta$ ) and velocity of outlet  $VK$ . FERTILIZER A.

TABLE 5.6. FERTILIZER B.

Review of the combinations of  $\omega_1$ ,  $\mu^*$ , and  $\varepsilon^*$  which give experimental results for  $\overline{VK}$ ,  $\bar{t}$ , and  $\bar{\beta}$ , that agree with the measured values. ( $20.0 < \overline{VK} < 21.0 \text{ m s}^{-1}$ ;  $0.034 < \bar{t} < 0.038 \text{ s}$ ;  $25.0 < \bar{\beta} < 28.0^\circ \rightarrow \text{all}$ ).

$\mu^* = 0.1$	$\varepsilon^*$					
$\omega_1 = -1000 \text{ rad s}^{-1}$					0.7	0.8
-2000					0.7	0.8
-3000					0.7	0.8
-4000					0.7	0.8
-5000					0.7	0.8
-6000					0.7	0.8
$\mu^* = 0.2$	$\varepsilon^*$					
$\omega_1 = -1000 \text{ rad s}^{-1}$	0.2	0.3	0.4	0.5		0.8
$\mu^* = 0.3$	$\varepsilon^*$					
$\omega_1 = -1000 \text{ rad s}^{-1}$	0.2	0.3	0.4	0.5	0.6	0.8
= -2000	0.2	0.3	0.4			
$\mu^* = 0.4$	$\varepsilon^*$					
$\omega_1 = -1000 \text{ rad s}^{-1}$	0.2	0.3	0.4	0.5	0.6	
-2000	0.2	0.3	0.4	0.5		
$\mu^* = 0.5$	$\varepsilon^*$					
$\omega_1 = -1000 \text{ rad s}^{-1}$			0.4	0.5	0.6	
-2000	0.2	0.3	0.4	0.5		
$\mu^* = 0.6$	$\varepsilon^*$					
$\omega_1 = -1000 \text{ rad s}^{-1}$		0.3	0.4	0.5	0.6	
-2000	0.2	0.3	0.4	0.5		
-3000	0.2	0.3				

and  $\overline{VK}$  are dependent on  $\omega_1$ . Furthermore, it is important that a value of  $\mu^* \geq 0.2$  provides the possibility for transition of a sliding to a rolling particle motion during the last phase of the stage of continuous contact so that  $\dot{x} = \omega \cdot r$ . It appears that the velocity and direction of the particles when leaving the sprout are mainly determined by the characteristics of particle motion during the last half period of sprout oscillation.

Since especially the estimated initial value of  $\omega_1$  must correspond reasonably with the terminal value of the particle rotation obtained during the previous oscillation period, one can conclude that for a value of  $\mu^* = 0.2$ , during a part of this period the acting forces  $FL$  and  $FN$  had such values that a considerable particle rotation could be obtained. For fertilizer type A, the measured mean value of the velocity component  $VKL$  at the end of this oscillation period was  $6.7 \text{ m s}^{-1}$ . Related to this, and taking into consideration the restrictions in the

TABLE 5.7. Part of the output of a simulation experiment showing that during the phase of continuous contact (CON) the kernel starts rolling (ROL) at relatively great values for the angle of oscillation ( $\theta$ ) when  $\mu^* \geq 0.2$ .

$R^*$ (m)	XKERNEL (m)	YKERNEL (m)	VBIMPC (m s <sup>-1</sup> )	VBIMPCL (m s <sup>-1</sup> )	VBIMPCN (m s <sup>-1</sup> )	VAIMPC (m s <sup>-1</sup> )	VAIMPCL (m s <sup>-1</sup> )	VAIMPCN (m s <sup>-1</sup> )	FI (deg)	ALPHA (deg)	TIME (s)	BNDR	ST/SL	IM/CO	ROTATION (rad s <sup>-1</sup> )	180°-BETA (deg)
.38	0.218	0.312	8.70	6.66	5.59	5.57	5.10	-2.24	28.36	0.00	0.000	R	SL	IMP	1609.72	93.67
.42	0.220	0.356	5.57	5.19	-2.02	7.12	4.55	-5.47	25.90	25.89	0.008	R	ST	IMP	2674.54	64.66
.43	0.212	0.375	7.12	4.75	-5.30	8.23	4.75	-6.72	23.78	35.29	0.011	R	ST	IMP	2674.77	58.05
.43	0.207	0.382	8.23	4.87	-6.63	8.69	4.86	-7.21	22.78	38.93	0.012	R	ST	IMP	2693.62	55.75
.44	0.204	0.386	8.69	4.91	-7.17	8.88	4.90	-7.40	22.36	40.37	0.012	R	ST	IMP	2704.46	54.88
.44	0.206	0.388	8.88	4.90	-7.40	9.85	6.53	-7.38	22.36	41.18	0.013	R	SLI	CON	2771.24	62.85
.44	0.204	0.391	9.85	6.53	-7.38	9.95	6.48	-7.55	22.11	41.99	0.013	R	SLI	CON	2838.24	61.74
.44	0.203	0.393	9.95	6.48	-7.55	10.06	6.44	-7.73	21.86	42.80	0.013	R	SLI	CON	2905.46	60.66
.44	0.202	0.395	10.06	6.44	-7.73	10.16	6.39	-7.90	21.61	43.61	0.014	R	SLI	CON	2972.86	59.58
.44	0.201	0.397	10.16	6.39	-7.90	10.27	6.35	-8.07	21.35	44.42	0.014	R	SLI	CON	3040.41	58.53
.45	0.199	0.399	10.27	6.35	-8.07	10.27	6.31	-8.25	21.08	45.23	0.014	R	SLI	CON	3108.11	57.49
.45	0.198	0.401	10.38	6.31	-8.25	10.38	6.27	-8.42	20.81	46.04	0.014	R	SLI	CON	3175.92	56.47
.45	0.196	0.404	10.50	6.27	-8.42	10.50	6.23	-8.59	20.54	46.85	0.015	R	SLI	CON	3243.82	55.46
.45	0.195	0.406	10.61	6.23	-8.59	10.61	6.19	-8.77	20.26	47.66	0.015	R	SLI	CON	3311.79	54.47
.45	0.193	0.408	10.73	6.19	-8.77	10.73	6.15	-8.94	19.98	48.47	0.015	R	SLI	CON	3379.79	53.50
.45	0.192	0.410	10.85	6.15	-8.94	10.85	6.11	-9.11	19.69	49.28	0.016	R	SLI	CON	3447.81	52.55
.45	0.190	0.412	10.98	6.11	-9.11	10.98	6.18	-9.29	19.40	50.09	0.016	R	ROL	CON	3431.49	52.02
.46	0.188	0.415	11.15	6.18	-9.29	11.15	6.24	-9.46	19.10	50.90	0.016	R	ROL	CON	3462.93	51.51
.46	0.186	0.417	11.33	6.24	-9.46	11.33	6.30	-9.63	18.80	51.71	0.016	R	ROL	CON	3495.09	51.00
.46	0.185	0.419	11.51	6.30	-9.63	11.51	6.37	-9.81	18.49	52.52	0.016	R	ROL	CON	3528.01	50.50

KERNEL TYPE: B

RESTITUTION: 0.40

FRICTION: 0.20

KERNEL ROTATION: -1000.00 rad s<sup>-1</sup>

\* The abbreviations are explained in the list of symbols (page 214).

model that  $\omega \cdot r = \dot{x} \leq VKL$ , an initial particle rotation of  $-4000 \text{ rad s}^{-1}$  seems to be acceptable ( $|\omega \cdot r| = 6 \text{ m s}^{-1}$ ). It can be added that it appears from the analyses that the particles are losing contact with the sprout wall during the last part of the phase of retardation of the sprout. At that time the value of  $VWL$  has an order of size of  $0.5 \text{ m s}^{-1}$  so that  $\omega \cdot r \approx |VKL - VWL|$ . According to the limitations of the model, the combinations in which  $\omega_1 \geq -5000 \text{ rad s}^{-1}$  are unlikely since the initial value of the particle rotation is too high.

Summarizing, it can be stated that it is justifiable to state that for fertilizer type A, the mean particle velocity of outlet  $\overline{VK}$ , angle of dispatch  $\overline{\beta}$ , and duration of particle movement  $\overline{t}$  within the sprout can be calculated with the aid of the theory included in the model. The values which have to be entered for the variables  $\omega_1$ ,  $\mu^*$  and  $\varepsilon^*$  are reasonable. The best agreement between measured and simulated values are obtained if  $\omega_1 = -4000 \text{ rad s}^{-1}$ ,  $\mu^* = 0.2$  and  $\varepsilon^* = 0.4$ . The results of the simulation experiments for the abovementioned combination of set values of the variables is presented in Fig. 5.25 together with the measured values of  $VK$  and  $\beta$ .

For the simulated values of  $VK$  and  $\beta$  the variance is smaller than for the measured values. The standard deviations were resp.  $2.9 \text{ m s}^{-1}$  and  $13.5^\circ$  against  $3.7 \text{ m s}^{-1}$  and  $16.0^\circ$ . An explanation for this can be found when considering the fact that the simulated values are a result of the adjustment during the whole process of particle motion of constant values for the variables  $\omega_1$  and  $r$  together with constant values for  $\mu^*$  and  $\varepsilon^*$ . In addition, the model calculations are based on spherical particles with trajectories which coincide with the horizontal section of the sprout.

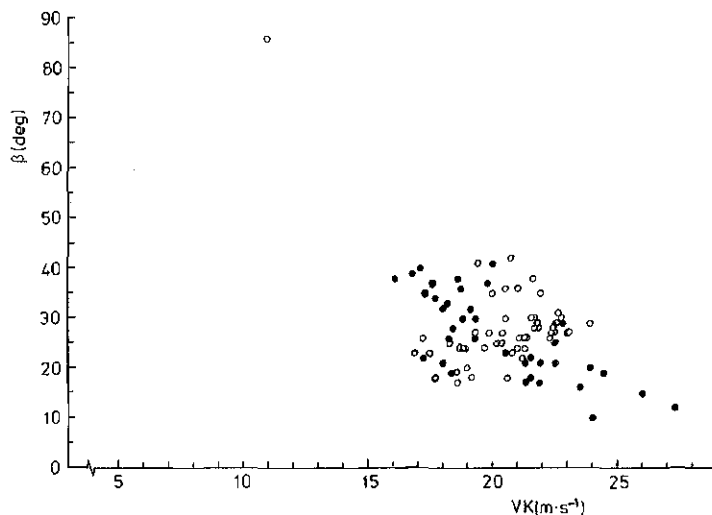


FIG. 5.26. The relation between simulated (○) and measured values (●) of the angles of particle dispatch ( $\beta$ ) and velocity of outlet  $VK$ . FERTILIZER B.



The results of the simulation experiments for type B are presented in Fig. 5.24. The curves representing the results of  $\overline{VK}$  and  $\bar{i}$  show a similar tendency as fertilizer A. This can be easily understood since the mean initial values of the input variables were only different to a small extent. The initial velocity components were somewhat higher for fertilizer B. These small differences appear also in the experimental results. The level of the mean velocity of outlet  $\overline{VK}$  is somewhat higher for fertilizer B. On the other hand, the level of  $\bar{i}$  is lower for the same combinations of  $\omega_1$ ,  $\varepsilon^*$  and  $\mu^*$ .

The results of the simulation experiments obtained with values for  $\mu^* \geq 0.2$  show that a relatively great number of combinations give acceptable values of  $\overline{VK}$ ,  $\bar{i}$  and  $\bar{\beta}$  (Table 5.6). However, nearly all these combinations have an initial particle rotation of  $-1000$  or  $-2000 \text{ rad s}^{-1}$ . In addition, we ignore the hardly possible combinations with  $\mu^* = 0.6$  and  $\varepsilon^* = 0.2$ , and  $0.3$ .

Similar to what was noted for fertilizer A before, further analyses of the simulation experiments for values of  $\mu^* \geq 0.2$  show that during the last oscillation period a value of the angle of oscillation  $\phi$  is obtained rather quickly, for which a rolling motion of the particles can occur at values of  $\dot{\phi} > 20 \text{ rad s}^{-1}$ . As an example, Table 5.7 shows a part of the results of a simulation experiment: it should be noted that in the output the angle of rotation  $\alpha$  shows a difference in phase of  $180^\circ$ .

Within this framework, it is interesting to refer to the theoretical analyses of particle motion on rotating discs with vanes presented by PATTERSON and REECE (1962). It appeared that particles which were supplied on such a spinning disc at a radius of  $0.15 \text{ m}$  immediately started rolling along the vanes when the tangential speed was  $3.2 \text{ m s}^{-1}$  and the coefficient of friction was  $\mu \geq 0.3$ .

With respect to the question if the oscillation characteristic of the distributor device of the reciprocating sprout fertilizer broadcaster can create similar velocity levels, the following remarks can be made. Starting from the maximum value of  $\dot{\phi}$ , for  $C = 0.475$  and  $\omega = 56.55 \text{ rad s}^{-1}$ , a resulting angular velocity of oscillation of  $30.54 \text{ rad s}^{-1}$  will create a similar tangential velocity level at a value of  $RB$  of  $0.105 \text{ m}$  (see Fig. 4.6). As a matter of fact, an increase of  $RB$  will result in similar velocity levels at an earlier phase of the oscillation period. For example, a combination  $RB = 0.19 \text{ m}$  and  $\phi = 22.5^\circ$  can be mentioned. For the reciprocating sprout broadcasters a frictional force component (caused by the tangential acceleration) has to be added to frictional force caused by the Coriolis acceleration. As a consequence, it is very reasonable to state that for the reciprocating sprout broadcaster, a rolling motion of spherical particles will be possible for values  $RB \geq 0.15 \text{ m}$  at the mentioned values of the imaginary coefficient of friction. For spinning disc broadcasters, a value for the coefficient of friction  $\mu \geq 0.17$ , enables the transition of particle motion from a sliding to a rolling mode, since in practice values  $\geq 200 \text{ min}^{-1}$  for the rotary frequency of the disc, and values  $\geq 0.3 \text{ m}$  for the disc diameter are applied. It can be stated that a value of  $\mu^* \geq 0.17$  also enables a rolling mode of particle motion for the reciprocating sprout broadcaster.

TABLE 5.8. Example of output of simulation experiments showing that for  $\mu^* = 0.1$  and  $\varepsilon^* = 0.7$ ; particle motion completely consists of impact (IMP) with a sliding character (SL).

<i>R*</i>	<i>YKERNEL</i>	<i>YKERNEL</i>	<i>VBIMPC</i>	<i>VBIMPCL</i>	<i>VBIMPCN</i>	<i>VAIMPC</i>	<i>VAIMPCL</i>	<i>VAIMPCN</i>
.39	0.222	0.321	9.70	7.54	6.10	7.78	6.50	- 4.27
.47	0.211	0.424	7.78	6.97	- 3.46	13.56	6.10	-12.11
.52	0.137	0.505	13.56	8.26	-10.76	18.56	7.64	-16.91
.57	0.037	0.572	18.56	10.72	-15.15	21.63	10.33	-19.01
KERNEL LEAVES THE SPROUT.								
	<i>YKERNEL</i>	<i>YKERNEL</i>	<i>VAFTER</i>	<i>VAFTRX</i>	<i>VAFTRY</i>	<i>ALPHA</i>	<i>TIME</i>	<i>BETA</i>
	-0.099	0.642	21.635	-19.236	9.902	113.452	0.035	27.238
<i>R</i>	<i>YKERNEL</i>	<i>YKERNEL</i>	<i>VBIMPC</i>	<i>VBIMPCL</i>	<i>VBIMPCN</i>	<i>VAIMPC</i>	<i>VAIMPCL</i>	<i>VAIMPCN</i>
.35	0.204	0.285	9.90	6.95	7.05	7.58	5.75	- 4.93
.44	0.175	0.407	7.58	6.56	- 3.80	15.04	5.54	-13.98
.51	0.046	0.509	15.04	9.44	-11.71	20.20	8.79	-18.19
KERNEL LEAVES THE SPROUT.								
	<i>YKERNEL</i>	<i>YKERNEL</i>	<i>VAFTER</i>	<i>VAFTRX</i>	<i>VAFTRY</i>	<i>ALPHA</i>	<i>TIME</i>	<i>BETA</i>
	-0.180	0.616	20.203	-18.262	8.642	129.142	0.040	25.324
<i>R</i>	<i>YKERNEL</i>	<i>YKERNEL</i>	<i>VBIMPC</i>	<i>VIMPCL</i>	<i>VBIMPCN</i>	<i>VAIMPC</i>	<i>VAIMPCL</i>	<i>VAIMPCN</i>
.40	0.227	0.329	9.10	5.80	- 7.01	6.73	4.61	- 4.91
.47	0.192	0.428	6.73	5.34	- 4.10	14.43	4.38	-13.75
.52	0.069	0.516	14.43	7.98	-12.12	19.69	7.35	-18.26
KERNEL LEAVES THE SPROUT.								
	<i>YKERNEL</i>	<i>YKERNEL</i>	<i>VAFTER</i>	<i>VAFTRX</i>	<i>VAFTRY</i>	<i>ALPHA</i>	<i>TIME</i>	<i>BETA</i>
	-0.153	0.616	19.688	-17.976	8.031	124.274	0.038	24.073
<i>R</i>	<i>YKERNEL</i>	<i>YKERNEL</i>	<i>VBIMPC</i>	<i>VIMPCL</i>	<i>VBIMPCN</i>	<i>VAIMPC</i>	<i>VAIMPCL</i>	<i>VAIMPCN</i>
.38	0.218	0.312	10.30	6.71	- 7.69	7.62	5.40	- 5.38
.47	0.179	0.435	7.62	6.34	- 4.24	16.04	5.24	-15.16
.54	0.024	0.544	16.04	9.88	-12.63	21.34	9.22	-19.24
KERNEL LEAVES THE SPROUT.								
KERNEL TYPE:		B						
RESTITUTION:		$\varepsilon^* = 0.70$						
FRICTION:		$\mu^* = 0.10$						
KERNEL ROTATION:		$\omega_1 = -3000.00 \text{ rad s}^{-1}$						

\* The abbreviations are explained in the list of symbols (page 214).

However, for fertilizer B the value of  $\omega_1 \cdot r$  has to equal  $\dot{x}$  and thus  $|VKL - VWL|$  under those conditions. As the value of  $\dot{x}$  is about  $6.3 \text{ m s}^{-1}$ , given the mean value of  $VKL$  and the characteristic of particle motion within the sprout, it can be concluded that the combinations for  $\mu^* \geq 0.2$  and  $\omega_1 = -1000$  and  $-2000 \text{ rad s}^{-1}$  are unlikely.

Based on these considerations, it is our opinion that a reasonable agreement between the results of the simulation experiments and the measured values can be obtained for fertilizer B when introducing values of 0.7 for the imaginary

TABLE 5.8. Continuation.

<i>FI</i>	<i>ALPHA</i>	<i>TIME</i>	<i>BNDR</i>	<i>ST/SL</i>	<i>IM/CO</i>	<i>ROTATION</i>	180°- <i>BETA</i>
28.36	0.00	0.000	R	SL	IMP	-1270.42	84.04
21.44	43.33	0.013	R	SL	IMP	172.18	47.17
10.66	69.59	0.021	R	SL	IMP	1197.19	33.99
-0.29	90.53	0.028	R	SL	IMP	1840.35	27.24

<i>FI</i>	<i>ALPHA</i>	<i>TIME</i>	<i>BNDR</i>	<i>ST/SL</i>	<i>IM/CO</i>	<i>ROTATION</i>	180°- <i>BETA</i>
28.36	0.00	0.000	R	SL	IMP	-1002.77	76.74
17.79	53.53	0.017	R	SL	IMP	694.97	38.41
0.52	89.03	0.027	R	SL	IMP	1775.38	25.32

<i>FI</i>	<i>ALPHA</i>	<i>TIME</i>	<i>BNDR</i>	<i>ST/SL</i>	<i>IM/CO</i>	<i>ROTATION</i>	180°- <i>BETA</i>
28.36	0.00	0.000	R	SL	IMP	-1013.36	70.56
19.05	50.23	0.016	R	SL	IMP	595.01	35.71
3.14	84.17	0.026	R	SL	IMP	1635.24	24.07

<i>FI</i>	<i>ALPHA</i>	<i>TIME</i>	<i>BNDR</i>	<i>ST/SL</i>	<i>IM/CO</i>	<i>ROTATION</i>	180°- <i>BETA</i>
28.36	0.00	0.000	R	SL	IMP	-822.20	72.46
17.22	54.97	0.017	R	SL	IMP	997.88	35.30
-1.75	93.24	0.029	R	SL	IMP	2100.17	22.86

coefficient of restitution  $\varepsilon^*$ , and 0.1 for the imaginary coefficient of friction  $\mu^*$ . Under these circumstances the initial value of  $\omega_1$  does not influence the results of  $\overline{VK}$ ,  $\bar{t}$ , and  $\bar{\beta}$  as the phase of impact can be completely described by the equations which were given for a sliding impact (see Table 5.8).

Fig. 5.26 shows agreement between simulated and measured values. With respect to the deviation of  $\overline{VK}$ , it holds that the value is greater for the measured values than for the simulated ones. They are 2.7 and 2.1 m s<sup>-1</sup> respectively.

Contrary to the results for fertilizer A, the standard deviation of the simulated values of  $\beta$  is greater than of the measured ones (10.0° resp. 8.3°). This is somewhat in disagreement with the expectation. This contradiction, however, is mainly determined by one single large deviating value of  $\beta$  (86.3°). Without this value the deviation of  $\beta$  would be reduced to 5.5°, the value of  $\bar{\beta}$  would decrease

to  $26.8^\circ$ , that of  $\overline{VK}$  would increase to  $20.5 \text{ m s}^{-1}$ , and the value of  $\bar{t}$  would not change at all.

#### 5.4.6. Discussion

It appears to be possible to develop a model which enables the calculation of the mean velocities and directions of the particles when leaving the oscillating sprout.

In the development of the theory and the successive set-up of the model, the following simplifications are introduced:

- Particle movement takes place in the plane which coincides with the horizontal section of the sprout.
- The theory holds for that part of the sprout where the particles have completed the process of sorting-in, and this includes a certain rate of synchronism between sprout and particle movement.
- The variables  $\varepsilon^*$  and  $\mu^*$  which represent restitution and friction properties of the materials are considered to be constant during the complete process of particle motion.
- It is assumed that the fertilizer particles have a spherical shape. Their size is represented by a constant value for the diameter.

The simulation experiments which were performed for the testing of the value of the model, show the following.

For values of the imaginary coefficient of friction  $\mu^* = 0.10$  it appears that for both types of fertilizer, the relative particle velocity does not depend on the initial particle rotation  $\omega_1$ . This includes the fact that the characteristic of particle motion during the stage of discontinuous contact can be described with the aid of the theory for sliding particle impacts.

For both fertilizer types reasonable agreement can be obtained between the measured and simulated values as well as for the mean particle velocity of outlet, the mean time needed for particle movement through the sprout, and the mean angle of dispatch. For that purpose, an initial particle rotation of  $-4000 \text{ rad s}^{-1}$  and values for the imaginary coefficients of friction and restitution of 0.2 and 0.4 for fertilizer A have to be used as input variables in the simulation model. These values are both explainable and/or reasonable. For fertilizer B, values for  $\mu^*$  and  $\varepsilon^*$  of resp. 0.1 and 0.7 have to be used in the model. As a result, the value of the initial particle rotation  $\omega_1$  has no influence on particle motion during the phase of impact. These values are also reasonable to explain. It should be emphasized that the actual values for the coefficients of restitution and friction (which are in good agreement) were determined at a later stage of the research work.

The fact that the values for  $\mu^*$ ,  $\varepsilon^*$  and  $\omega_1$  have to be estimated can be considered a weakness of the model. However, taking into consideration the relatively small number of particles which are used for the comparison of simulated and measured results, in our opinion the final conclusion is justified that the developed model enables reasonable possibilities for the calculation of the velocity and direction of outlet of the particles depending on the broadcaster design and fertilizer properties.

It should be mentioned that the application rate was decreased to the very low value of  $0.5 \text{ kg min}^{-1}$ . The mutual affection of particles could be neglected in the experiments. In practice, when application rates of  $60\text{--}120 \text{ kg min}^{-1}$  are used, mutual particle affection can occur. As the consequence, it can be expected that the variation in particle trajectories and velocities will increase. To a certain extent, such an effect can act favourably on the distribution pattern.

## 6. EFFECTS OF DESIGN VARIABLES ON THE DISTRIBUTION PROCESS

### 6.1. INTRODUCTION

In the previous chapter attention was paid to the development of a simulation model for the description of particle dynamics. The next sections deal with experiments whose objective is to use the model for examination of the effects of changing various design parameters on the process of particle motion and, as a consequence, on the distribution process. In addition, laboratory experiments are performed with comparable designs of the reciprocating sprout broadcaster.

The effects of various design variables on the distribution process are studied in order to examine possibilities for:

- enlargement of the spreading width (and, as a consequence, the working width); and
- realization of some well-defined ranges of bout width for specific practical conditions.

As bout width depends on both particle velocities of outlet and angles of dispatch, the discussion of the experimental results is based on the values of these two variables.

Attention will be paid to the choice of the initial values of the particle input variables since it can be expected that they have interactions with alteration of design variables of the broadcaster.

It has been widely proved by experiments that without further provisions, the kinematics of the distributor device realizes a diverging particle flow after dispatch. As a result, a two-peak, hollow cone transverse distribution pattern is obtained, which is unwanted in practice with respect to evenness of the compound transverse distribution pattern. Within this framework, the effect of an additional device at the end of the sprout, and a specific design of the orifice on particle motion will be examined.

### 6.2. SPROUT DESIGN AND THE EFFECTS ON PARTICLE VELOCITIES AND ANGLES OF OUTLET

In its present design the reciprocating sprout broadcaster is equipped with a round converging steel or polyester sprout. The convergent shape is expressed by the value of the sprout angle  $\gamma$ , (which is usually about  $1^\circ$ ). In the next sections results from experiments are discussed which were performed to examine the effects on the distribution pattern of sprout types with more convergent ( $\gamma = +4^\circ$ ), divergent ( $\gamma = -4^\circ$ ), and parallel walls ( $\gamma = 0^\circ$ ).

Experiments of MENNEL and REECE (1963) have shown that the section of the vanes on spinning disc broadcasters highly effects the variation in the values of the angles of outlet in the vertical plane.

Contrary to the objective of reducing or controlling these variations when designing spinning disc broadcasters, it was expected that for reciprocating sprout broadcasters a certain rate of variation in the vertical angles of dispatch would act positively on the distribution pattern. For this reason, experiments with three types of sprout design (with circular, rhombic, and rectangular sections) were performed.

#### 6.2.1. *Materials and methods*

The kinematic characteristics of the distributor device used in the experiments can be described with equations similar to those described in sections 4.2.1 and 4.2.2. The value of the crank length  $RA$  was 0.082 m and that of the connecting rod  $L$ : 0.194 m. This results in a value of  $C = 0.422$ , providing a value of the angle of oscillation  $\phi$  of  $24^\circ$ . Sprout length defined by  $RB$  was 0.63 m. The rotary frequency ( $N$ ) of the driving shaft was  $480 \text{ min}^{-1}$ . The distributor device was placed in a stationary laboratory set-up. Preliminary experiments proved that this set-up, combined with the particular set value of  $N: 480 \text{ min}^{-1}$ , maintained symmetry in the oscillation pattern to a sufficiently usable degree. The sprouts involved in the experiments were made from aluminium.

Particles were supplied to the distributor devices through a central hole which was positioned above and around the point of oscillation.

The distribution patterns obtained with the various sprout types were examined by using the following methods. Primarily, velocities and angles of outlet projected in the horizontal plane were studied, using the previously-described high speed film technique. The camera was placed at a height of about three meters above the distributor device. Since analyses of movie films require a considerable amount of labour, a second method for analyzing the distribution pattern was introduced. This technique was used for the more extensive experiments and was similar to that described in the work of GÖHLICH and KESTEN (1972). Behind the distributor device a half circular blackboard was placed, divided into vertical columns and horizontal rows in such a way that squares of  $0.10 \times 0.10 \text{ m}$  were obtained. The distance of the blackboard from the centre of oscillation  $P$  was 1.5 m. For marking the points of impact on the blackboard, the particles were traced with a fluorescent powder. Points of impact were recorded, providing the determination of the distribution patterns in both the horizontal and vertical planes.

In preliminary experiments, the experimental results obtained with the high speed movie technique were compared with the distribution patterns on the blackboard. The relationships which were found, were used afterwards in order to translate the distribution characteristics of the particles on the blackboard in terms of estimation of particle velocities and angles of outlet.

#### 6.2.2. *Experimental results*

Preliminary experiments show that there exists a high rate of symmetry between the left and right half of the distribution pattern. As a consequence, it is possible to add the number of impacts of identical column and row numbers of the left and right half of the blackboard. In addition, values of  $\beta \geq 90^\circ$  can be transformed to

their supplementary angles and added to values of  $\beta < 90^\circ$ .

When combining an analyses of the high speed films with the position of the impacting traced particles on the blackboard, it appears that there exists a linear relationship between the column number of the square in which a particle impacts and the mean angle of dispatch  $\bar{\beta}$  per column. This relationship can be expressed

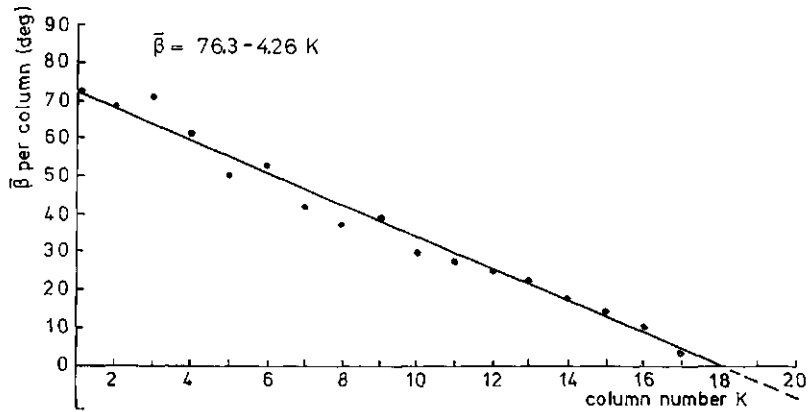


FIG. 6.1. The values of the mean angle of particle dispatch per column ( $\bar{\beta}$ ) as a function of column number  $K$ .

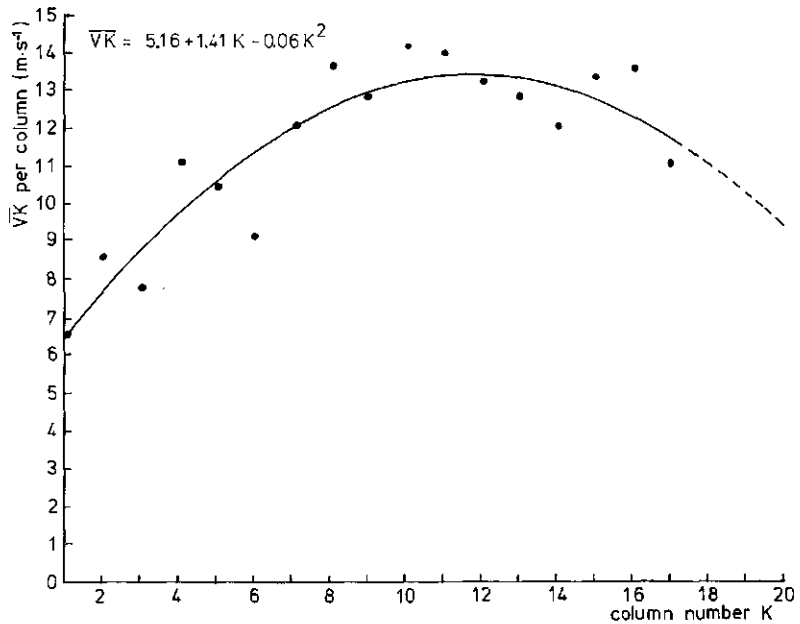


FIG. 6.2. The values of the mean velocity of particle dispatch per column ( $\bar{VK}$ ) as a function of column number  $K$ .



TABLE 6.1. The 80% range of particle velocities of outlet ( $VK$ ) of nine sprout types.

Shape of sprout walls; % of particles	Mean values of $VK$ per column ( $m s^{-1}$ ) and shape of the sections		
	<i>rectangular</i>	<i>rhombic</i>	<i>circular</i>
<i>divergent walls</i>			
10-50%	11.5-13.4	11.7-13.3	12.1-13.3
50-90%	13.4-13.1	13.3-12.4	13.3-13.1
<i>parallel walls</i>			
10-50%	11.5-13.4	11.7-13.3	12.4-13.3
50-90%	13.4-13.2	13.3-13.1	13.3-13.2
<i>convergent walls</i>			
10-50%	12.0-13.4	12.6-13.2	12.4-13.2
50-90%	13.4-12.9	13.2-12.7	13.3-12.8

as:  $\bar{\beta} = 76.3 - 4.34 K$  in which  $\bar{\beta}$  represents the mean value of the angle of dispatch for a certain column number  $K$ . (Fig. 6.1). In addition, a similar relationship was found between the mean values of particle velocity of outlet per column and the column numbers. This relationship can be expressed by  $\overline{VK} = 5.16 + 1.41 K - 0.06 K^2$ . (Fig. 6.2). With the aid of these relationships it is possible to derive from the distribution pattern obtained on the blackboard an estimation of the spectra of particle velocities and angles of outlet for the various sprout types.

From the results on the blackboard it can be observed that all the sprout types involved produce a two-peak transverse distribution pattern, since on an average about 60% of all particles impact in the columns numbered 9 to 13. Therefore, the majority of the particles have angles of dispatch within the range of 20-40 deg resulting in the creation of two main diverging mass flows of fertilizer particles.

The following aspects of particle velocity of dispatch appear (Table 6.1) from the experimental results on the blackboard. On an average, 80% of the particles have values for this velocity which are concentrated within a relatively small range of 11.4 to 13.4  $m s^{-1}$ . The highest values for the mean velocity of outlet are found in column number 12.

The cumulative distribution curves of the particles over the columns (based on 400 particles), depending on the various sprout types examined, are presented in Fig. 6.3. The differences between the various distribution patterns are rather small. A larger effect from the shape of the sprout wall is found for the rhombic and circular sections of the sprout. The rhombic section combined with divergent sprout walls gives the highest percentage of particles which impact at lower and higher column numbers on the blackboard. As a result, the percentage of particles which have lower velocities of outlet is somewhat higher for this specific type of sprout. In addition, the variation of the values of the angles of outlet is somewhat greater.

The vertical distribution pattern of the points of impact on the blackboard

shows that with the divergent sprout (combined with the rhombic section) a larger variation in the vertical plane was obtained (Fig. 6.4). This is partly due to the greater percentage of particles with lower values of the velocity of outlet, which results in a lower height of impact on the blackboard. In Fig. 6.4 this phenomenon is represented by the impacts at the higher row numbers. In addition, it is very well tenable that this specific combination of section and sprout shape creates opportunities for a greater variation in angles of outlet in the vertical plane (angles of elevation). Obviously the phase of particle impact can play a more dominant role, since for spinning disc broadcasters (where a sliding or rolling particle motion along the vanes dominates) a rhombic section resulted in the lowest

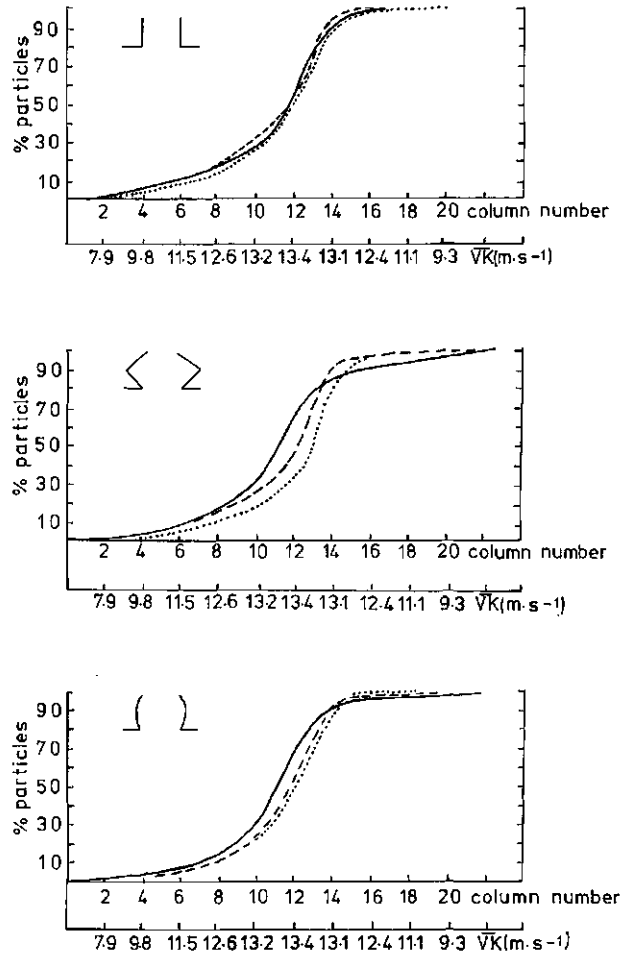


FIG. 6.3. Cumulative distribution curves of the particle impacts over the column numbers, representing the distribution curves of the values of the mean velocities of particle outlet per column  $\bar{V}_K$ . Sections of the sprout are: rectangular (J L), rhombic (◊), and circular (⊖). Sprout walls: —: divergent, ---: parallel, ·····: convergent.

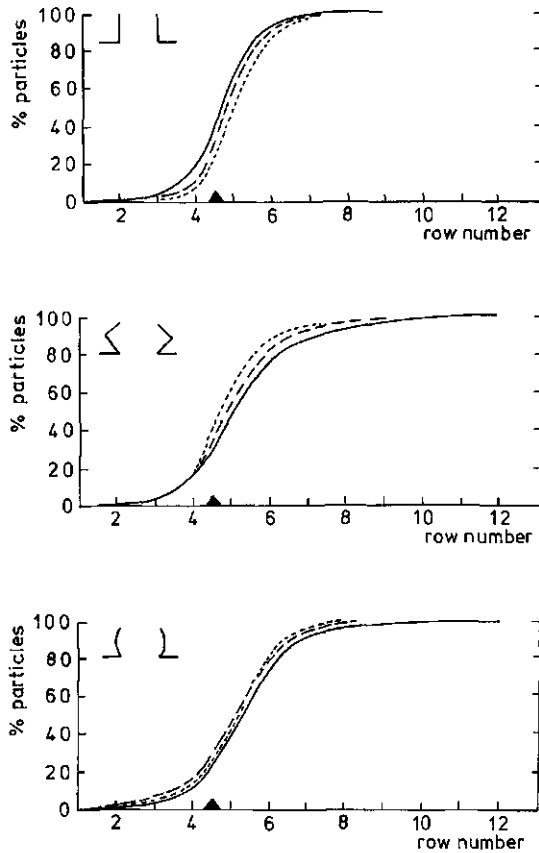


FIG. 6.4. Cumulative distribution curves of particle impacts in the vertical plane represented by the row numbers. Height of the sprout is indicated by:  $\blacktriangle$ . Sections of the sprout are: rectangular (J I), rhombic (L N), and circular (O P). Sprout walls: —: divergent, ---: parallel, .....: convergent.

variations of the angles of elevation (MENNEL and REECE, 1963). It must be added that the convergent rhombic sprout type also results in a low variation of the points of particle impact in the vertical plane.

### 6.2.3. Simulation experiments

In addition to the laboratory experiments, a number of simulation experiments were performed using the model which is described in the previous chapter. This simulation model, however, did not permit the examination of possible differences between various sections of the sprout. In addition, the assumption was made that the process of sorting-in of the particles in PEETEN's (1975) equipment had the characteristic that within the range  $0.15 \leq R_0 \leq 0.24$  m each interval  $\Delta R_0 = 0.01$  m has the same relative frequency of fertilizer particles. This assumption was based on examination of the points of reversal of the direction of particle motion using traced particles.

It should be noted that the specific problems concerned with the choice of the data file, describing the initial conditions of particle motion, will be discussed more extensively later on in this chapter.

Simulation experiments performed were based on the following initial values for  $VK$ ,  $\psi$ ,  $R_0$  and  $r$ . Values increased according to  $VK = 2.5 (0.1) 3.4 \text{ m s}^{-1}$ , at increasing values of the initial radius, according to  $R_0 = 0.15 (0.01) 0.24 \text{ m}$ . For the entire data file the initial values of the angles of impact  $\psi$  and the particle radius  $r$  are kept constant. The values were  $35^\circ$  and  $0.0015 \text{ m}$ . The same was done for the value of the initial particle rotation  $\omega_1$ , being  $-1000 \text{ rad s}^{-1}$ .

From experiments by INNS and REECE (1962) a value for the coefficient of restitution of 0.17 for impact of calcium ammonium nitrate on aluminium was gained. In the experiments of HOEDJES (1978) a value of 0.23 was mentioned. From additional experiments in which the height of rebound of particles dropped from 1.0 m on an aluminium plate was recorded, a value of 0.26 was calculated for the coefficient of restitution. Based on these results, the use of a value of 0.2 for the imaginary coefficient of restitution  $\epsilon^*$  is tenable.

The experimental results of the friction measurements described in sections 7.2 and 7.3 lead to the introduction of a value of 0.4 for the imaginary coefficient of friction  $\mu^*$ .

#### 6.2.4. *Experimental results*

Comparison between the analyses of high speed films and simulation experiments shows the following.

For parallel sprout walls ( $\gamma = 0^\circ$ ), the simulation experiments give mean values for  $\overline{VK}$  and  $\overline{\beta}$  of  $13.1 \text{ m s}^{-1}$  and  $29.1^\circ$ . The measured mean values of the three sections of this sprout type are  $12.8 \text{ m s}^{-1}$  and  $31.0^\circ$ . For the convergent sprout type ( $\gamma = +4^\circ$ ) the simulated values of  $\overline{VK}$  and  $\overline{\beta}$  are  $11.0 \text{ m s}^{-1}$  and  $34.9^\circ$ . The values obtained from the analyses are  $11.8 \text{ m s}^{-1}$  and  $30^\circ$ . The divergent sprout walls ( $\gamma = -4^\circ$ ) result in simulated values of  $13.5 \text{ m s}^{-1}$  and  $28.2^\circ$ . The mean measured values for  $\overline{VK}$  and  $\overline{\beta}$  are  $13.8 \text{ m s}^{-1}$  and  $29^\circ$ .

It can be concluded that the agreement between simulated and measured values of  $\overline{VK}$  and  $\overline{\beta}$ , obtained with the previously-mentioned file of initial data, was good. Some additional simulations performed showed that an increase of the initial level of  $VK$  by  $0.5 \text{ m}$  influences the values of the output data to a relatively small extent. On an average, the value of  $\overline{VK}$  increased by  $0.3 \text{ m s}^{-1}$ . Increase of the value of  $\omega_1$  to  $-1500 \text{ rad s}^{-1}$  lead to an average decrease of  $\overline{VK}$  of  $0.7 \text{ m s}^{-1}$ .

### 6.3. CONSEQUENCES OF ALTERATION OF DESIGN VARIABLES FOR PARTICLE DISPATCH

#### 6.3.1. *Introduction*

From previous sections, the conclusion can be drawn that it is possible to use the simulation model as an additional tool for estimation of the effects of changed construction variables on particle motion. The next section deals with simulation experiments which were performed with modified design variables of the distribution device of the reciprocating sprout broadcaster.

### 6.3.2. The input data file

The choice of the values describing the initial particle motion (and used in the model) need some additional considerations and explanations.

From preliminary experiments by VERHOFSTADT (1978) it appeared that there existed certain interactions between the input data file (describing initial particle conditions) and the effect of alteration of a construction variable (e.g. sprout length). In the experiments of VERHOFSTADT (1978) initial radii were varied according to  $R_o = 0.16$  (0.2) 0.22 m. Additionally, angles of impact varied according to  $\psi_1 = 40.0$  (5.0)  $45.0^\circ$ , and particle velocities before impact varied according to  $\overline{VK} = 4.6$  (0.2)  $5.2 \text{ m s}^{-1}$ . In this way 48 combinations created the data file which was used for the experiments.

As was expected, the results showed that mean particle velocity of outlet increased with increasing values of the sprout length. Consequently, the mean values for the angle of dispatch decreased. However, some experiments gave results of a different character. Firstly, an increase of  $\overline{VK}$  was noticed at increased values of sprout length. Secondly, after reaching a maximum of, for example, a sprout length of 0.71 m, the value of  $\overline{VK}$  decreased with continuing increase of sprout length to a value of 0.75 m.

Obviously, the mass flow of particles remains concentrated and particles are not equally distributed over the last 0.4 m of the sprout. The decrease in the mean value of  $\overline{VK}$  can be explained assuming that part of the particle flow is intercepted by the sprout wall. This results in impacts and, as a consequence, in a decrease in the mean level of the velocities of outlet (Fig. 6.5).

In addition, it is tenable to assume that there can exist interactions between the process of sorting-in of the particles along the sprout wall and the oscillation pattern of the sprout. Therefore, frequency distribution of the particles over the part of sprout where this process takes place can vary with specific shapes of the sprout or angles of oscillation. Furthermore, flow properties of the fertilizer can affect this process.

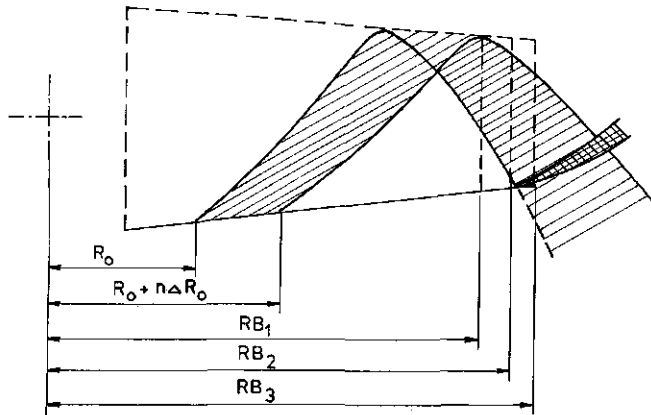


FIG. 6.5. Interception of a part of the particle flow when increasing the length of the sprout from  $RB_2$  to  $RB_3$ . The range of initial radii is represented by  $R_o$  and  $R_o + n\Delta R_o$ .

Since more detailed knowledge of the process of sorting-in of the particles is not available, some assumptions have to be made with respect to the development of a 'standard' data file which is usable for the performance of the simulation experiments.

Firstly, it is assumed that the process of sorting-in takes place within the sprout section which is limited by the values of  $R_o = 0.10$  and  $0.24$  m. This assumption is reasonable when referring to the analyses of particle motion. In addition, it is assumed that the initial particle velocity linearly increases with increased values of the initial radius  $R_o$ . The initial radii determining the particle positions at the beginning of the simulation experiments have the values of  $R_o = 0.10(0.01)0.24$  m. Consequently, the initial particle velocities have values of  $3.0(0.1)4.4$  m s<sup>-1</sup>. The levels of these velocities agree reasonably with those noted in the analyses of the high speed films. Particle radius is kept at a constant value of  $r = 0.0015$  m and the initial angle of impact at a value of  $35^\circ$ . The value of the latter is also in the same order of size as the values obtained from particle motion analyses.

Friction and restitution properties of the fertilizers in the model represented by  $\mu^*$  and  $\varepsilon^*$ , were  $0.2$  and  $0.4$  for fertilizer type I, and  $0.1$  and  $0.6$  for fertilizer type II. It can be assumed that the initial particle rotation  $\omega_1$  does not greatly affect particle motion of fertilizer II, due to the low value of the imaginary coefficient of friction. For both types of fertilizer a value of  $-1000$  rad s<sup>-1</sup> was adjusted to the initial particle rotation  $\omega_1$ . These values are not unrealistic when considering the levels of the components of relative particle velocity. Moreover, preliminary investigations made clear that an increase of  $\omega_1$  to  $-2000$  rad s<sup>-1</sup> does not greatly affect mean particle velocities of outlet. In addition, it appeared that there was no need for changing the diameter of the sprout entrance. Therefore, the size of the entrance was kept at a constant value of  $0.10$  m (VERHOFSTADT, 1978).

### 6.3.3. Interpretation of the experimental results

Knowledge of the process of sorting-in of particles is only available on a limited scale. As a consequence, the character of the initial frequency distribution of the particles over intervals of  $0.01$  m (in the range  $R_o = 0.10$ – $0.24$  m) is unknown under more specific conditions. For this reason the following strategy was applied to examine the experimental results obtained from the simulation studies.

Firstly, the experimental results expressed by the particle velocities of outlet  $VK$  and angles of dispatch  $\beta$  were presented in relation to the initial starting positions  $R_o$  of the particles. A complete review of the experimental results is given in Appendix I. These data enable the research workers as well as the broadcaster designers, to study in more detail the effects of alteration of various construction parameters. The set of data can be used as a basis for further examination, for example by means of the introduction of various more specific frequency distributions which represent the possible features of the process of particle sorting-in. Nevertheless, it should be emphasized that there still exists the need for performance of more extensive, future studies in order to obtain a better knowledge of the fundamentals of this process.

Secondly, it was examined to what extent the mean values of  $VK$  and  $\beta$  were

affected by various design parameters, based on the assumption that particle frequency is equal for each interval  $\Delta R_0$  of 0.01 m within the range of initial radii  $R_0$ : 0.10 – 0.24 m.

Thirdly, a part of the set of experimental results was treated with a certain frequency distribution where the relative frequency of the number of particles starting from a certain interval  $\Delta R_0$  decreased with increasing values of  $R_0$ . Using this frequency distribution, it was assumed that 20% of the particles started from an initial radius  $R_0 = 0.10$  m, and only 2% started from an initial radius of 0.24 m. A detailed specification of this frequency distribution is shown in Fig. 6.8a. Based on these assumptions the values for  $\overline{VK}$  and  $\overline{\beta}$  were calculated.

#### 6.3.4. Experimental results

A complete review of the results of the simulation experiments is given in Appendix I for both types of fertilizers used. In the following section alterations of construction variables and their effects on particle motion will be discussed.

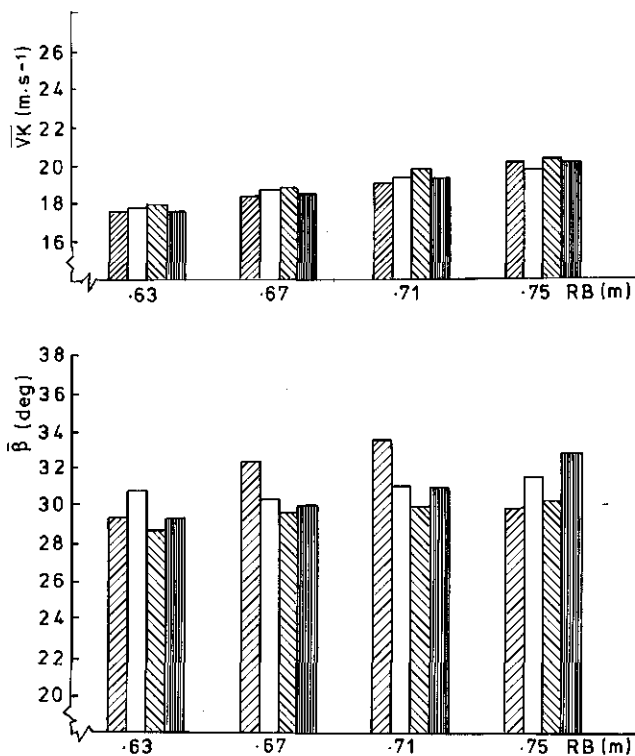


FIG. 6.6a. The mean values of particle velocities of outlet  $\overline{VK}$  and angles of dispatch  $\overline{\beta}$  as functions of the sprout length  $RB$  and sprout angle  $\gamma$ :  $////$ :  $\gamma = 1^\circ$ ;  $\square$ :  $\gamma = 0^\circ$ ;  $||||$ :  $\gamma = -1^\circ$ ;  $||||$ :  $\gamma = -2^\circ$ . ( $N = 540 \text{ min}^{-1}$ ;  $C = 0.475$ .) FERTILIZER I.

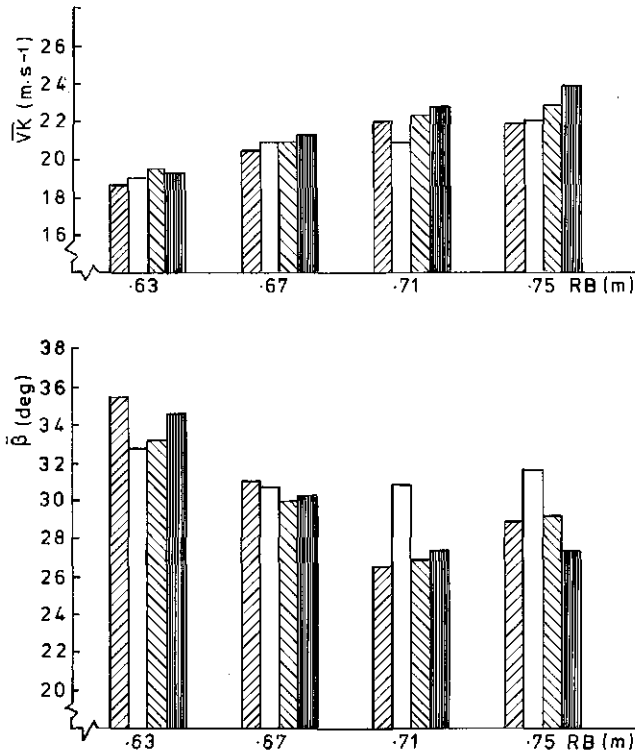


FIG. 6.6b. The mean values of particle velocities of outlet  $\overline{VK}$  and angles of dispatch  $\bar{\beta}$  as functions of the sprout length  $RB$  and sprout angle  $\gamma$ ;  $////$ :  $\gamma = 1^\circ$ ;  $\square$ :  $\gamma = 0^\circ$ ;  $||||$ :  $\gamma = -1^\circ$ ;  $||||$ :  $\gamma = -2^\circ$ . ( $N = 540 \text{ min}^{-1}$ ;  $C = 0.475$ .) FERTILIZER II.

#### 6.3.4.1. Sprout length and sprout angle

The effects of alteration of sprout length  $RB$  ( $RB = 0.63, 0.67, 0.71$ , and  $0.75$  m), and sprout angle  $\gamma$  ( $\gamma = 1^\circ, 0^\circ, -1^\circ$ , and  $-2^\circ$ ), on the values of  $\overline{VK}$ ,  $\bar{\beta}$ , and  $t$  per individual starting position  $R_o$ , are shown in Appendix I. 1.1.1 to I. 1.4.8. Values for  $C$  ( $= RA/L$ ) and  $N$  were set at  $0.475$  and  $540 \text{ min}^{-1}$ . Sprout diameter at the entrance was set at  $0.10$  m since preliminary studies showed that alteration of the variable towards a higher level generally lead to negative effects for particle motion (VERHOFSTADT, 1978).

It can be noticed that the effect of various sprout angles on the values of  $\overline{VK}$  is rather small for all sprout lengths (Fig. 6.6a and 6.6b). The mean value of the angle of dispatch ( $\bar{\beta}$ ) shows greater variation; however, it is not possible to determine a particular tendency.

For these reasons, further experiments were done by using a slightly convergent sprout with a sprout angle of  $\gamma = 1^\circ$ .

Fig. 6.7a and 6.7b give as examples the relations between the values of the particles velocity of outlet  $\overline{VK}$  and the initial radii  $R_o$  depending on sprout length  $RB$ . It can be noted that for certain parts of the range of  $R_o$ , similar values for  $\overline{VK}$  are



obtained for both types of fertilizer. Apparently, for those values of  $R_o$ , differences in sprout length do not influence the values of the velocity of outlet. On the other hand, there are also parts in the range of  $R_o$  for which the effect of alteration of the sprout length is quite clear. Fig. 6.7a shows, for example, that for a sprout length of 0.75 m the value of  $VK$  starts at a relatively high level at an initial radius of 0.10 m. For the successive intervals  $R_o = 0.11-0.13$  m, the values of  $VK$  strongly decrease.

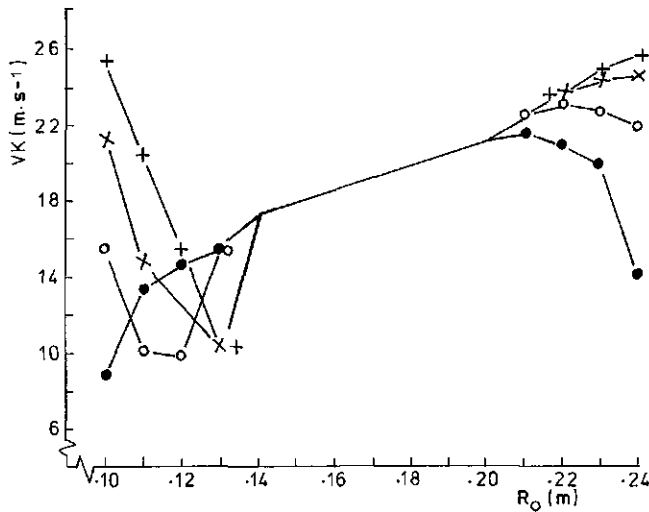


FIG. 6.7a. The value of particle velocity of outlet  $VK$  as a function of the initial radius  $R_o$ . ●:  $RB = 0.63$  m, ○:  $RB = 0.67$  m, ×:  $RB = 0.71$  m, +:  $RB = 0.75$  m. ( $\gamma: 1^\circ$ ;  $C: 0.475$ ;  $N: 540 \text{ min}^{-1}$ .) FERTILIZER I.

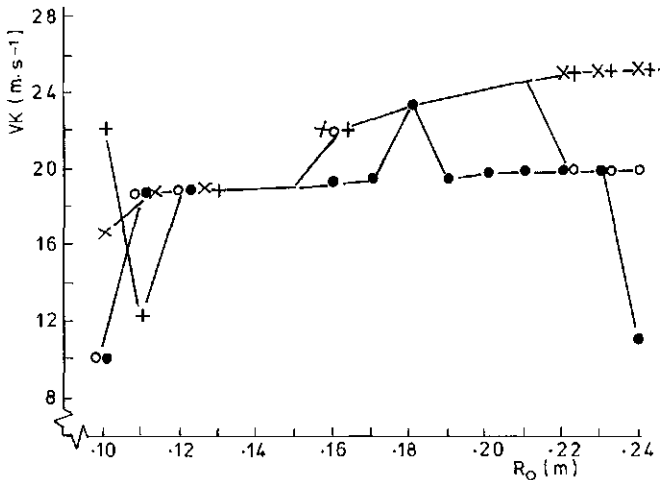


FIG. 6.7b. The value of the particle velocity of outlet  $VK$  as a function of the initial radius  $R_o$ . ●:  $RB = 0.63$  m, ○:  $RB = 0.67$  m, ×:  $RB = 0.71$  m, +:  $RB = 0.75$  m. ( $\gamma: 1^\circ$ ;  $C: 0.475$ ;  $N: 540 \text{ min}^{-1}$ .) FERTILIZER II.

A similar tendency is noticed for fertilizer II at a sprout length of 0.75 m (Fig. 6.7b). As a result, the mean value of the velocity of outlet ( $\overline{VK}$ ) slightly decreases when increasing the value of the sprout length from 0.71 m to 0.75 m.

Differences in the process of sorting-in of the particles along the sprout wall – which are represented by two frequency distributions A and B in the range  $R_o = 0.10$ –0.24 m (Fig. 6.8a) – show the following aspects. Due to the high percentage of

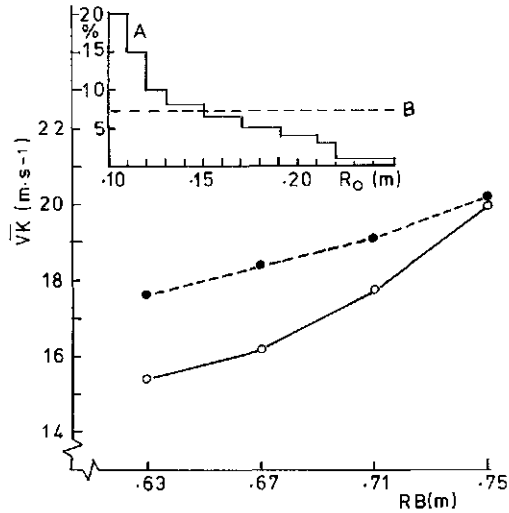


FIG. 6.8a. The effect of two types of frequency distributions (A: ○—○; and B: ●—●) within the range of initial values  $0.10 \leq R_o \leq 0.24$  m, on the mean values of the velocity of particle outlet  $\overline{VK}$ , at four sprout lengths  $RB$ . ( $\gamma: 1^\circ$ ;  $C: 0.475$ ;  $N: 540 \text{ min}^{-1}$ .) FERTILIZER I.

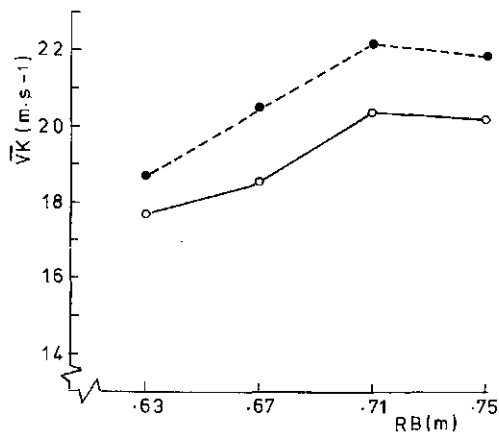


FIG. 6.8b. The effect of two types of frequency distributions (A: ○—○; and B: ●—●) within the range of initial values  $0.10 \leq R_o \leq 0.24$  m, on the mean values of the velocity of particle outlet  $\overline{VK}$ , at four sprout lengths  $RB$ . ( $\gamma: 1^\circ$ ;  $C: 0.475$ ;  $N: 540 \text{ min}^{-1}$ .) FERTILIZER II.

particles with lower values for the initial radii  $R_0$  (resulting in relatively low values of the velocity of outlet), the mean values for  $\overline{VK}$  are lower for the distribution curve A than for the distribution curve B. It can be noted that the effect of an increase of the sprout length shows similar tendencies for both frequency distributions. For fertilizer I,  $\overline{VK}$  increases with an increase of the sprout length from 0.63 to 0.75 m. For fertilizer II,  $\overline{VK}$  also increases with an increase of the sprout length from 0.63 to 0.71 m; a further increase to a value of 0.75 m results in a small decrease of the value of  $\overline{VK}$  (Fig. 6.8b).

Generally it can be stated that high values of  $\overline{VK}$  are attended by low values of  $\bar{\beta}$ , and conversely. The conclusion can be drawn, therefore, that an increase of sprout length creates possibilities for increase of the level of particle velocities of outlet. This increase is, on an average, linearly related to an increase in the values of the sprout length. The value of this increase is estimated at about  $0.5\text{--}1.0\text{ m s}^{-1}$  per  $0.04\text{ m}$  increase of sprout length, depending on the type of fertilizer. Alteration of the sprout angle appears to have no practical effects.

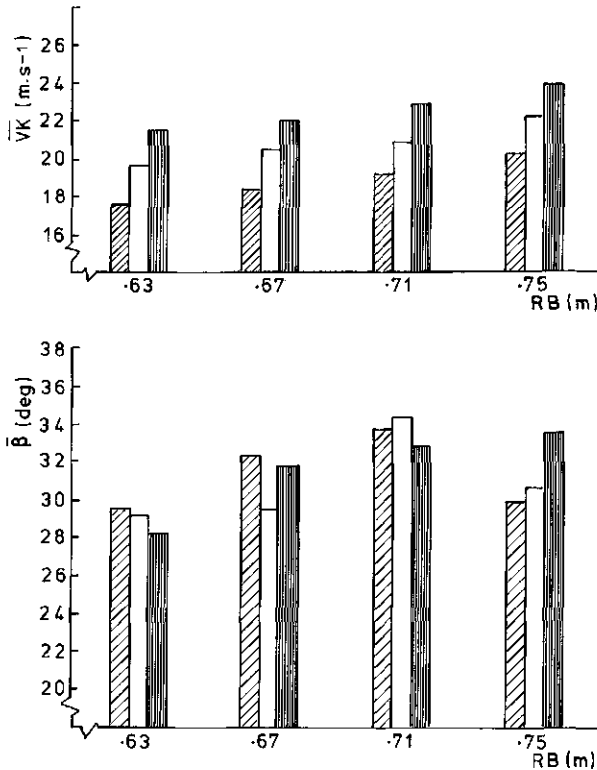


FIG. 6.9a. The mean values of particle velocities of outlet  $\overline{VK}$  and angles of dispatch  $\bar{\beta}$  as functions of the sprout length  $RB$ , and the rotary frequency of the driving shaft  $N$ .  
 ///:  $N=540\text{ min}^{-1}$ ; □:  $N=600\text{ min}^{-1}$ ; |||:  $N=660\text{ min}^{-1}$ . ( $\gamma=1^\circ$ ;  $C=0.475$ ) FERTILIZER I.

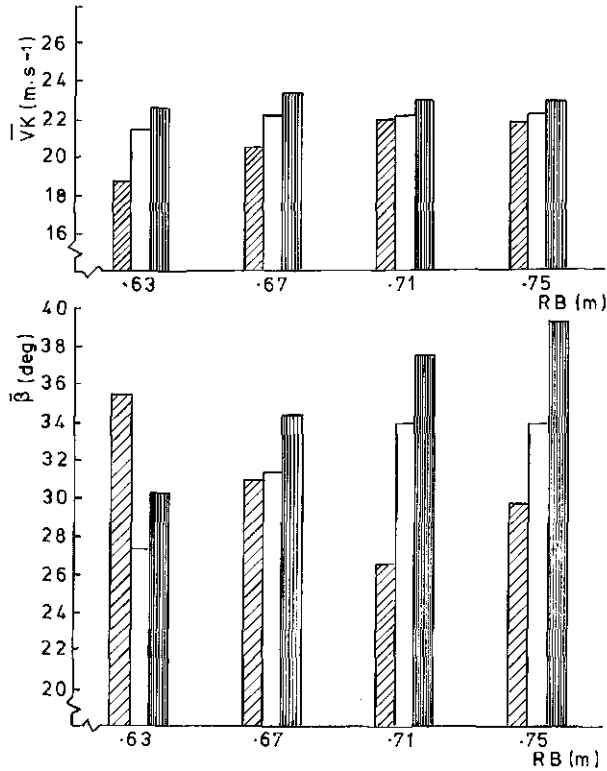


FIG. 6.9b. The mean values of particles velocities of outlet  $\overline{VK}$  and angles of dispatch  $\bar{\beta}$  as functions of the sprout length  $RB$ , and the rotary frequency of the driving shaft  $N$ .  
 ///:  $N=540 \text{ min}^{-1}$ ; □:  $N=600 \text{ min}^{-1}$ ; |||:  $N=660 \text{ min}^{-1}$ . ( $\gamma=1^\circ$ ;  $C=0.475$ ) FERTILIZER II.

#### 6.3.4.2. Sprout length and rotary frequency of the driving shaft

It can be expected that besides an increase of the length of the sprout, an increase of the rotary frequency of the driving shaft ( $N$ ) can create opportunities for increase of the level of  $VK$  since angular velocity of the sprout depends on  $\omega$ .

The experimental results which were obtained from the studies of these parameters are shown in Appendix I.2.1 to I.2.16, and in Fig. 6.9a and 6.9b.

When applying the frequency distribution B for fertilizer I, an increase of  $N$  leads to an increase of the values of  $\overline{VK}$  for all the four values of the sprout length. On an average, the velocity of outlet  $\overline{VK}$  increased with about  $2 \text{ m s}^{-1}$  when the value of  $N$  increased with  $60 \text{ min}^{-1}$ .

The effect of an increase of  $N$  on the mean value of the angle of outlet ( $\bar{\beta}$ ) varies with sprout length. The 'normal' effect showing a decrease of  $\bar{\beta}$  with increasing values of  $\overline{VK}$ , is noticed at a sprout length of 0.63 m. Contrary to what was expected, the mean value of  $\bar{\beta}$  appeared to increase with an increase of the value of  $\overline{VK}$  at a sprout length of 0.75 m. From the results listed in Appendix I. 2.14, it can be seen that this high value of  $\bar{\beta}$  is mainly caused by the occurrence of only two

extreme high values for  $\beta$  ( $86.3^\circ$  and  $88.5^\circ$ ) at initial values of  $R_0$ : 0.14 and 0.15 m. These two extremes must be explained by impacts of the particles on the opposite sprout wall before leaving the sprout, since the values for  $t$  are not extreme. As a consequence, the values of  $VK$  for these particular initial radii are relatively low; however, their effect on the mean value of  $VK$  is not so pronounced.

Since the number of initial radii was limited to 15 values, such an 'opposite' effect of increase of  $\bar{\beta}$  (together with increase of  $\bar{VK}$ ) indicates that there are extremes for both in the experimental results. Generally speaking, these extremes for  $\beta$  are in the order of  $70$ – $85^\circ$  in size, and their frequency is limited to  $10$ – $25\%$ . This does not change the fact that in practice the transverse distribution pattern will still show a two-peak character.

For fertilizer II the increase of  $\bar{VK}$  at increasing values of  $N$  is less pronounced for the two higher values of the sprout length. The high values which are found for  $\bar{\beta}$  indicate that the number of relatively low values of  $VK$  is comparatively high (e.g. four in Appendix I.2.16).

Nevertheless, it can be stated that an increase of the number of the rotary frequency of the driving shaft (and as a result, an increase of the angular velocity of the sprout) can create a higher level of the mean particle velocity of outlet.

When using the standard data file and frequency distribution B, this increase of  $\bar{VK}$  can reach values of about  $4 \text{ m s}^{-1}$  when increasing the rotary frequency from  $540$  to  $660 \text{ min}^{-1}$ .

#### 6.3.4.3. Sprout length and angle of oscillation

An increase of the ratio between length of the crank ( $RA$ ) and the connecting rod ( $L$ ) results in higher values of the angle of oscillation, and higher mean and maximum values of angular velocity of the sprout.

A recently introduced design of the reciprocating sprout broadcaster has a possibility for variation of the angle of oscillation  $\phi$  in three steps:  $\phi = 19.0^\circ$  ( $C = 0.325$ ),  $\phi = 23.7^\circ$  ( $C = 0.400$ ), and  $\phi = 28.4^\circ$  ( $C = 0.475$ ). In addition the effect of an increase of  $C$  towards  $0.6$ , resulting in a value for the angle of oscillation of  $36.5^\circ$ , was examined. The value of the rotary frequency  $N$  was kept constant at  $540 \text{ min}^{-1}$ .

Experimental results are shown in Appendix I.3.1 to I.3.24 and in Fig. 6.10a and 6.10b. It appears that the level of the velocity of outlet increases with increased values of the angle of oscillation at all sprout lengths and for both fertilizers. In the range of  $C = 0.325$  to  $0.475$  the value of  $\bar{VK}$  appears to increase about linearly. On an average, this increase is in the order of size of  $3$ – $4 \text{ m s}^{-1}$  for each increase of the value of  $C$  with  $0.075$  ( $\phi = 4.7^\circ$ ) at all sprout lengths observed.

For practical purposes this effect creates the opportunity to establish different ranges in working width. Ranges of  $6$ – $8$ ,  $8$ – $10$ , and  $10$ – $12 \text{ m}$  are mentioned in the broadcaster manufacturer's specifications.

It should be repeated that the values for  $\bar{\beta}$  do not show a uniform tendency; the variations are considerable. High values for  $\bar{\beta}$  can be explained by the occurrence of a number of extreme values of  $\beta$ : for example, the value of  $\bar{\beta}$ :  $45.9^\circ$  obtained for fertilizer II at a sprout length of  $0.75 \text{ m}$  and  $C = 0.325$  is the result of four ex-

tremely high values of  $\beta$ :  $78.8^\circ$ – $88.4^\circ$ . They are situated in the range of initial radii  $R_o$  of 0.20–0.23 m (see Appendix I.3.16).

The variation in the number of extreme values for  $\beta$ , and thus the variation of the relative frequency of these angles of dispatch, can lead to the following practical consequences. Since fertilizer is dispatched from the sprout in two divergent flows, considerable variations in the value of  $\beta$  implies that the special devices at the end of the sprout (such as bows, etc.) need to be adapted to specific characteristics of particle motion. Adaptations in design of such devices obviously also depend on the type of fertilizer which has to be spread. As a result, unwanted and unexpected variations in the shape of the transverse distribution pattern can occur when applying one single type of bow at the end of the oscillating sprout.

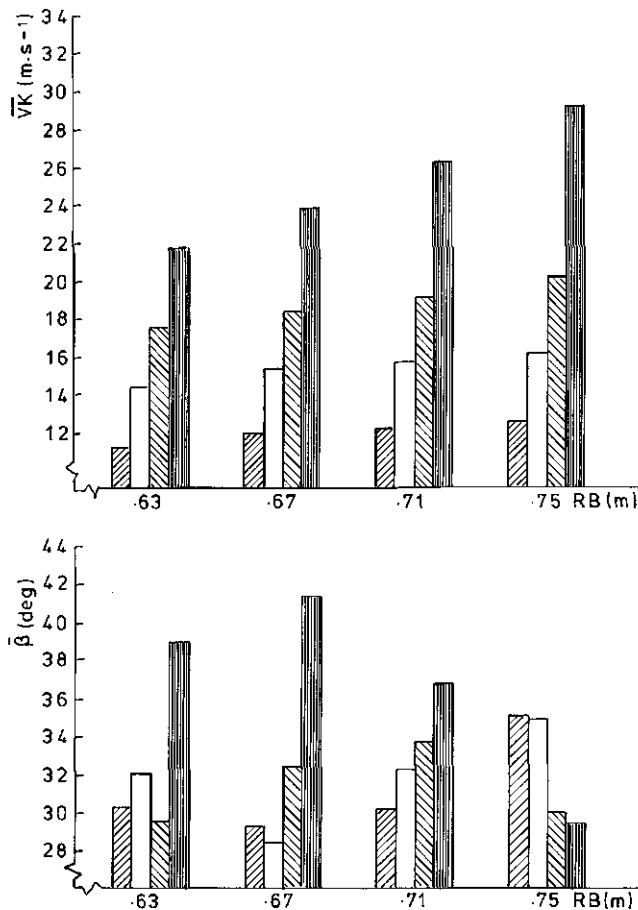


FIG. 6.10a. The mean values of particle velocities of outlet  $\bar{V}_K$ , and the angles of dispatch ( $\bar{\beta}$ ) as functions of the sprout length  $RB$ , and the ratio  $C$  between crank ( $RA$ ) and connecting rod ( $L$ ).  $////$ :  $C = 0.325$ ;  $\square$ :  $C = 0.400$ ;  $||||$ :  $C = 0.475$ ;  $||||$ :  $C = 0.600$ . ( $\gamma = 1^\circ$ ;  $N = 540 \text{ min}^{-1}$ ) FERTILIZER I.

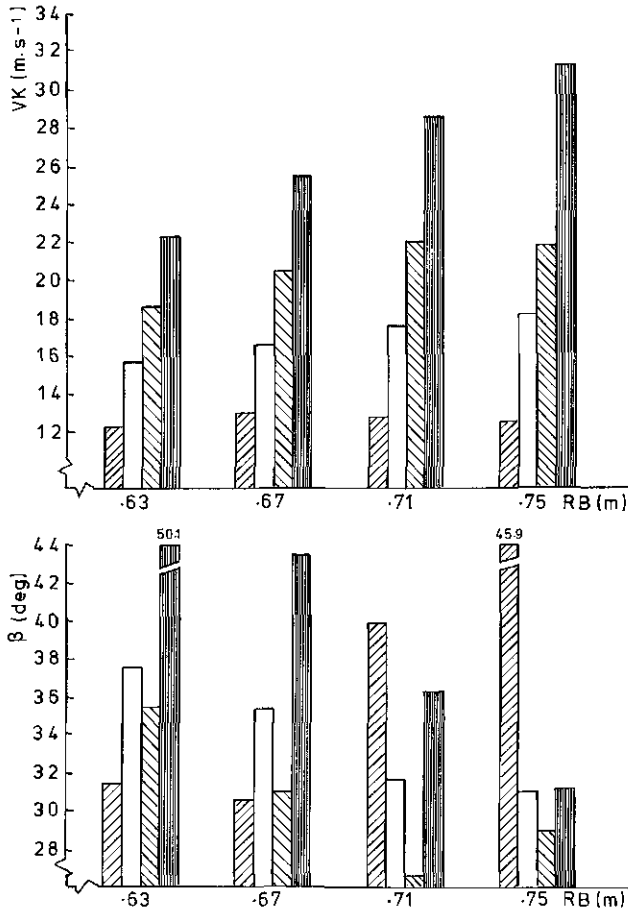


FIG. 6.10b. The mean values of particle velocities of outlet  $\overline{VK}$ , and the angles of dispatch ( $\beta$ ) as functions of the sprout length  $RB$ , and the ratio  $C$  between crank ( $RA$ ) and connecting rod ( $L$ ).  
 ////:  $C = 0.325$ ; □:  $C = 0.400$ ; \\\\\:  $C = 0.475$ ; ||||:  $C = 0.600$ . ( $\gamma = 1^\circ$ ;  $N = 540 \text{ min}^{-1}$ )  
 FERTILIZER II.

#### 6.3.4.4. Sprout length, angle of oscillation, and rotary frequency of the driving shaft

In the previous sections it was indicated that increase of sprout length, angle of oscillation, and rotatory speed of the driving shaft, create opportunities for an increase of the level of the values of velocity of particle outlet.

Experimental results obtained for  $C = 0.6$  ( $\phi = 36.5^\circ$ ) and  $N = 660 \text{ min}^{-1}$  are listed in Appendix I.4.1 to I.4.8. In addition, mean values are compared with those obtained for the 'normal' design parameters (Fig. 6.11a and Fig. 6.11b). It can be noticed that a considerable increase of the mean values for  $\overline{VK}$  is obtained when applying the high values for the design parameters  $C$ ,  $N$ , and  $RB$ . On an average, the differences in mean velocity of outlet are about  $10 \text{ m s}^{-1}$  at the lower value of

$RB = 0.63$  m. For each increase of  $RB$  of  $0.04$  the differences increase about  $2.1$  to  $2.3 \text{ m s}^{-1}$  to a maximum of about  $17 \text{ m s}^{-1}$ . According to DOBLER and FLATOW (1968) the mean value of the particle trajectories would increase by about  $5.0$  m, up to  $12.0$  m when particles dispatch horizontally.

It can be noticed that the values for  $\bar{\beta}$  show the expected tendency: an increase of the values of  $\overline{VK}$  is attended by a decrease of  $\bar{\beta}$ . On the estimation that the fertilizer is distributed with a spreading angle of  $120^\circ$  (see also Fig. 3.2), an increase of the mean value of the spreading width of about  $4.4$  m can be obtained. Under these circumstances – taking into consideration the variations of  $VK$  – the width of the basic transverse distribution pattern can reach values of  $30.0$  m.

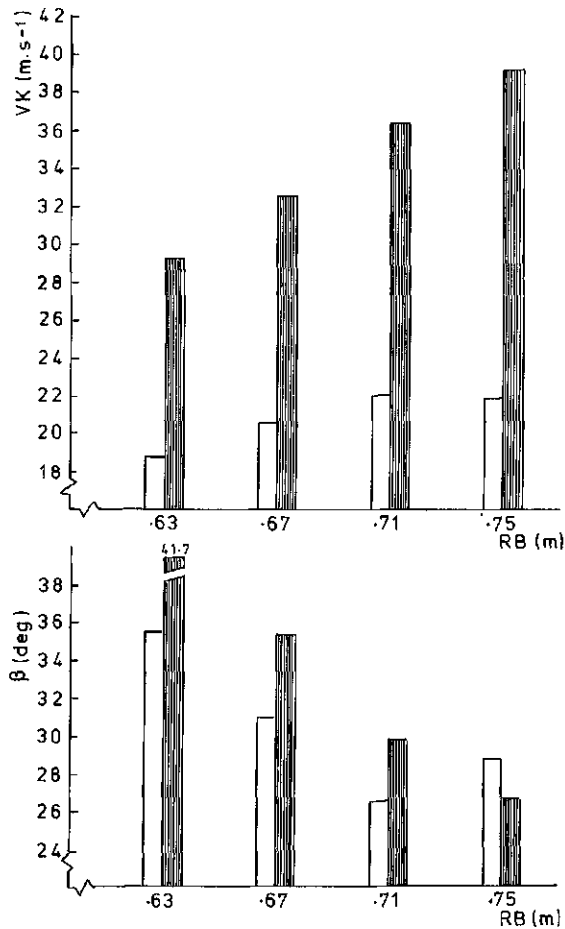


FIG. 6.11a. The main values of particle velocities of outlet  $\overline{VK}$  and the angles of dispatch  $\bar{\beta}$  as functions of the sprout length  $RB$ , and the combination of ratio  $C$  and the rotary frequency of the shaft  $N$ .

□:  $C = 0.475$  and  $N = 540 \text{ min}^{-1}$ ; ||||:  $C = 0.600$  and  $N = 660 \text{ min}^{-1}$  ( $\gamma = 1^\circ$ ). FERTILIZER I.



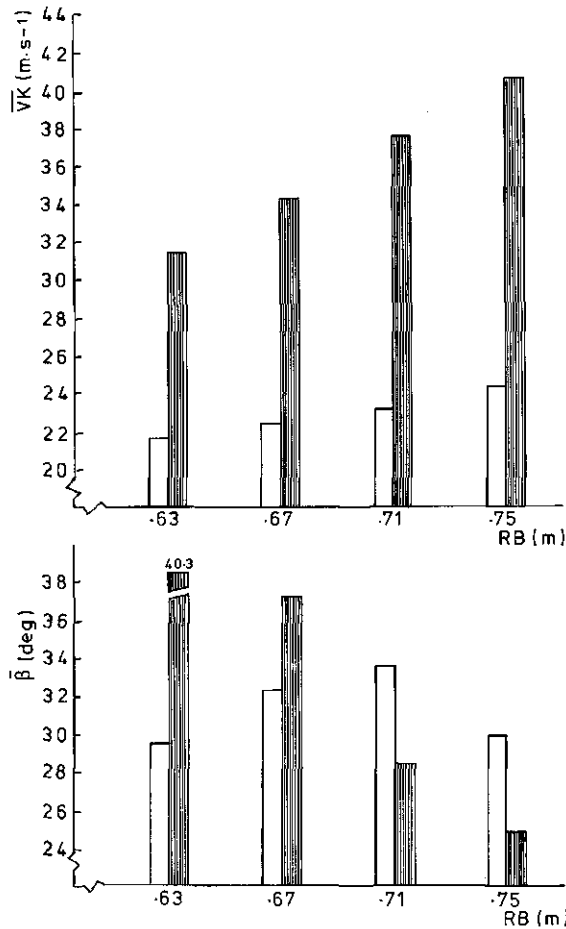


FIG. 6.11b. The mean values of particle velocities of outlet  $\bar{VK}$  and the angles of dispatch  $\bar{\beta}$  as functions of the sprout length  $RB$ , and the combination of ratio  $C$  and the rotary frequency of the shaft  $N$ .

□:  $C = 0.475$  and  $N = 540 \text{ min}^{-1}$ ; |||:  $C = 0.600$  and  $N = 660 \text{ min}^{-1}$  ( $\gamma = 1^\circ$ ). FERTILIZER II.

#### 6.4. EFFECTS OF ACCESSORIES AT THE SPROUT END ON THE BASIC DISTRIBUTION PATTERN

Due to the specific oscillation characteristics of the sprout (and particle dynamics within it) fertilizer will dispatch from the sprout in two divergent flows. This phenomenon results in a two-peak transverse distribution pattern acting negatively on the evenness of the compound distribution pattern. In addition, a limitation to the tolerable variation in the ratio of overlap must be expected. To obtain a one-peak symmetrical transverse distribution pattern, the reciprocating sprout broadcaster is equipped with a sprout which has a special design. At the end

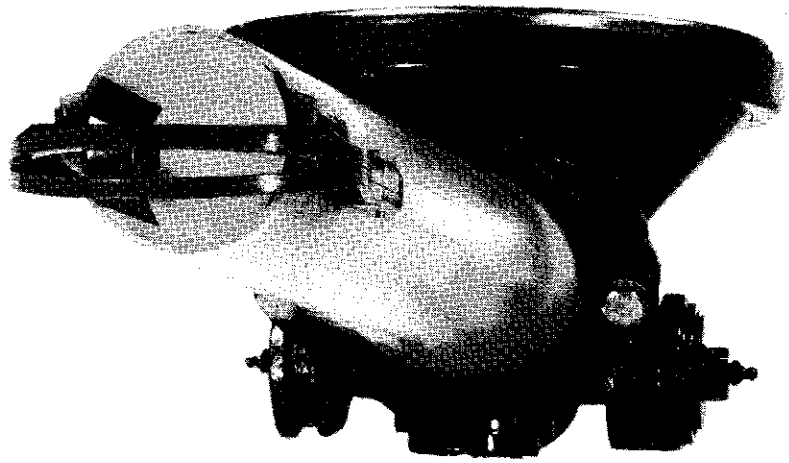


FIG. 6.12. The orifice of the sprout with grooves and bow.

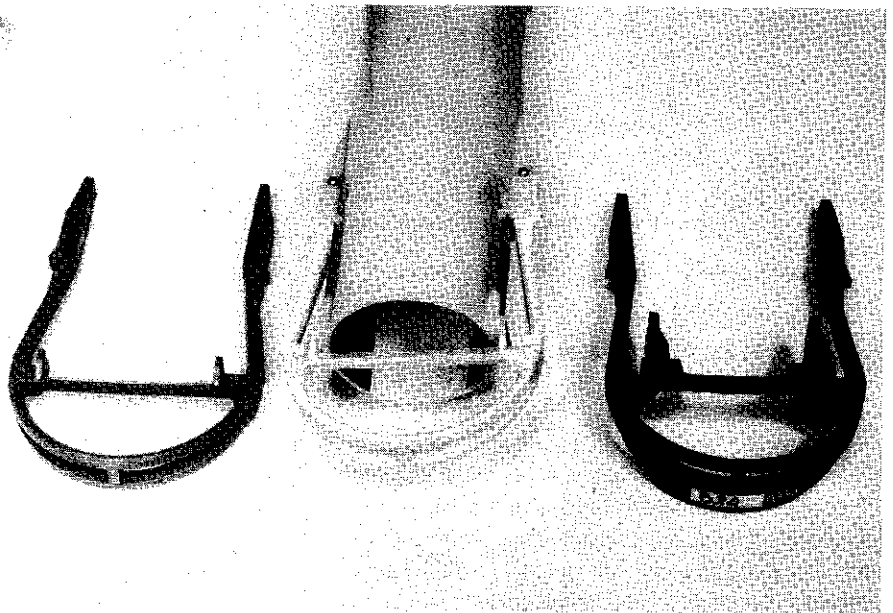


FIG. 6.13. Some examples of bows for various types of fertilizers.

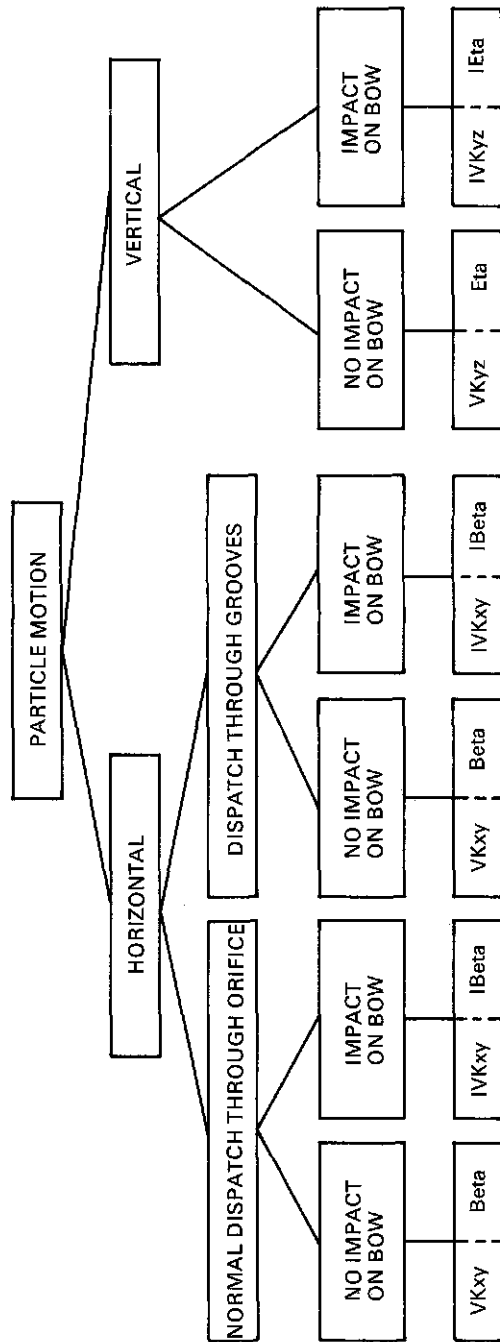


FIG. 6.14. Possibilities for particle motion, particle velocity of outlet, and angles of dispatch in the horizontal ( $x-y$ ) and the vertical ( $y-z$ ) plane. Particle velocities of outlet, angles of dispatch in the horizontal plane, and angles of elevation after impact on the bow are indicated with  $I$ .

TABLE 6.2. Review of the results of analyses of particle motion, projected in the horizontal (x-y) plane. (According to PEELEN, 1976.)

		n	$\overline{Beta}; \overline{IBeta}$ resp. (180°-Beta; $\overline{IBeta}$ ) (deg)	St.dev. Beta; $\overline{IBeta}$ (deg)	$\overline{VKxy}$ resp. $\overline{IVKxy}$ (m s <sup>-1</sup> )	St.dev. VKxy; $\overline{IVKxy}$ (m s <sup>-1</sup> )	%
1. Dispatch through orifice; no impact on bow	Beta <90	100	23.1	19.7	17.5	3.3	34.4
	Beta ≥90	86	158.9(29.1)	18.4	17.4	3.4	
2. Dispatch through grooves; no impact on bow	Beta <90	62	28.1	27.0	14.7	3.3	23.2
	Beta ≥90	63	153.8(26.2)	24.8	15.4	3.4	
3. Dispatch through orifice; before impact on bow	Beta <90	70	26.9	14.3	18.1	2.7	25.1
	Beta ≥90	66	152.2(27.8)	14.8	18.2	3.3	
4. Dispatch through orifice; after impact on bow	Beta <90	69	7.6	13.5	19.6	2.9	(25.0)
	Beta ≥90	66	174.8 (5.2)	8.4	19.5	3.6	
5. Dispatch through grooves; before impact on bow	Beta <90	47	33.0	26.1	15.4	3.7	17.4
	Beta ≥90	47	148.9(31.1)	39.1	14.8	7.0	
6. Dispatch through grooves; after impact on bow	Beta <90	48	17.6	20.3	17.9	5.5	(17.2)
	Beta ≥90	45	166.4(13.6)	16.6	18.8	4.7	
7. Effect of sprout without bow (Σ1+2+3+5)	Beta <90	279	26.8	21.1	16.7	3.5	100
	Beta ≥90	262	153.2(25.8)	22.7	16.7	4.4	
8. Effect of sprout with bow (Σ1+2+4+6)	Beta <90	279	19.4	21.7	17.5	4.1	99.6
	Beta ≥90	260	163.0(17.0)	20.8	17.6	4.0	

n = number of particles; St.dev. = standard deviation)

of the sprout, the side walls are provided with grooves which are enclosed by a horizontal bow (Fig. 6.12). It can be mentioned that for various types of fertilizers, different combinations of grooves and bows are required and are experimentally designed (Fig. 6.13).

In the next sections we will deal with experiments which were performed to obtain a basic understanding of the action of these accessories at the end of the sprout.

#### 6.4.1. *Materials and methods*

Particle behaviour is examined with the aid of a high speed movie technique. Particles passing the last part of the sprout are filmed at 1500 p.p.s. in the horizontal and vertical plane. With this method information can be obtained about particle dispatch through the grooves and orifice, and the possible impacts on the bow. The sprout used in these experiments has the same dimensions as that which was used in the experiments by MEULEMAN (1975). The sprout is mounted on a Vicon broadcaster permitting a value of the angle of oscillation  $\phi$  of  $28.36^\circ$ . (Note: the sprout thus oscillates over an angle of  $56.72^\circ$ .) The sprout length is 0.63 m; the diameter at the entrance is 0.10 m. The sprout has a convergent shape; the value of the sprout angle  $\gamma$  is  $1^\circ$ . The rotary frequency of the driving shaft is  $540 \text{ min}^{-1}$ .

The fertilizer used is Chilisaltper of the sieve fraction 2.8–3.4 mm. The 1000 kernel weight of these particles is 19.7 g.

Particle characteristics are determined with the aid of a film motion analyzer in the horizontal ( $x$ - $y$ ) and vertical ( $y$ - $z$ ) plane. Fig. 6.14 shows the various possibilities for the particles to leave the sprout and impact on the bow, as well as particle velocities and directions before and after dispatch.

#### 6.4.2. *Experimental results*

A review of the results of the analyses of particle motion projected in the horizontal ( $x$ - $y$ ) plane is given in Table 6.2. The sprout equipped with a bow shows a similar and sufficient rate of symmetry of the distribution pattern when compared to one without a bow. This rate of symmetry is shown by the almost equal percentage of angles of dispatch with a value  $< 90^\circ$  and  $\geq 90^\circ$ , the mean values of these angles of dispatch, the mean velocities of outlet, and the standard deviation of both.

The percentage of particles with values of  $Beta$ ,  $IBeta < 90^\circ$  is 51.6% and thus the values  $\geq 90^\circ$  are 48.4%. The mean values of the angles of dispatch ( $Beta$ ,  $IBeta$  respectively ( $180^\circ - Beta$ ,  $180^\circ - IBeta$ ) are  $19.4^\circ$  and  $17.0^\circ$ , and the standard deviations are  $21.7^\circ$  and  $20.8^\circ$ . Since this rate of symmetry exists, all further values for the angle of dispatch will be expressed by  $Beta$ ,  $IBeta$ .

Particles dispatch with a mean value of outlet of  $17.5 \text{ m s}^{-1}$  ( $Beta$ ,  $IBeta < 90^\circ$ ), and  $17.6 \text{ m s}^{-1}$  ( $Beta$ ,  $IBeta \geq 90^\circ$ ). The values for the standard deviations are 4.1 and  $4.0 \text{ m s}^{-1}$ .

It appears that 40.6% of all particles ( $n = 539$ ) analyzed, leave the sprout while passing the grooves in the sides of the sprout. Almost 43% of these particles impact

the bow. Apparently, that contact between the bow and these particles results in an increase of the mean velocity of outlet ( $\overline{VK}_{xy} = 18.4 \text{ m s}^{-1}$ ). The mean value of the angle of dispatch ( $\overline{IBeta}$ ) decreases significantly ( $\overline{Beta} = 32.1^\circ$ ;  $\overline{IBeta} = 15.6^\circ$ ) and the variance is relatively small.

The conclusion is drawn, therefore, that particles which leave the sprout through the grooves obviously obtain a higher level of velocity due to the contact with the bow. This fact has to be explained by observing the relationship between the moment of particle impact on the bow and the momentary value of the angle of oscillation of the sprout. From analyses of high speed movies it appears that a part of the particles is leaving the sprout during its accelerating phase (PEELEN, 1976). Since sprout wall velocity increases relatively to particle velocity, and the direction of motion of both coincide, an impact between bow and particles can create opportunities for obtaining a higher level of particle velocity. In addition, the impact can occur at a higher value of what is described as the effective radius (see also section 5.3.3.2).

It appears that 59.5 % of all the particles analyzed, leave the sprout through the orifice. About 41.5 % of these particles will impact on the bow. This contact with the bow results in a somewhat higher velocity of outlet ( $\overline{VK}_{xy} = 18.1 \text{ m s}^{-1}$ ;  $\overline{IVK}_{xy} = 19.5 \text{ m s}^{-1}$ ). The mean value of the angles of dispatch of the impacting particles decreases significantly ( $\overline{Beta} = 27.4^\circ$ ;  $\overline{IBeta} = 6.4^\circ$ ). The variance of  $\overline{IBeta}$  is relatively small.

On the other hand it is clear that 57.6 % of all particles do not contact the bow at all.

Particles which are leaving the orifice (about 60%) have a significantly higher velocity of outlet than those which are leaving the sprout through the grooves. The mean values for the mean velocity of outlet are about 17.5 and 15.0  $\text{m s}^{-1}$ . This lower mean velocity of outlet can be explained by considering the fact that particles which are dispatching through the orifice have a higher value of the mean effective radius (0.66 m compared with 0.62 m), which enables the creation of a higher level of particle velocity.

It can be observed that particles which will later impact on the bow appear to have a higher mean value of  $Beta$  obtained during their previous motion within the sprout, compared to particles which do not impact.

Summarizing, the following combined effect of grooves and bow on particle motion in the horizontal plane can be recorded. The angle of dispatch ( $\overline{IBeta}$ ) decreases significantly with a value of about  $8^\circ$ . The values of  $Beta$  and  $\overline{IBeta}$  show a similar variance. The mean value of the particle velocity of outlet is somewhat higher. Obviously, the higher velocity of outlet of the particles leaving the sprout through the orifice compensates for the lower values of outlet of the particles dispatching through the grooves.

Regarding the action of the grooves and the bow in the horizontal plane, it must be concluded that they do not contribute to the creation of a more convergent character of the particle flows. As a result, the objective of these accessories, being the creation of a one-peak transverse distribution pattern, must be obtained by their action on particle motion and trajectories in the vertical plane.

TABLE 6.3. Review of the results of analyses of particle motion projected in the vertical ( $y$ - $z$ ) plane.

		n	$\overline{Eta}; \overline{IEta}$ ( $\geq 0$ ; $< 0$ ) (deg)	$\overline{Eta}; \overline{IEta}$ (deg)	St. dev. $\overline{Eta}; \overline{IEta}$ (deg)	%																																				
1. Dispatch through grooves and orifice; no impact on bow	$Eta \geq 0$	126	20.2	+1.9	29.8	57.7																																				
	$Eta < 0$	112	-18.6				2. Dispatch through grooves and orifice; before impact on bow	$Eta \geq 0$	78	25.8	+1.6	51.3	42.2	$Eta < 0$	96	-18.1	3. Dispatch through grooves and orifice; after impact on bow	$IEta \geq 0$	62	40.2	-19.3	52.8	41.7	$IEta < 0$	110	-52.8	4. Effect of sprout without bow	$Eta \geq 0$	204	22.3	+1.8	47.2	100	$Eta < 0$	208	-18.4	5. Effect of sprout with bow	$Eta; IEta \geq 0$	188	26.8	-7.0	52.4
2. Dispatch through grooves and orifice; before impact on bow	$Eta \geq 0$	78	25.8	+1.6	51.3	42.2																																				
	$Eta < 0$	96	-18.1				3. Dispatch through grooves and orifice; after impact on bow	$IEta \geq 0$	62	40.2	-19.3	52.8	41.7	$IEta < 0$	110	-52.8	4. Effect of sprout without bow	$Eta \geq 0$	204	22.3	+1.8	47.2	100	$Eta < 0$	208	-18.4	5. Effect of sprout with bow	$Eta; IEta \geq 0$	188	26.8	-7.0	52.4	99.5	$Eta; IEta < 0$	222	-35.5						
3. Dispatch through grooves and orifice; after impact on bow	$IEta \geq 0$	62	40.2	-19.3	52.8	41.7																																				
	$IEta < 0$	110	-52.8				4. Effect of sprout without bow	$Eta \geq 0$	204	22.3	+1.8	47.2	100	$Eta < 0$	208	-18.4	5. Effect of sprout with bow	$Eta; IEta \geq 0$	188	26.8	-7.0	52.4	99.5	$Eta; IEta < 0$	222	-35.5																
4. Effect of sprout without bow	$Eta \geq 0$	204	22.3	+1.8	47.2	100																																				
	$Eta < 0$	208	-18.4				5. Effect of sprout with bow	$Eta; IEta \geq 0$	188	26.8	-7.0	52.4	99.5	$Eta; IEta < 0$	222	-35.5																										
5. Effect of sprout with bow	$Eta; IEta \geq 0$	188	26.8	-7.0	52.4	99.5																																				
	$Eta; IEta < 0$	222	-35.5																																							

The analyses of the filmed particle trajectories in the vertical ( $y$ - $z$ ) plane give some difficulties. In the extreme positions of the sprout and at low values for  $Beta$  and  $IBeta$ , an accurate determination of the particle trajectories appears to be difficult. For this reason, the measured particle velocities  $\overline{VKyz}$  and  $\overline{IVKyz}$  are additionally compared with the values that are obtained by transformation of the mean velocities of outlet  $\overline{VKxy}$  and  $\overline{IVKxy}$ . First, the values of  $\overline{VKy}$  and  $\overline{IVKy}$  were calculated by multiplying  $\overline{VKxy}$  and  $\overline{IVKxy}$  with the value of  $\sin Beta$  or  $\sin IBeta$ . In addition, the values of these velocity components were divided by  $\cos \overline{Eta}$  or  $\cos \overline{IEta}$  resulting in the calculated values for  $\overline{VKyz}$  and  $\overline{IVKyz}$ .

A review of the results of the analyses of high speed films in the vertical ( $y$ - $z$ ) plane is presented in Table 6.3. The followings aspects can be presented.

Particles that leave the sprout without contacting the bow (about 58%) have a mean measured value for the angle of elevation  $Eta$  of  $1.9^\circ$ . The percentage of particles which do not impact agrees well with the percentage which are found from the analyses of the films in the ( $x$ - $y$ ) plane. The value of the mean particle velocity  $\overline{VKyz}$  is  $6.4 \text{ m s}^{-1}$ . Again there exists a reasonable agreement with the mean calculated value which is derived from  $\overline{VKxy}$ . A further comparison between the mean measured and calculated values  $\overline{VKyz}$  and  $\overline{IVKyz}$  shows a reasonably good rate of agreement. Therefore it can be stated that there does not exist a discrepancy between the analyses in the ( $x$ - $y$ ) and ( $y$ - $z$ ) plane.

The particles that impact on the bow (leaving the sprout through grooves and orifice) have a mean value of  $Eta$  before impact of  $1.6^\circ$ . The mean velocity ( $\overline{VKyz}$ ) is  $8.0 \text{ m s}^{-1}$ . It can be recorded that about 45% of the particles have a value of  $Eta \geq 0^\circ$ , indicating that particles are moving upwards. This portion of the particles

a mean value of  $\overline{Eta}$  of  $25.8^\circ$ . The particles that are moving downwards (about 55%), indicated by values for  $\overline{Eta} < 0$ , have a mean value for the angle of elevation of  $-18.1^\circ$ . The standard deviation of (all values) of  $\overline{Eta}$  has a higher value than the particles which do not contact the bow.

Impact of the particles on the bow has the following effects for particle motion after the contact. The mean angle of elevation ( $\overline{IEta}$ ) shows a considerably increased negative value. The particle velocity projected in the ( $y-z$ ) plane decreases considerably to a value for  $\overline{VKyz}$  of  $3.8 \text{ m s}^{-1}$ . This can be explained by the fact that after particles impact the bow, they obtain considerably lower values for  $\overline{IBeta}$ : mean values recorded in the ( $x-y$ ) plane are  $6.4^\circ$  for the particles that are impacting after leaving the grooves, and  $15.6^\circ$  for particles impacting after leaving the orifice of the sprout. As a result, the particles are directed more towards the soil, which is emphasized by the higher (64%) amount of particles with an angle of elevation  $\overline{IEta} < 0$ . The mean value of the angle of elevation for this part of the particles is now  $-52.8^\circ$ . The other part of the particles is directed more upwards, represented by a value of  $\overline{IEta}$  of  $40.2^\circ$ . The value of the standard deviation of  $\overline{IEta}$  increases considerably.

The effect in the ( $y-z$ ) plane of the adjustment of a bow on the total amount of particles leaving the sprout is an alteration for the mean angle of dispatch ( $\overline{Eta}$ ;  $\overline{IEta}$ ) to a negative mean value of  $-7.0^\circ$  together with a lower mean value of the velocity of dispatch.

Summarizing the actions of grooves and bow, the following remarks can be made with respect to the three dimensional effect on particle motion and trajectories.

The mean value of the absolute velocity of particle dispatch is hardly affected, although there exists a tendency towards an increased mean level in the ( $x-y$ ) plane. In combination with the decrease of the mean values for  $\overline{IBeta}$ , in principle the opportunity is created for obtaining an increase of the spreading angle  $\lambda$  (see Fig. 3.2), and even for a small increase of the working width. As was stated before, this phenomenon is opposite to the objectives of these accessories. The transformation of the resulting two-peak character of the transverse distribution pattern to a one-peak pattern is completely realized by the action of the devices in the ( $y-z$ ) plane. It appears that, on an average, the particle stream is more directed towards the soil since  $\overline{IEta}$  has a negative value of  $-7.0^\circ$ . However, it must be assumed that the 64% of the particles that have negative values for  $\overline{IEta}$  after impact with the bow, play a more important role in this transformation. The high mean negative value of the angles of elevation of this part of the particle flow creates opportunities for particle landings near the centre of the distribution device. In principle, the remaining 36% of the particles (for which  $\overline{IEta} \geq 0$ ) can contribute to a certain extent to an increase of the particle trajectories after dispatch, and as a consequence to an increase in working width.



## 6.5. DISCUSSION

Laboratory experiments were performed with nine sprout types (being combinations of the sections: circular, rectangular, and rhombic; together with the sprout angles  $\gamma = 4^\circ$ ,  $0^\circ$ , and  $-4^\circ$ ). The design of the sprouts shows only small effects on the transverse distribution patterns.

The frequency distributions of points of impact in the horizontal plane on the blackboard show that the majority of particles impact within a small range of similar column numbers. As a result, variation in particle velocity of outlet and angles of outlet is rather small. The basic transverse distribution patterns keep their two-peak character.

The largest variations in particle velocity of outlet are obtained with a divergent ( $\gamma = -4^\circ$ ) sprout type combined with a rhombic section. A similar effect is found with variations in the angles of outlet. The increasing frequency of particles impacting in the lower and higher column numbers indicates that the relative frequency of particles with lower velocities of outlet is higher with the divergent sprout types.

Observations in the vertical plane show that the smallest variations of the points of impact on the blackboard are obtained with a convergent, rhombic sprout type. On the other hand, largest variation are noted for the divergent rhombic sprout. This effect can be explained by the higher percentage of particles with lower values for velocity of outlet, and the somewhat greater variation in the angles of elevation. As a result, the possibilities for particle landings near the centre of the broadcaster can be somewhat more favourable for this specific sprout design. Nevertheless, special adjustments at the end of the sprout will remain necessary to support this effect to such an extent that an acceptable one-peak basic transverse distribution pattern is realized in practice.

Since particle motion in the vertical plane has a more uniform character when using a convergent rhombic sprout type, the assumption is tenable that the design of a bow at the end of the sprout can be more easily optimized for this particular sprout type.

The results of some simulation experiments show a very reasonable agreement with the results of the laboratory experiments using the various sprout types, although assumptions have to be made with respect to some initial characteristics of particle motion. These assumptions emphasize the need for more extensive, future examinations of the process of sorting-in of the particles at the entrance of the sprout. This still existing lack of fundamental knowledge can be considered a weakness in the interpretation of the results of the simulation experiments which were performed with various construction variables.

In principle, the effects of alteration of the construction variables (sprout length  $RB$ , sprout angle  $\gamma$ , rotary frequency of the driving shaft  $N$ , and angle of oscillation  $\phi$ ) on the mean velocities and angles of outlet, have to be considered in relation to the specific characteristics of the process of sorting-in of the particles. In other words, the specific character of a frequency distribution within the range of initial starting radii ( $R_0$ ) can affect the absolute values of the mean values of  $VK$  and  $\beta$ , since there

exist interactions between the initial radius and (for example) sprout length, angle of oscillation, and rotary frequency.

For this reason the results of the simulation experiments are primarily presented individually in relation to the value of the initial radius. Secondly, values of  $\overline{VK}$  and  $\overline{\beta}$  are calculated on the assumption that all intervals of  $\Delta R_0$  have the same frequency  $\Delta R_0 = 0.01$  m;  $0.10 \leq R_0 \leq 0.24$  m). In addition, some values of  $\overline{VK}$  and  $\overline{\beta}$  are given based on the assumption that the relative frequency of  $\Delta R_0$  decreases with an increase of  $R_0$ .

The following conclusions from the simulation experiments can be drawn. The effect of alteration of the sprout angle ( $\gamma = -2, -1, 0, \text{ and } +1^\circ$ ) on mean values of the velocity of outlet and angle of dispatch is small. There is no need to change the present design of the sprout ( $\gamma = +1^\circ$ ).

Increase of the other construction variables increases the level of the mean velocity of dispatch. As a result, opportunities are created for an increase of the spreading width. The rate of increase of the mean velocity of dispatch sometimes depends on the type of fertilizer, and on interactions between construction variables. For example, the effect of an increase of the rotary frequency  $N$  obviously depends on the sprout length and the fertilizer properties represented by  $\mu^*$  and  $\varepsilon^*$ .

Increase of the angle of oscillation of the sprout (by alteration of the value of  $C$  according to  $C = 0.325, 0.400, 0.475, \text{ and } 0.600$ ) leads to a considerably steady increase of  $\overline{VK}$  for both fertilizers at all sprout lengths. For the designers, such an effect provides practical opportunities to establish various ranges of working width. A combination of increases of  $C$  to a value 0.600,  $RB$  to a value 0.75 m, and  $N$  to  $660 \text{ min}^{-1}$  results in an increase of  $\overline{VK}$  of  $17 \text{ m s}^{-1}$  (which is about two times the value that is obtained with the normal present design of the reciprocating sprout broadcaster). It is almost superfluous to emphasize that under such circumstances, an extreme adaption of the construction of the distribution device is required since mass forces acting on the system will change extraordinarily in level as well as in character.

The effect of alteration of construction variables on the mean values of the angles of dispatch varies considerably due to the (varying) frequency of the occurrence of extreme high values.

Since this complex of interactions exists (including fertilizer properties), the following strategy for the advantageous application of the simulation technique is recommended to the reciprocating sprout broadcaster designers.

The number of construction variables examined should be considerably limited to those which have special practical and/or commercial interests. In the simulation studies, the effects of various frequency distributions within the range of initial radii should be examined more extensively. The use of a range of initial radii similar to that in our experiments is tolerable and not unrealistic. The same holds for the values which were used to define the other initial particle conditions.

The process of sorting-in of the particles should be the subject of future research work. Research results can contribute to a more accurate understanding of the initial particle motion. This will increase the value of the simulation technique.

Moreover, it is imaginable that a better knowledge of particle behaviour in the bowl and at the entrance of the sprout can contribute to a controlled process of distribution and motion.

The application of a combination of grooves and a bow at the end of the sprout has the following consequences for the basic transverse distribution pattern. About 40% of all particles that leave the sprout through grooves and orifice impact on the bow. In the horizontal plane these impacts result in an increase of the mean velocity of outlet of the particles. The mean value of the angle of outlet, however, decreases; this can result in an increase of spreading width. In the vertical plane, impact of particles on the bow results in increased variation of the angles of elevation. The negative mean value of the angles of elevation after impact indicates that a majority of the particle trajectories are directed more towards the centre of the transverse distribution pattern. This effect, combined with that portion of the particles which leave the sprout with high values for the angles of dispatch, creates an opportunity for the realization of a one-peak basic transverse distribution pattern. Since the process of particle dispatch depends to a certain extent on specific physical properties of the fertilizers, and thus on the (previous) character of particle motion within the sprout, the design of the bow must be adapted and optimized for various types of granular fertilizers. The present designs are optimized in an experimental way. It should be taken into consideration whether further extension and improvement of the simulation model in the future can contribute to optimizing the design of this extremely important part of the distributor device of this type of broadcaster.

## 7. PHYSICAL PROPERTIES OF FERTILIZERS AND THEIR CONSEQUENCES FOR THE DISTRIBUTION PROCESS

### 7.1. INTRODUCTION

The physical properties of fertilizers are of major common interest to both fertilizer manufacturers and distributor designers. In general, fertilizer manufacturers pay foremost attention to those factors which determine the structure of a certain fertilizer and its maintenance during transport, storage, and handling. For instance, if fertilizer granules are too soft or fragile, they break apart during handling or during spreading (since impacts within the oscillating sprout can also be a source of particle breakdown). As a consequence, the particle size distribution changes, which can result in a decrease of the working width of a fertilizer broadcaster. Soft granules also tend to cake more than firm ones. Therefore, the most desirable fertilizer granules or prills are those which can pass certain minimum requirements for hardness. The specific procedures for the determination of crushing strength and the resistance of granules to degradation by abrasive or impactive actions (HARDESTY and ROSS, 1938; BROWN et al., 1968; UKF, 1974) will not be discussed in detail as they are primarily a matter of responsibility for the fertilizer manufacturers. However, those properties which affect more directly the spreading width and evenness of distribution are of special importance for fertilizer broadcaster designers.

In agricultural engineering research some attention has been paid to the effects of particle size, particle size distribution, bulk density, and angle of repose on working quality (OEHRING, 1963; HEYMAN et al., 1971; N.I.A.E., 1971; BRÜBACH, 1973). In the testing procedure for fertilizer distributors according to O.E.C.D. standards (1967), the fertilizers used for the tests are defined by particle size distribution and bulk density. Unfortunately these values are not directly related to working performances such as the quality of the transverse and longitudinal distribution patterns.

In this section we will deal with the results of a number of experiments which were carried out to obtain information about the effects of various physical properties on the distribution process of the reciprocating sprout broadcaster, including the process of particle motion. Attention has been paid to those factors which can possibly contribute to an increase in working width, evenness of distribution, and acceptable variations in ratio of overlap. Physical properties of the fertilizers are primarily studied from an agricultural engineering point of view. Nevertheless, some aspects are useful for both the agricultural machine designer and the fertilizer technologist as they can create a basis for a further mutual adaption of fertilizer and distribution equipment.

## 7.2. OBJECTIVES, MATERIALS AND METHODS

The experiments performed are divided into three groups.

A. The first series dealt with an examination of the frictional and elastic properties of fertilizers. As described in chapter 5, the prediction of particle movement in the sprout depends on the values of  $\mu^*$  and  $\varepsilon^*$ . The values of these variables, which were required in order to obtain a reasonable agreement between simulated and measured values, can be explained in a satisfactory way. Further investigations will make clear that the assumptions applied in the model are supported by the results of actual friction and restitution measuring experiments of the fertilizers.

B. The objective of the second series was an examination of the effects of some physical properties of fertilizer on spreading performance with the reciprocating broadcaster. For this purpose three types of calcium ammonium nitrate were examined. Fertilizer I consisted of granular material, fertilizer II of low-density prills, and fertilizer III of high-density prills (see Tables 7.3 and 7.4). Physical properties were expressed in terms of: particle size (Mass Median Diameter or  $d_{50}$ ), variation in particle size distribution ( $d_{90}-d_{10}$  or  $d_{95}-d_{05}$ ), bulk density, moisture content, angle of repose, coefficient of restitution, and 1000 kernel weight. Spreading performance was examined in terms of optimal working width (indicated by the minimal value of the coefficient of variation), maximum working width, and the range of working widths over which the coefficient of variation does not exceed the value of 15 % (see also Fig. 3.3). In addition, the possible correlations between the physical properties mentioned before were studied.

C. The third series was a continuation of series B. Based upon the results of series B, some specially prepared sieve fractions of fertilizers I, II and III were tested with respect to their spreading performances with three types of distributors (reciprocating sprout broadcaster, two-spinning disc type broadcaster, and pneumatic distributor). Within the objectives of this thesis we will only report the results obtained with the reciprocating sprout broadcaster.

For series B the transverse distribution pattern was studied on a patternator which was specially developed for testings of the reciprocating sprout broadcaster (Fig. 7.1a). Tests were performed using a stationary set-up of the broadcaster. Fertilizer was collected in 80 trays of 0.25 m wide and 4.00 m long. Spreading height was 0.75 m. The rotary frequency of the p.t.o. was  $540 \text{ min}^{-1}$ . Two aspects have to be noted with respect to this method. Contrary to practical circumstances, there is no effect caused by an additional acting velocity component due to driving speed. Secondly, the length of the trays is of great importance since their size should coincide with the backward projection of the particles. This means that the area of the horizontal distribution pattern should not exceed the size of the collecting area (i.e. 4 m long and 20 m wide). To collect all particles, vertical sheets were placed in front and behind the trays. This enables, in principle, ricochetting of the particles from the sheets. This phenomenon can affect the shape of the transverse distribution pattern in an uncontrolled way.

The application rates were 30, 60 and  $90 \text{ kg min}^{-1}$ ; actual spreading time for one experiment was 0.5 min.



FIG. 7.1a. Determination of the basic transverse distribution pattern of the reciprocating sprout broadcaster on a patternator (stationary set-up of the broadcaster).

During testing series C, the distribution patterns were examined according to a method which was in agreement with the O.E.C.D. standard testing procedure. The fertilizer was spread by a driving broadcaster (Fig. 7.1b). Driving speed was  $6 \text{ km h}^{-1}$ . The fertilizer was collected in 40 trays of 0.5 m wide and 2 m long. The application rates were  $500$  and  $1000 \text{ kg ha}^{-1}$  which are comparable to  $60$  and  $120 \text{ kg min}^{-1}$ . Height of the broadcaster was  $0.75 \text{ m}$ , and rotary frequency of the p.t.o. was  $540 \text{ min}^{-1}$ . As a result of the driving speed and the length of the trays, the patternator was passed in about  $1.2 \text{ s}$ . Contrary to the previous method described for B, the forward speed of the broadcaster can affect particle trajectories to some extent and therefore the transverse distribution pattern.

For determination of the basic distribution pattern the amount of fertilizer per tray was weighed and recorded.

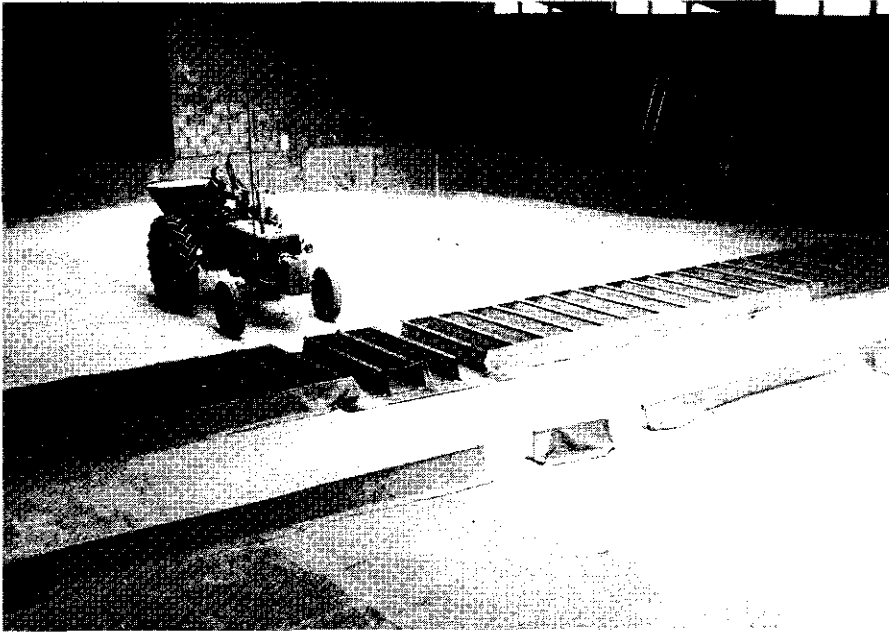


FIG. 7.1b. Determination of the basic transverse distribution pattern on a patternator with a driving tractor-mounted broadcaster.

The compound distribution patterns at various working widths and ratios of overlap were calculated, and plotted with the aid of a computer.

#### 7.2.1. *Determination of physical properties*

When determining physical properties, a description of the different methods used is most important. In general, values of physical properties as they are mostly presented in literature, should not be transferred to specific situations without an additional description of the applied measuring procedures used. The values must be considered relative ones, due to interactions with measuring methods.

##### 7.2.1.1. Coefficient of friction

As mentioned before, frictional properties directly influence particle movement in the sprout since they are expressed by the variable  $\mu^*$ . It is assumed that the parameter  $\mu^*$  can be correlated to a certain extent with the value of the kinetic coefficient of friction. The methods used to determine static and kinetic coefficients of friction for agricultural materials have usually been designed to suit the particular conditions of the materials tested (MOHSEIN, 1968; INNS and REECE, 1962; JIE-A-LOOI, 1968). For determination of dynamic frictional properties, the materials are mostly placed in contact with a positively-driven surface having a known relative velocity. The materials samples are loaded with a weight; this results in a normal force. The horizontal frictional force can be measured by e.g. a

spring scale, a system of beams and linkages with strain gages, or with force transducers.

Examination of the dynamic frictional properties of the fertilizers was made with the following two methods. The first method is described by HUISMAN (1977). Measurement of the coefficient of friction was made with the aid of a friction meter which was originally developed for the examination of the frictional properties of straw pieces (Fig. 7.2). The coefficient of friction was determined by placing a fertilizer particle in the under-fetching device (2). Small pieces of polyester and aluminium were placed in the upper device (1). Normal force was obtained by the placement of a 5 g mass on the upper device. During measurement the upper device (1) had a constant relative velocity of  $4 \text{ mm s}^{-1}$ . Since the relative velocity is low, the method could be described as a determination of the static coefficient of friction (BRUBAKER and POS, 1965). However, as the system allows a certain

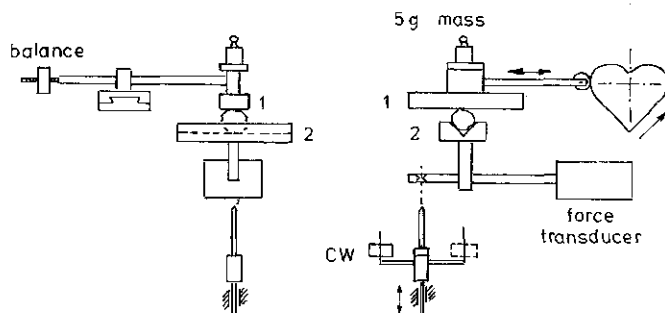


FIG. 7.2. Schematic representation of the friction measuring device. (According to HUISMAN, 1977.)

degree of elastic freedom of the relative moving surfaces, the frictional process can be described in terms of 'stick-slip' (MOHSEININ, 1968). As a result, the average frictional forces measured in this method depend on both the static and the kinetic coefficients of friction, the first being the highest. The results obtained must be considered a 'semi' kinetic coefficient of friction because the values tend towards an overestimation of the 'pure' kinetic coefficient of friction.

Taking into account a calibration value  $C$ , which is the result of the force  $CW \cdot A$  acting on the force transducer ( $CW$  is the value of the calibration mass, and  $A$  represents a constant which depends on the construction of the friction meter) the values for the coefficients of friction  $\mu$  could be computed from:

$$\mu = \frac{M}{C} \cdot CW \cdot A \quad (7.1)$$

$A$  has a value of: 1.18 and  $CW$  the value of: 1.02 g.  $M$  now represents the horizontal frictional force acting on the force transducer. Its value, just like that of  $C$ , was registered on a paper writer. For the calculation of the value of  $\mu$ , 100 fertilizer particles were examined.

In addition, a second method described by HOEDJES (1978) was used. It should be noted that the possible interactions between the values obtained and this



measuring method are still subject to further studies. Calculation of the kinetic coefficient of friction was based on a simplification of the theory described in section 5.4.2 (which dealt with the phenomenon of sliding impact). The equations presented there for the calculation of particle velocity after impact also enable calculation of the value of  $\mu$  (and  $\varepsilon$ ). For this reason, particle status before impact (particle velocity, angle of impact, particle rotation) was compared with particle status after impact using a stroboscopic-photographic technique. It was expected that the values of the coefficient of friction obtained by this method would support the values of  $\mu^*$  which had to be used in the model, particularly during the phase of discontinuous contact.

#### 7.2.1.2. Coefficient of restitution

The coefficient of restitution ( $\varepsilon$ ) is widely employed in analysis of engineering problems. Its value indicates the degree of elasticity or plasticity during impact. It has been agreed and well-proved that the coefficient of restitution is not a constant but varies with the velocity of impact (MOHSENIN, 1968; HOEDJES, 1978).

In the process of particle movement inside the reciprocating sprout, the coefficient of restitution proved to be of fundamental significance.

Values of the coefficients of restitution of fertilizer during an impact on polyester were determined by REILING (1976). As mentioned before, the method used by HOEDJES (1978) also enabled the calculation of the values of  $\varepsilon$ . A widely-used method for determination of the coefficient of restitution deals with a comparison of the height of a vertically dropped particle with the height of its rebound (INNS and REECE, 1962; VOLLHEIM, 1971; MOHSENIN 1968).

In our experiments particle movement was filmed (72 p.p.s.). Particles were dropped vertically from a height of 1.0 m. Maximum height of rebound was recorded using a film motion analyzer. Coefficient of restitution was derived from:

$$\varepsilon = \frac{V_2}{V_1} = \left( \frac{H_2}{H_1} \right)^{1/2} \quad (7.2)$$

in which:  $V_1$  = initial velocity;  $V_2$  = velocity after rebound;  $H_1$  = height of dropping (1.00 m);  $H_2$  = maximum height of rebound.

When analyzing maximum height of rebound, only those particle trajectories were taken into consideration which deviated less than  $13^\circ$  from the vertical.

#### 7.2.1.3. Particle size distribution

Spreading width is influenced by particle size. Retardation of particle velocity due to air resistance increases as particle diameter decreases. Consequently, the working width of fertilizer broadcasters increases with the increasing diameter of fertilizer particles. According to HEYMANN et al. (1971) working width increased from 6 to 14 m as the percentage of particles  $> 2$  mm increased from 2.5 to 96.5%. For fertilizer distributors of the spinning disc system it was recommended that the lower and upper limits of particle size should be 1.5 to 4.0 mm.

In our experiments particle size distribution was measured using A.S.T.M. thread sieves. The sizes of the sieve holes were 1.6, 2.0, 2.5, 2.8, 3.5 and 4.0 mm. The amount of sieved fertilizer was 250 g per experiment. When the overflow over 4.0 mm exceeded 25 g, this fraction was resieved using holes of 5.0 mm as well. The sieving apparatus was a Retsch sieve type 3 D. Sieving time of a sample was 5 min. Particle size distribution was plotted cumulatively. From these graphs the Mass Median Diameter ( $d_{50}$ ) or 50 % point, as well as the variation in particle size represented by the value of  $d_{95}-d_{05}$  (series B) and  $d_{90}-d_{10}$  (series C) were calculated.

#### 7.2.1.4. Bulk density

Bulk density was determined according to the O.E.C.D. standards DAA/T/102 (1967). A measuring cube of known weight having a size of  $0.25 \times 0.25 \times 0.25$  m was filled with fertilizer, using a funnel, until the fertilizer had reached its maximum angle of repose (i.e. piled above the cube in the form of a pyramid). After removing the excess, the cube was weighed and bulk density calculated; this was expressed in  $\text{kg dm}^{-3}$ .

#### 7.2.1.5. Angle of repose

The angle of repose measured in our experiments represented the momentary angle of repose of a free surface. The method used was described by KOUWENHOVEN and TERPSTRA (1975). A vertically rotating drum (0.35 m, in dia.) was filled to 30 % with fertilizer. Inside, the drum was covered with a ribbed rubber coat. Peripheral speed of the drum was  $0.008 \text{ m s}^{-1}$ ; when the product started sliding, the momentary angle of repose was measured. It should be noted that the values recorded depended both on peripheral speed and the diameter of the drum. For this reason the values should only be considered relatively.

#### 7.2.1.6. Thousand kernel weight

Thousand kernel weight was determined according to the method prescribed by the Dutch Governmental Seed Testing Station. The weight of 100 kernels was measured 8 times and the mean was calculated. Multiplication by 10 resulted in the 1000 kernel weight.

#### 7.2.1.7. Moisture content

Moisture content was determined by the fertilizer manufacturers according to the Karl Fisher titration method.

### 7.3. EXPERIMENTAL RESULTS

#### 7.3.1. *Coefficients of friction and restitution*

Results of the examination of the friction and elastic properties of some fertilizers are presented in Tables 7.1 and 7.2. Using the method of HUISMAN (1977), friction forces obtained from fertilizer particles in contact with a sample of

TABLE 7.1. Friction properties of several fertilizers.

Material	Fertilizer	Coefficient of friction $\mu$	Standard deviation $\sigma_{\mu}$
Method of 'semi' kinetic measurement (HUISMAN, 1977)			
Polyester	Chilisalt peter granules (fertilizer A)	0.23	0.03
	Ammonium nitrate prills (fertilizer B)	0.17	0.02
Aluminium	Calcium ammonium nitrate granules*	0.38	0.04
	Calcium ammonium nitrate prills (fertilizer III)	0.42	0.06
	Urea granules	0.34	0.04
	Ammonium nitrate prills (fertilizer B)	0.29	0.02
Method of friction / impact measurement (HOEDJES, 1978)			
Steel	Calcium ammonium nitrate granules*	0.21	0.08

\* same fertilizer

the polyester sprout are found to be lower than those values obtained from fertilizer in contact with aluminium. This can be explained by the fact that the friction force depends upon the nature of the materials in contact; this results in different shearing and deforming as well as adhesion and cohesion processes.

From the figures presented by HOEDJES (1978) the following conclusions can be drawn. For comparable materials, the values of the computed friction forces are much lower (ranging from 0.16–0.28, with a mean value of the coefficient of kinetic friction of 0.21). Within the range of initial relative velocities studied ( $V$ : 6.3–8.5 m s<sup>-1</sup>), the value of the coefficient of friction  $\mu$  was correlated with the relative velocity according to  $\mu = 0.04 V - 0.09$  ( $r^2 = 0.40$ ). Explanation for these differences may be found in the fact that with the HOEDJES (1978) method, an extremely short duration of the contact time between the materials is obtained. In other words, time of actual contact is extremely short (in the order of milliseconds). Translation of the results obtained by one method into another should be avoided.

It seems fair to state that the values of the coefficient of friction for fertilizers A and B obtained from Huisman's method, support the theoretical values. These should be added to the variable  $\mu^*$  in the mathematical model in order to obtain agreement between measured and simulated values of velocity and angle of outlet (see section 5.4.5.).

Related to the model developed for the description of particle movement inside

the sprout, the friction process can be explained in a quantitative way partly by the friction forces measured with the method of Huisman, and partly by the results obtained with the method of Hoedjes. When explaining the friction process during particle movement, the values obtained by Huisman's method are apparently more applicable as far as they concern the phase of continuous contact. On the other hand, it appears that during the phase of discontinuous contact the values for the coefficient of friction according to the Hoedjes' method better support the actual character of particle movement.

Therefore, it can be stated that the friction forces during particle movement act in a complex way. Their character supports, in our opinion, the introduction of a variable  $\mu^*$  in the model, which can be considered as an imaginary kinetic coefficient of friction.

The elastic properties of the fertilizer, indicated by the presented values of the coefficient of restitution, vary with the different kinds of fertilizer used (Table 7.2). The effect of the Mass Median Diameter of the different sieve fractions on the values of the coefficient of restitution is not clear within one group of fertilizers. On the contrary, the coefficient of restitution varies from one type of fertilizer to the other. Fertilizer B proved to have the highest value of the coefficient of restitution, followed by the so-called high-density prills (Fertilizer III).

It has been proved in experiments that the value of the coefficient of restitution is dependent on the initial velocity of impact (MOHSEIN, 1968). In our experiments the initial velocity of the impacting fertilizer particles was about  $4.5 \text{ m s}^{-1}$ , using Reiling's method. The impact velocity during the phase of discontinuous contact of particle movement within the sprout varied considerably, especially since successive impacts were possible. For this reason the conditions under which the actual values of  $\epsilon$  were obtained only permit a limited comparison with the process of energy transfer within the sprout to a moving fertilizer particle. This is true insofar as the character of the transfer deals with elastic properties of the materials.

However, it seems reasonable to conclude that the values measured for the coefficient of restitution with the method used by Reiling support the values which were used in the mathematical model for the imaginary variable  $\epsilon^*$ .

### 7.3.2. *Other physical properties*

The values of the other physical properties for the fertilizers used in the experiments are given in Tables 7.3 and 7.4.

According to the manufacturers specifications, particle size distributions are the following.

– Fertilizer I:

- a. 1.5–2.0 mm: minimum 90% within this fraction;
- b. 60/20/20: 60% in 1.5–2.5 mm, 20% in 2.5–3.15 mm,  
20% in 3.15–4.0 mm;
- c. 33/33/33: 33% in 1.5–2.5 mm, 33% in 2.5–3.15 mm,  
33% in 3.15–4.0 mm;

TABLE 7.2. Restitution properties of several fertilizers.

Fertilizer / Mass Median Diameter (mm)	Coefficient of restitution $\varepsilon$	Standard Deviation $\sigma_{\varepsilon}$
Impact on polyester according to REILING (1976)		
A. Chilisalt peter /3.0	0.48	0.04
B. Ammonium nitrate /3.0	0.73	0.06
I. Calcium ammonium nitrate;		
granules		
a./1.7	0.51	0.09
b./2.4	0.49	0.04
c./2.9	0.48	0.03
d./3.1*	0.46	0.03
e./3.5	0.47	0.03
f./3.6	0.46	0.05
II. Calcium ammonium nitrate;		
prills		
a./1.9	0.46	0.08
b./2.2	0.46	0.09
c./2.3*	0.46	0.07
III. Calcium ammonium nitrate;		
prills		
a./2.2	0.60	0.06
b./2.3	0.59	0.05
c./2.8	0.58	0.06
d./2.8*	0.57	0.08
e./3.4	0.64	0.05
f./3.9	0.52	0.09
Impact on steel, according to HOEDJES (1978)		
I. Calcium ammonium nitrate;		
granules		
d./3.1*	0.23	0.10

Trade products are marked with \*

e. 20/20/60: 20% in 1.5–2.5 mm, 20% in 2.5–3.15 mm,  
60% in 3.15–4.0 mm;

f. 3.5–4.0 mm: minimum 90% within this fraction.

For the trade products as well as the types I: g–k, II: d–f, and III: g–i, no previous specifications were supplied by the manufacturers.

– Fertilizer II:

a. 1.6–2.0 mm: minimum 90% within this fraction;

b. 2.0–2.5 mm: minimum 90% within this fraction.

– Fertilizer III:

a. 2.0–2.48 mm: minimum 90% within this fraction;

b. 60/20/20: 60% in 1.53–2.48 mm, 20% in 2.48–3.35 mm,

TABLE 7.3. Physical properties of the fertilizers used.

Fraction	Mass Median Diameter; $d_{50}$ (mm)	$d_{95} - d_{05}$ (mm) or $d_{90} - d_{10}$	bulk density (kg dm <sup>-3</sup> )	angle of repose (deg)	moisture content (% H <sub>2</sub> O)	1000 kernel weight (g)
<b>I. Calcium ammonium nitrate; granules</b>						
a.	1.7	0.6	0.99	33	0.12	7.1
b.	2.4	2.2	1.04	34	0.22	22.7
c.	2.9	2.3	1.04	36	0.29	29.2
d.*	3.1	1.9	1.00	36	0.17	35.9
e.	3.5	2.4	1.05	35	0.19	40.3
f.	3.6	0.9	1.03	36	0.20	44.8
g.	2.1	0.4	1.03		0.23	
h.	2.8	1.0	1.03		0.23	
i.*	2.9	1.6	1.04		0.24	
j.	3.7	0.9	1.01		0.23	
k.	4.4	0.7	1.01		0.24	
<b>II. Calcium ammonium nitrate; prills ('low-density')</b>						
a.	1.9	0.9	0.94	35	1.00	6.7
b.	2.2	0.7	0.95	37	0.80	11.6
c.*	2.3	1.1	0.95	37	0.82	11.7
d.	1.9	0.5	0.99		0.68	
e.	2.3	0.3	0.98		0.63	
f.*	2.4	0.8	0.98		0.98	
<b>III. Calcium ammonium nitrate; prills ('high-density')</b>						
a.	2.2	1.0	1.08	28	0.28	11.9
b.	2.3	2.7	1.11	30	0.30	20.0
c.	2.8	2.7	1.09	30	0.34	31.5
d.*	2.8	2.0	1.06	29	0.18	27.3
e.	3.4	2.5	1.09	31	0.34	40.2
f.	3.9	1.3	1.08	32	0.34	54.4
g.	2.4	0.6	1.09		0.06	
h.*	3.1	1.8	1.09		0.09	
i.	3.2	1.1	1.09		0.10	

Trade products are marked with \*

- 30% in 3.35–5.15 mm;  
 c. 33/33/33: 33% in 1.53–2.48 mm, 33% in 2.48–3.35 mm,  
 33% in 3.35–5.15 mm;  
 e. 20/20/60: 20% in 1.53–2.48 mm, 20% in 2.48–3.35 mm,  
 60% in 3.35–5.15 mm;  
 f. 3.35–4.03 mm: minimum 90% within this fraction.

TABLE 7.4. Sieve fractions of the fertilizers used.

Product / sieve fraction or compound	Sieve fractions (%)					
	< 1.6 (mm)	1.6-2.0 (mm)	2.0-2.8 (mm)	2.8-3.35 (mm)	3.35-4.0 (mm)	> 4.0 (mm)
I a. 1.5-2.0 mm	36.6	61.2	1.8	-	-	-
b. 60/20/20	2.4	22.0	42.7	13.2	15.8	3.9
c. 33/33/33	3.9	13.6	28.2	25.4	25.4	3.5
d.*trade	-	0.8	24.7	38.5	29.1	5.9
e. 20/20/60	1.1	7.3	15.5	19.0	46.3	10.8
f. 3.5-4.0 mm	-	0.1	1.7	31.6	66.3	-
g. 1.5-3.0 mm	2.2	21.0	73.7	1.7	1.1	0.2
h. 2.5-3.5 mm	0.3	0.7	42.6	46.4	9.8	0.1
i.* trade	1.2	3.4	37.3	33.3	20.9	3.9
j. 3.5-4.5 mm	0.2	0.1	0.6	17.6	67.8	13.6
k. > 4.5 mm	0.1	0.1	0.2	0.3	7.5	92.9
II a. 1.6-2.0 mm	10.0	77.9	11.7	0.3	0.1	-
b. 2.0-2.5 mm	0.1	8.1	91.1	0.6	0.1	-
c.*trade	2.5	18.2	74.6	4.3	0.3	0.1
d. 1.6-2.0 mm	5.5	63.3	31.1	-	-	-
e. 2.0-2.5 mm	0.2	6.7	90.9	2.0	0.1	-
f.* trade	1.3	11.3	79.9	7.0	0.7	0.2
III a. 2.0-2.48 mm	0.6	29.8	69.5	0.1	-	-
b. 60/20/20	0.7	14.5	58.1	9.2	9.9	7.6
c. 33/33/33	0.7	8.9	42.2	15.4	19.3	13.5
d.*trade	0.3	4.9	47.7	25.0	17.9	4.2
e. 20/20/60	0.7	7.4	28.5	11.9	28.9	22.8
f. 3.35-4.03 mm	0.1	0.1	0.2	6.3	68.2	25.1
g. 1.6-2.8 mm	0.8	8.1	88.2	2.9	-	-
h.*trade	0.3	1.6	29.5	31.8	23.4	13.4
i. > 2.8 mm	0.1	0.1	12.8	55.5	25.4	6.0

The results of the sieve analyses show that not all products had a particle size distribution which was in complete agreement with the manufacturers' specifications (see Table 7.4). The fertilizers I f. and III f. are examples showing disagreement. For fertilizer I f. the amount of particles < 3.5 mm is too high. On the other hand, for type III f. the amount of too-coarse particles exceeds their limits.

The so-called 'high-density' prills showed the highest values for bulk density (1.06 to 1.09 kg dm<sup>-3</sup>); the 'low-density' prills showed the lowest values (0.94 to 0.99 kg dm<sup>-3</sup>). Moisture content varied considerably with the type of fertilizer; this can be explained by the differences in technology used in the production of the prills.

## 7.4. EFFECTS OF PHYSICAL PROPERTIES OF FERTILIZERS ON THE QUALITY OF THE TRANSVERSE DISTRIBUTION PATTERN

### 7.4.1. Introduction

One method which can be used for the estimation of the effects of physical properties on the quality of the distribution pattern is to define the relationship between variables which represent some main physical properties and parameters that represent the quality of the transverse distribution pattern.

The quality of the compound transverse distribution patterns was expressed by means of:

- The optimum working width, which is that working width larger than 5 m at which the most even distribution was obtained. The evenness of distribution was expressed by means of the coefficient of variation ( $C.V.$ ) and/or Burema's number of irregularity ( $R$ ).
- The (minimum) values of  $C.V.$  and/or  $R$  of the optimal working width.
- The maximum working width, indicating that value of the working width for which the values of  $C.V.$  and/or  $R$  do not exceed the limits of 15% and 75.
- The size of the workable trajectory below this maximum working width (based on the same limits for  $C.V.$  and  $R$ ).

The values of these trajectories indicate the possibilities for tolerable variations in the ratio of overlap. For example, a maximum working width of 11.0 m and a workable trajectory of 5.0 m, means that for working widths of 6.0 to 11.0 m the values of  $C.V.$  or  $R$  do not exceed 15% or 75. Consequently, one will find the optimum working width within this range to be 8.5 m which shows a minimum value for  $C.V.$  of 8.3%.

For test series C the possible consequences of variations in the ratio of overlap were further expressed by the minimum mean values for  $R$  of three and five neighbouring trajectories of 0.5 m each. In practice these ranges are situated around the optimum working width. It is clear that a relatively low value of  $\bar{R}_{min}$  in practice will reduce the increase in the rate of unevenness of the compound transverse distribution pattern which is caused by variations in the ratio of overlap.

In his work, REILING (1976) has tried to develop a more fundamental statistical basis for the explanation of the effects of physical properties on distribution patterns by examining the correlation between these and the variables indicating the quality of the distribution pattern. Experimental results were treated by using methods like forward stepwise regression and another method developed by DANIEL and WOOD (1971), with the aim of obtaining equations which express the relations between both the explaining variables (physical properties) and the variables which must be explained (quality aspects of distribution patterns).

It appeared that due to unavoidable imperfections in the set-up of the experiments, a complete statistical treatment of the results was at least debatable. In addition, it should be emphasized that the experiments were primarily focused on the consequences of particle size (distribution) for the quality of the transverse distribution pattern.



TABLE 7.5a. Relations between particle size (distribution) and features of the compound transverse distribution patterns.

Fertilizer	M.M.D. or $d_{50}$ (mm)	$d_{95}-d_{05}$ (mm)	Optimum working width (m) for			Coefficient of variation C.V. (%) for			Maximum working width (m) and workable trajectory ( ) for		
			30	60	90	30	60	90	30	60	90
			kg min <sup>-1</sup>			kg min <sup>-1</sup>			kg min <sup>-1</sup>		
I a.	1.7	0.6	7.0	7.0	7.0	10.1	10.3	8.0	7.5 (1.0)	7.5 (0.5)	7.5 (1.0)
b.	2.4	2.2	9.0	9.0	8.0	4.9	8.1	8.2	11.0 (3.5)	11.5 (4.0)	12.5 (6.5)
c.	2.9	2.3	9.0	9.0	8.5	5.4	9.5	10.1	12.0 (6.0)	11.5 (3.5)	12.0 (4.5)
d.*	3.1	1.9	9.0	9.0	9.0	7.5	6.2	10.5	11.5 (5.5)	12.0 (4.0)	11.5 (3.0)
e.	3.5	2.4	9.5	11.0	9.0	5.5	7.7	8.8	12.5 (5.0)	12.5 (4.0)	12.5 (7.0)
f.	3.6	0.9	9.5	10.0	9.0	6.1	8.1	9.6	13.0 (7.0)	12.5 (4.0)	13.0 (5.0)
II a.	1.9	0.9	7.0	7.0	7.0	8.6	10.6	7.7	7.5 (1.0)	7.5 (0.5)	7.5 (1.0)
b.	2.2	0.7	8.0	8.0	8.0	5.3	11.6	12.0	9.0 (2.0)	9.0 (1.5)	8.0 (1.5)
c.*	2.3	1.1	8.0	8.0	8.0	4.9	9.4	12.6	9.0 (3.0)	9.0 (1.5)	8.0 (1.5)
III a.	2.2	1.0	8.0	9.0	9.0	4.7	5.6	8.2	10.5 (4.5)	15.0 (9.0)	12.5 (6.5)
b.	2.3	2.7	8.5	9.5	9.5	6.2	5.4	8.4	11.5 (5.5)	15.0 (9.0)	13.0 (4.5)
c.	2.8	2.7	9.5	10.0	9.5	7.2	5.7	9.2	13.5 (7.0)	15.0 (9.0)	13.5 (5.0)
d.*	2.8	2.0	8.5	9.0	9.5	9.1	7.6	9.6	10.0 (3.5)	14.0 (8.0)	14.0 (5.5)
e.	3.4	2.5	9.5	10.0	12.5	5.9	6.2	9.0	14.0 (8.0)	14.5 (8.5)	14.0 (5.5)
f.	3.9	1.3	9.0	10.0	13.0	7.2	8.8	8.2	14.5 (8.5)	14.5 (8.5)	14.5 (8.5)

trade products are marked with \*

TABLE 7.5b. Relations between particle size (distribution) and features of the compound transverse distribution patterns.

Fertilizer	M.M.D. or $d_{50}$ (mm)	$d_{90}-d_{10}$ (mm)	Optimum working width (m)		Number of irregularity $R$		Coefficient of variation C.V. (%)		$\bar{R}_{min}$ 1.5 m		$\bar{R}_{min}$ 2.5 m		Maximum working width and workable trajectory ( )	
			for		for		for		for		for		for	
			500	1000	500	1000	500	1000	500	1000	500	1000	500	1000
I g.	2.1	0.4	7.0	7.0	42	40	8.8	7.6	54	55	67	70	8.0 (1.5)	7.5 (1.0)
h.	2.8	1.0	8.5	7.0	50	40	11.9	8.6	52	48	56	60	9.0 (2.0)	8.0 (1.0)
i.*	2.9	1.6	7.5	7.0	36	38	8.2	8.4	40	49	46	60	9.5 (2.5)	8.5 (1.5)
j.	3.7	0.9	8.5	7.5	41	44	8.3	9.3	44	49	48	56	11.0 (5.0)	9.0 (3.0)
k.	4.4	0.7	9.0	8.0	39	47	8.4	10.3	43	50	50	54	11.5 (5.5)	10.0 (4.0)
II d.	1.9	0.5	6.5	6.5	43	36	9.4	7.6	63	70	75	83	7.0 (0.5)	6.5 (0.0)
e.	2.3	0.3	7.0	7.0	57	45	11.4	9.9	63	59	71	73	7.5 (1.0)	7.0 (0.5)
f.*	2.4	0.8	7.0	6.5	57	38	11.0	8.7	62	56	70	70	8.0 (1.5)	7.0 (0.5)
III g.	2.4	0.6	7.5	7.5	34	32	7.0	6.9	38	45	40	51	9.0 (3.0)	8.0 (2.0)
h.*	3.1	1.8	8.5	8.0	23	52	4.7	10.6	29	55	36	61	11.5 (5.5)	9.5 (3.5)
i.	3.2	1.1	9.0	8.5	52	57	11.0	12.2	56	62	53	66	9.5 (2.0)	9.0 (1.5)

trade products are marked with \*

Moreover, there developed a certain rate of mutual adaption between fertilizers and fertilizer broadcasters since the basic knowledge of the characteristics of distribution mechanisms (especially the spinning disc broadcasters) has increased. The common aim of improvement of the distribution pattern has resulted in a tendency to produce uniform types of granular fertilizers.

The values of some physical properties like bulk density and moisture content are closely related to specific production technologies of the manufacturers. Variations between the levels of these physical properties were small since the number of fertilizer manufacturers participating in the experiments was limited to three, for unavoidable confidential reasons.

The experimental results, and therefore the conclusions drawn, will indicate those physical properties which mainly explain the quality of the distribution pattern.

#### 7.4.2. Experimental results

The experimental results are presented in Table 7.5a (test series B) and Table 7.5b (test series C).

This subdivision of the results is useful because of the differences in testing methods which resulted in considerable differences in the experimental results for comparable fertilizers. This phenomenon will be discussed later in this section.

For all the experiments a workable trajectory and an optimum working width for which the limits of  $C.V. < 15\%$  or  $R < 75$  were not exceeded, could be found. For the greater part of the fertilizers tested, values of  $C.V. < 10\%$  ( $R < 50$ ) were obtained.

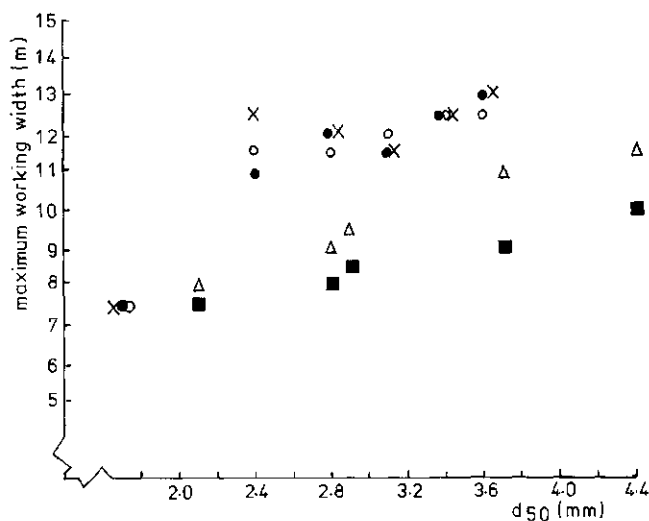


FIG. 7.3a. The maximum working width as a function of the Mass Median Diameter ( $d_{50}$ ). Application rates: ●: 30 kg min<sup>-1</sup>, ○: 60 kg min<sup>-1</sup>, ×: 90 kg min<sup>-1</sup>, (series B); △: 500 kg ha<sup>-1</sup>, ■: 1000 kg ha<sup>-1</sup> (series C). FERTILIZER I.

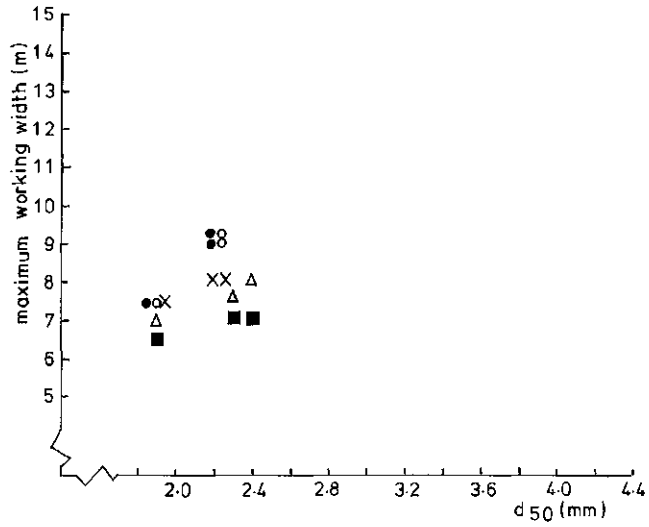


FIG. 7.3b. The maximum working width as a function of the Mass Median Diameter ( $d_{50}$ ). Application rates: ●: 30 kg min<sup>-1</sup>, ○: 60 kg min<sup>-1</sup>, ×: 90 kg min<sup>-1</sup>, (series B); △: 500 kg ha<sup>-1</sup>, ■: 1000 kg ha<sup>-1</sup> (series C). FERTILIZER II.

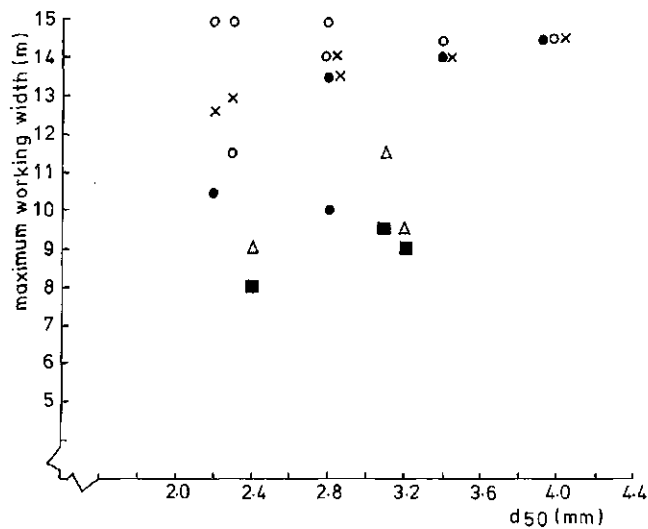


FIG. 7.3c. The maximum working width as a function of the Mass Median Diameter ( $d_{50}$ ). Application rates: ●: 30 kg min<sup>-1</sup>, ○: 60 kg min<sup>-1</sup>, ×: 90 kg min<sup>-1</sup>, (series B); △: 500 kg ha<sup>-1</sup>, ■: 1000 kg ha<sup>-1</sup> (series C). FERTILIZER III.

Some types of fertilizer show a relationship between the application rate and the quality of the compound transverse distribution patterns. For coarse fractions (e. and f.) of fertilizer I, the optimum working width is somewhat higher when metering  $60 \text{ kg min}^{-1}$ . The coarse fractions (e. and f.) of fertilizer III provide a distinctly higher optimum working width with a metering of  $90 \text{ kg min}^{-1}$ .

Generally, all fertilizer types show a tendency towards increases of maximum working width if the Mass Median Diameter of the fractions (and the 1000 kernel weight which appears to be closely correlated to this) increased (Fig. 7.3a-c). This tendency interacts with the application rate. For fertilizer III with a metering of  $60 \text{ kg min}^{-1}$ , there is no effect of particle size on the maximum working width; on the contrary, at  $90 \text{ kg min}^{-1}$  this effect is rather clear in test series B (Fig. 7.3c). In addition, at the latter application rate the optimum working width also tends to increase with increasing values of  $d_{50}$  (Fig. 7.4c).

For fertilizer I in test series C the positive influence of an increased value of the M.M.D. or  $d_{50}$  on the maximum working width is quite clear for both application rates of  $500 \text{ kg ha}^{-1}$  ( $\approx 60 \text{ kg min}^{-1}$ ) and  $1000 \text{ kg ha}^{-1}$  ( $\approx 120 \text{ kg min}^{-1}$ ). For this type of fertilizer it is evident that a fine sieve fraction - represented by a low value of  $d_{50}$  and a high percentage (36.6 %) of particles  $< 1.6 \text{ mm}$ , together with a low value of  $d_{95}-d_{05}$  - negatively affects the optimum working width, and especially the maximum working width and the size of the workable trajectory. As a result, steering faults or other deviations from the optimum ratio of overlap have strong negative effects. Similar effects are noticed for sieve fraction a. and somewhat less conclusively for fraction d. of fertilizer type II.

The effects of particles of a sieve fraction  $< 1.6 \text{ mm}$  on the distribution pattern is clearly demonstrated by Fig. 7.5a. which represents the sieve fractions in the collecting trays after spreading of series B fertilizers). The working width is limited and the shape of the basic transverse distribution pattern differs considerably from the other fractions. The same is true for fertilizer III (Fig. 7.5b)

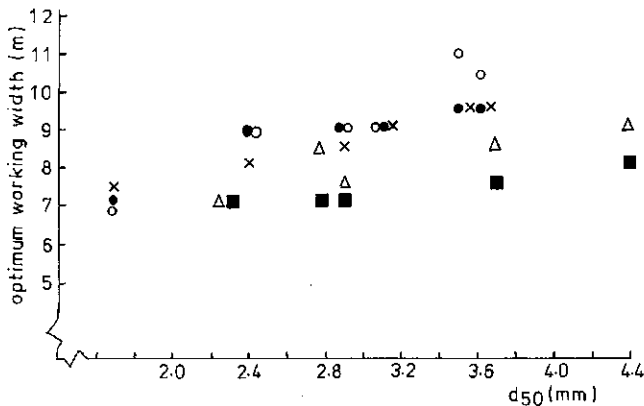


FIG. 7.4a. The optimum working width as a function of the Mass Median Diameter ( $d_{50}$ ). Application rates: ●:  $30 \text{ kg min}^{-1}$ , ○:  $60 \text{ kg min}^{-1}$ , ×:  $90 \text{ kg min}^{-1}$  (series B); △:  $500 \text{ kg ha}^{-1}$ , ■:  $1000 \text{ kg ha}^{-1}$  (series C). FERTILIZER I.

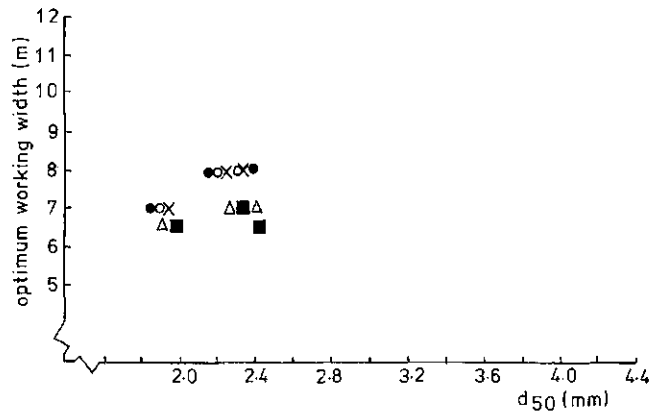


FIG. 7.4b. The optimum working width as a function of the Mass Median Diameter ( $d_{50}$ ). Application rates: ●: 30 kg min<sup>-1</sup>, ○: 60 kg min<sup>-1</sup>, ×: 90 kg min<sup>-1</sup> (series B); △: 500 kg ha<sup>-1</sup>, ■: 1000 kg ha<sup>-1</sup> (series C). FERTILIZER II.

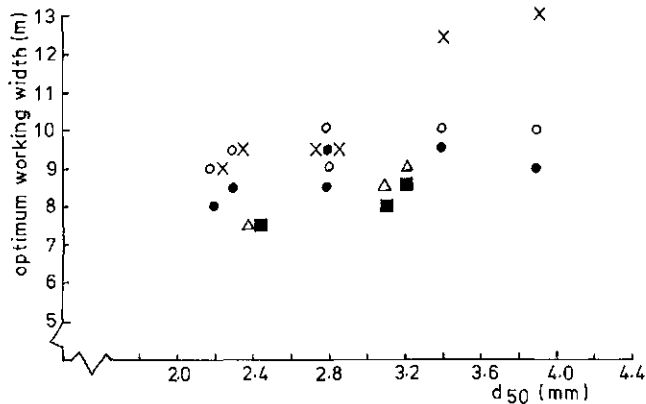


FIG. 7.4c. The optimum working width as a function of the Mass Median Diameter ( $d_{50}$ ). Application rates: ●: 30 kg min<sup>-1</sup>, ○: 60 kg min<sup>-1</sup>, ×: 90 kg min<sup>-1</sup> (series B); △: 500 kg ha<sup>-1</sup>, ■: 1000 kg ha<sup>-1</sup> (series C). FERTILIZER III.

although the amount of this particular fine sieve fraction is very small for this type. From both figures the conclusion can be drawn that coarser fractions create possibilities for increases in the working width.

For all fractions of fertilizer II the size of the workable trajectory is small, especially at higher application rates. Again, a low value of  $d_{50}$  acts in a negative way. The same is true for the fine sieve fractions of fertilizer I (Fig. 7.6a). This type of fertilizer shows the general tendency to an increasing size of the workable trajectory when the value of  $d_{50}$  increases, although there is some interaction with the application rate.

Fertilizer type III shows the highest levels of workable trajectories (Fig. 7.6b). Obviously, the value of the workable trajectory does not depend on the value of  $d_{50}$  at application rates of 30 kg min<sup>-1</sup>. For the other application rates of test series B,

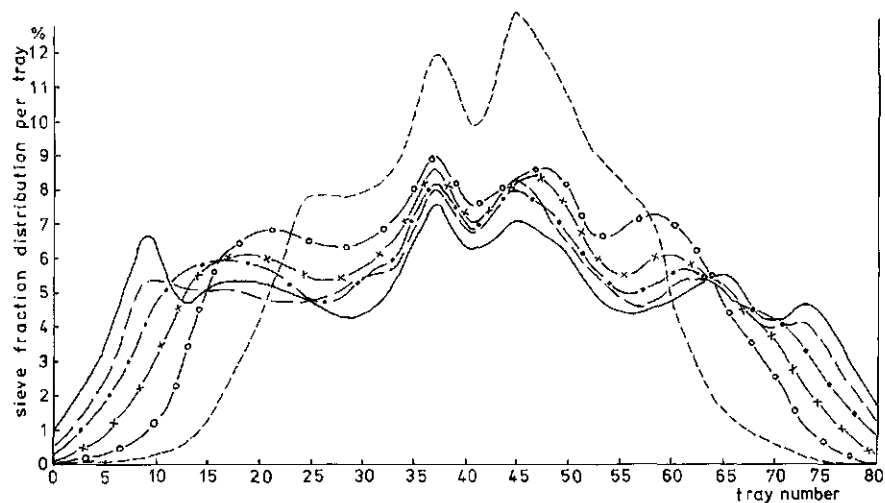


FIG. 7.5a. Sieve fraction distributions of the fertilizer per collecting tray after spreading. Sieve fractions: ----: < 1.6 mm, —○—: 1.6–2.0 mm, —×—: 2.0–2.8 mm, —●—: 2.8–3.35 mm, — —: 3.35–4.0 mm, —: > 4.0 mm. FERTILIZER I (series B).

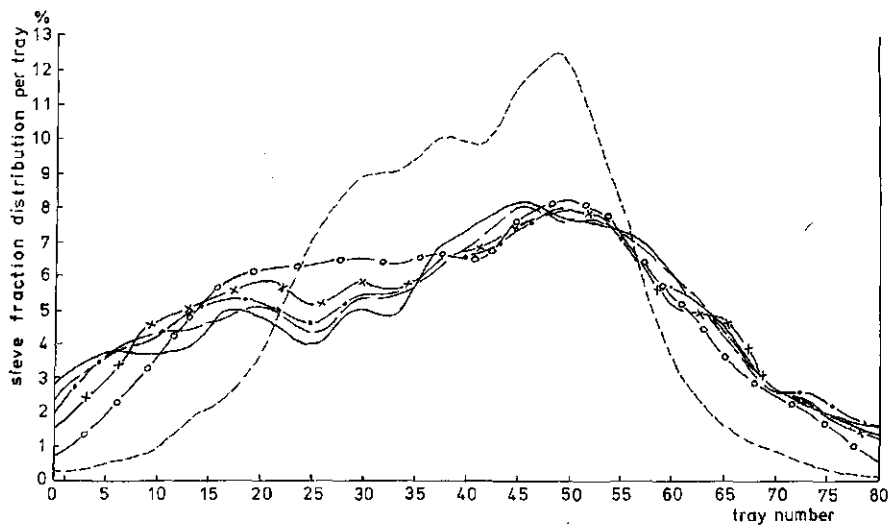


FIG. 7.5b. Sieve fraction distributions of the fertilizer per collecting tray after spreading. Sieve fractions: ----: < 1.6 mm, —○—: 1.6–2.0 mm, —×—: 2.0–2.8 mm, —●—: 2.8–3.35 mm, — —: 3.35–4.0 mm, —: > 4.0 mm. FERTILIZER III (series B).

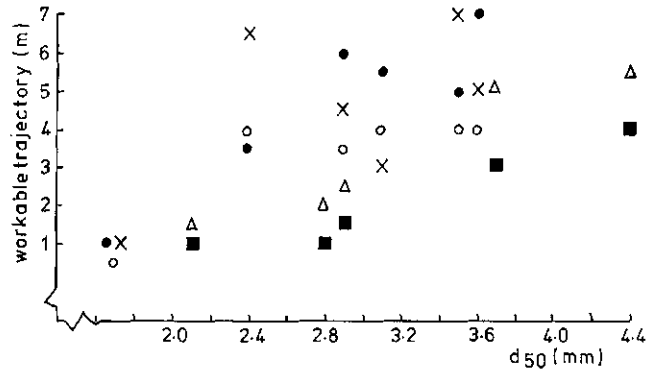


FIG. 7.6a. Workable trajectory as a function of the Mass Median Diameter ( $d_{50}$ ). Application rates: ●: 30 kg min<sup>-1</sup>, ○: 60 kg min<sup>-1</sup>, ×: 90 kg min<sup>-1</sup> (series B); △: 500 kg ha<sup>-1</sup>, ■: 1000 kg ha<sup>-1</sup> (series C). FERTILIZER I.

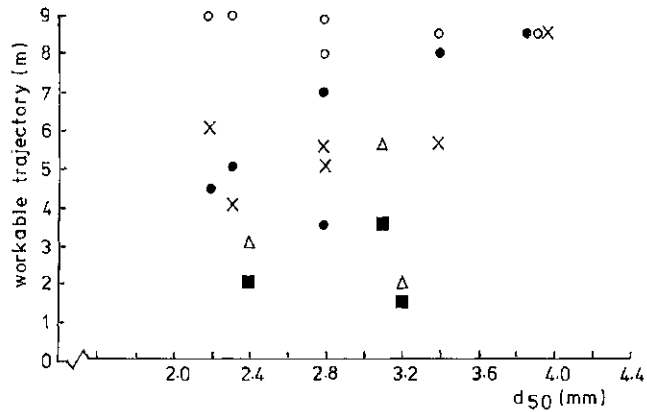


FIG. 7.6b. Workable trajectory as a function of the Mass Median Diameter ( $d_{50}$ ). Application rates: ●: 30 kg min<sup>-1</sup>, ○: 60 kg min<sup>-1</sup>, ×: 90 kg min<sup>-1</sup> (series B); △: 500 kg ha<sup>-1</sup>, ■: 1000 kg ha<sup>-1</sup> (series C). FERTILIZER III.

there is a similar tendency to an increasing size of the workable trajectory with increasing values of  $d_{50}$ .

These results agree reasonably with those obtained from similar experiments performed by the N.I.A.E. (1971) in which it appeared that a large particle size permitted greater tolerance of driving errors.

A comparison between different fertilizers, including the three application rates, shows the following aspects (Table 7.6) based on similarity in sieve fractions and/or  $d_{50}$  and  $d_{95} - d_{05}$ .

For the fine sieve fractions of fertilizers I and II there is no difference with respect to the mean optimum working width, the mean value of *C.V.*, and the mean workable trajectory (limited by *C.V.* < 15%). For all the other comparable combinations, the high-density prills were superior to both the granules and the



TABLE 7.6. Comparison between similar sieve fractions of different types of fertilizers with respect to distribution quality.

Type of fertilizer	Sieve fraction (mm)/or compound	Bulk density (kg dm <sup>-3</sup> )	Mean optimum working width (m)	Mean value of C.V. (%)	Mean workable trajectory (m)
I a.	1.5 -2.0	0.99	7.0	9.5	0.8
II b.	1.6 -2.0	0.94	7.0	9.0	0.8
I b.	2.0 -2.5	0.95	8.0	9.6	1.3
III a.	2.0 -2.4	1.08	8.7	6.2	6.7
I f.	3.5 -4.0	1.03	9.5	7.9	5.3
III b.	3.35-4.03	1.11	10.7	8.1	8.3
I e.	20/20/60	1.05	9.8	7.3	5.5
III e.	20/20/60	1.09	10.7	7.0	7.3
I b.	60/20/20	1.04	8.7	7.1	4.7
III b.	60/20/20	1.11	9.2	6.7	6.3
I c.	33/33/33	1.04	8.8	8.3	4.7
III c.	33/33/33	1.09	9.7	7.4	7.0
I f.	trade product	0.98	6.7	9.9	7.5
III g.	1.6-2.8	1.09	7.5	7.0	8.5

low-density prills. This supports the statements of HEYMANN et al. (1971) and REILING (1976) that high bulk density of granular fertilizers contributes to an increase of the optimum working width. It can be added that other quality aspects of the transverse distribution pattern improve also, since the values of *C.V.* are lower and those of the workable trajectory are higher.

A comparison between fertilizers I and III shows that at comparable levels of  $d_{50}$ , an increase of the value of  $d_{95}-d_{05}$  or  $d_{90}-d_{10}$  leads to an increase of the evenness of the compound distribution pattern. Values for *C.V.* and *R* are somewhat lower at the optimum working width. Apparently the spreading process of the reciprocating sprout broadcaster is favourably influenced by a certain rate of variation in particle size.

It is notable that the results of the experiments of series B and C especially for fertilizers I and III, show a rather great difference at comparable levels of  $d_{50}$ . Both the values of the maximum working width and the optimum working width are at a lower level, although the set values of the spreading height and the number of revolutions of the driving shaft are the same for all experiments. Until now it was not possible to give a complete explanation for this phenomenon. Partly it may be explained by aspects concerned with the collecting methods described in section 7.2. It can be concluded, however, that one should take care when transferring the results of experiments obtained on a certain type of patternator to situations under different conditions.

## 7.5. DISCUSSION

The following conclusions could be drawn from the friction and restitution experiments. The values which were added to the imaginary coefficient of friction ( $\mu^*$ ) and restitution ( $\varepsilon^*$ ) in the mathematical model are in reasonable agreement with those obtained from actual friction and restitution experiments.

The coefficients of friction for fertilizers A and B with a polyester plate, obtained with the method of 'semi' kinetic measurement, were 0.23 and 0.17. In the simulation experiments, values of 0.2 and 0.1 for the imaginary coefficient of friction gave the best agreement between calculated and measured values of  $\bar{V}K$ ,  $\bar{i}$ , and  $\bar{\beta}$ .

In the model, theoretical values of 0.4 and 0.7 were added to the imaginary coefficient of restitution  $\varepsilon^*$  for fertilizers A and B. In the actual restitution experiments values of 0.48 and 0.73 were obtained for both fertilizers.

Although the character of particle motion within the sprout can be complicated, it is tenable to introduce imaginary coefficients of friction and restitution in the simulation model. It appears that the values which must be added to these variables can be obtained from performance of rather simple model experiments as described in this chapter.

The quality of the transverse distribution patterns (indicated by the optimum bout width for which the value of *C.V.* is minimal, the range of the workable trajectory:  $C.V. < 15\%$ , and the maximum working width) is mainly affected by:

particle size, bulk density and particle size distribution. Effects of other physical properties such as moisture content, coefficient of restitution, and possible interactions between the properties involved in these experiments, could not be examined to a more extensive rate. This was due to unavoidable imperfections in the performance of the experiments.

Sieve fractions  $< 1.6$  mm must be eliminated from granular fertilizers which are to be spread by a reciprocating sprout broadcaster since they limit working width, and therefore capacity. In addition, their transverse distribution pattern differs considerably from that of other fractions in the compound; this can act in a negative way on evenness of distribution.

Generally, increased values of the Mass Median Diameter and the correlated 1000 kernel weight act positively on the quality of the distribution pattern, although sometimes there is noticeable interaction with application rates. Nevertheless, coarse particles enable the realization of greater optimum and maximum working widths. This effect is supported by high values of bulk density (as they were found for fertilizer III). In addition, the larger particle sizes give distribution patterns with a greater tolerance of driving errors. These conclusions are in agreement with results of similar experiments mentioned in relevant literature cited in this chapter.

As far as its value has a relationship with the quality of the distribution pattern, an upper limit on particle size is not quite clear. The experimental results partly show an interaction with the testing methods applied and the application rates. For fertilizer I in test series B hardly any influence of a M.M.D.  $> 2.4$  mm can be noticed. The values of both optimum and maximum working widths are at an almost constantly high level. On an average the same is true for fertilizer III in test series B, although an exception has to be made for the optimum working width at an application rate of  $90 \text{ kg min}^{-1}$ . The tests with the driving broadcaster (series C) show a continuous increase of the maximum working width with increased values of the M.M.D. for fertilizer I. Moreover, the upper limit of particle size depends on various other factors such as minimum application rates and dimensions of the metering devices. Especially for the reciprocating sprout broadcaster, it seems that the intensity of particle impacts within the sprout can be a limiting factor for particle size since generally speaking, particle breakdown will be higher for larger particles.

A variation in particle size seems to act favourably on the evenness of the compound transverse distribution pattern of the reciprocating sprout broadcaster. This is in contrast to what is generally noticed for spinning disc types. For this reason an increasingly close cooperation between fertilizer and broadcaster manufacturers is recommended.

The differences which were found between the stationary and the driving testing method described in this chapter require further examination since, especially for coarse fertilizers, the differences in maximum working width were considerable.

## SUMMARY

### *Introduction*

Since the end of the 1950's, variable bout width distributors were used for broadcast application of granular fertilizers. The bout width is a multiple of the width of the metering and distribution devices. The most important types are the spinning disc and reciprocating sprout broadcasters. The distribution device mainly transfers translation energy to the particles so that they are distributed over a large area.

The construction of the distribution and metering devices is simple; the broadcasters are relatively cheap to purchase and maintain. The combination of a high bout width (8–15 m) and a high driving speed enables high capacities at high application rates of fertilizer. Work load and operation costs are relatively low.

### *Objectives of this study*

Contrary to the spinning disc system, the reciprocating sprout broadcaster has been the subject of fundamental research only on a limited scale. The objective of this research work described in the previous chapters was to give a first impulse for more fundamental analysis of factors which determine the distribution process of the reciprocating sprout broadcaster. Within this framework, attention was paid to:

- the kinematic aspects of the oscillating distributor device;
- an analysis of the characteristics of motion of separate particles within the sprout and after dispatch;
- the formulation of a theory and the development of a model for the calculation of particle trajectories and velocities;
- the consequence of alterations of relevant construction parameters for both the oscillatory characteristic of the distributor device and particle motion resulting in the basic transverse distribution pattern;
- the influences of fertilizer properties on the quality of the distribution pattern, which e.g. is represented by the optimum and maximum bout width and the evenness of the compound distribution pattern.

### *Developments*

From the outline of the development of fertilizer distributors (chapter 2), it appears that in the beginning the evenness of the transverse distribution pattern of the reciprocating sprout broadcaster was poor. The evenness of the compound transverse distribution pattern is a dominating factor for the quality of the distribution process. Maintenance of the correct ratio of overlap was difficult because of the steep slopes of the basic transverse patterns. However, comparative machine testings, experimental research work of the manufacturers, and a progressing mutual adaption of fertilizers and broadcasters resulted in a considerable increase of the quality of the spreading process.

It can be stated that in their present designs the reciprocating sprout and

spinning disc broadcasters are equal to each other with respect to operation quality. Values of the coefficient of variation  $< 10\%$  for the transverse compound distribution patterns can be realized when these types of broadcasters are carefully used in practice.

Nevertheless, yield losses of 1–3% which were still noted in practice at the beginning of 1970, emphasize the need for continuous attention to the evenness of the transverse distribution pattern. The most serious source of failures in practice is application at an incorrect ratio of overlap.

The need for increase of the working width is supported by the timeliness of fertilizing and the desirability for a decrease of the number of wheel tracks. Depending on factors such as working speed, application rate, and hopper content, the net working times ( $\text{h ha}^{-1}$ ) can decrease by about 10 and 20% respectively, when increasing the bout width from 8 to 10 m and from 10 to 15 m.

#### *Distribution patterns*

Chapter 3 deals with the determination, representation, and interpretation of the evenness of distribution. Determination of the size of the standard sampling area depends on fertilizing-technical, climatological, soil, and cultivation factors. The specific characteristics of the transverse distribution pattern should be taken into consideration.

It appears that for broadcast application of fertilizer, irregularities within areas of  $0.5 \times 0.5$  m hardly influence crop yields. As a consequence, the width of the collecting trays (0.5 m) which are recommended in the O.E.C.D. standard testing procedure, can be qualified as acceptable.

The most frequently used coefficients of irregularity are the coefficient of variation  $C.V.$ , the linear deviation from the mean  $\bar{d}$ , and Burema's number of irregularity  $R$ . The relationships between these coefficients are presented.

The shape of the basic transverse distribution pattern determines the evenness of the compound pattern, the ratio overlap, and the optimum and maximum working widths. The optimum working width is defined by that width  $> 5.0$  m at which the values for  $C.V.$  and/or  $R$  are minimal. The maximum working width is limited by values for  $C.V. < 15\%$  and/or  $R < 75$ .

Partly based on practical considerations, a number of requirements have been formulated for the shape of the compound transverse distribution pattern. In section 3.3 a number of basic transverse distribution patterns are discussed which enable a good rate of evenness (e.g.  $C.V. < 8\%$ ) at a low ratio of overlap (e.g.  $O = 0.4$ ). Two- or more-peak basic transverse distribution patterns have to be refused.

The complexity of external factors prevents the formulation of a uniform standard for evenness of distribution which is based on agricultural requirements. Results of incidentally performed field trials tend towards more generous standards for the tolerable rate of unevenness than those used by testing departments.

Increase of the application rate of (N) fertilizers or increase of their concentration justifies a tightening of the standards for the coefficients of irregularity. The higher costs of the progressing technical development of distributors has to be weighed against the financial advantages of increased yields.

### *Characteristics of oscillation*

Studies of the characteristics of the oscillation pattern of the distributor device deals with the relation between relevant construction parameters (angular velocity  $\omega$ , or rotary frequency  $N$  of the driving shaft, ratio  $C$  between the length of the crank and the connecting rod, and the length of the sprout  $RB$ ) and the angles of oscillation, angular velocities, and angular accelerations. Additionally, the velocity and acceleration components of the sprout are discussed (chapter 4).

Velocity and accelerations are linearly and quadratically proportional to the rotatory velocity of the driving shaft. The influence of the ratio between crank and connecting rod is somewhat more complicated. For values of  $C \geq 0.408$ , the angular acceleration  $\dot{\phi}$  increases from  $\alpha=0$ . After reaching its maximum value  $\dot{\phi}_{max}$  at  $\alpha_c$ ,  $\dot{\phi}$  decreases to 0 at  $\alpha=\pi/2$ . For  $C < 0.408$ ,  $\dot{\phi}$  continuously decreases during the period  $0 \leq \alpha \leq \pi/2$ .

Increase of the values of  $\omega$ ,  $RB$ , and  $C$  creates possibilities for an increase of the level of energy of the oscillating sprout. As a consequence, occasions arise for an increase of the spreading width. Alteration of these design variables must be attended by adaption of parts of the broadcaster in order to maintain a sufficient rate of symmetry in the characteristic of oscillation. In its present design, deviations from the nominal value of the rotary frequency  $N$  of  $540 \text{ min}^{-1}$  should be avoided. For tractor-mounted distributors, deviations can lead to asymmetry in the oscillation pattern.

### *Particle motion*

Particle motion was studied with the aid of a high speed movie technique (chapter 5). In the characteristic of particle motion two stages can be distinguished:

1. A stage of discontinuous contact between sprout wall and separate particles. This process of impacts can include a period during which friction and restitution properties define particle translation, and a period during which only restitution properties are defining the process of motion. Under these circumstances particle translation is defined also by the momentary value of particle rotation.
2. Successively, a stage of discontinuous contact can be distinguished during which particles slide and/or roll. The values which had to be adjusted to:
  - a. initial particle rotation  $\omega_1$  and
  - b. the imaginary coefficient of friction and restitution  $\mu^*$ , and  $e^*$– in order to obtain agreement between results of motion analyses and simulation experiments – could be explained to a reasonable extent. In addition, experimental research in a later stage supported these values (chapter 7).

It can be concluded that the simulation technique provides possibilities for the calculation of trajectories and velocities of separate particles. Increase of the application rate (which was  $0.5 \text{ kg min}^{-1}$  during the experiments) to more practical values of  $60\text{--}120 \text{ kg min}^{-1}$  increases the mutual affection of the particles. It can be expected that this will lead to an increase of variation in particle trajectories and velocities. The character of the process of sorting-in of the particles must be subject to further research.

### *Design variables*

Shape and section of the sprout influence particle motion (chapter 6). The sprout types investigated show only relatively small differences. A divergent sprout type ( $\gamma = -4^\circ$ ) with a rhombic section increases the variation of the velocities of outlet of the particles and the variation of the horizontal and vertical angles of dispatch. It can be derived from simulation experiments that increase of the length of the sprout  $RB$ , the rotary frequency of the driving shaft  $N$ , and the angle of oscillation  $\phi$  ( $C$ ), lead to an increase of the mean velocity of outlet of the particles  $\bar{V}K$ . An increase of the value  $C$  to 0.600;  $N$  to  $660 \text{ min}^{-1}$  and  $RB$  to 0.75 m results in values for  $\bar{V}K$  of about  $39 \text{ m s}^{-1}$ . Generally speaking, an increase of the value of  $\bar{V}K$  is attended by a lower mean value of the angle of dispatch ( $\bar{\beta}$ ).

Without additional sprout accessories, the basis transverse distribution pattern tends towards a more pronounced two-peak characteristic. The relative frequency of the occurrence of extreme (high) values of  $\beta$  varies. It depends on the type of fertilizer ( $\mu^*$  and  $\epsilon^*$ ) and the design properties of the broadcaster ( $RB$ ,  $C$  and  $N$ ). Therefore, the value of  $\bar{\beta}$  varies. As a result, dimensions and shape of the grooves and the bow at the sprout end must be adjusted to fertilizer and broadcaster properties, since both accessories have to change the two-peak character into the one-peak character of the transverse basic distribution pattern.

It has been proven that filling of the centre of the distribution pattern is realized by directing downwards a part ( $\approx 60\%$ ) of the particles that impact the bow ( $\approx 40\%$ ). In addition, the bow can increase the spreading width, since the value of  $\bar{\beta}$  decreases significantly and the value of  $\bar{V}K$  increases slightly. These effects are supported by that part of the particles which are leaving the sprout with a positive angle of elevation.

### *Fertilizer properties*

Experimental results in chapter 7 show that an increase of the Mass Median Diameter of the particles (and the correlated 1 000 kernel weight) positively affects the quality of the transverse distribution pattern. Sieve fractions  $< 1.6 \text{ mm}$  must be avoided. A relatively high value for bulk density, which was noticed for the high-density prills, supports the favourable effect of the M.M.D. mentioned above. Contrary to what is frequently stated for spinning disc fertilizer broadcasters, it was noticed that increase of the variation of particle diameters positively affects the quality of the compound transverse distribution pattern of the reciprocating sprout broadcaster.

The study which is described in this thesis has contributed to an increase of knowledge of characteristics of particle behaviour in the oscillating distributor device of the reciprocating sprout broadcaster. The characteristics of motion for both the distributor device and the particles are more complicated than for the spinning disc broadcaster. Based on present standards, both types of broadcasters can realize a good quality of the distribution pattern.

Both broadcasters create opportunities for an increase of capacity by means of increase of the bout width. For this purpose an increase of both the velocity of

outlet of the particles and the value of the spreading angle  $\lambda$  is necessary. This requires adaptations in construction of both types of broadcasters. For the reciprocating sprout broadcaster it can be stated that adaptation of the design to a modified oscillation characteristic will be complicated. For the spinning disc type the necessity for the outwards transport of a higher fertilizer mass by the vanes will affect the process of sorting-in and can cause unwanted mutual affection of the particles which prevents a smooth motion. Adaptation of those fertilizer properties which increase the discharge distances of the particles after dispatch will be necessary.

For the reciprocating broadcaster further studies of the processes of particle flow and sorting-in at the sprout entrance and the effects of dimensions and shapes of grooves and bow at the orifice on particle dispatch are recommended.



## ACKNOWLEDGEMENTS

This publication was prepared at the Department of Agricultural Engineering of the Agricultural University Wageningen.

The author is much indebted to the Heads of the Department: Prof. Ir. A. Moens and Prof. Ir. G. J. Quast for their stimulating guidance and technical assistance. The helpfulness and friendship of all members of the Department have been of great profit.

The research work could be performed with the aid of the financial and technical support of:

- Vicon: Agricultural machinery Division Ltd. at Nieuw Venneep;
- IMAG; testing department and photo and film department at Wageningen;
- CTI/TNO; at Apeldoorn;
- Agricultural Office of the Dutch Nitrogen Fertilizer Industries (DSM, MEKOG, NSM) at The Hague.

The discussions with Drs. M. H. Hendriks, Drs. B. R. Damsté, Dr. Ir. F. J. C. Rademacher, Ir. G. Haaker and Prof. Dr. G. R. Veldkamp are kindly acknowledged.

## SAMENVATTING

### *Inleiding*

Sedert het einde van de vijftiger jaren wordt voor de toediening van granulaire kunstmeststoffen gebruik gemaakt van breedwerpige strooiers met een variabele werkbreedte. De werkbreedte bedraagt een veelvoud van de breedte van de doseer- en verdeelorganen. De belangrijkste uitvoeringsvormen zijn de centrifugaal- en pendelstrooiers. Door de verdeelorganen wordt in hoofdzaak translatie-energie op de korrels overgebracht, waardoor deze over een groot oppervlak kunnen worden verspreid.

De constructie van de verdeel- en doseerorganen is eenvoudig: de strooiers zijn relatief goedkoop in aanschaf en onderhoud. Door een combinatie van grote werkbreedte (8-15 m) en hoge rijsnelheid kunnen ook bij hoge meststofgiften grote capaciteiten worden bereikt, met een voor de mens relatief geringe fysieke belasting en relatief lage bewerkingskosten.

### *Doel van het onderzoek*

In tegenstelling tot de centrifugaalstrooiers, is de pendelstrooier slechts op bescheiden schaal onderwerp geweest van onderzoek. Doel van het hier beschreven onderzoek is geweest, het geven van een eerste aanzet voor een meer fundamentele analyse van factoren, die in belangrijke mate bepalend zijn voor het verdeelproces van de pendelstrooier. In dit kader is aandacht besteed aan:

- de kinematische aspecten van het oscillerende verdeelorgaan;
- de analyse van het bewegingsgedrag van afzonderlijke deeltjes in de strooiplaat en bij het verlaten ervan;
- de formulering van theoretische betrekkingen en het opstellen van een model waarmee banen en snelheden van deeltjes kunnen worden beschreven;
- de gevolgen van veranderingen van relevante constructie parameters voor de oscillatiekarakteristiek van het verdeelorgaan en het deeltjesgedrag alsmede het daarmee samenhangende enkelvoudige transversale strooibeeld;
- de betekenis van meststofeigenschappen voor de kwaliteit van het verdeelpatroon, zoals dat wordt aangegeven door de optimale en maximale werkbreedte en de regelmaat van de samengestelde transversale strooibeelden.

### *Ontwikkelingen*

Uit de in hoofdstuk 2 geschetste ontwikkeling blijkt, dat de regelmaat van het transversale verdeelpatroon - waardoor de bewerkingskwaliteit in belangrijke mate wordt bepaald - bij de pendelstrooier aanvankelijk slecht was. Het handhaven van de juiste overlappingsgraad was kritisch, tengevolge van de steil oplopende flanken van het enkelvoudige transversale strooibeeld.

Door vergelijkende beproevingen, experimenteel onderzoek, alsmede voortschrijdende wederzijdse afstemming van meststoffen en strooiers op elkaar, kon een aanzienlijke verbetering worden gerealiseerd. Gesteld kan worden, dat in hun huidige vorm, pendel- en centrifugaalstrooiers voor wat de bewerkingskwaliteit betreft aan elkaar gelijkwaardig zijn. Variatiecoëfficiënten  $< 10\%$  voor de breedte-verdeling zijn bij zorgvuldig gebruik in de praktijk bereikbaar.

Niettemin nopen de nog in het begin van de jaren zeventig onder praktijkomstandigheden geconstateerde opbrengstverliezen van 1–3%, tot voortdurende aandacht voor het aspect van de regelmaat van het transversale verdeelpatroon. Daarbij is een belangrijke foutenbron gelegen in het strooien bij een onjuiste overlappingsgraad. Mede gelet op de periodegebondenheid van de bewerking en de wenselijkheid tot vermindering van rijsporen, blijft de behoefte tot vergroting van de werkbreedte bestaan. Afhankelijk van factoren als rijnsnelheid, gift, en bakinhoud, kunnen bij vergroting van de werkbreedte van 8 tot 10 m resp. van 10 tot 15 m, de zuivere werktijden ( $\text{h ha}^{-1}$ ) dalen met ongeveer 10%, resp. 20%.

### *Verdeelpatronen*

In hoofdstuk 3 is uitgebreid aandacht geschonken aan de bepaling, weergave en interpretatie van de strooiregelmaat. Bij de bepaling van de standaardgrootte van de bemonsteringsoppervlakken dient rekening te worden gehouden met bemestingstechnische, teeltkundige, bodemkundige en klimatologische factoren. De specifieke karakters van de dwarsverdeling van de meststof dienen mede in de beschouwing te worden betrokken.

Gebleken is, dat onregelmatigheden binnen oppervlakken van  $0.5 \times 0.5$  m, in het algemeen niet of nauwelijks leiden tot opbrengstdalingen, bij een breedwerpig toediening van kunstmest. Derhalve kan de in de O.E.S.O. standaard procedure aanbevolen breedte van de opvangbakken van 0.5 m acceptabel worden genoemd.

Veelvuldig gebruikte kengetallen voor de weergave van de strooiregelmaat zijn: de variatiecoëfficiënt  $C.V.$ , de gemiddelde lineaire afwijking ten opzichte van het gemiddelde  $\bar{d}$  en Burema's onregelmatigheidsgetal  $R$ . De tussen genoemde indices bestaande relaties zijn aangegeven.

De vorm van het enkelvoudige transversale strooibeeld is bepalend voor de regelmaat van het samengestelde beeld, de overlappingsgraad en derhalve voor de optimale en de maximale werkbreedte. De optimale werkbreedte wordt gedefinieerd als die werkbreedte  $> 5$  m, waarbij de waarden voor  $C.V.$  en/of  $R$  minimaal zijn. De maximale werkbreedte wordt begrensd door de waarden van  $C.V. < 15\%$  dan wel  $R < 75$ . In dit verband is een aantal normen geformuleerd, waaraan – mede op praktische gronden – het verdeelpatroon dient te voldoen. In paragraaf 3.3 wordt een aantal basisvormen van transversale strooibeelden besproken, die bij een lage overlappingsgraad (b.v.  $O = 0.4$ ), een goede regelmaat van de samengestelde verdeelpatronen mogelijk maken (b.v.  $C.V. < 8\%$ ). Meertoppige asymmetrische enkelvoudige transversale strooibeelden moeten worden afgewezen.

De complexiteit van uitwendige factoren maakt het formuleren van een uniforme norm voor de regelmaat, gebaseerd op landbouwkundige eisen, onmogelijk.

Incidenteel uitgevoerde proeven tenderen naar mildere normen, dan die welke door beproevingsinstellingen worden gehanteerd. Verhoging van (N) meststofgiften c.q. concentraties, rechtvaardigt een verscherping. Tegen het te verwachten geldelijke voordeel van meeroebrenghen dienen de meerkosten van voortschrijdende technische verbeteringen van de strooiwerkhuizen te worden afgewogen.

#### *Oscillatiekarakteristiek*

Het onderzoek van de oscillatiekarakteristiek van het strooiorgaan richt zich op de verbanden tussen relevante constructieparameters (hoeksnelheid  $\omega$ , of het toerental  $N$  van de aandrijvende as, verhouding kruk en drijfstaanglengte  $C$ , lengte van de strooi pijp  $RB$ ) en de oscillatiehoeken, hoeksnelheden en hoekversnellingen, alsmede daarmee samenhangende snelheids- en versnellingscomponenten van het verdeelorgaan (hoofdstuk 4). Snelheid en versnellingen zijn lineair, resp. kwadratisch gerelateerd aan de rotatiesnelheid van de aandrijvende as. De invloed van de verhouding tussen kruk- en drijfstaanglengte  $C$  op de oscillatiekarakteristiek is van gecompliceerder aard. Voor  $C \geq 0.408$  toont de hoekversnelling  $\dot{\phi}$  een stijgend verloop vanaf  $\alpha = 0$ . Na het bereiken van de maximale waarde  $\dot{\phi}_{max}$  voor  $\alpha_c$  daalt  $\dot{\phi}$  tot 0 voor  $\alpha = \pi/2$ . Voor  $C < 0.408$  daalt  $\dot{\phi}$  continu op  $0 \leq \alpha \leq \pi/2$ .

Vergroting van de waarden van  $\omega$ ,  $RB$  en  $C$  biedt mogelijkheden tot verhoging van het energieniveau van de strooi pijp en derhalve eveneens mogelijkheden voor vergroting van de strooibreedte. Verandering van deze constructieparameters dient gepaard te gaan met een aanpassing van onderdelen van de strooier, teneinde in voldoende mate de symmetrie in de oscillatiekarakteristiek te handhaven. Ook bij de huidige constructie dient niet van het nominale toerental van 540 omw/min te worden afgeweken, daar dit bij aanbouwstrooiers kan leiden tot een asymmetrische oscillatiekarakteristiek.

#### *Deeltjesbeweging*

De deeltjesbeweging in de strooi pijp werd bestudeerd met behulp van een high speed filmtchniek (hoofdstuk 5). In de bewegingskarakteristiek kunnen twee fasen worden onderscheiden:

1. Een fase, waarin discontinu contact tussen pijp wand en de afzonderlijke korrels bestaat. Dit proces van botsingen kan een gedeelte omvatten, waarin wrijvings- en elasticiteitseigenschappen bepalend zijn voor de deeltjestranslatie en rotatie en een deel waarin alleen elasticiteitseigenschappen van de materialen bepalend zijn. In dit geval wordt de translatie mede bepaald door de momentane grootte van de deeltjesrotatie.
2. Aansluitend kan een fase van continu contact (glijden/rollen) worden onderscheiden.

De waarden, die – bij overeenstemming tussen analyse- en simulatieresultaten – in het ontwikkelde bewegingsmodel zijn toegevoegd aan de instelvariabelen:

- a. de initiële deeltjesrotatie  $\omega_1$  en
- b. de schijnwrijvings- en restitutiecoëfficiënten  $\mu^*$  resp.  $\varepsilon^*$ , konden op redelijke wijze worden verklaard. Door experimenteel onderzoek kon bovendien de waarde van de grootheden  $\mu^*$  en  $\varepsilon^*$  worden ondersteund (hoofdstuk 7).

Geconcludeerd kan worden dat de simulatietechniek mogelijkheden biedt voor het berekenen van banen en snelheden van afzonderlijke deeltjes. Vergroting van de massastroom van  $0,5 \text{ kg min}^{-1}$  tijdens de experimenten, tot praktischere waarden van  $60\text{--}120 \text{ kg min}^{-1}$  zal leiden tot een grotere mate van wederzijdse beïnvloeding der kunstmestdeeltjes en derhalve tot een grotere variatie van korrelsnelheden en -richtingen. Het karakter van het insorteerproces dient nader te worden onderzocht.

### *Constructieparameters*

De vorm en de doorsnede van de strooi pijp hebben invloed op de deeltjesbeweging (hoofdstuk 6). Bij de in het onderzoek betrokken varianten waren de onderlinge verschillen gering. Een divergerende pijpvorm ( $\gamma = -4^\circ$ ) met een ruitvormige doorsnede verhoogt de variatie in uittredesnelheden en horizontale en verticale uittredehoeken. Vergroting van lengte van de strooi pijp  $RB$ , van het toerental van de aandrijvende as  $N$  en van de oscillatiehoek  $\phi$  ( $C$ ) leidt, blijkens de uitgevoerde simulatie-experimenten tot verhoging van de gemiddelde uittredesnelheid der deeltjes  $\overline{VK}$ . Bij vergroting van  $C$  tot  $0,600$ ;  $N$  tot  $660 \text{ min}^{-1}$ ; en  $RB$  tot  $0,75 \text{ m}$ , werden waarden voor  $\overline{VK}$  van  $\approx 39 \text{ m s}^{-1}$  gerealiseerd. In het algemeen zal een verhoging van  $\overline{VK}$  gepaard gaan met een lagere gemiddelde waarde voor de uittredehoek ( $\beta$ ). Zonder verdere voorzieningen aan de strooi pijp zal het enkelvoudige transversale strooi beeld neigen tot een sterkere mate van tweetoppigheid. De relatieve frequentie waarmee extreem hoge waarden voor  $\beta$  voorkomen varieert en is mede afhankelijk van de meststofsoort ( $\mu^*$  en  $\varepsilon^*$ ) en de strooiereigenschappen ( $RB$ ,  $C$  en  $N$ ). Derhalve kan ook de waarde voor  $\beta$  variëren. Als gevolg hiervan zullen dimensies en vorm van zijlsleuven en beugel aan het einde van de strooi pijp – die het tweetoppig karakter van het transversale strooi beel dienen te modificeren tot een ééntoppig, symmetrisch beeld – aangepast dienen te worden aan meststof en strooiereigenschappen.

Aangetoond werd dat het opvullen van het centrum van het strooi beeld gerealiseerd wordt door het naar beneden richten (afwerpen met negatieve elevatiehoeken), van een gedeelte ( $\approx 60\%$ ) van de korrelstroom, dat met de beugel in aanraking komt ( $\approx 40\%$ ) bij het verlaten van de strooi pijp. Additioneel werkt de beugel vergrotend op de strooi breedte door een significante afname van de uittredehoeken  $\beta$  en een geringe niet significante toename van de afwerpsnelheden  $\overline{VK}$ . Dit effect wordt ondersteund door een deel der korrels dat onder een positieve elevatiehoek de strooi pijp verlaat.

### *Meststofeigenschappen*

Van het complex van meststofeigenschappen, zoals dat in hoofdstuk 7 wordt behandeld, beïnvloedt een toename van de grootte van de mediane korreldiameter en het daarmee gecorreleerde duizendkorrelgewicht, de kwaliteit van het transversale strooi beeld in gunstige zin. Zee fracties  $< 1,6 \text{ mm}$  dienen te worden vermeden. Een relatief hoge waarde voor de bulkdichtheid – zoals die werd aangetroffen bij high-density prills – ondersteunt het genoemde gunstige effect van de mediane korreldiameter. In tegenstelling tot wat veelal wordt beschreven bij centrifugaal-

strooiers, blijkt een vergroting van de spreiding in korreldiameters een positief effect te hebben op de regelmaat van het samengestelde transversale strooibeeld van de pendelstrooier.

Het hier beschreven onderzoek heeft bijgedragen tot vergroting van de inzichten van het deeltjesgedrag in het oscillerend verdeelorgaan van de pendelstrooier. De bewegingskarakteristiek van het verdeelorgaan en de deeltjes is gecompliceerder van aard dan bij de centrifugaalstrooier. Gerekend volgens de huidige normen kan met beide typen strooiers een goede kwaliteit van het verdeelpatroon worden gerealiseerd.

De twee strooiers bieden mogelijkheden voor vergroting van de capaciteit, door vergroting van de werkbreedte. Daartoe is vergroting van de uittredesnelheid der deeltjes en de waarde van de strooihoek  $\lambda$  noodzakelijk, hetgeen voor beide typen strooiers constructieve aanpassingen vereist. Bij de pendelstrooier zal de aanpassing van de constructie aan de veranderende oscillatiekarakteristiek van het verdeelorgaan gecompliceerd zijn. Bij de centrifugaalstrooier dient rekening te worden gehouden met de noodzakelijke hogere massastroom die door de schoepen moet worden verwerkt en de gevolgen hiervan voor het proces van insortering en mogelijke stuwwerking. Aanpassing van die kunstmesteigenschappen die de werpafstand vergroten is noodzakelijk.

Voor de pendelstrooier wordt verdere studie van het proces van instroming en insortering van de korrels in de strooi pijp en de effecten van de dimensies en vorm van de uitstroomopeningen met inbegrip van de verschillende beugeltypen op het proces van afwerpen van de korrels aanbevolen.

## REFERENCES

- ADAM, O. (1960) Untersuchungen über die Vorgänge in feststoffbeladenen Gasströmen. Thesis. Köln.
- ANONYMUS (1928) Gedenkboek Veenkoloniale Boerenbond 1903-1928. Veendam: 24.
- ANONYMUS (1958) Vicon Spandicar. *Landbouwmechanisatie* 9: 556.
- ANONYMUS (1967) Beproeving centrifugaal en pendelstrooiers. I.L.R. publ. 113. Wageningen.
- ANONYMUS (1972) Fertilizer spreaders: official reports. Farming in S.A.: 33-41.
- ANONYMUS (1974) Merkenonderzoek kunstmeststrooiers. I.L.R. publikatie no. 184. Wageningen.
- ANONYMUS (1976) Intern verslag Werkgroep Korreldiameter. IMAG. Wageningen (unpublished).
- BAECKE, A. (1976) Personal communication.
- BAKKER ARKEMA, P. W. (1957) in: RIEMER, G. *Handboek voor landbouwwerktuigen en trekkers*. Zwolle: 335-370.
- BERG, F. L. M. T. VAN DEN (1970) De verwerking van kunstmest bij de Rijksdienst voor de IJsselmeerpolders. Intern rapport no. 224. Rijksdienst voor de IJsselmeerpolders. Lelystad, The Netherlands.
- BERRY, P. E. (1970) Influence of the form of the basic pattern on total overlapped patterns in the case of one-way overlapping systems of fertilizer distributions. N.I.A.E. Note No. 44/0901. Silsoe, England.
- BOSMA, J. (1976) Verslag simulatie-opdracht pendelstrooier. Vakgroep Natuur- en Weerkunde, Landbouwhogeschool Wageningen (unpublished).
- BRINSFIELD, R. B. and J. W. HUMMEL (1975) Simulation of a new centrifugal distributor design. *Transactions of the ASAE* 18: 213-216/220.
- BROWN, M. L. et al. (1968) *J. Agr. Food Chem.* 16: 373-377.
- BRUBAKER, J. E. and J. POS (1965) Determining static coefficients of friction of grains on a structural surface. *Transactions of the ASAE* 8: 53-55.
- BRUTSCHKE, F. (1900) *Jahrbuch D.L.G.* 15. in: FRANZ, G. *Die Geschichte der Landtechnik im XX Jahrhundert*. Frankfurt/Main 1969: 164-177.
- BRÜBACH, M. (1969) Ein Versuchstand zur Ermittlung der Verteilungsgüte von Verteilgeräten und Probleme der Auswertung. *Grundlagen der Landtechnik* 19: 163-165.
- BRÜBACH, M. (1970) Der Einfluss von Arbeitsbreite und Abwurfhöhe auf das Streubild des Schleuderstreuers. *Landtechnische Forschung* 18: 5-8.
- BRÜBACH, M. (1973) Der Einfluss der Düngerqualitätsigenschaften auf die Verteilung. *Landtechnik* 9, (Juni).
- BUREMA, H. J. (1968) Beoordeling van de strooiermaat van centrifugaal kunstmeststrooiers. Rapport 110 I.L.R.. Wageningen.
- BUREMA, H. J. (1970) Evenness of spread of spinner broadcasters. Research Report 1. Institute of Agricultural Engng. and Rationalization. Wageningen.
- BURG, P. F. J. VAN (1968) Nitrogen fertilizing of grassland in spring. *Neth. Nitr. Techn. Bull.* 6: 28-29.
- CASELLA, A. (1956/57) Prove di laboratorio di una spandiconcime a spaglio con un tubo di lancio oscillante. *Atti C.N.M.A.* 1956-'57. Vol. II: 185-192.
- CBS (1965, 1970, 1975) *Landbouwstelling*. Voorburg.
- CLEINE, G. and T. A. J. YZERMAN (1976) *Kunstmestpendelstrooier, simulatie-opdracht*. Afdeling Electrotechniek, TH Twente (unpublished).
- COOLMAN, F. and J. M. G. VAN DER POEL (1964) Van gareel tot aftakas. I.L.R. publikatie no. 78. Wageningen.
- DANIEL, C. and F. S. WOOD (1971) *Fitting Equations to Data*. Wiley Intersc. New York/London.
- DAVIES, G. R. (1972) The spinning disc distributor, part 1. Project Report P/8 University of Canterbury, New Zealand.
- DAVIES, G. R. (1973) The spinning disc distributor, part 2. Project Report P/9 University of Canterbury, New Zealand.
- DAVIS, P. F. (1971) The best basic distribution pattern for a spray nozzle or fertilizer distributor. *J. agric. Engng. Res.* 16: 316-323.

- DELITZ, M. (1969) Berechnung von Schleuderscheiben. *Deutsche Agrartechnik* **19**: 239-241.
- DIEST, A. VAN (1971) Opbrengstwetten. Laboratorium voor Landbouwscheikunde, Landbouwhogeschool Wageningen.
- DIXHOORN, J. J. VAN (1972) Netwerkgrafen en bondgrafen. Afdeling Electrotechniek. 1241.0937. TH Twente.
- DOBLER, K. and J. FLATOW (1968) Berechnung der Wurfvorgänge beim Schleuderdüngerstreuer. *Grundlagen der Landtechnik* **18**: 129-134.
- DOBLER, K. and J. FLATOW (1969) Konstruktive Ausbildung der Streuorgane von Schleuderdüngerstreuern zur Erzielung eines optimalen Streubildes. *Grundlagen der Landtechnik* **19**: 55-60.
- ELLEN, H. (1973) Landbouwtechnische aspecten van de toepassing van gegranuleerde bestrijdingsmiddelen. Doctoraalscriptie Landbouwwerktuigkunde. Vakgroep Landbouwtechniek, Landbouwhogeschool Wageningen.
- EYTH, M. (1906) Lebendige Kräfte (Sieben Vorträge auf dem Gebiete der Technik). In: FRANZ, G. *Geschichte der Landtechnik im XX Jahrhundert*. Frankfurt/Main 1969: 177.
- FISCHER, G. (1910) Die Entwicklung des Landwirtschaftlichen Maschinenwesens in Deutschland. Berlin.
- FOEKEN, D. and G. KIERS (1977) *Merkengids*. Instituut voor Mechanisatie, Arbeid en Gebouwen. Wageningen.
- FUSSEL, G. E. (1952) *The farmers tools*. London.
- GASPARETTO, E. (1969) La produzione di alcune colture in funzione della regolarità traversale di distribuzione degli spandiconcime centrifughi. *Revisita Il Riso Anno XVIII*. N 2/3. Milano.
- GESCHIERE, J. (1976) Personal communication.
- GLOVER, J. W. and J. V. BAIRD (1973) Performance of spinner type fertilizer spreaders. *Transactions of the ASAE* **16**: 48-51.
- GÖHLICH, H. and E. KESTEN (1972) Einflüsse auf das Verhalten von Haufwerkströmen auf Schleuderscheiben von Mineräldüngerstreuern 1/2. *Grundl. der Landtechnik* **22**: 11-15/43-46.
- GREEN, T. L. (1968) Even spread with solid materials. *Farm Mechanization and Buildings* **20**: 51-52.
- HANUSCH, L. (1969) Untersuchungen über die zweckmäßigste Gestaltung vollmechanisierter Transport- und Ausbringverfahren für feste Mineräldüngemittel. Thesis. Meissen.
- HARDESTY, J. O. and W. H. ROSS (1938) *Ind. Eng. Chem.* **30**: 668-672.
- HERPERD, R. Q. and J. H. PASCAL (1959) The transverse distribution of fertilizer by conventional types of distributors. *J. agric. Engng. Res.* **4**: 95-107.
- HEYDE, H. (1957) Zur Bewertung der Streugenauigkeit von Düngerstreuern. *Landtechnische Forschung* **7**: 53-55.
- HEYDE, H. (1963) *Landmaschinenlehre*. Band I. Berlin: 402-412.
- HEYMANN, W. et al. (1971) Arbeitsqualität und Streuleistung von Düngerstreumaschinen in Abhängigkeit von der Düngerqualität. *Deutsche Agrartechnik* **21**: 187-191.
- HOEDJES, P. J. (1978) Empirisch onderzoek naar het botsgedrag van kunstmestkorrels met behulp van fotografische gegevens. Doctoraalscriptie Werktuigkunde. Vakgroep Landbouwtechniek, Landbouwhogeschool Wageningen.
- HOLLMANN, W. (1962) Untersuchungen über die Düngerverteilung von Schleuderstreuern. Thesis. T. U. Berlin.
- HOLLMANN, W. and A. MATHES (1962) Untersuchungen an Schleuderdüngerstreuern. *Landtechnische Forschung* **12**: 179-186.
- HOLMES, M. R. J. (1968) Fertilizer application: The degree of accuracy required. *Farm Mechanization and Buildings* **20**: 51-52.
- HOOGLAND, E. J. N. (1955) Strooi-beelden bij kunstmeststrooiers. *Landbouwmechanisatie* **6**: 498-501.
- HUISMAN, W. (1977) Moisture content, coefficient of friction and modulus of elasticity in relation to walker losses in a combine harvester. *ASAE Publ.* 1-78: 25-29.
- INNS, F. M. and A. R. REECE (1962) The theory of the centrifugal distributor II. *J. agric. Engng. Res.* **7**: 345-353.
- ISENSEE, E. (1973) Beurteilung von Arbeitsverfahren der Mineräldüngung. *Die Landarbeit* **24**: 25-29.
- JAGTENBERG, W. D. (1966) *Stikstof* **5**: 216-222.
- JIE-A-LOOI, F. J. (1968) Methoden en apparaten voor de bepaling van enkele fysische eigenschappen



- van landbouwprodukten. Scriptie Landbouwwerktuigkunde. Vakgroep Landbouwtechniek, Landbouwhogeschool Wageningen.
- JÜRGENS, G. (1971) Vergleichende Untersuchungen über die Wirkung von wasserfreien Ammoniak, Stickstoff-Lösungen und Stickstoff-Salzdüngemitteln. KTBL Berichte über Landtechnik 142.
- KANAFOJSKI, C. (1972) in: BERNACKI H. et al. Agricultural Machines, Theory and Construction. Vol. I. Warsaw, Poland: 571-618.
- KLAPP, E. (1965) Theorie der Verteilung von Feststoffteilchen mittels Schleuderscheiben. Forsch. Ing. Wesen 31: 83-86.
- KOUWENHOVEN, J. K. and R. TERPSTRA (1975) Effect of sphere diameter on the mechanical behaviour of glass spheres. J. agric. Engng. Res. 20: 363.
- KRUTIKOW, N. P. et al. (1955) Theorie, Berechnung und Konstruktion der Landmaschinen. Band I. Berlin: 607.
- LEEK, J. H. VAN DER (1977) Granulieren. Procestechniek 33: 137-141.
- LORENZ, F. (1954) Handarbeit oder Maschinenverwendung. Landtechnik 9: 406-408.
- LORENZ, F. (1955) Varianzanalyse, eine Methode zur Messung der Streugenauigkeit von Düngerstreumaschinen. Landtechnische Forschung 5: 31-32.
- LORENZ, F. (1957) Zwei Bewertungsmethoden für die Streugenauigkeit von Düngerstreuern. Landtechnische Forschung 7: 111-112.
- LORENZ, F. and A. MATHES (1955) Die Streufähigkeit von mineralischen Düngemitteln. Landtechnische Forschung 5: 53-60.
- LOON, J. H. VAN (1959) Arbeidsfysiologie in en rond de boerderij. Landbouwk. Tijdschrift 71: 459-466.
- MARKS, K. (1959) Zur Problematik der Schleuderdüngerstreuer. Landtechnische Forschung 9: 21-34.
- MARKS, K. (1963) KTBL Arbeitsblatt für Landtechnik Nr. F-Du 101. Frankfurt.
- MASCHE, H. (1955) Die Varianzanalyse, eine Methode zur Messung der Streugenauigkeit von Düngerstreumaschinen. Landtechnische Forschung 5: 125-126.
- MATHES, A. (1960) Breitstreuer oder Schleudestreuer. Landtechnik 15: 574-576.
- MATHES, A. (1969) in: FRANZ, G. Die Geschichte der Landtechnik im XX Jahrhundert. Frankfurt/Main: 164-177.
- MATHES, A. and W. PREISBERG (1967) Das Auswerten landtechnischer Versuchsreihen mit programmgesteuerten Rechenanlagen. Grundlagen der Landtechnik 17: 155-159.
- MENNEL, R. M. and A. R. REECE (1963) The theory of the centrifugal distributor III. J. agric. Engng. Res. 8: 78-84.
- MESKENS, L. (1975) De evolutie van de produktie, de buitenlandse handel en het verbruik van kunstmeststoffen. Landbouwtijdschrift 28: 1023-1053.
- MEULEMAN, J. (1976) De beweging van de oscillerende strooipijp en het gedrag van kunstmestkorrels hierin I, II. Doctoraalscriptie Landbouwwerktuigkunde. Vakgroep Landbouwtechniek, Landbouwhogeschool Wageningen.
- MITCHELL, D. (1974) Uneven application leads to £6./acre grain losses. Power Farming (May).
- MITCHELL, D. (1975) Accuracy counts. Power Farming (March).
- MOHSENIN, N. N. (1968) Physical properties of plant and animal materials. Part II of Vol. I. Dept. Agric. Engng. Pennsylvania State University: 441-445 and 618-647.
- N.I.A.E. (1971) National Institute of Agricultural Engineering. Report R 71/7560. Silsoe, Bedford.
- NORBY, A. and J. HAMAN (1965) The effect of the liquid cone form on spray distribution of hollow cone nozzles. J. agric. Engng. Res. 10: 322-327.
- O.E.C.D. (1967) Standard Testing Procedure for Fertiliser Distributors. Paris.
- OEHRING, J. (1963) Wie genau Düngerstreuen? Landtechnik 18: 76-80.
- OEHRING, J. (1964) Zur Überlappung bei Schleuderdüngerstreuern. Landtechnische Forschung 14: 30-32.
- OOSTENDORP, D. (1964) Stikstofbemesting en grasgroei in het voorjaar. Landbouwkundig Tijdschrift 76: 101-110.
- PAAUW, F. VAN DER (1940) Proeven over de betekenis van een gelijkmatige verdeling van den kunstmest. Versl. Landbk. Onderz. 46: 409-438.
- PATTERSON, D. E. and A. R. REECE (1962) The theory of the centrifugal distributor I. J. agric. Engng. Res. 7: 232-240.

- PAPATHEODOSSIOU, T. (1970) Optimiering der Korn- und Granulatverteilung beim Breitstreuen insbesondere von Herbiziden. KTBL Berichte über Landtechnik 138. Wolfratshausen.
- PEELEN, H. T. J. (1976) Het effect van een beugel en perforaties aan het uiteinde van de strooi pijp van een pendelstrooier op het strooibeeld. Doctoraalscriptie Landbouwwerktuigkunde. Vakgroep Landbouwtechniek, Landbouwhogeschool Wageningen.
- PEETEN, J. M. G. (1975) De invloed van de vorm en de stand van de pijpwand op de uittredehoek en snelheid van de korrels bij het verlaten van het strooiorgaan van de pendelstrooier. Doctoraalscriptie Landbouwwerktuigkunde. Vakgroep Landbouwtechniek, Landbouwhogeschool Wageningen.
- PELLIZZI, G. (1958) Cinematica e sperimentazione dettagliata di spandiconcime ad azione centrifuga. Estratto dal Fasc V e VI / 1957 delle Memorie ed Atti del Centro di Studi per l'Ingegneria Agraria. Milano.
- PESCHIER, D. N. (1974) Personal communication.
- POEL, J. M. G. VAN DER and G. REINDERS (1962) Landbouwtechniek en rationalisatie in het midden van de 19e eeuw. Warffum.
- POEL, J. M. G. VAN DER (1967) Honderd jaar landbouwmechanisatie in Nederland. Wageningen.
- PRUMMEL, J. et al. (1959) Onderzoek naar de strooi regelmaat van kunstmeststrooiers. Landbouwvoorlichting 16: 134-144.
- PRUMMEL, J. and P. DATEMA (1962) Strooi regelmaat van kunstmeststrooiers en de betekenis daarvan voor de opbrengst. Landbouwmechanisatie 13: 742-753.
- QUAST, G. J. (1971) Mechanismen. Vakgroep Landbouwtechniek, Landbouwhogeschool Wageningen: J 22-J 25.
- REED, W. B. and E. WACKER (1970) Determing distribution patterns of dry-fertilizer applicators. Transactions of the ASAE 13: 85-89.
- REILING, J. (1976) De invloed van enige fysische eigenschappen van kunstmest op de kwaliteit van het strooibeeld van de Vicon pendelstrooier. Doctoraalscriptie Landbouwwerktuigkunde. Vakgroep Landbouwtechniek, Landbouwhogeschool Wageningen.
- REINDERS, G. (1892) Handboek voor de Nederlandse landbouw en veeteelt. Groningen: 396-397.
- RINSEMA, W. T. (1959) Bemesting en meststoffen. Zwolle.
- ROMANELLO, G. (1969) Studio cinematico del distributore di uno spandiconcime a tubo oscillante. Machine e Motori Agricoli 27: 63-69.
- ROOS, V. S. (1978). De beweging van een kunstmestkorrel in de strooi pijp van een pendelstrooier; ontwikkeling van een model. Doctoraalscriptie Landbouwwerktuigkunde. Vakgroep Landbouwtechniek, Landbouwhogeschool Wageningen.
- RÜHLE, K. (1975) Die Verteilgenauigkeit pneumatischer Düngerstreuer. KTBL Schrift 198. Darmstadt/Kranichstein.
- SANTEN, G. W. VAN (1950) Inleiding tot het gebied der mechanische trillingen. Amsterdam.
- SCHAAFSTAL, H. A. and H. M. DE LINT (1973) Arbeidsbehoefte, in: Verlichting en besparing van arbeid bij de bemesting. Min. van Landbouw en Visserij en Ned. Kunstmest Federatie: 25-41.
- SCHILLING, E. (1958) Landmaschinen. Band 3. Köln: 73-101.
- SELKE, W. (1965) Die Düngung. Berlin.
- SHARMA, R. K. and W. K. BILANSKI (1971) Coefficients of restitution of grains. Transactions of the ASAE 14: 216-218.
- SIMONS, D. and F. TRAPHAGEN (1961) in: DENCKER C. Handbuch der Landtechnik. Hamburg: 405-422.
- SMEETS, J. A. H. (1964) Het gedrag van kunstmestkorrels op de werpschijf van een centrifugaalstrooier. Bepaling van strooibeelden. Scriptie 156. Vakgroep Landbouwtechniek, Landbouwhogeschool Wageningen.
- SPEELMAN, L. (1972) Zaai- en verzorgingstechniek. Vakgroep Landbouwtechniek, Landbouwhogeschool Wageningen.
- SPIJKERMAN, A. J. C. (1956) Smitfield Show 1955. Landbouwmechanisatie 6: 12-14.
- SPOELSTRA, L. H. (1973) Arbeidsverlichting, in: Verlichting en besparing van arbeid bij de bemesting. Min. van Landbouw en Visserij en Ned. Kunstmestfederatie: 42-45.
- TAMBOER, J. (1976) Personal communication.
- UKF (1974) Intern Rapport 12-74.4. IJmuiden.

- VERHOFSTADT, J. J. G. G. (1978) Invloed van enige konstruktieparameters en korreleigenschappen op korrelsnelheid en -richting bij de pendelstroofier. Doctoraalscriptie Landbouwwerktuigkunde. Vakgroep Landbouwtechniek, Landbouwhogeschool Wageningen.
- VOLLHEIM, R. (1971) Pneumatischer Transport. Leipzig: 30-37.
- VOLLMER, F. J. (1967) Düngen mit flüssigem Stickstoff. Ingenieurschule für Landbau. Brühl/Köln.
- WEBER, E. (1957) Grundriss der biologischen Statistik. Jena.
- WEST, W. J. et al. (1940) The effects of an unevenly distributed top-dressing on the yield of wheat. *Agric. Engng. Record*. (June): 23.
- WIDT, R. A. DE (1955) Landbouwmechanisatie. Economische en sociale aspecten van de mechanisatie van de landbouw in de Verenigde Staten van Noord-Amerika en Nederland. Zwolle.
- WIRTHS, W. (1956) Die Körperliche Belastung beim Düngerstreuen. *Internat. Z. Physiol. einsch. Arbeitsphysiol.* **16**: 237-249.
- ZANDER, J. (1972) Ergonomics in machine design. *Communications Agric. Univ. Wageningen, The Netherlands*. 72.6 (1972).
- ZSCHUPPE, H. (1967) Die Bewertung von Arbeitsqualität von Düngerstreuern. *Deutsche Agrartechnik* **17**: 61-64.
- ZSCHUPPE, H. (1968) Untersuchungen über den Einfluss der Streugenauigkeit von Düngerstreuern auf den Pflanzenertrag. *Arch. Landtechnik* **7**: 111-120.

## APPENDIX I

Appendix I. 1.1.1./1.1.5

BROADCASTER						
sprout length ( $RB$ ) = 0.63 m			sprout angle ( $\gamma$ ) = $+1^\circ$			
ratio crank/connecting rod ( $C$ ) = 0.475			rotary frequency ( $N$ ) = 540 min <sup>-1</sup>			
FERTILIZER						
$\mu^* = 0.2, \varepsilon^* = 0.4, \omega_1 = -1000 \text{ rad s}^{-1}$			$\mu^* = 0.1, \varepsilon^* = 0.6, \omega_1 = -1000 \text{ rad s}^{-1}$			
$R_0$ (m)	$VK$ (m s <sup>-1</sup> )	$\beta$ (deg)	$t$ (s)	$VK$ (m s <sup>-1</sup> )	$\beta$ (deg)	$t$ (s)
.10	8.8	80.2	0.122	10.2	89.4	0.117
.11	13.4	24.3	0.115	18.7	21.6	0.103
.12	14.7	22.5	0.111	19.0	23.2	0.101
.13	15.5	22.7	0.108	19.2	24.6	0.098
.14	17.6	26.6	0.103	19.4	26.0	0.097
.15	17.9	23.8	0.102	19.6	27.4	0.094
.16	18.5	22.2	0.098	19.7	28.8	0.093
.17	19.2	21.0	0.095	19.8	30.0	0.090
.18	19.9	20.1	0.093	23.5	22.9	0.089
.19	20.5	19.4	0.090	19.8	32.4	0.087
.20	21.4	21.9	0.087	19.9	33.6	0.084
.21	21.6	25.8	0.084	20.0	34.7	0.082
.22	21.1	31.1	0.081	20.0	35.8	0.079
.23	20.0	37.6	0.078	20.0	36.8	0.075
.24	14.2	43.7	0.075	11.2	65.4	0.074
Mean values	17.6	19.5	0.096	18.7	35.5	0.091

Appendix I. 1.1.2./1.1.6

BROADCASTER						
sprout length ( $RB$ ) = 0.67 m			sprout angle ( $\gamma$ ) = $+1^\circ$			
ratio crank/connecting rod ( $C$ ) = 0.475			rotary frequency ( $N$ ) = 540 min <sup>-1</sup>			
FERTILIZER						
$\mu^* = 0.2, \varepsilon^* = 0.4, \omega_1 = -1000 \text{ rad s}^{-1}$			$\mu^* = 0.1, \varepsilon^* = 0.6, \omega_1 = -1000 \text{ rad s}^{-1}$			
$R_0$ (m)	$VK$ (m s <sup>-1</sup> )	$\beta$ (deg)	$t$ (s)	$VK$ (m s <sup>-1</sup> )	$\beta$ (deg)	$t$ (s)
.10	15.5	46.1	0.128	10.2	89.4	0.122
.11	10.1	74.4	0.122	18.7	21.6	0.107
.12	9.8	85.5	0.116	19.0	23.2	0.103
.13	15.5	22.7	0.111	19.2	24.6	0.101
.14	17.6	26.6	0.106	19.4	26.0	0.100
.15	17.9	23.8	0.104	19.6	27.4	0.097
.16	18.5	22.2	0.102	22.0	22.3	0.095
.17	19.2	21.0	0.099	22.9	22.3	0.094
.18	19.9	20.1	0.096	23.5	22.9	0.093
.19	20.5	19.2	0.094	24.0	23.8	0.089
.20	21.1	18.6	0.092	24.4	24.8	0.088
.21	22.5	21.1	0.089	24.8	25.7	0.085
.22	23.1	24.2	0.086	20.0	35.8	0.083
.23	22.8	27.9	0.083	20.0	36.8	0.080
.24	21.9	31.6	0.080	20.0	37.8	0.078
Mean values	18.4	32.3	0.101	20.5	31.0	0.094

Appendix I. 1.1.3./1.1.7

BROADCASTER						
sprout length ( <i>RB</i> ) = 0.71 m			sprout angle ( $\gamma$ ) = +1°			
ratio crank/connecting rod ( <i>C</i> ) = 0.475			rotary frequency ( <i>N</i> ) = 540 min <sup>-1</sup>			
I			II			
$\mu^* = 0.2, \varepsilon^* = 0.4, \omega_1 = -1000 \text{ rad s}^{-1}$			$\mu^* = 0.1, \varepsilon^* = 0.6, \omega_1 = -1000 \text{ rad s}^{-1}$			
<i>R<sub>o</sub></i> (m)	FERTILIZER			FERTILIZER		
	<i>VK</i> (m s <sup>-1</sup> )	$\beta$ (deg)	<i>t</i> (s)	<i>VK</i> (m s <sup>-1</sup> )	$\beta$ (deg)	<i>t</i> (s)
.10	21.6	38.2	0.133	16.7	52.3	0.128
.11	14.6	51.0	0.127	18.7	21.6	0.108
.12	9.8	85.5	0.120	19.0	23.2	0.107
.13	10.2	87.8	0.116	19.2	24.6	0.105
.14	17.6	26.6	0.110	19.4	26.0	0.102
.15	17.9	23.8	0.107	19.6	27.4	0.101
.16	18.5	22.2	0.105	22.0	22.3	0.099
.17	19.2	21.0	0.103	22.9	22.3	0.096
.18	19.9	20.1	0.101	23.5	22.9	0.094
.19	20.5	19.2	0.097	24.0	23.8	0.093
.20	21.1	18.6	0.095	24.4	24.8	0.091
.21	22.4	20.3	0.093	24.8	25.7	0.089
.22	23.7	21.4	0.090	25.0	26.7	0.088
.23	24.5	23.7	0.087	25.2	27.6	0.085
.24	24.6	26.1	0.085	25.4	28.5	0.082
Mean values	19.1	33.7	0.105	22.0	26.6	0.098

Appendix I. 1.1.4./1.1.8

BROADCASTER						
sprout length ( <i>RB</i> ) = 0.75 m			sprout angle ( $\gamma$ ) = +1°			
ratio crank/connecting rod ( <i>C</i> ) = 0.475			rotary frequency ( <i>N</i> ) = 540 min <sup>-1</sup>			
I			II			
$\mu^* = 0.2, \varepsilon^* = 0.4, \omega_1 = -1000 \text{ rad s}^{-1}$			$\mu^* = 0.1, \varepsilon^* = 0.6, \omega_1 = -1000 \text{ rad s}^{-1}$			
<i>R<sub>o</sub></i> (m)	FERTILIZER			FERTILIZER		
	<i>VK</i> (m s <sup>-1</sup> )	$\beta$ (deg)	<i>t</i> (s)	<i>VK</i> (m s <sup>-1</sup> )	$\beta$ (deg)	<i>t</i> (s)
.10	25.4	31.6	0.137	22.0	40.5	0.132
.11	21.4	41.0	0.131	12.6	67.9	0.112
.12	15.4	50.9	0.126	19.0	23.2	0.108
.13	10.2	87.8	0.119	19.2	24.6	0.107
.14	17.6	26.6	0.112	19.4	26.0	0.105
.15	17.9	23.8	0.111	19.6	27.4	0.103
.16	18.5	22.2	0.109	22.0	22.3	0.101
.17	19.2	21.0	0.105	22.9	22.3	0.100
.18	19.9	20.1	0.103	23.5	22.9	0.098
.19	20.5	19.2	0.101	24.0	23.8	0.096
.20	21.1	18.6	0.099	24.4	24.8	0.093
.21	22.4	20.3	0.096	24.8	25.7	0.092
.22	23.6	21.0	0.093	25.0	26.7	0.089
.23	24.8	21.5	0.090	25.2	27.6	0.088
.24	25.7	22.8	0.088	25.4	28.5	0.086
Mean values	20.2	29.9	0.108	21.9	28.9	0.101

## Appendix I. 1.2.1./1.2.5

BROADCASTER						
sprout length ( <i>RB</i> ) = 0.63 m			sprout angle ( $\gamma$ ) = 0°			
ratio crank/connecting rod ( <i>C</i> ) = 0.475			rotary frequency ( <i>N</i> ) = 540 min <sup>-1</sup>			
I			II			
$\mu^* = 0.2, \varepsilon^* = 0.4, \omega_1 = -1000 \text{ rad s}^{-1}$			$\mu^* = 0.1, \varepsilon^* = 0.6, \omega_1 = -1000 \text{ rad s}^{-1}$			
<i>R<sub>o</sub></i> (m)	<i>VK</i> (m s <sup>-1</sup> )	$\beta$ (deg)	<i>t</i> (s)	<i>VK</i> (m s <sup>-1</sup> )	$\beta$ (deg)	<i>t</i> (s)
.10	9.4	77.7	0.121	13.7	23.4	0.116
.11	14.0	23.1	0.114	19.2	20.7	0.102
.12	14.5	25.1	0.110	19.8	21.8	0.100
.13	15.9	23.0	0.107	20.3	23.0	0.099
.14	16.6	24.1	0.104	20.7	24.3	0.095
.15	17.5	23.9	0.101	21.1	24.5	0.094
.16	19.4	26.3	0.097	21.3	26.7	0.091
.17	19.9	24.2	0.094	21.6	27.9	0.090
.18	20.6	22.9	0.092	21.7	29.0	0.088
.19	21.5	23.7	0.089	22.0	30.0	0.085
.20	22.1	26.6	0.086	22.2	31.1	0.083
.21	22.2	31.3	0.083	22.4	32.0	0.080
.22	20.0	31.1	0.081	12.9	57.4	0.078
.23	16.5	39.6	0.078	12.9	58.7	0.076
.24	16.6	40.5	0.074	12.9	60.0	0.072
Mean values	17.8	30.9	0.095	19.0	32.8	0.090

## Appendix I. 1.2.2./1.2.6

BROADCASTER						
sprout length ( <i>RB</i> ) = 0.67 m			sprout angle ( $\gamma$ ) = 0°			
ratio crank/connecting rod ( <i>C</i> ) = 0.475			rotary frequency ( <i>N</i> ) = 540 min <sup>-1</sup>			
I			II			
$\mu^* = 0.2, \varepsilon^* = 0.4, \omega_1 = -1000 \text{ rad s}^{-1}$			$\mu^* = 0.1, \varepsilon^* = 0.6, \omega_1 = -1000 \text{ rad s}^{-1}$			
<i>R<sub>o</sub></i> (m)	<i>VK</i> (m s <sup>-1</sup> )	$\beta$ (deg)	<i>t</i> (s)	<i>VK</i> (m s <sup>-1</sup> )	$\beta$ (deg)	<i>t</i> (s)
.10	13.8	52.3	0.127	13.6	67.8	0.120
.11	10.5	75.1	0.118	19.2	20.7	0.106
.12	14.5	25.1	0.114	19.8	21.8	0.104
.13	15.9	23.0	0.110	20.3	23.0	0.102
.14	16.6	24.1	0.108	20.7	24.3	0.099
.15	17.5	23.9	0.104	21.1	25.5	0.098
.16	19.4	26.3	0.100	21.3	26.7	0.095
.17	19.9	24.2	0.098	21.6	27.9	0.092
.18	20.6	22.9	0.095	21.7	29.0	0.091
.19	21.2	22.0	0.093	22.0	30.0	0.089
.20	21.9	21.0	0.090	22.2	31.1	0.086
.21	22.9	23.5	0.088	22.4	32.0	0.084
.22	23.3	26.8	0.085	22.5	33.0	0.083
.23	23.0	32.2	0.082	22.7	33.9	0.079
.24	20.3	33.1	0.080	22.8	34.8	0.077
Mean values	18.7	30.4	0.099	20.9	30.8	0.094

## Appendix I. 1.2.3./1.2.7

BROADCASTER						
sprout length ( $RB$ ) = 0.71 m			sprout angle ( $\gamma$ ) = $0^\circ$			
ratio crank/connecting rod ( $C$ ) = 0.475			rotary frequency ( $N$ ) = 540 min $^{-1}$			
I			FERTILIZER		II	
$\mu^* = 0.2, \varepsilon^* = 0.4, \omega_1 = -1000 \text{ rad s}^{-1}$					$\mu^* = 0.1, \varepsilon^* = 0.5, \omega_1 = -1000 \text{ rad s}^{-1}$	
$R_0$ (m)	$VK$ (m s $^{-1}$ )	$\beta$ (deg)	$t$ (s)	$VK$ (m s $^{-1}$ )	$\beta$ (deg)	$t$ (s)
.10	20.5	41.5	0.131	13.6	67.8	0.126
.11	10.5	75.1	0.123	19.2	20.7	0.108
.12	11.9	69.9	0.117	19.8	21.8	0.106
.13	15.9	23.0	0.114	20.3	23.0	0.104
.14	16.6	24.1	0.111	20.7	24.3	0.102
.15	17.5	23.9	0.108	21.1	25.5	0.099
.16	19.4	26.3	0.104	21.3	26.7	0.098
.17	19.9	24.2	0.102	21.6	27.9	0.096
.18	20.6	22.9	0.098	21.7	29.0	0.095
.19	21.2	22.0	0.096	22.0	30.0	0.092
.20	21.9	21.0	0.094	22.2	31.1	0.090
.21	22.6	20.4	0.092	22.4	32.0	0.087
.22	23.4	20.8	0.089	22.5	33.0	0.087
.23	24.2	23.9	0.086	22.7	33.9	0.084
.24	24.3	27.5	0.084	22.8	34.8	0.082
Mean values	19.4	31.1	0.103	20.9	30.8	0.097

## Appendix I. 1.2.4./1.2.8

BROADCASTER						
sprout length ( $RB$ ) = 0.75 m			sprout angle ( $\gamma$ ) = $0^\circ$			
ratio crank/connecting rod ( $C$ ) = 0.475			rotary frequency ( $N$ ) = 540 min $^{-1}$			
I			FERTILIZER		II	
$\mu^* = 0.2, \varepsilon^* = 0.4, \omega_1 = -1000 \text{ rad s}^{-1}$					$\mu^* = 0.1, \varepsilon^* = 0.6, \omega_1 = -1000 \text{ rad s}^{-1}$	
$R_0$ (m)	$VK$ (m s $^{-1}$ )	$\beta$ (deg)	$t$ (s)	$VK$ (m s $^{-1}$ )	$\beta$ (deg)	$t$ (s)
.10	24.9	34.1	0.136	13.6	67.8	0.129
.11	18.7	44.1	0.130	13.4	78.7	0.111
.12	11.9	69.9	0.123	19.8	21.8	0.109
.13	11.5	79.6	0.117	20.3	23.0	0.106
.14	16.6	24.1	0.113	20.7	24.3	0.104
.15	17.5	23.9	0.111	21.1	25.5	0.103
.16	19.4	26.3	0.106	21.3	26.7	0.100
.17	19.9	24.2	0.104	21.6	27.9	0.099
.18	20.6	22.9	0.101	23.5	23.8	0.097
.19	21.2	22.0	0.099	25.0	22.9	0.094
.20	21.9	21.0	0.097	25.9	23.2	0.092
.21	22.6	20.4	0.095	26.6	23.8	0.091
.22	23.3	19.7	0.093	27.2	24.5	0.090
.23	24.0	19.1	0.090	27.7	25.2	0.087
.24	25.3	22.3	0.088	22.8	34.8	0.086
Mean values	19.9	31.6	0.107	22.0	31.6	0.100

Appendix I. 1.3.1./1.3.5

BROADCASTER						
sprout length ( $RB$ ) = 0.63 m			sprout angle ( $\gamma$ ) = $-1^\circ$			
ratio crank/connecting rod ( $C$ ) = 0.475			rotary frequency ( $N$ ) = 540 $\text{min}^{-1}$			
FERTILIZER						
I			II			
$\mu^* = 0.2, \varepsilon^* = 0.4, \omega_1 = -1000 \text{ rad s}^{-1}$			$\mu^* = 0.1, \varepsilon^* = 0.6, \omega_1 = -1000 \text{ rad s}^{-1}$			
$R_0$ (m)	$VK$ ( $\text{m s}^{-1}$ )	$\beta$ (deg)	$t$ (s)	$VK$ ( $\text{m s}^{-1}$ )	$\beta$ (deg)	$t$ (s)
.10	13.7	21.0	0.117	12.6	34.5	0.114
.11	14.6	21.9	0.113	19.3	21.0	0.102
.12	15.2	23.5	0.111	20.3	21.1	0.100
.13	15.8	25.3	0.106	21.1	21.8	0.098
.14	17.0	23.8	0.104	21.7	22.8	0.096
.15	17.9	24.1	0.100	22.3	23.9	0.093
.16	18.5	25.1	0.098	22.8	25.0	0.092
.17	19.6	24.7	0.095	23.2	26.0	0.089
.18	21.9	28.3	0.091	23.5	27.0	0.087
.19	22.7	29.4	0.089	23.9	27.9	0.084
.20	21.3	26.8	0.086	24.3	28.9	0.081
.21	20.6	30.1	0.084	14.5	52.5	0.080
.22	18.5	36.1	0.080	14.5	53.6	0.078
.23	18.7	37.0	0.076	14.6	54.7	0.074
.24	12.5	54.4	0.072	14.7	55.8	0.072
Mean values	17.9	28.8	0.095	19.5	33.1	0.089

Appendix I. 1.3.1./1.3.6

BROADCASTER						
sprout length ( $RB$ ) = 0.67 m			sprout angle ( $\gamma$ ) = $-1^\circ$			
ratio crank/connecting rod ( $C$ ) = 0.475			rotary frequency ( $N$ ) = 540 $\text{min}^{-1}$			
FERTILIZER						
I			II			
$\mu^* = 0.2, \varepsilon^* = 0.4, \omega_1 = -1000 \text{ rad s}^{-1}$			$\mu^* = 0.1, \varepsilon^* = 0.6, \omega_1 = -1000 \text{ rad s}^{-1}$			
$R_0$ (m)	$VK$ ( $\text{m s}^{-1}$ )	$\beta$ (deg)	$t$ (s)	$VK$ ( $\text{m s}^{-1}$ )	$\beta$ (deg)	$t$ (s)
.10	10.6	71.3	0.124	12.6	34.5	0.118
.11	14.6	21.9	0.116	19.3	21.0	0.106
.12	15.2	23.5	0.113	20.3	21.1	0.103
.13	15.8	25.3	0.109	21.1	21.8	0.101
.14	17.0	23.8	0.107	21.7	22.8	0.100
.15	17.9	24.1	0.104	22.3	23.9	0.097
.16	18.5	25.1	0.102	22.8	25.0	0.094
.17	19.6	24.7	0.099	23.2	26.0	0.093
.18	21.7	27.4	0.094	23.5	27.0	0.090
.19	22.1	25.3	0.092	23.9	27.9	0.089
.20	23.0	26.1	0.089	24.3	28.9	0.087
.21	23.8	28.5	0.087	24.6	29.8	0.084
.22	22.2	28.3	0.085	24.9	30.6	0.082
.23	21.2	32.0	0.082	14.6	54.7	0.079
.24	18.9	37.8	0.079	14.7	55.8	0.077
Mean values	18.8	29.7	0.099	20.9	30.0	0.093



## Appendix I. 1.3.3./1.3.7

BROADCASTER						
sprout length ( $RB$ ) = 0.71 m			sprout angle ( $\gamma$ ) = $-1^\circ$			
ratio crank/connecting rod ( $C$ ) = 0.475			rotary frequency ( $N$ ) = $540 \text{ min}^{-1}$			
I			II			
FERTILIZER			FERTILIZER			
$\mu^* = 0.2, \varepsilon^* = 0.4, \omega_1 = -1000 \text{ rad s}^{-1}$			$\mu^* = 0.1, \varepsilon^* = 0.6, \omega_1 = -1000 \text{ rad s}^{-1}$			
$R_p$ (m)	$VK$ ( $\text{m s}^{-1}$ )	$\beta$ (deg)	$t$ (s)	$VK$ ( $\text{m s}^{-1}$ )	$\beta$ (deg)	$t$ (s)
.10	18.6	44.1	0.130	12.6	34.5	0.121
.11	11.2	73.2	0.122	19.3	21.0	0.107
.12	15.2	23.5	0.116	20.3	21.1	0.107
.13	15.8	25.3	0.113	21.1	21.8	0.103
.14	17.0	23.8	0.109	21.7	22.8	0.101
.15	17.9	24.1	0.108	22.3	23.9	0.100
.16	18.5	25.1	0.104	22.8	25.0	0.097
.17	19.6	24.7	0.101	23.2	26.0	0.094
.18	21.7	27.4	0.097	23.5	27.0	0.094
.19	22.1	25.3	0.095	23.9	27.9	0.091
.20	22.7	24.2	0.093	24.3	28.9	0.090
.21	23.4	23.4	0.090	24.6	29.8	0.088
.22	24.4	25.3	0.088	24.9	30.6	0.085
.23	25.0	28.8	0.085	25.2	31.4	0.083
.24	25.1	32.5	0.083	25.4	32.2	0.081
Mean values	19.9	30.0	0.102	22.3	26.9	0.096

## Appendix I. 1.3.4./1.3.8

BROADCASTER						
sprout length ( $RB$ ) = 0.75 m			sprout angle ( $\gamma$ ) = $-1^\circ$			
ratio crank/connecting rod ( $C$ ) = 0.475			rotary frequency ( $N$ ) = $540 \text{ min}^{-1}$			
I			II			
FERTILIZER			FERTILIZER			
$\mu^* = 0.2, \varepsilon^* = 0.4, \omega_1 = -1000 \text{ rad s}^{-1}$			$\mu^* = 0.1, \varepsilon^* = 0.6, \omega_1 = -1000 \text{ rad s}^{-1}$			
$R_p$ (m)	$VK$ ( $\text{m s}^{-1}$ )	$\beta$ (deg)	$t$ (s)	$VK$ ( $\text{m s}^{-1}$ )	$\beta$ (deg)	$t$ (s)
.10	23.5	38.6	0.134	19.0	53.8	0.127
.11	16.6	50.4	0.128	19.3	21.0	0.111
.12	12.3	71.4	0.121	20.3	21.1	0.108
.13	15.8	25.3	0.116	21.1	21.8	0.107
.14	17.0	23.8	0.113	21.7	22.8	0.103
.15	17.9	24.1	0.109	22.3	23.9	0.102
.16	18.5	25.1	0.107	22.8	25.0	0.099
.17	19.6	24.7	0.104	23.2	26.0	0.098
.18	21.7	27.4	0.100	23.5	27.0	0.095
.19	22.1	25.3	0.098	23.9	27.9	0.095
.20	22.7	24.2	0.096	24.3	28.9	0.092
.21	23.4	23.2	0.094	24.6	29.8	0.090
.22	24.1	22.4	0.092	24.9	30.6	0.089
.23	25.1	23.2	0.089	25.2	31.4	0.087
.24	25.8	25.7	0.087	25.4	32.2	0.084
Mean values	20.4	30.3	0.106	22.8	28.8	0.099

Appendix I. 1.4.1./1.4.5

BROADCASTER						
sprout length ( $RB$ ) = 0.63 m			sprout angle ( $\gamma$ ) = $-2^\circ$			
ratio crank/connecting rod ( $C$ ) = 0.475			rotary frequency ( $N$ ) = $540 \text{ min}^{-1}$			
I			FERTILIZER			II
$\mu^* = 0.2, \epsilon^* = 0.4, \omega_1 = -1000 \text{ rad s}^{-1}$						$\mu^* = 0.1, \epsilon^* = 0.6, \omega_1 = -1000 \text{ rad s}^{-1}$
$R_s$ (m)	$VK$ ( $\text{m s}^{-1}$ )	$\beta$ (deg)	$t$ (s)	$VK$ ( $\text{m s}^{-1}$ )	$\beta$ (deg)	$t$ (s)
.10	13.7	22.2	0.117	13.4	33.5	0.113
.11	14.9	21.8	0.114	18.4	24.3	0.101
.12	15.8	22.5	0.110	20.2	21.8	0.099
.13	16.5	23.6	0.106	21.3	21.5	0.097
.14	17.2	25.1	0.103	22.3	21.9	0.095
.15	17.7	26.5	0.100	23.2	22.7	0.094
.16	19.1	24.5	0.098	23.9	23.5	0.091
.17	20.1	24.9	0.093	24.5	24.4	0.088
.18	20.8	25.7	0.092	25.0	25.3	0.087
.19	21.4	26.5	0.089	15.9	47.4	0.084
.20	19.8	32.0	0.085	16.0	48.5	0.082
.21	20.2	32.9	0.083	16.1	49.5	0.080
.22	20.5	33.7	0.079	16.3	50.5	0.076
.23	13.9	49.1	0.076	16.4	51.4	0.073
.24	14.1	50.2	0.072	16.5	52.3	0.071
Mean values	17.7	29.4	0.094	19.3	34.6	0.089

Appendix I. 1.4.2./1.4.6

BROADCASTER						
sprout length ( $RB$ ) = 0.67 m			sprout angle ( $\gamma$ ) = $-2^\circ$			
ratio crank/connecting rod ( $C$ ) = 0.475			rotary frequency ( $N$ ) = $540 \text{ min}^{-1}$			
I			FERTILIZER			II
$\mu^* = 0.2, \epsilon^* = 0.4, \omega_1 = -1000 \text{ rad s}^{-1}$						$\mu^* = 0.1, \epsilon^* = 0.6, \omega_1 = -1000 \text{ rad s}^{-1}$
$R_s$ (m)	$VK$ ( $\text{m s}^{-1}$ )	$\beta$ (deg)	$t$ (s)	$VK$ ( $\text{m s}^{-1}$ )	$\beta$ (deg)	$t$ (s)
.10	12.7	61.7	0.123	13.4	33.5	0.117
.11	14.9	21.8	0.115	18.4	24.3	0.105
.12	15.8	22.5	0.113	20.2	21.8	0.103
.13	16.5	23.6	0.110	21.3	21.5	0.101
.14	17.2	25.1	0.106	22.3	21.9	0.099
.15	17.7	26.5	0.104	23.2	22.7	0.096
.16	19.1	24.5	0.100	23.9	23.5	0.094
.17	20.1	24.9	0.097	24.5	24.4	0.091
.18	20.8	25.7	0.095	25.0	25.3	0.091
.19	21.9	25.2	0.093	25.6	26.1	0.088
.20	22.5	25.8	0.089	26.1	27.0	0.085
.21	22.4	28.1	0.087	26.6	27.8	0.083
.22	22.8	28.9	0.084	16.3	50.5	0.081
.23	20.9	34.6	0.082	16.4	51.4	0.079
.24	14.1	50.2	0.077	16.5	52.3	0.077
Mean values	18.6	30.0	0.098	21.3	30.3	0.093

## Appendix I. 1.4.3./1.4.7

BROADCASTER						
sprout length ( $RB$ ) = 0.71 m			sprout angle ( $\gamma$ ) = $-2^\circ$			
ratio crank/connecting rod ( $C$ ) = 0.475			rotary frequency ( $N$ ) = $540 \text{ min}^{-1}$			
I			II			
FERTILIZER						
$\mu^* = 0.2, \epsilon^* = 0.4, \omega_1 = -1000 \text{ rad s}^{-1}$			$\mu^* = 0.1, \epsilon^* = 0.6, \omega_1 = -1000 \text{ rad s}^{-1}$			
$R_o$ (m)	$VK$ ( $\text{m s}^{-1}$ )	$\beta$ (deg)	$t$ (s)	$VK$ ( $\text{m s}^{-1}$ )	$\beta$ (deg)	$t$ (s)
.10	12.7	61.7	0.128	13.4	33.5	0.120
.11	12.6	67.6	0.120	18.4	24.3	0.108
.12	15.8	22.5	0.115	20.2	21.8	0.105
.13	16.5	23.6	0.111	21.3	21.5	0.102
.14	17.2	25.1	0.108	22.3	21.9	0.101
.15	17.7	26.5	0.105	23.2	22.7	0.099
.16	19.1	24.5	0.103	23.9	23.5	0.096
.17	20.1	24.9	0.101	24.5	24.4	0.095
.18	20.8	25.7	0.099	25.0	25.3	0.092
.19	21.9	25.2	0.095	25.6	26.1	0.092
.20	22.7	25.4	0.094	26.1	27.0	0.089
.21	23.5	25.7	0.090	26.6	27.8	0.087
.22	24.0	26.6	0.088	27.1	28.5	0.084
.23	23.3	29.7	0.085	27.5	29.2	0.082
.24	23.7	30.4	0.083	16.5	52.3	0.080
Mean values	19.4	31.0	0.102	22.8	27.3	0.095

## Appendix I. 1.4.4./1.4.8

BROADCASTER						
sprout length ( $RB$ ) = 0.75 m			sprout angle ( $\gamma$ ) = $-2^\circ$			
ratio crank/connecting rod ( $C$ ) = 0.475			rotary frequency ( $N$ ) = $540 \text{ min}^{-1}$			
I			II			
FERTILIZER						
$\mu^* = 0.2, \epsilon^* = 0.4, \omega_1 = -1000 \text{ rad s}^{-1}$			$\mu^* = 0.1, \epsilon^* = 0.6, \omega_1 = -1000 \text{ rad s}^{-1}$			
$R_o$ (m)	$VK$ ( $\text{m s}^{-1}$ )	$\beta$ (deg)	$t$ (s)	$VK$ ( $\text{m s}^{-1}$ )	$\beta$ (deg)	$t$ (s)
.10	19.6	44.7	0.133	19.2	56.9	0.125
.11	12.6	67.6	0.125	18.4	24.3	0.110
.12	13.3	69.2	0.120	20.2	21.8	0.108
.13	16.5	23.6	0.115	21.3	21.5	0.106
.14	17.2	25.1	0.112	22.3	21.9	0.104
.15	17.7	26.5	0.109	23.2	22.7	0.101
.16	19.1	24.5	0.107	23.9	23.5	0.100
.17	20.1	24.9	0.104	24.5	24.4	0.097
.18	20.8	25.7	0.101	25.0	25.3	0.096
.19	21.9	25.2	0.098	25.6	26.1	0.093
.20	22.7	25.4	0.097	26.1	27.0	0.093
.21	24.7	27.6	0.093	26.6	27.8	0.090
.22	25.3	26.6	0.091	27.1	28.5	0.088
.23	26.4	28.3	0.088	27.5	29.2	0.085
.24	25.1	27.7	0.086	27.9	30.0	0.085
Mean values	20.2	32.8	0.105	23.9	27.4	0.099

## Appendix I. 2.1./2.3

BROADCASTER						
sprout length ( $RB$ ) = 0.63 m			sprout angle ( $\gamma$ ) = $+1^\circ$			
ratio crank/connecting rod ( $C$ ) = 0.475			rotary frequency ( $N$ ) = 600 $\text{min}^{-1}$			
I			FERTILIZER		II	
$\mu^* = 0.2, \varepsilon^* = 0.4, \omega_1 = -1000 \text{ rad s}^{-1}$					$\mu^* = 0.1, \varepsilon^* = 0.6, \omega_1 = -1000 \text{ rad s}^{-1}$	
$R_c$ (m)	$VK$ ( $\text{m s}^{-1}$ )	$\beta$ (deg)	$t$ (s)	$VK$ ( $\text{m s}^{-1}$ )	$\beta$ (deg)	$t$ (s)
.10	15.3	48.4	0.114	18.9	19.4	0.098
.11	10.5	76.6	0.107	19.6	20.3	0.096
.12	15.7	22.1	0.102	20.2	21.6	0.094
.13	16.4	23.2	0.101	20.4	23.0	0.092
.14	17.4	22.9	0.097	20.8	24.5	0.090
.15	19.4	25.3	0.093	21.0	25.9	0.088
.16	19.9	23.2	0.091	21.3	27.3	0.086
.17	20.6	21.8	0.088	23.9	22.0	0.084
.18	21.3	20.7	0.086	25.1	22.0	0.082
.19	22.0	19.7	0.084	21.7	31.0	0.080
.20	22.8	19.3	0.081	21.7	32.2	0.078
.21	23.7	21.6	0.079	21.8	33.3	0.076
.22	24.0	25.8	0.076	21.9	34.4	0.073
.23	23.5	30.4	0.074	21.9	35.4	0.071
.24	22.4	36.6	0.071	21.9	36.4	0.069
Mean values	19.7	29.2	0.090	21.5	27.3	0.084

## Appendix I. 2.2./2.4

BROADCASTER						
sprout length ( $RB$ ) = 0.63 m			sprout angle ( $\gamma$ ) = $+1^\circ$			
ratio crank/connecting rod ( $C$ ) = 0.475			rotary frequency ( $N$ ) = 660 $\text{min}^{-1}$			
I			FERTILIZER		II	
$\mu^* = 0.2, \varepsilon^* = 0.4, \omega_1 = -1000 \text{ rad s}^{-1}$					$\mu^* = 0.1, \varepsilon^* = 0.6, \omega_1 = -1000 \text{ rad s}^{-1}$	
$R_c$ (m)	$VK$ ( $\text{m s}^{-1}$ )	$\beta$ (deg)	$t$ (s)	$VK$ ( $\text{m s}^{-1}$ )	$\beta$ (deg)	$t$ (s)
.10	21.7	42.1	0.108	13.0	82.2	0.092
.11	10.9	78.5	0.101	20.5	19.3	0.090
.12	16.3	23.4	0.095	21.3	20.4	0.088
.13	17.6	22.6	0.093	21.8	21.8	0.086
.14	18.6	22.7	0.090	22.2	23.2	0.084
.15	19.5	22.9	0.087	22.6	24.7	0.082
.16	21.4	24.3	0.084	22.8	26.0	0.080
.17	22.0	22.6	0.082	23.1	27.4	0.078
.18	22.9	21.4	0.080	26.2	21.8	0.076
.19	23.6	20.6	0.078	27.4	21.9	0.074
.20	24.3	19.5	0.076	23.5	31.0	0.073
.21	25.4	19.6	0.073	23.6	32.1	0.071
.22	26.2	22.3	0.071	23.8	33.2	0.069
.23	26.3	26.5	0.069	23.8	34.3	0.068
.24	25.6	31.7	0.066	23.9	35.3	0.066
Mean values	21.5	28.1	0.084	22.6	30.3	0.078

## Appendix I. 2.5./2.7

BROADCASTER						
sprout length ( <i>RB</i> ) = 0.67 m			sprout angle ( $\gamma$ ) = $+1^\circ$			
ratio crank/connecting rod ( <i>C</i> ) = 0.475			rotary frequency ( <i>N</i> ) = 600 min <sup>-1</sup>			
I			II			
FERTILIZER			FERTILIZER			
$\mu^* = 0.2, \varepsilon^* = 0.4, \omega_1 = -1000 \text{ rad s}^{-1}$			$\mu^* = 0.1, \varepsilon^* = 0.6, \omega_1 = -1000 \text{ rad s}^{-1}$			
<i>R<sub>o</sub></i> (m)	<i>VK</i> (m s <sup>-1</sup> )	$\beta$ (deg)	<i>t</i> (s)	<i>VK</i> (m s <sup>-1</sup> )	$\beta$ (deg)	<i>t</i> (s)
.10	22.0	39.4	0.119	12.4	75.5	0.102
.11	15.2	52.1	0.112	12.9	70.1	0.098
.12	10.4	83.7	0.109	20.2	21.6	0.097
.13	16.4	23.2	0.102	20.4	23.0	0.094
.14	17.4	22.9	0.100	20.8	24.5	0.093
.15	19.4	25.3	0.096	21.0	25.9	0.090
.16	19.9	23.2	0.094	21.3	27.3	0.089
.17	20.6	21.8	0.092	23.9	22.0	0.088
.18	21.3	20.7	0.089	25.1	22.0	0.085
.19	22.0	19.7	0.087	25.8	22.7	0.083
.20	22.8	19.0	0.085	26.4	23.5	0.082
.21	23.4	18.4	0.083	26.8	24.5	0.079
.22	25.1	21.6	0.080	27.1	25.4	0.078
.23	25.8	24.2	0.078	27.4	26.3	0.076
.24	25.5	27.6	0.075	21.9	36.4	0.074
Mean values	20.5	29.5	0.093	22.2	31.4	0.087

## Appendix I. 2.6./2.8

BROADCASTER						
sprout length ( <i>RB</i> ) = 0.67 m			sprout angle ( $\gamma$ ) = $+1^\circ$			
ratio crank/connecting rod ( <i>C</i> ) = 0.475			rotary frequency ( <i>N</i> ) = 660 min <sup>-1</sup>			
I			II			
FERTILIZER			FERTILIZER			
$\mu^* = 0.2, \varepsilon^* = 0.4, \omega_1 = -1000 \text{ rad s}^{-1}$			$\mu^* = 0.1, \varepsilon^* = 0.6, \omega_1 = -1000 \text{ rad s}^{-1}$			
<i>R<sub>o</sub></i> (m)	<i>VK</i> (m s <sup>-1</sup> )	$\beta$ (deg)	<i>t</i> (s)	<i>VK</i> (m s <sup>-1</sup> )	$\beta$ (deg)	<i>t</i> (s)
.10	27.2	33.3	0.112	13.0	82.2	0.095
.11	19.2	45.3	0.106	13.4	73.8	0.093
.12	11.9	75.8	0.101	14.1	70.5	0.091
.13	11.8	84.3	0.096	21.8	21.8	0.088
.14	18.6	22.7	0.093	22.2	23.2	0.086
.15	19.5	22.9	0.090	22.6	24.7	0.084
.16	21.4	24.3	0.087	22.8	26.0	0.083
.17	22.0	22.6	0.085	23.1	27.4	0.081
.18	22.9	21.4	0.084	26.2	21.8	0.079
.19	23.6	20.6	0.081	27.4	21.9	0.077
.20	24.3	19.5	0.079	28.2	22.6	0.076
.21	25.3	19.0	0.077	28.7	23.4	0.074
.22	25.9	18.2	0.075	29.3	24.4	0.072
.23	27.9	22.2	0.072	29.7	25.3	0.071
.24	28.4	25.0	0.070	30.0	26.2	0.069
Mean values	22.0	31.8	0.087	23.5	34.3	0.081

Appendix I. 2.9./2.11

BROADCASTER						
sprout length (RB) = 0.71 m			sprout angle ( $\gamma$ ) = $+1^\circ$			
ratio crank/connecting rod (C) = 0.475			rotary frequency (N) = 600 min <sup>-1</sup>			
I			FERTILIZER		II	
$\mu^* = 0.2, \epsilon^* = 0.4, \omega_1 = -1000 \text{ rad s}^{-1}$					$\mu^* = 0.1, \epsilon^* = 0.6, \omega_1 = -1000 \text{ rad s}^{-1}$	
$R_0$ (m)	VK (m s <sup>-1</sup> )	$\beta$ (deg)	$t$ (s)	VK (m s <sup>-1</sup> )	$\beta$ (deg)	$t$ (s)
.10	26.6	31.9	0.123	12.4	75.5	0.105
.11	21.6	44.8	0.117	12.9	70.1	0.101
.12	14.5	55.7	0.113	13.7	69.4	0.098
.13	11.2	83.6	0.107	20.4	23.0	0.097
.14	11.5	87.6	0.103	20.8	24.5	0.094
.15	19.4	25.3	0.099	21.0	25.9	0.093
.16	19.9	23.2	0.097	21.3	27.3	0.091
.17	20.6	21.8	0.095	23.9	22.0	0.089
.18	21.3	20.7	0.093	25.1	22.0	0.088
.19	22.0	19.7	0.092	25.8	22.7	0.087
.20	22.8	19.0	0.088	26.4	23.5	0.084
.21	23.4	18.4	0.086	26.8	24.5	0.083
.22	25.1	20.5	0.084	27.1	25.4	0.081
.23	26.3	21.6	0.081	27.4	26.3	0.079
.24	27.2	23.5	0.079	27.7	27.2	0.078
Mean values	20.9	34.5	0.097	22.2	34.0	0.090

Appendix I. 2.10/2.12

BROADCASTER						
sprout length (RB) = 0.71 m			sprout angle ( $\gamma$ ) = $+1^\circ$			
ratio crank/connecting rod (C) = 0.475			rotary frequency (N) = 660 min <sup>-1</sup>			
I			FERTILIZER		II	
$\mu^* = 0.2, \epsilon^* = 0.4, \omega_1 = -1000 \text{ rad s}^{-1}$					$\mu^* = 0.1, \epsilon^* = 0.6, \omega_1 = -1000 \text{ rad s}^{-1}$	
$R_0$ (m)	VK (m s <sup>-1</sup> )	$\beta$ (deg)	$t$ (s)	VK (m s <sup>-1</sup> )	$\beta$ (deg)	$t$ (s)
.10	30.4	28.1	0.115	13.0	82.2	0.099
.11	27.1	36.7	0.110	13.4	73.8	0.096
.12	20.0	46.2	0.105	14.1	70.5	0.092
.13	11.8	84.3	0.100	14.8	70.9	0.091
.14	12.3	86.3	0.095	22.2	23.2	0.088
.15	19.5	22.9	0.093	22.6	24.7	0.087
.16	21.4	24.3	0.089	22.8	26.0	0.084
.17	22.0	22.6	0.087	23.1	27.4	0.083
.18	22.9	21.4	0.085	26.2	21.8	0.082
.19	23.6	20.6	0.084	27.4	21.9	0.080
.20	24.3	19.5	0.082	28.2	22.6	0.078
.21	25.3	19.0	0.080	28.7	23.4	0.077
.22	25.9	18.2	0.078	29.3	24.4	0.075
.23	27.9	20.9	0.076	29.7	25.3	0.074
.24	29.2	22.1	0.073	30.0	26.2	0.073
Mean values	22.9	32.9	0.090	23.0	37.6	0.084

## Appendix I. 2.13/2.15

BROADCASTER						
sprout length ( $RB$ ) = 0.75 m			sprout angle ( $\gamma$ ) = $+1^\circ$			
ratio crank/connecting rod ( $C$ ) = 0.475			rotary frequency ( $N$ ) = 600 $\text{min}^{-1}$			
I			II			
$\mu^* = 0.2, \varepsilon^* = 0.4, \omega_1 = -1000 \text{ rad s}^{-1}$			$\mu^* = 0.1, \varepsilon^* = 0.6, \omega_1 = -1000 \text{ rad s}^{-1}$			
$R_o$ (m)	$VK$ ( $\text{m s}^{-1}$ )	$\beta$ (deg)	$t$ (s)	$VK$ ( $\text{m s}^{-1}$ )	$\beta$ (deg)	$t$ (s)
.10	29.3	27.0	0.127	12.4	75.5	0.109
.11	26.7	35.0	0.121	12.9	70.1	0.105
.12	22.4	43.5	0.117	13.7	69.4	0.101
.13	15.4	56.1	0.111	20.4	23.0	0.099
.14	11.5	87.6	0.106	20.8	24.5	0.097
.15	19.4	25.3	0.101	21.0	25.9	0.096
.16	19.9	23.2	0.099	21.3	27.3	0.094
.17	20.6	21.8	0.097	23.9	22.0	0.092
.18	21.3	20.7	0.095	25.1	22.0	0.090
.19	22.0	19.7	0.093	25.8	22.7	0.088
.20	22.8	19.0	0.091	26.4	23.5	0.087
.21	23.4	18.4	0.089	26.8	24.5	0.086
.22	25.1	20.5	0.087	27.1	25.4	0.083
.23	26.3	21.2	0.084	27.4	26.3	0.082
.24	27.4	21.4	0.082	27.7	27.2	0.080
Mean values	22.2	30.7	0.100	22.2	34.0	0.093

## Appendix I. 2.14/2.16

BROADCASTER						
sprout length ( $RB$ ) = 0.75 m			sprout angle ( $\gamma$ ) = $+1^\circ$			
ratio crank/connecting rod ( $C$ ) = 0.475			rotary frequency ( $N$ ) = 660 $\text{min}^{-1}$			
I			II			
$\mu^* = 0.2, \varepsilon^* = 0.4, \omega_1 = -1000 \text{ rad s}^{-1}$			$\mu^* = 0.1, \varepsilon^* = 0.6, \omega_1 = -1000 \text{ rad s}^{-1}$			
$R_o$ (m)	$VK$ ( $\text{m s}^{-1}$ )	$\beta$ (deg)	$t$ (s)	$VK$ ( $\text{m s}^{-1}$ )	$\beta$ (deg)	$t$ (s)
.10	32.0	24.5	0.118	19.8	58.4	0.102
.11	31.5	30.3	0.113	13.4	73.8	0.098
.12	27.5	38.1	0.109	14.1	70.5	0.095
.13	19.9	48.2	0.105	14.8	70.9	0.093
.14	12.3	86.3	0.100	15.7	74.3	0.090
.15	12.8	88.5	0.097	22.6	24.7	0.088
.16	21.4	24.3	0.092	22.8	26.0	0.087
.17	22.0	22.6	0.090	23.1	27.4	0.085
.18	22.9	21.4	0.088	26.2	21.8	0.083
.19	23.6	20.6	0.086	27.4	21.9	0.081
.20	24.3	19.5	0.085	28.2	22.6	0.080
.21	25.3	19.0	0.083	28.7	23.4	0.079
.22	25.9	18.2	0.081	29.3	24.4	0.078
.23	27.9	20.9	0.078	29.7	25.3	0.075
.24	29.2	21.3	0.076	30.0	26.2	0.075
Mean value	23.9	33.6	0.093	23.0	39.4	0.086

Appendix I. 3.1./3.5

BROADCASTER						
sprout length ( $RB$ ) = 0.63 m			sprout angle ( $\gamma$ ) = $+1^\circ$			
ratio crank/connecting rod ( $C$ ) = 0.400			rotary frequency ( $N$ ) = 540 $\text{min}^{-1}$			
I			FERTILIZER		II	
$\mu^* = 0.2, \varepsilon^* = 0.4, \omega_1 = -1000 \text{ rad s}^{-1}$					$\mu^* = 0.1, \varepsilon^* = 0.6, \omega_1 = -1000 \text{ rad s}^{-1}$	
$R_s$ (m)	$VK$ ( $\text{m s}^{-1}$ )	$\beta$ (deg)	$t$ (s)	$VK$ ( $\text{m s}^{-1}$ )	$\beta$ (deg)	$t$ (s)
.10	17.3	24.9	0.147	14.4	42.2	0.133
.11	17.3	22.8	0.143	10.8	59.3	0.127
.12	17.1	30.5	0.137	12.5	52.9	0.123
.13	13.0	39.2	0.130	9.9	67.6	0.118
.14	7.2	75.0	0.122	8.9	83.8	0.113
.15	7.9	71.9	0.115	17.1	22.2	0.100
.16	12.4	24.4	0.112	17.4	22.8	0.099
.17	13.4	22.7	0.109	17.7	23.7	0.095
.18	13.8	23.4	0.105	17.8	24.5	0.094
.19	14.4	23.1	0.102	18.0	25.4	0.091
.20	14.9	23.1	0.100	18.1	26.3	0.090
.21	16.3	25.6	0.095	18.3	27.2	0.088
.22	16.7	24.2	0.093	18.4	28.0	0.085
.23	17.2	23.3	0.090	18.5	28.9	0.083
.24	17.8	25.5	0.087	18.5	29.7	0.080
Mean values	14.4	32.0	0.112	15.7	37.6	0.101

Appendix I. 3.2./3.6

BROADCASTER						
sprout length ( $RB$ ) = 0.67 m			sprout angle ( $\gamma$ ) = $+1^\circ$			
ratio crank/connecting rod ( $C$ ) = 0.400			rotary frequency ( $N$ ) = 540 $\text{min}^{-1}$			
I			FERTILIZER		II	
$\mu^* = 0.2, \varepsilon^* = 0.4, \omega_1 = -1000 \text{ rad s}^{-1}$					$\mu^* = 0.1, \varepsilon^* = 0.6, \omega_1 = -1000 \text{ rad s}^{-1}$	
$R_s$ (m)	$VK$ ( $\text{m s}^{-1}$ )	$\beta$ (deg)	$t$ (s)	$VK$ ( $\text{m s}^{-1}$ )	$\beta$ (deg)	$t$ (s)
.10	17.3	24.9	0.151	18.0	32.7	0.138
.11	17.2	20.6	0.148	17.8	35.1	0.133
.12	18.9	25.4	0.142	12.5	52.9	0.128
.13	18.0	31.5	0.136	9.9	67.6	0.123
.14	13.5	40.6	0.129	8.9	83.8	0.118
.15	7.9	71.9	0.122	17.1	22.2	0.104
.16	12.4	24.4	0.115	17.4	22.8	0.102
.17	13.4	22.7	0.113	17.7	23.7	0.099
.18	13.8	23.4	0.110	17.8	24.5	0.098
.19	14.4	23.1	0.106	18.0	25.4	0.095
.20	14.9	23.1	0.103	18.1	26.3	0.094
.21	16.3	25.6	0.099	18.3	27.2	0.091
.22	16.7	24.2	0.097	18.4	28.0	0.089
.23	17.1	22.9	0.094	18.5	28.9	0.088
.24	17.6	22.0	0.092	18.5	29.7	0.085
Mean values	15.3	28.4	0.117	16.5	35.4	0.106



## Appendix I. 3.3./3.7

BROADCASTER						
sprout length ( $RB$ ) = 0.71 m			sprout angle ( $\gamma$ ) = $+1^\circ$			
ratio crank/connecting rod ( $C$ ) = 0.400			rotary frequency ( $N$ ) = 540 $\text{min}^{-1}$			
I			II			
FERTILIZER			FERTILIZER			
$\mu^* = 0.2, \varepsilon^* = 0.4, \omega_1 = -1000 \text{ rad s}^{-1}$			$\mu^* = 0.1, \varepsilon^* = 0.6, \omega_1 = -1000 \text{ rad s}^{-1}$			
$R_o$ (m)	$VK$ ( $\text{m s}^{-1}$ )	$\beta$ (deg)	$t$ (s)	$VK$ ( $\text{m s}^{-1}$ )	$\beta$ (deg)	$t$ (s)
.10	17.3	24.9	0.155	20.0	28.4	0.144
.11	17.2	20.6	0.153	17.8	35.1	0.138
.12	19.1	23.5	0.147	20.6	30.9	0.133
.13	20.0	26.2	0.141	17.6	37.6	0.130
.14	18.7	32.7	0.135	8.9	83.8	0.124
.15	14.6	39.7	0.130	17.1	22.2	0.107
.16	8.5	69.4	0.123	17.4	22.8	0.104
.17	8.0	80.1	0.119	17.7	23.7	0.102
.18	13.8	23.4	0.114	17.8	24.5	0.101
.19	14.4	23.1	0.111	18.0	25.4	0.098
.20	14.9	23.1	0.109	18.1	26.3	0.097
.21	16.3	25.6	0.103	18.3	27.2	0.095
.22	16.7	24.2	0.101	18.4	28.0	0.094
.23	17.1	22.9	0.098	18.5	28.9	0.091
.24	17.6	22.0	0.096	18.5	29.7	0.089
Mean values	15.6	32.1	0.122	17.6	31.6	0.110

## Appendix I. 3.4./3.8

BROADCASTER						
sprout length ( $RB$ ) = 0.75 m			sprout angle ( $\gamma$ ) = $+1^\circ$			
ratio crank/connecting rod ( $C$ ) = 0.400			rotary frequency ( $N$ ) = 540 $\text{min}^{-1}$			
I			II			
FERTILIZER			FERTILIZER			
$\mu^* = 0.2, \varepsilon^* = 0.4, \omega_1 = -1000 \text{ rad s}^{-1}$			$\mu^* = 0.1, \varepsilon^* = 0.6, \omega_1 = -1000 \text{ rad s}^{-1}$			
$R_o$ (m)	$VK$ ( $\text{m s}^{-1}$ )	$\beta$ (deg)	$t$ (s)	$VK$ ( $\text{m s}^{-1}$ )	$\beta$ (deg)	$t$ (s)
.10	17.3	24.9	0.159	20.9	26.4	0.146
.11	17.2	20.6	0.158	21.7	26.8	0.143
.12	19.1	23.5	0.151	20.6	30.9	0.139
.13	20.5	23.6	0.146	17.6	37.6	0.136
.14	21.1	27.2	0.140	15.2	45.9	0.130
.15	19.5	32.9	0.135	10.6	71.7	0.110
.16	15.8	38.7	0.130	17.4	22.8	0.107
.17	11.5	50.8	0.125	17.7	23.7	0.106
.18	8.4	79.6	0.119	17.8	24.5	0.105
.19	8.5	83.2	0.115	18.0	25.4	0.102
.20	14.9	23.1	0.112	18.1	26.3	0.101
.21	16.3	25.6	0.107	18.3	27.2	0.098
.22	16.7	24.2	0.105	18.4	28.0	0.097
.23	17.1	22.9	0.103	20.0	24.1	0.095
.24	17.6	22.0	0.101	21.1	23.1	0.094
Mean values	16.1	34.9	0.127	18.2	31.0	0.114

## Appendix I. 3.9./3.13

BROADCASTER						
sprout length ( $RB$ ) = 0.63 m			sprout angle ( $\gamma$ ) = $+1^\circ$			
ratio crank/connecting rod ( $C$ ) = 0.325			rotary frequency ( $N$ ) = 540 $\text{min}^{-1}$			
I			FERTILIZER			
$\mu^* = 0.2, \varepsilon^* = 0.4, \omega_1 = -1000 \text{ rad s}^{-1}$			$\mu^* = 0.1, \varepsilon^* = 0.6, \omega_1 = -1000 \text{ rad s}^{-1}$			
$R_0$ (m)	$VK$ ( $\text{m s}^{-1}$ )	$\beta$ (deg)	$t$ (s)	$VK$ ( $\text{m s}^{-1}$ )	$\beta$ (deg)	$t$ (s)
.10	11.5	25.3	0.161	13.0	27.5	0.153
.11	12.0	25.6	0.158	13.8	27.5	0.147
.12	12.5	26.2	0.154	14.1	29.2	0.140
.13	13.1	27.7	0.151	14.0	31.0	0.135
.14	12.8	24.1	0.150	12.8	36.6	0.129
.15	13.4	23.8	0.145	8.3	61.2	0.124
.16	14.0	26.1	0.142	8.8	59.4	0.120
.17	13.5	29.5	0.137	9.1	34.1	0.116
.18	10.6	34.5	0.131	9.2	34.9	0.112
.19	5.5	68.3	0.123	11.4	23.9	0.109
.20	5.8	69.0	0.116	12.9	20.8	0.106
.21	10.9	22.9	0.111	13.6	20.7	0.102
.22	11.1	23.8	0.109	14.2	21.0	0.098
.23	11.2	24.8	0.104	14.6	21.5	0.095
.24	12.1	22.4	0.101	15.0	22.1	0.092
Mean values	11.3	31.6	0.133	12.3	31.4	0.119

## Appendix I. 3.10./3.14

BROADCASTER						
sprout length ( $RB$ ) = 0.67 m			sprout angle ( $\gamma$ ) = $+1^\circ$			
ratio crank/connecting rod ( $C$ ) = 0.325			rotary frequency ( $N$ ) = 540 $\text{min}^{-1}$			
I			FERTILIZER			
$\mu^* = 0.2, \varepsilon^* = 0.4, \omega_1 = -1000 \text{ rad s}^{-1}$			$\mu^* = 0.1, \varepsilon^* = 0.6, \omega_1 = -1000 \text{ rad s}^{-1}$			
$R_0$ (m)	$VK$ ( $\text{m s}^{-1}$ )	$\beta$ (deg)	$t$ (s)	$VK$ ( $\text{m s}^{-1}$ )	$\beta$ (deg)	$t$ (s)
.10	11.5	25.3	0.167	13.0	27.5	0.138
.11	12.0	25.6	0.163	13.8	27.5	0.152
.12	12.5	26.2	0.160	15.6	31.6	0.145
.13	13.1	27.7	0.156	15.4	27.0	0.141
.14	12.8	24.1	0.156	12.8	36.6	0.136
.15	13.4	23.8	0.152	13.9	34.7	0.131
.16	13.9	24.0	0.149	8.8	59.4	0.127
.17	14.1	21.6	0.144	10.7	48.7	0.122
.18	14.4	27.1	0.138	9.2	34.9	0.117
.19	11.7	33.3	0.132	11.4	23.9	0.114
.20	9.4	42.3	0.124	12.9	20.8	0.109
.21	6.2	67.7	0.118	13.6	20.7	0.106
.22	11.1	23.8	0.114	14.2	21.0	0.104
.23	11.2	24.8	0.109	14.6	21.5	0.100
.24	12.1	22.4	0.108	15.0	22.1	0.097
Mean values	12.0	29.3	0.139	13.0	30.5	0.124

BROADCASTER						
sprout length ( $RB$ ) = 0.71 m			sprout angle ( $\gamma$ ) = $+1^\circ$			
ratio crank/connecting rod ( $C$ ) = 0.325			rotary frequency ( $N$ ) = 540 $\text{min}^{-1}$			
I			FERTILIZER		II	
$\mu^* = 0.2, \varepsilon^* = 0.4, \omega_1 = -1000 \text{ rad s}^{-1}$					$\mu^* = 0.1, \varepsilon^* = 0.6, \omega_1 = -1000 \text{ rad s}^{-1}$	
$R_0$ (m)	$VK$ ( $\text{m s}^{-1}$ )	$\beta$ (deg)	$t$ (s)	$VK$ ( $\text{m s}^{-1}$ )	$\beta$ (deg)	$t$ (s)
.10	7.3	62.0	0.173	13.0	27.5	0.162
.11	12.0	25.6	0.169	13.8	27.5	0.156
.12	12.5	26.2	0.165	15.5	30.9	0.150
.13	13.1	27.7	0.162	15.4	27.0	0.147
.14	12.8	24.1	0.161	15.8	27.9	0.143
.15	13.4	23.8	0.158	13.9	34.7	0.138
.16	13.9	24.0	0.154	14.8	33.7	0.133
.17	14.1	21.6	0.151	10.7	48.7	0.129
.18	15.2	23.4	0.145	11.8	45.4	0.125
.19	15.4	27.0	0.139	8.8	61.8	0.121
.20	14.0	34.0	0.132	7.5	80.4	0.116
.21	9.9	42.1	0.126	7.5	88.4	0.113
.22	6.6	65.2	0.122	14.2	21.0	0.107
.23	11.2	24.8	0.115	14.6	21.5	0.106
.24	12.1	22.4	0.111	15.0	22.1	0.103
Mean values	12.2	31.6	0.146	12.8	39.9	0.130

BROADCASTER						
sprout length ( $RB$ ) = 0.75 m			sprout angle ( $\gamma$ ) = $+1^\circ$			
ratio crank/connecting rod ( $C$ ) = 0.325			rotary frequency ( $N$ ) = 540 $\text{min}^{-1}$			
I			FERTILIZER		II	
$\mu^* = 0.2, \varepsilon^* = 0.4, \omega_1 = -1000 \text{ rad s}^{-1}$					$\mu^* = 0.1, \varepsilon^* = 0.6, \omega_1 = -1000 \text{ rad s}^{-1}$	
$R_0$ (m)	$VK$ ( $\text{m s}^{-1}$ )	$\beta$ (deg)	$t$ (s)	$VK$ ( $\text{m s}^{-1}$ )	$\beta$ (deg)	$t$ (s)
.10	11.5	37.9	0.182	13.0	27.5	0.165
.11	7.5	65.0	0.175	13.8	27.5	0.161
.12	12.5	26.2	0.169	15.5	30.9	0.154
.13	13.1	27.7	0.165	15.4	27.0	0.152
.14	12.8	24.1	0.166	15.8	27.9	0.148
.15	13.4	23.8	0.161	16.9	26.5	0.143
.16	13.9	24.0	0.159	14.8	33.7	0.139
.17	14.1	21.6	0.157	17.7	27.3	0.136
.18	15.2	23.4	0.150	11.8	45.4	0.132
.19	16.1	23.8	0.145	8.8	61.8	0.126
.20	16.3	26.5	0.139	7.5	80.4	0.123
.21	15.2	31.2	0.134	7.5	88.4	0.118
.22	12.4	36.0	0.129	7.7	83.6	0.113
.23	7.1	61.9	0.124	8.0	78.8	0.109
.24	6.4	72.8	0.119	15.0	22.1	0.106
Mean values	12.5	35.0	0.152	12.6	45.9	0.135

## Appendix I. 3.17./3.21

BROADCASTER						
sprout length ( <i>RB</i> ) = 0.63 m			sprout angle ( $\gamma$ ) = +1°			
ratio crank/connecting rod ( <i>C</i> ) = 0.600			rotary frequency ( <i>N</i> ) = 540 min <sup>-1</sup>			
I			II			
FERTILIZER			FERTILIZER			
$\mu^* = 0.2, \varepsilon^* = 0.4, \omega_1 = -1000 \text{ rad s}^{-1}$			$\mu^* = 0.1, \varepsilon^* = 0.6, \omega_1 = -1000 \text{ rad s}^{-1}$			
<i>R<sub>o</sub></i> (m)	<i>VK</i> (m s <sup>-1</sup> )	$\beta$ (deg)	<i>t</i> (s)	<i>VK</i> (m s <sup>-1</sup> )	$\beta$ (deg)	<i>t</i> (s)
.10	22.9	17.0	0.099	26.9	22.3	0.096
.11	24.0	16.0	0.098	27.6	24.6	0.094
.12	25.4	15.2	0.095	30.4	22.2	0.091
.13	28.9	19.7	0.091	31.2	24.0	0.088
.14	30.5	22.9	0.088	28.5	30.6	0.086
.15	30.6	27.9	0.085	28.8	32.4	0.085
.16	29.5	31.9	0.082	28.9	34.0	0.082
.17	26.7	38.1	0.079	22.4	45.4	0.079
.18	20.6	44.8	0.076	22.4	46.9	0.077
.19	16.5	56.1	0.072	22.4	48.4	0.074
.20	11.8	82.3	0.069	12.8	80.0	0.071
.21	12.0	84.9	0.065	12.9	82.1	0.067
.22	12.3	87.4	0.063	12.9	84.3	0.065
.23	16.2	20.0	0.060	13.0	86.3	0.063
.24	16.9	19.9	0.058	13.2	88.2	0.061
Mean values	21.7	38.9	0.079	22.3	50.1	0.079

## Appendix I. 3.18./3.22

BROADCASTER						
sprout length ( <i>RB</i> ) = 0.67 m			sprout angle ( $\gamma$ ) = +1°			
ratio crank/connecting rod ( <i>C</i> ) = 0.600			rotary frequency ( <i>N</i> ) = 540 min <sup>-1</sup>			
I			II			
FERTILIZER			FERTILIZER			
$\mu^* = 0.2, \varepsilon^* = 0.4, \omega_1 = -1000 \text{ rad s}^{-1}$			$\mu^* = 0.1, \varepsilon^* = 0.6, \omega_1 = -1000 \text{ rad s}^{-1}$			
<i>R<sub>o</sub></i> (m)	<i>VK</i> (m s <sup>-1</sup> )	$\beta$ (deg)	<i>t</i> (s)	<i>VK</i> (m s <sup>-1</sup> )	$\beta$ (deg)	<i>t</i> (s)
.10	22.9	17.0	0.102	26.9	22.3	0.098
.11	24.0	16.0	0.100	29.1	21.0	0.096
.12	25.4	15.2	0.097	30.4	22.2	0.094
.13	28.8	18.6	0.094	31.2	24.0	0.092
.14	31.1	20.4	0.090	31.8	25.8	0.089
.15	32.4	22.9	0.088	32.3	27.5	0.087
.16	32.8	26.5	0.085	32.6	29.1	0.084
.17	31.4	31.5	0.082	29.0	35.5	0.083
.18	29.5	36.0	0.080	29.2	37.0	0.081
.19	25.5	43.1	0.076	22.4	48.4	0.078
.20	20.0	49.2	0.074	22.4	49.9	0.076
.21	16.6	60.1	0.069	22.3	51.3	0.073
.22	12.3	87.4	0.066	12.9	84.3	0.070
.23	12.4	89.8	0.064	13.0	86.3	0.068
.24	12.7	87.9	0.062	13.2	88.2	0.064
Mean values	23.8	41.4	0.082	25.3	43.5	0.082

## Appendix I. 3.19./3.23

BROADCASTER						
sprout length ( $RB$ ) = 0.71 m			sprout angle ( $\gamma$ ) = $+1^\circ$			
ratio crank/connecting rod ( $C$ ) = 0.600			rotary frequency ( $N$ ) = 540 $\text{min}^{-1}$			
I			II			
FERTILIZER			FERTILIZER			
$\mu^* = 0.2, \varepsilon^* = 0.4, \omega_1 = -1000 \text{ rad s}^{-1}$			$\mu^* = 0.1, \varepsilon^* = 0.6, \omega_1 = -1000 \text{ rad s}^{-1}$			
$R_0$ (m)	$VK$ ( $\text{m s}^{-1}$ )	$\beta$ (deg)	$t$ (s)	$VK$ ( $\text{m s}^{-1}$ )	$\beta$ (deg)	$t$ (s)
.10	22.9	17.0	0.105	26.9	22.3	0.099
.11	24.0	16.0	0.104	29.1	21.0	0.098
.12	25.4	15.2	0.100	30.4	22.2	0.096
.13	28.8	18.6	0.096	32.3	21.8	0.093
.14	31.0	19.0	0.093	33.3	23.2	0.092
.15	33.1	20.5	0.090	34.1	24.9	0.090
.16	34.4	23.2	0.088	34.6	26.4	0.087
.17	34.6	26.5	0.085	32.9	30.6	0.085
.18	33.8	30.0	0.083	33.1	32.0	0.084
.19	31.5	35.3	0.080	33.3	33.4	0.082
.20	28.4	40.2	0.077	29.3	39.7	0.079
.21	24.1	48.6	0.074	22.3	51.3	0.077
.22	16.7	62.2	0.071	22.3	52.7	0.075
.23	12.4	89.8	0.068	22.3	54.1	0.072
.24	12.7	87.9	0.066	13.2	88.2	0.068
Mean values	26.2	36.7	0.085	28.6	36.3	0.085

## Appendix I. 3.20./3.24

BROADCASTER						
sprout length ( $RB$ ) = 0.75 m			sprout angle ( $\gamma$ ) = $+1^\circ$			
ratio crank/connecting rod ( $C$ ) = 0.600			rotary frequency ( $N$ ) = 540 $\text{min}^{-1}$			
I			II			
FERTILIZER			FERTILIZER			
$\mu^* = 0.2, \varepsilon^* = 0.4, \omega_1 = -1000 \text{ rad s}^{-1}$			$\mu^* = 0.1, \varepsilon^* = 0.6, \omega_1 = -1000 \text{ rad s}^{-1}$			
$R_0$ (m)	$VK$ ( $\text{m s}^{-1}$ )	$\beta$ (deg)	$t$ (s)	$VK$ ( $\text{m s}^{-1}$ )	$\beta$ (deg)	$t$ (s)
.10	22.9	17.0	0.107	26.9	22.3	0.101
.11	24.0	16.0	0.106	29.1	21.0	0.100
.12	25.4	15.2	0.103	30.4	22.2	0.098
.13	28.8	18.6	0.098	32.3	21.8	0.095
.14	31.0	19.0	0.095	34.0	22.1	0.093
.15	33.0	19.1	0.093	35.5	22.7	0.092
.16	35.1	20.6	0.090	36.3	24.0	0.090
.17	36.3	23.1	0.088	36.3	26.4	0.087
.18	36.6	25.6	0.086	36.7	27.8	0.086
.19	36.0	29.4	0.083	33.3	33.4	0.083
.20	34.0	33.3	0.081	33.5	34.7	0.083
.21	30.7	38.5	0.078	33.6	35.9	0.080
.22	26.0	45.2	0.075	29.3	42.2	0.078
.23	20.1	54.5	0.072	22.3	54.1	0.076
.24	16.8	66.1	0.070	22.4	55.4	0.072
Mean values	29.1	29.4	0.088	31.5	31.1	0.088

## Appendix I. 4.1./4.5

BROADCASTER						
sprout length ( $RB$ ) = 0.63 m			sprout angle ( $\gamma$ ) = $+1^\circ$			
ratio crank/connecting rod ( $C$ ) = 0.600			rotary frequency ( $N$ ) = 660 $\text{min}^{-1}$			
I			FERTILIZER			II
$\mu^* = 0.2, \varepsilon^* = 0.4, \omega_1 = -1000 \text{ rad s}^{-1}$						$\mu^* = 0.1, \varepsilon^* = 0.6, \omega_1 = -1000 \text{ rad s}^{-1}$
$R_s$ (m)	$VK$ ( $\text{m s}^{-1}$ )	$\beta$ (deg)	$t$ (s)	$VK$ ( $\text{m s}^{-1}$ )	$\beta$ (deg)	$t$ (s)
.10	26.2	18.7	0.085	30.2	19.9	0.081
.11	27.5	17.0	0.082	31.7	21.8	0.080
.12	29.1	16.0	0.080	32.7	23.9	0.077
.13	30.5	15.3	0.078	35.9	21.6	0.077
.14	34.6	19.1	0.075	37.2	23.2	0.075
.15	36.9	21.7	0.073	38.1	24.9	0.072
.16	37.7	25.3	0.070	34.6	31.4	0.070
.17	37.1	29.7	0.068	34.9	33.0	0.069
.18	34.3	35.6	0.066	35.1	34.5	0.067
.19	30.8	41.3	0.063	27.0	45.9	0.065
.20	23.0	48.8	0.060	27.0	47.4	0.063
.21	20.0	57.0	0.057	27.2	48.8	0.059
.22	14.3	83.9	0.055	15.4	80.8	0.058
.23	14.6	86.2	0.053	15.4	82.9	0.056
.24	14.8	88.4	0.050	15.7	84.8	0.053
Mean values	27.4	40.3	0.068	29.2	41.7	0.068

## Appendix I. 4.2./4.6

BROADCASTER						
sprout length ( $RB$ ) = 0.67 m			sprout angle ( $\gamma$ ) = $+1^\circ$			
ratio crank/connecting rod ( $C$ ) = 0.600			rotary frequency ( $N$ ) = 660 $\text{min}^{-1}$			
I			FERTILIZER			II
$\mu^* = 0.2, \varepsilon^* = 0.4, \omega_1 = -1000 \text{ rad s}^{-1}$						$\mu^* = 0.1, \varepsilon^* = 0.6, \omega_1 = -1000 \text{ rad s}^{-1}$
$R_s$ (m)	$VK$ ( $\text{m s}^{-1}$ )	$\beta$ (deg)	$t$ (s)	$VK$ ( $\text{m s}^{-1}$ )	$\beta$ (deg)	$t$ (s)
.10	26.2	18.7	0.088	30.2	19.9	0.084
.11	27.5	17.0	0.085	31.7	21.8	0.082
.12	29.1	16.0	0.082	33.8	21.3	0.079
.13	30.5	15.3	0.080	35.9	21.6	0.078
.14	34.5	18.5	0.077	37.2	23.2	0.076
.15	37.2	19.7	0.075	38.1	24.9	0.075
.16	39.2	22.0	0.073	38.8	26.6	0.072
.17	40.2	25.0	0.071	39.3	28.1	0.071
.18	39.3	29.5	0.068	35.1	34.5	0.069
.19	37.3	34.0	0.066	35.2	35.9	0.068
.20	33.8	39.2	0.064	35.3	37.3	0.066
.21	29.4	46.3	0.061	27.2	48.8	0.064
.22	20.1	59.0	0.058	27.1	50.2	0.062
.23	14.6	86.2	0.056	27.0	51.5	0.060
.24	14.8	88.4	0.054	15.7	84.8	0.058
Mean values	30.2	35.7	0.071	32.5	35.4	0.071

## Appendix I. 4.3./4.7

BROADCASTER						
sprout length ( $RB$ ) = 0.71 m			sprout angle ( $\gamma$ ) = $+1^\circ$			
ratio crank/connecting rod ( $C$ ) = 0.600			rotary frequency ( $N$ ) = 660 $\text{min}^{-1}$			
I			II			
FERTILIZER			FERTILIZER			
$\mu^* = 0.2, e^* = 0.4, \omega_1 = -1000 \text{ rad s}^{-1}$			$\mu^* = 0.1, e^* = 0.6, \omega_1 = -1000 \text{ rad s}^{-1}$			
$R_p$ (m)	$VK$ ( $\text{m s}^{-1}$ )	$\beta$ (deg)	$t$ (s)	$VK$ ( $\text{m s}^{-1}$ )	$\beta$ (deg)	$t$ (s)
.10	26.2	18.7	0.089	30.2	19.9	0.086
.11	27.5	17.0	0.087	31.7	21.8	0.083
.12	29.1	16.0	0.085	33.8	21.3	0.080
.13	30.5	15.3	0.084	35.9	21.6	0.079
.14	34.5	18.5	0.079	37.2	23.2	0.077
.15	37.0	18.9	0.077	39.8	22.5	0.076
.16	39.7	19.9	0.075	40.8	24.0	0.074
.17	41.6	22.1	0.073	41.6	25.5	0.073
.18	42.3	25.2	0.071	42.2	26.9	0.071
.19	42.2	28.1	0.069	40.0	31.0	0.069
.20	40.0	32.7	0.067	40.2	32.3	0.069
.21	37.2	37.4	0.065	40.6	33.6	0.067
.22	32.3	43.2	0.062	35.6	39.8	0.065
.23	24.8	50.7	0.060	27.0	51.5	0.063
.24	20.2	62.7	0.058	27.1	52.8	0.061
Mean values	33.7	28.4	0.073	36.3	29.8	0.073

## Appendix I. 4.4./4.8

BROADCASTER						
sprout length ( $RB$ ) = 0.75 m			sprout angle ( $\gamma$ ) = $+1^\circ$			
ratio crank/connecting rod ( $C$ ) = 0.600			rotary frequency ( $N$ ) = 660 $\text{min}^{-1}$			
I			II			
FERTILIZER			FERTILIZER			
$\mu^* = 0.2, e^* = 0.4, \omega_1 = -1000 \text{ rad s}^{-1}$			$\mu^* = 0.1, e^* = 0.6, \omega_1 = -1000 \text{ rad s}^{-1}$			
$R_p$ (m)	$VK$ ( $\text{m s}^{-1}$ )	$\beta$ (deg)	$t$ (s)	$VK$ ( $\text{m s}^{-1}$ )	$\beta$ (deg)	$t$ (s)
.10	26.2	18.7	0.090	30.2	19.9	0.087
.11	27.5	17.0	0.088	31.7	21.8	0.085
.12	29.1	16.0	0.087	33.8	21.3	0.083
.13	30.5	15.3	0.085	35.9	21.6	0.081
.14	34.5	18.5	0.081	38.1	21.6	0.079
.15	37.0	18.9	0.079	39.8	22.5	0.078
.16	39.5	19.0	0.077	41.8	22.6	0.077
.17	42.0	20.2	0.074	43.5	23.2	0.075
.18	43.9	22.2	0.073	44.4	24.5	0.073
.19	44.7	24.5	0.071	44.2	26.7	0.071
.20	44.5	27.4	0.069	44.7	28.0	0.070
.21	42.8	31.6	0.067	40.6	33.6	0.068
.22	39.9	35.7	0.065	40.8	34.8	0.068
.23	35.7	41.0	0.063	40.8	36.0	0.066
.24	31.1	46.3	0.061	35.8	42.2	0.064
Mean values	36.6	24.8	0.075	39.1	26.7	0.075

## LIST OF SYMBOLS AND ABBREVIATIONS

$\alpha$	angle of rotation
$\alpha$	angle of slope of the disc (Fig. 5.2)
$\alpha_c$	critical value of the angle of rotation (section 4.2.2.3)
$\beta$	angle of particle dispatch
$\beta$	angle of backwards distortion of the vane (Fig. 5.2)
$\gamma$	sprout angle
$\delta$	angle between centre line and particle distance from the oscillation point (Fig. 5.18, section 5.4.3)
$\varepsilon$	coefficient of restitution
$\varepsilon^*$	imaginary coefficient of restitution
$\theta$	angle, representing a function of the angle of oscillation and the sprout angle (section 5.4.2)
$\lambda$	spreading angle
$\mu$	coefficient of friction
$\mu^*$	imaginary coefficient of friction
$\tau$	time constant (section 4.3.1)
$\phi$	angle of oscillation
$\phi_{max}$	maximum angle of oscillation
$\dot{\phi}$	angular velocity of the sprout
$\dot{\phi}_{max}$	(absolute) maximum value of the angular velocity of the sprout
$\phi_{gem}$	mean value of the angular velocity of the sprout
$\ddot{\phi}$	angular acceleration of the sprout
$\dot{\phi}_{max}$	maximum value of the angular acceleration of the sprout
$\ddot{\phi}_{gem}$	mean value of the angular acceleration of the sprout
$\psi$	angle of particle impact
$\omega$	angular velocity of the driving shaft
$\omega_1$	initial particle rotation before impact
$\omega_2$	particle rotation after impact
$\Omega$	angular velocity of the driving shaft (section 4.3.1)
$a$	(momentary) radial particle position on the disc (section 5.2)
$a_1$	radius of particle supply (section 5.2)
$a_2$	radius of the disc (section 5.2)
$a_v$	free radius of the disc (section 5.2)
$a_f$	value for $a$ where particles start sliding (section 5.2)
$\dot{a}$	radial velocity (section 5.2)
$\ddot{a}$	radial acceleration (section 5.2)
$b$	spreading width
$b_e$	working width
$c$	variable, depending on the diameter of the sprout at the entrance



$\bar{d}$	linear deviation from the mean
$d_{max}$	maximum deviation from the mean
$d_{50}$	Mass Median Diameter
$g$	gravitational acceleration
$k_1$	constant (section 5.2)
$m$	mass of the particle
$P$	constant (section 5.4.2)
$r$	radius of a particle
$v$	difference between the two most extreme values
$x,y,z$	level lines for the value of C.V. (Fig. 3.5)
$A$	constant (section 7.2.1)
$B$	point at the centre line of the sprout
$C$	ratio between length of the crank and the connecting rod
$C$	constant (section 5.2)
$C.V.$	coefficient of variation
$CW$	calibration mass (section 7.2.1)
$D$	variable depending on $\mu$ (section 5.2)
$F_C$	Coriolis force
$F_R$	friction force
$F_Z$	centrifugal force
$G$	mass flow of fertilizer inside the sprout (section 4.3.1)
$J$	mass moment of inertia of a spherical particle
$J_1$	mass moment of inertia of the flywheel
$J_2$	sum of mass moment of inertia of sprout, bowl, counterweight, and forked connection
$K$	torsion spring
$L$	length of the connecting rod
$M$	friction force (section 7.2.1)
$N$	rotary frequency of the driving shaft
$O$	ratio of overlap
$P$	oscillation point (Fig. 4.1)
$R$	Burema's number of irregularity (section 3.2.2)
$R_o$	initial starting position of the particle
$R$	distance between the position of a particle in the sprout and the center of oscillation
$\dot{R}$	radial velocity of a particle
$\ddot{R}$	radial acceleration of a particle
$RA$	length of the crank
$RB$	length of the sprout
$W$	coefficient of irregularity according to Heyde (section 3.2.2)
$a_{BCEN}$	centripetal acceleration of the point $B$ at the sprout
$a_{BTAN}$	tangential acceleration of the point $B$ at the sprout
$a_{BCENGEM}$	mean value of the centripetal acceleration of the sprout

<i>aBCENMAX</i>	maximum value of the centripetal acceleration of the sprout
<i>aBTANGEM</i>	mean value of the tangential acceleration of the sprout
<i>aBTANMAX</i>	maximum value of the tangential acceleration of the sprout
<i>ALPHA</i>	angle of rotation ( $\alpha$ )
<i>Beta</i>	angle of dispatch in the horizontal ( $x$ - $y$ ) plane (section 6.4.1/6.4.2)
<i>BNDR</i>	indication for contact between particle and left ( $L$ ) or right ( $R$ ) wall
<i>Eta</i>	angle of particle dispatch in the vertical ( $y$ - $z$ ) plane (section 6.4.1/6.4.2)
<i>FI</i>	angle of oscillation ( $\phi$ )
<i>FL</i>	force acting on a particle parallel to the sprout wall
<i>FN</i>	force acting on a particle perpendicular to the sprout wall
<i>IBeta</i>	angle of particle dispatch in the horizontal ( $x$ - $y$ ) plane after contact with the bow (section 6.4.1/6.4.2)
<i>IEta</i>	angle of particle dispatch in the vertical ( $y$ - $z$ ) plane after contact with the bow (section 6.4.1/6.4.2)
<i>IM/CO</i>	phase at particle impact ( <i>IMP</i> ) or continuous contact ( <i>CON</i> )
<i>ROL</i>	rolling motion of particle during continuous contact
<i>ROTATION</i>	particle rotation ( $\omega$ )
<i>SLI</i>	sliding motion of particle during continuous contact
<i>ST/SL</i>	stick ( <i>ST</i> ) or sliding ( <i>SL</i> ) impact
<i>VABS</i>	absolute particle velocity of outlet (section 5.2)
<i>VAIMPC</i>	absolute particle velocity after contact with sprout wall
<i>VAIMPC<sub>L</sub></i>	component of <i>VAIMPC</i> parallel to the sprout wall
<i>VAIMPC<sub>N</sub></i>	component of <i>VAIMPC</i> perpendicular to the sprout wall
<i>VBIMPC</i>	absolute particle velocity before contact with sprout wall
<i>VBIMPC<sub>L</sub></i>	component of <i>VBIMPC</i> parallel to the sprout wall
<i>VBIMPC<sub>N</sub></i>	component of <i>VBIMPC</i> perpendicular to the sprout wall
<i>VB<sub>TAN</sub></i>	tangential velocity of the point <i>B</i> at the sprout
<i>VB<sub>TANGEM</sub></i>	mean value of the tangential velocity of the sprout
<i>VB<sub>TANMAX</sub></i>	maximum value of the tangential velocity of the sprout
<i>VB<sub>X</sub></i>	component of tangential velocity in <i>X</i> -direction
<i>VB<sub>Y</sub></i>	component of the tangential velocity in <i>Y</i> -direction
<i>VK</i>	absolute particle velocity of outlet
<i>VK<sub>L</sub></i>	particle velocity component parallel to the sprout wall
<i>VK<sub>N</sub></i>	particle velocity component perpendicular to the sprout wall
<i>VK<sub>RAD</sub></i>	radial component of particle velocity
<i>VK<sub>TAN</sub></i>	tangential component of particle velocity
<i>VK<sub>X</sub></i>	<i>X</i> -component of particle velocity <i>VK</i>
<i>VK<sub>Y</sub></i>	<i>Y</i> -component of particle velocity <i>VK</i>
<i>VW</i>	velocity of the sprout wall at the point of impact <i>A</i> (section 5.4.2)
<i>VW<sub>L</sub></i>	velocity component of <i>VW</i> parallel to the sprout wall

<i>VWN</i>	velocity component of <i>VW</i> perpendicular to the sprout wall
<i>WK</i>	absolute particle velocity after impact
<i>WKL</i>	particle velocity after impact parallel to the sprout wall
<i>WKN</i>	particle velocity after impact perpendicular to the sprout wall
<i>XKERNEL</i>	<i>X</i> -coordinate of a kernel (Table 5.7)
<i>YKERNEL</i>	<i>Y</i> -coordinate of a kernel (Table 5.7)

## CURRICULUM VITAE

Lambertus Speelman werd op 2 augustus 1942 te Assen geboren. Na het behalen van het MULO-B diploma te Assen, werd de opleiding voortgezet aan de Rijks Hogere Landbouwschool te Groningen.

In 1961 werd het eindexamen afgelegd. Aansluitend werd begonnen met de studie aan de Landbouwhogeschool. Het Ingenieursdiploma in de studierichting Landbouwwerktuigkunde werd in januari 1968 behaald.

Naast het hoofdvak omvatte de ingenieursstudie Grondbewerking, Werktuigkunde en Landbouwplantenteelt.

Sedert 1 februari 1968 is de auteur werkzaam geweest bij de vakgroep Landbouwtechniek van de Landbouwhogeschool, laatstelijk als wetenschappelijk hoofdmedewerker belast met onderwijs en onderzoek in de zaai- en verzorgingstechniek en de produkttechniek.

Op 1 april 1979 werd de vakgroep verlaten teneinde de huidige functie van Directeur van de Rijks Hogere Landbouwschool te Groningen te vervullen.